



The feasibility of using brown seaweed, *Laminaria digitata* as feedstock for generating bioenergy and biomaterials.

Being a thesis presented by

MEMBERE EDWARD AMASAYE

In application for

THE DEGREE OF DOCTOR OF PHILOSOPHY

To Newcastle University

The work embodied here-in was carried out in the School of Civil Engineering and Geosciences, Faculty of Agriculture and Engineering, Newcastle University upon Tyne,

NE1 7RU.

March, 2018



## Abstract

The societal need to develop sustainable renewable energy sources has seen a recent increase in the amount of research on anaerobic digestion technologies. Biofuels from algae, known as third generation biofuels, are taking a lead interest in this regard. The characteristics of the biopolymer components of seaweed, particularly brown algae, make it suitable for methanogenic digestion, and brings advantages over other biofuel feedstocks which displace terrestrial food crops from agricultural production.

This thesis investigates the feasibility of using brown seaweed, *Laminaria digitata* (LD), as a viable feedstock for continuous generation of bioenergy (methane) via the anaerobic digestion process, and biomaterial production from thermochemical processes. Results of methane yield from an initial bio-methane potential (BMP) assessment, using a modified BMP method, on pre-treated and dried samples gave yields of between  $141 \pm 5.77 \text{ mL CH}_4 \text{ gVS}^{-1}$  and  $207 \pm 0.07 \text{ mL CH}_4 \text{ gVS}^{-1}$ . Analysis of the thermochemical properties of the seaweed by pyrolysis gas chromatography-mass spectrometry (Py-GC-MS) identified sixty-four compounds present in all samples, twenty which have been previously reported as major pyrolysis products of *Laminaria digitata*. Proton Nuclear Magnetic Resonance ( $^1\text{H}$  NMR) analysis of extracted sodium alginate (biomaterial) fraction, gave results in agreement with reported literature on mono and diad frequencies, homopolymeric mannuronic  $F_M$  (0.36 - 0.46) ( $F_{MM} = 0.33 - 0.47$ ), guluronic (0.54 - 0.64) ( $F_{GG} = 0.19 - 0.25$ ) blocks with alternating block fractions of ( $F_{GM} = 0.17 - 0.21$ ) and ( $F_{MG} = 0.17 - 0.21$ ). The M/G ratio obtained (1.18 - 1.79) is an indication that the alginate extracted from *L. digitata* can be used to produce soft and elastic gels rather than brittle ones. Alginate is a major polysaccharide component of brown seaweeds which degrades to glyceraldehyde-3-phosphate and pyruvate as final products during anaerobic digestion. The triad frequencies ( $F_{GGG} = 0.14 - 0.17$ ,  $F_{MGM} = 0.11 - 0.126$ ,  $F_{GGM} = F_{MGG} = 0.05 - 0.09$ ) and the average block lengths are ( $N_G = 2.15 - 2.22$  and  $N_M = 2.61 - 3.85$ ) were also evaluated.

BMP studies on the effect of temperature on biogas production from *L. digitata* feedstock showed the trend  $35 \text{ }^\circ\text{C} > 25 \text{ }^\circ\text{C} > 45 \text{ }^\circ\text{C} > 55 \text{ }^\circ\text{C}$ , similar results being found in continuous fermentations, with mesophilic (35 °C) reactors giving better

cumulative methane yield than thermophilic (55 °C) reactors. Optimisation of the process using a multivariate technique, fit and multiple regression model, showed the interaction terms  $X_2^2$  (VFAs) and  $X_1 \times X_2$  (COD, VFAs) for mesophilic and thermophilic reactors were the best indicators of optimal methane production compared to other terms.

Research into the potential of mixed co-digestion of the *L. digitata* feedstock is important as it helps to overcome the limitations of using a mono-digestion feedstock of *L. digitata*, such as high hydrogen sulphide production, limited availability of *L. digitata* biomass, and seasonal variation in algal composition. Mono- and co-digestion of *L. digitata* (LD) with a stimulated food waste (SFW) were assessed using various mix ratios  $LD_{100:0\%}$ ,  $LD_{90:10\%}$ ,  $LD_{75:25\%}$ ,  $LD_{50:50\%}$ . BMP results showed the co-digested mix ratios exhibited both antagonist ( $LD_{90:10\%}$ ) and synergetic ( $LD_{75:25\%}$ ) effects. In the continuous study, the mono-digestion of  $LD_{100:0\%}$  was characterized by an accumulation of high total volatile fatty acids (tVFA) concentrations, reduced pH, and an increased FOS: TAC ratio, when the organic loading rate (OLR) was increased, leading to reactor failure. It was proposed that co-digestion brought about the dilution of inhibitory compounds, faster acclimatization of microorganisms to high salinity (chloride) levels in the presence of low ammonia concentrations at high loading rate.

Trace element supplementation (TES) during anaerobic digestion of the macroalgae feedstock in various mix ratios: control (TES 0), TES 1 (0.1 mg/l Se, 0.1 mg/l W), TES 2 (0.1 mg/l Se, 0.1 mg/l W, 0.5 mg/l Co, 0.1 mg/l Mo), TES 3 (0.1 mg/l Se, 0.1 mg/l W, 0.5 mg/l Co, 0.1 mg/l Mo, 0.5 mg/l Ni, 0.05 mg/l Cu) and TES 4 (0.1 mg/l Se, 0.1 mg/l W, 0.5 mg/l Co, 0.1 mg/l Mo, 0.5 mg/l Ni, 0.05 mg/l Cu, 0.5 mg/l Fe, 0.1 mg/l Zn) in batch reactors improved methane yield by 17% - 50%, and stimulated a steady digestion process in a continuous reactor when added weekly with increase in OLR compared to a reactor without trace element which led to reactor instability, and eventually failure.

## Acknowledgements

I like to express my sincere gratitude to Tertiary Education Trust Fund (TEFUND) Nigeria and the University of Port Harcourt, Choba, Nigeria for sponsorship of this PhD studies.

I would like to immensely thank my supervisors Dr. Paul Sallis and Prof. David Graham for their advice, guidance, and support throughout the duration of this study.

Special thanks to the College of Civil and Geosciences and School of Chemistry, Newcastle University where the studies were undertaken. I like to especially thank David Race, David Early, Bernard Bowler, Paul Donohoe and Corine Wills for all their help and technical support.

I appreciate all my friends and colleagues for their thoughtfulness and advice during this study.

My profound heartfelt gratitude to my wife and children who stood by and encouraged me when it was needed most.

Above all I give glory to the Almighty God who sustained and saw me through this study.



Dedication

For mother

For Victoria, Ella, Owass and Favour

## **Glossary**

<i>AD</i>	<i>anaerobic digestion</i>
<i>ASTM</i>	<i>American Society for Testing and Materials</i>
<i>BEF</i>	<i>Biomethane efficiency factor</i>
<i>BMP</i>	<i>Biomethane potential</i>
<i>BTU</i>	<i>British thermal unit</i>
<i>CH<sub>4</sub></i>	<i>Methane</i>
<i>CO<sub>2</sub></i>	<i>Carbon dioxide</i>
<i>COD</i>	<i>Chemical oxygen demand</i>
<i>DTG</i>	<i>Derivative thermogravimetry</i>
<i>FOS:TAC</i>	<i>Volatile organic acids content: buffer capacity</i>
<i>HCL</i>	<i>Hydrogen chloride</i>
<i><sup>1</sup>HNMR</i>	<i>Proton Nuclear Magnetic Resonance Spectroscopy</i>
<i>H<sub>2</sub>S</i>	<i>Hydrogen sulphide</i>
<i>ISP</i>	<i>Integrated systems approach</i>
<i>K</i>	<i>Decay constant</i>
<i>LD</i>	<i>Laminaria digitata</i>
<i>MY</i>	<i>Methane yield</i>
<i>M / G</i>	<i>Mannuronic / Guluronic ratio</i>
<i>mg</i>	<i>Milligram</i>
<i>NaOH</i>	<i>Sodium hydroxide</i>
<i>Py-GC/MS</i>	<i>Pyrolysis gas chromatography- mass spectrometry</i>
<i>R<sup>2</sup></i>	<i>Coefficient of regresssion</i>
<i>TGA</i>	<i>Thermogravimetric analysis</i>
<i>tVFAs</i>	<i>Total volatile fatty acids</i>
<i>TS</i>	<i>Total solids</i>
<i>TTHA</i>	<i>Triethylenetetraminehexaacetic acid</i>
<i>μ</i>	<i>Growth rate</i>
<i>μg</i>	<i>Microgram</i>
<i>VS</i>	<i>Volatile solids</i>
<i>SWF</i>	<i>Stimulated food waste</i>
<i>λ</i>	<i>Lag phase</i>



# Table of Contents

<b>Chapter 1. Introduction .....</b>	<b>25</b>
1.1 Background .....	25
1.2 The aim of the thesis .....	28
1.3 Specific Objectives .....	34
1.4 The thesis outline .....	35
<b>Chapter 2. Literature Review .....</b>	<b>36</b>
2.1 Marine biomass, Macroalgae as feedstock for bio-refinery .....	36
2.2 Biomass a renewable energy resource. ....	38
2.2.1 Classification of biomass feedstocks .....	40
2.2.2 Biofuels .....	41
2.3 Overview of biofuels policy framework. ....	43
2.4 Macroalgae biomass as third generation biofuels. ....	45
2.4.1 Algae .....	45
2.4.2 Macroalgae .....	46
2.5 Macroalgae taxonomical and biochemical compositions .....	48
2.6 Advantages of macroalgae as biomass feedstock .....	50
2.7 Macroalgae biomass cultivation and production .....	51
2.8 Brown seaweed .....	54
2.8.1 Cellulose .....	57
2.8.2 Alginate .....	57
2.8.3 Laminarin .....	58
2.8.4 Fucoidans .....	58
2.8.5 Mannitol .....	58
2.8.6 Brown Algae Phlorotannins .....	59
2.9 Anaerobic digestion process .....	60

2.10 The Fundamental biochemical AD process .....	61
2.10.1 Disintegration phase .....	62
2.10.2 Hydrolysis.....	63
2.10.3 Acidogenesis.....	63
2.10.4 Acetogenesis.....	64
2.10.5 Methanogenesis.....	65
2.11 Factors influencing digesters performance .....	66
2.11.1 pH and Alkalinity .....	67
2.11.2 Temperature.....	68
2.11.3 Retention Times .....	69
2.11.4 Organic Loading rate (OLR).....	70
2.11.5 Carbon to Nitrogen ratio (C: N) .....	71
2.11.6 Mixing.....	71
2.12 Inhibition of AD process .....	72
2.12.1 Oxygen.....	72
2.12.2 Ammonium (NH <sub>4</sub> <sup>+</sup> ) and Ammonia (NH <sub>3</sub> ).....	73
2.12.3 Sulphur compounds .....	76
2.12.4 Total Volatile fatty acids (TVFAs).....	78
2.12.5 Heavy metals .....	80
2.12.6 Light metals.....	81
2.12.7 Sodium .....	82
2.12.8 Potassium .....	82
2.13 Anaerobic digestion of macroalgae biomass for biogas production. ....	82

2.14 Toxicity to macroalgae digestion .....	85
2.14.1 Polyphenols .....	85
2.14.2 NaCl toxicity .....	85
2.15 Organic fraction of municipal solid waste (OFMSW) .....	86
2.16 Co-digestion of Macroalgae with OFMSW .....	87
2.17 Nutrient requirement for anaerobic digestion .....	89
2.18 Kinetic Models for biogas production .....	91
2.18.1 Mathematical models .....	91
2.18.2 Theoretical biogas yield .....	91
2.18.3 Reaction kinetics model .....	92
2.19 Anaerobic biodegradability assessment .....	96
2.20 Thermochemical processes for biomass conversion .....	99
<b>Chapter 3. Materials and Methods .....</b>	<b>103</b>
3.1 Collection, pre-treatment, and storage .....	103
3.1.1 Experimental design/reactor system .....	104
3.1.2 Inoculum and operation .....	104
3.2 Laboratory analytical methods .....	105
3.2.1 pH and Solids .....	105
3.2.2 Chemical oxygen demand (COD) .....	105
3.2.3 Ammonical nitrogen (NH <sub>3</sub> -N) .....	106
3.2.4 Total Kjeldahl Nitrogen (TKN) .....	106
3.2.5 Total organic carbon (TOC) .....	106
3.2.6 Elemental Composition (CNS) analysis .....	106
3.2.7 Sulphate (SO <sub>4</sub> <sup>2-</sup> ) .....	107
3.2.8 Volatile fatty acids (VFAs) .....	107

3.2.9 Biogas and methane measurement .....	107
3.2.10 Hydrogen sulphide and CO <sub>2</sub> gas measurement. ....	108
3.2.11 Trace metals extraction .....	109
3.2.12 Trace metals analysis by inductively coupled plasma optical emission spectrometry (ICP-OES). ....	109

**Chapter 4. Bio-methane Potential Test (BMP) using inert gas sampling bags with macroalgae feedstock. .... 110**

4.1 Introduction .....	111
4.2 Materials and Methods .....	111
4.2.1 Collection, pretreatment, and storage .....	111
4.2.2 Inoculum .....	111
4.2.3 Characterization of the sample.....	112
4.2.4 Assessment of Bio-methane potential energy from the Buswell equation .....	113
4.2.5 Modified Bio-methane potential assessment of pre-treated Substrate. ....	114
4.2.6 Biogas collection .....	115
4.2.7 Biogas and methane measurement .....	116
4.2.8 Determination of the kinetic decay constant and lag phase. ....	116
4.2.9 Validation samples .....	117
4.3 Results and discussion .....	118
4.3.1 Inoculum .....	118
4.3.2 Characterisation of macroalgal substrates .....	119
4.3.3 CH <sub>4</sub> production .....	121

4.3.4 Methane Production (Validation samples) .....	124
4.4 Conclusion.....	127
<b>Chapter 5. Thermochemical characterization of brown seaweed, <i>Laminaria digitata</i> from UK shores. ....</b>	<b>129</b>
5.1 Introduction.....	130
5.2 Material and Methods.....	130
5.2.1 Collection, pretreatment, and storage.....	130
5.2.2 Thermal Analysis .....	130
5.2.3 Pyrolysis-gas chromatography-mass spectrometry analysis (Py-GC-MS).....	131
5.2.4 Alginate extraction .....	131
5.2.5 Proton Nuclear Magnetic Resonance ( <sup>1</sup> H NMR) Analysis .....	132
5.3 Results and Discussion .....	132
5.3.1 Thermal Gravimetric Analysis (TGA) .....	132
5.3.2 Pyrolysis-gas chromatography-mass spectrometry analysis .....	135
5.3.3 <sup>1</sup> H NMR Analysis .....	138
5.4 Conclusion.....	144
<b>Chapter 6. Effect of temperature on kinetics of biogas production from macroalgae.....</b>	<b>146</b>
6.2 Materials and methods .....	147
6.2.1 Algae collection, pretreatment, and storage.....	147
6.2.2 Substrate characterization and analysis .....	147
6.3 BMP studies at different temperatures .....	148
6.3.1 Batch studies .....	148

6.3.2 Kinetic study on batch experiment .....	149
6.4 Results and Discussion .....	151
6.4.1 Experimental batch study.....	151
6.4.2 Kinetic study using modified Gompertz and logistics model.....	157
6.5 Conclusion .....	160
<b>Chapter 7. Continuous reactor study of macroalgae feedstock under mesophilic and thermophilic conditions.....</b>	<b>161</b>
7.2 Materials and methods .....	163
7.2.1 Experimental procedure .....	163
7.2.2 Algae collection, pretreatment, and storage .....	163
7.3 Results and discussion .....	163
7.3.1 Methane production profiles: Mesophilic and thermophilic digesters	163
7.4 Process performance indicators .....	171
7.4.1 pH, VFAs, and alkalinity .....	171
7.4.2 Ammonium ion (NH <sub>4</sub> <sup>+</sup> ) and free ammonia (NH <sub>3</sub> ) nitrogen .....	177
7.4.3 Solids, COD, and Anions .....	181
7.4.4 Statistical Analysis .....	188
7.5 Conclusion.....	191
<b>Chapter 8. Optimisation of methane production from macroalgae feedstock using regression analysis under mesophilic and thermophilic conditions .....</b>	<b>192</b>
8.2 Materials and methods .....	193
8.2.1 Experimental procedure .....	193
8.2.2 Algae collection, pretreatment, and storage .....	193

8.2.3 Optimisation methodology used.....	193
8.3 Results and Discussion .....	194
8.3.1 Model equation generation: Mesophilic temperature .....	194
8.3.2 Surface and contour plots analysis for mesophilic reactor.....	197
8.3.3 Model equation generation: Thermophilic temperature.....	200
8.4 Conclusion.....	203
<b>Chapter 9. Co-digestion of macroalgae with simulated food waste (SFW)</b>	<b>205</b>
9.1 Introduction.....	206
9.2 Materials and Methods .....	206
9.2.1 Substrate, inoculum and chemical analysis .....	206
9.2.2 Synthetic food waste preparation.....	206
9.2.3 Experimental procedure.....	207
9.3 Results and Discussion .....	208
9.3.1 Characterisation of macroalgae and food substrates.....	208
9.4 Batch studies: CH <sub>4</sub> production.....	212
9.4.1 Kinetics of CH <sub>4</sub> production .....	215
9.4.2 Antagonistic or synergistic effects of co-digestion on methane yields .....	216
9.5 Continuous co-digestion studies.....	217
9.5.1 Assessment of mono-digestion of LD <sub>100%</sub> (100% <i>L. digitata</i> , 0% food waste) .....	221
9.5.2 Assessment of co-digestion of LD <sub>90:10 %</sub> (90% <i>L. digitata</i> , 10% food waste) .....	224
9.5.3 Assessment of co-digestion of LD <sub>75:25 %</sub> (75% <i>L. digitata</i> , 25% food waste) .....	226

9.5.4 Assessment of co-digestion of LD <sub>50:50%</sub> (50% <i>L. digitata</i> , 50% food waste) .....	228
9.5.5 Comparison of LD <sub>100%</sub> with other LD <sub>LD%: FW%</sub> mix reactors .....	229
9.5.6 Metal Concentrations .....	237
9.6 Conclusion .....	240
<b>Chapter 10. Anaerobic digestion of macroalgae with trace element supplementation: Batch and continuous studies .....</b>	<b>241</b>
10.1 Introduction .....	243
10.2 Materials and methods .....	243
10.2.1 Substrates and chemical analysis .....	243
10.2.2 Inoculum .....	243
10.2.3 Design of the Experiment .....	243
10.2.4 Continuous reactors .....	244
10.3 Results and discussion .....	245
10.3.1 Biomethane potential .....	245
10.3.2 Continuous reactors (Experiment 1) .....	247
10.3.3 Continuous reactors (Experiment 2) .....	261
10.4 Conclusion .....	267
<b>Chapter 11. General discussion and conclusion.....</b>	<b>268</b>
11.1 Recommendation.....	271
11.1.1 Areas recommended for further studies using brown seaweed.....	272
<b>Chapter 12. References .....</b>	<b>273</b>



<b>Appendix A. Expeded Py-GC/MS profile at 610°C for <i>Laminaria digitata</i> collected in January (Figure A-D).....</b>	<b>319</b>
<b>Appendix B. X-ray Diffraction intensity graphs for Algae samples collected in January, July, and December 2015. ....</b>	<b>321</b>
<b>Appendix C. Matrix plot of COD, VFA and alkalinity for mesophilic and thermophilic reactor .....</b>	<b>321</b>
<b>Appendix D. Correlation: reactor, pH, temperature, COD, VFA, ammonia, VS, and alkalinity (35°C).....</b>	<b>322</b>
<b>Appendix E. Correlation: reactor, pH, temperature, COD, VFA, ammonia, alkalinity (55 °C).....</b>	<b>323</b>

## List of Tables

Table 2-1: Categorization of biomass feedstock adapted from (Demirbas, 2009a)	41
Table 2-2: Advantages and disadvantages of different generations of biofuels.	43
Table 2-3: Approximate chemical composition of seaweeds	49
Table 2-4: Modified models for bacterial growth	96
Table 4-1: Characteristics of macroalgal samples	117
Table 4-2: Elemental and physical analysis of macroalgal samples	119
Table 4-3: Elemental components for generation of the stoichiometric equation for macroalgal samples.	119
Table 4-4: Theoretical prediction of biogas production from macroalgal samples using the Buswell Equation.	120
Table 4-5: Theoretical methane yields for pre-treated macroalgal samples	120
Table 4-6: BMP results compared to theoretical yield.	126
Table 5-1 TGA and elemental analysis results for algae samples	133
Table 5-2 Compounds identified in pyrograms from Py-GC/MS of <i>Laminaria digitata</i>	137
Table 5-3: Compositional data of alginate extracted from <i>Laminaria digitata</i> compared to other <i>Laminaries</i> species	143
Table 6-1: Physiochemical characteristics of <i>Laminaria digitata</i> of macroalgal feedstock	147
Table 6-2 Generation of the stoichiometric equation and theoretical assessment of biogas production from macroalgae (collected in July 2015)	152
Table 6-3 Bio-methane production for macroalgae using results of BMP and theoretical analysis	152
Table 6-4 Results of kinetics study (Modified Gompertz and Logistics model)	157
Table 7-1 Methane yields (mL CH <sub>4</sub> / g VS) of seaweed fermentation at mesophilic and thermophilic temperature at five OLR	164
Table 7-2 Analysis of variance (ANOVA) for reactors cumulative CH <sub>4</sub> means	189
Table 8-1 Variables used in fit and multiple regression analysis	194
Table 8-2 Analysis of Variance (ANOVA) for Mesophilic reactor MR 1	194

Table 8-3 Analysis of Variance (ANOVA) for Response surface model at thermophilic temperature (TR 1) .....	200
Table 9-1 Selected types of food substrates used. ....	206
Table 9-2 Ratios of LD with SFW used in both batch and continuous reactors study. ....	207
Table 9-3 Characteristics of inoculum, macroalgae, and food used for batch and continuous processes. ....	209
Table 9-4 Design mix used in the batch and continuous operations with BMP results of experimental and theoretical methane (CH <sub>4</sub> ) yields. ....	211
Table 9-5 Kinetic analysis of the different mix ratio using the modified Gompertz equation .....	212
Table 9-6 Antagonistic or synergistic effects of co-digestion on methane yields. ....	217
Table 9-7 Performance characteristics of the continuous reactors R1 - R4 .....	224
Table 9-8 Essential trace elements concentration of algae and stimulated food waste feedstock, inoculum, and continuous reactors R1, R2, R3 and R4.....	238
Table 10-1 Experimental design for both batch and CSTRs with trace element concentration. ....	244
Table 10-2 : Trace element concentration in algae substrate and inoculum at the start of the experiment, and the concentration in the reactors at the end of the experiment. ....	252
Table 10-3 Summary of the results for the continuous reactors with and without trace element supplementation (Experiment 2). ....	264
Table 10-4 Summary of the results for the continuous reactors with and without trace element supplementation (Experiment 2). ....	264

## List of Figures

Figure 2-1: Biorefinery and its role in the transformation of biomass .....	38
Figure 2-2: Potential pathways from marine algae to biofuels.....	42
Figure 2-3 Generic representation of alternating life cycle of seaweeds .....	46
Figure 2-4: Renewable fuel sources and bioproducts from algae .....	47
Figure 2-5: World production of farmed macroalgae from 2001 to 2010 .....	53
Figure 2-6: Redline indicates natural distribution of shallow water with potential for macroalgae cultivation .....	54
Figure 2-7: <i>Laminariales</i> distribution in UK, dominating rocky shores at, or just below low water mark.....	55
Figure 2-8: Life history of <i>Laminaria</i> .....	56
Figure 2-9: Hypothetical model of the biochemical organization of cell walls of brown algae.....	56
Figure 2-10: Structural presentation of polysaccharides abundant in seaweed biomass,.....	57
Figure 2-11 Phloroglucinol parent molecule (1, 3, 5 trihydroxybenzene) .....	59
Figure 2-12: The essentials of fermentation. ....	61
Figure 2-13 Overview of the four principle reaction steps of anaerobic digestion	62
Figure 2-14: The Cardinal temperature: minimum, optimum and maximum.....	68
Figure 2-15: Relative growth rate of psychrophilic, mesophilic, and thermophilic	69
Figure 2-16: Proposed mechanism of ammonia inhibition in methanogenic bacteria .....	75
Figure 2-17: Effect of heavy metal concentration on biological reactions by McCarthy (Gikas and Romanos, 2006). ....	81
Figure 2-18: Phases of bacteria growth curve.....	92
Figure 2-19. Bio-methane potential reactor and sampling illustration (Hansen et al., 2004). ....	98
Figure 2-20 An example of a DTG profile of alginic acid, Na and Ca-alginate in an inert (N <sub>2</sub> ) atmosphere (Ross <i>et al.</i> , 2011).....	101
Figure 3-1 <i>Laminaria digitata</i> feedstock preparation process.....	103

Figure 3-2 Continuous reactor set up and design .....	104
Figure 4-1. % Methane composition in biogas using waste beer as substrate..	112
Figure 4-2. Modified BMP reactor and gas collection bag.....	115
Figure 4-3 a) Plot of cumulative methane at different HAC concentration b) methane composition obtained at different concentrations HAC concentration.	118
Figure 4-4: A), Cumulative; and B), Daily BMP for macroalgal samples; FD, FHY, DD, DHY. ....	121
Figure 4-5: A) Macroalgal methane composition and, b) First order plot of the cumulative methane production of pre-treated macroalgal samples FD, FHY, DD and DHY. ....	123
Figure 4-6: A) Cumulative BMP and, B) Percentage of methane in biogas from the BMP test for the second sample of seaweeds. ....	125
Figure 4-7: First order plot of cumulative methane production for Figure 4-6. ...	126
Figure 5-1: TGA profile for <i>Laminaria digitata</i> collected in January 2015.....	134
Figure 5-2 Py-GC/MS profile at 610°C for <i>Laminaria digitata</i> collected in January, July, December (identified compounds are listed in Table 5-2). ....	136
Figure 5-3 The region of the <sup>1</sup> H NMR spectrum of alginate used for quantitative analysis .....	139
Figure 5-4 Some examples of typical <sup>1</sup> H-NMR spectra of some alginates.....	139
Figure 5-5: H <sup>1</sup> NMR spectra for solution of alginate from <i>Laminaria digitata</i> in D <sub>2</sub> O. 1. January 2. July 3. December, 2015.....	140
Figure 6-1 A) Cumulative biogas production B), % Methane .....	153
Figure 6-2 A) Cumulative methane production B) Daily methane production (mL CH <sub>4</sub> / gVS). ....	154
Figure 6-3 First order plot of cumulative methane production of <i>Laminaria digitata</i> at various temperature range. ....	156
Figure 6-4 Comparison of predicted A), modified Gompertz; and B), logistics models with experimental cumulative methane production.....	159
Figure 7-1 Daily and cumulative CH <sub>4</sub> production, % CH <sub>4</sub> and H <sub>2</sub> S composition and organic loading rate (OLR) for; A), MR 1, Control (algae only) at 35 °C; B), TR 1, Control (algae only) at 55 °C.....	165
Figure 7-2 Daily and cumulative CH <sub>4</sub> production, % CH <sub>4</sub> and H <sub>2</sub> S composition and organic loading rate (OLR) for; A), MR 2, Algae + NaHCO <sub>3</sub> addition at 35 °C; B), TR 2, Algae + NaHCO <sub>3</sub> addition at 55 °C. ....	166

Figure 7-3 Daily and cumulative CH <sub>4</sub> production, % CH <sub>4</sub> and H <sub>2</sub> S composition and organic loading rate (OLR) for; A), MR 3, Algae + FePO <sub>4</sub> addition at 35 °C; B), TR 3, Algae + FePO <sub>4</sub> addition at 55 °C.....	167
Figure 7-4 A), Variations in pH, B), VFAs, of both mesophilic (MR 1, 2, 3) and thermophilic (TR 1, 2, 3) digesters. ....	174
Figure 7-5 A), Variations in Alkalinity; and B), FOS: TAC ratio of both mesophilic (MR 1, 2, 3) and thermophilic (TR 1, 2, 3) digesters.....	175
Figure 7-6 Volatile fatty acids speciation from macroalgae during AD, a) Mesophilic (MR 1) and, b) thermophilic temperature (TR 1).....	176
Figure 7-7 A), Concentration profile for Total Kjeldahl (TKN); B), Total ammonia nitrogen (TAN) in mesophilic (MR 1, 2, 3) and thermophilic (TR 1, 2, 3) digesters. ....	177
Figure 7-8 A), Concentration profile for free ammonia (NH <sub>3</sub> ) nitrogen (FAN); B), ammonium ion (NH <sub>4</sub> <sup>+</sup> ) in mesophilic (MR 1, 2, 3) and thermophilic (TR 1, 2, 3) digesters.....	178
Figure 7-9 A), Concentration profile of soluble COD; B), Total COD in mesophilic (MR 1, 2, 3) and thermophilic (TR 1, 2, 3) reactors. ....	181
Figure 7-10 A), Concentration profile of sulphate; B), Chloride in mesophilic (MR 1, 2, 3) and thermophilic (TR 1, 2, 3) reactors.....	185
Figure 7-11 A), Concentration profile of total solids; B), Volatile solids in mesophilic (MR 1, 2, 3) and thermophilic (TR 1, 2, 3) reactors. ....	187
Figure 7-12 Main effects and interaction plot for cumulative CH <sub>4</sub> production for mesophilic (MR 1, 2, 3) and thermophilic (TR 1, 2, 3) reactors. ....	190
Figure 8-1 Main effects plot for mesophilic reactor (MR 1) on methane production. ....	196
Figure 8-2 Surface and contour plots for mesophilic reactor (MR 1). ....	198
Figure 8-3 Surface and contour plots for thermophilic reactor (TR 1) .....	199
Figure 8-4 Main effects plot for thermophilic reactor (TR I) on methane yield ...	201
Figure 9-1 Homogenous prepared food feedstock for the digesters .....	207
Figure 9-2 Cumulative and daily biogas profile for different design mix of algae to food ratio. ....	213
Figure 9-3 Cumulative and daily methane profile for different design mix of algae to food ratio. ....	213
Figure 9-4 Continuous reactors, co-digestion mixtures; A), Daily biogas production; B), Cumulative biogas production.....	219

Figure 9-5 Continuous reactors, co-digestion mixtures; A), % Methane; B), Cumulative methane production. ....	220
Figure 9-6 Assessment of continuous reactors, mono-digestion of <i>L. digitata</i> R1 (LD <sub>100%</sub> ): Variations in CH <sub>4</sub> production, MY, BMP (mL CH <sub>4</sub> / gVS), and FOS: TAC ratio with increasing OLR (gVS.L <sup>-1</sup> .d <sup>-1</sup> ). Vertical dashed line indicates organic loading rate (OLR). ....	222
Figure 9-7 Assessment of continuous reactors, co-digestion of <i>L. digitata</i> R2 (LD <sub>90:10%</sub> ): Variations in CH <sub>4</sub> production, MY, BMP (mL CH <sub>4</sub> / gVS), and FOS: TAC ratio with increasing OLR (gVS.L <sup>-1</sup> .d <sup>-1</sup> ). Vertical dashed line indicates organic loading rate (OLR). ....	225
Figure 9-8 Assessment of continuous reactors, co-digestion of <i>L. digitata</i> R3 (LD <sub>75:25%</sub> ): Variations in CH <sub>4</sub> production, MY, BMP (mL CH <sub>4</sub> / gVS), and FOS: TAC ratio with increasing OLR (gVS.L <sup>-1</sup> .d <sup>-1</sup> ). Vertical dashed line indicates organic loading rate (OLR). ....	227
Figure 9-9 Assessment of continuous reactors, co-digestion of <i>L. digitata</i> R4 (LD <sub>50:50%</sub> ): Variations in CH <sub>4</sub> production, MY, BMP (mL CH <sub>4</sub> / gVS), and FOS: TAC ratio with increasing OLR (gVS.L <sup>-1</sup> .d <sup>-1</sup> ). Vertical dashed line indicates organic loading rate (OLR). ....	228
Figure 9-10 Continuous reactors, co-digestion mixtures (A), pH; (B), FOS: TAC ratio; (C), Total volatile fatty acid (tVFAs) .....	231
Figure 9-11 Continuous reactors, co-digestion mixtures; (A), Alkalinity; (B), Total ammonia nitrogen (TAN). ....	233
Figure 9-12 Continuous reactors, co-digestion mixtures; (A), Free ammonia nitrogen (FAN); (B), Chemical oxygen demand (COD) .....	234
Figure 9-13 Continuous reactors, co-digestion mixtures; (A), Total solid; (%TS) (B), Volatile solid (%VS). ....	235
Figure 9-14 Continuous reactors, co-digestion mixtures; Chloride concentration. ....	237
Figure 10-1 Cumulative biogas and methane yield for Batch test 1 and 2 .....	246
Figure 10-2 A), Daily volumetric methane production in continuous reactors (RTES 0 and RTES 1); B), Daily volumetric methane production in continuous reactors (RTES 0 and RTES 2).....	248
Figure 10-3 A), Daily volumetric methane production in continuous reactors (RTES 0 and RTES 3); B), Daily volumetric methane production in continuous reactors (RTES 0 and RTES 4).....	249
Figure 10-4 A), Cumulative methane production; and B), % Methane content in continuous reactors (RTES 0 – 4). ....	250

Figure 10-5 % Hydrogen sulphide production in continuous reactors (RTES 0 – 4).....	251
Figure 10-6 A), Volatile fatty acids profile; and B), FOS: TAC ratio in continuous reactors RTES 0 - 4.....	255
Figure 10-7 A), pH, and B), Alkalinity profile in continuous reactors RTES 0 - 4. ....	256
Figure 10-8 A), TKN; and B), TAN concentration profile in continuous reactors RTES 0 - 4. ....	260
Figure 10-9 Soluble COD concentration profile in continuous reactors RTES 0 - 4. ....	261
Figure 10-10 Assessment of continuous reactors, reactor 1 and reactor 2 (TES-4) mix: Variations in CH <sub>4</sub> production, MY, BMP (mL CH <sub>4</sub> / gVS), and FOS: TAC ratio with increasing OLR (gVS.L <sup>-1</sup> .d <sup>-1</sup> ). Vertical dashed line indicates organic loading rate (OLR).....	262
Figure 10-11 A), Volatile fatty acid; and B), pH concentration profile in continuous reactors R 1 and R 2 (TES 4 mix). ....	265
Figure 10-12 A), Alkalinity; and B), COD concentration profile in continuous reactors R 1 and R 2 (TES 4 mix). ....	266



# Chapter 1. Introduction

## 1.1 Background

Energy sources are divided into three categories: fossil fuels (coal, petroleum and natural gas), renewable and nuclear sources (Demirbaş, 2001), and classified into two groups renewable and non-renewable sources (Experts, 2017). Within the first half of the 20<sup>th</sup> century, petroleum became widely available and the dominant source of energy. However, petroleum is now considered a limited and non-renewable resource (Stevens and Verhé, 2004). It is striking to note that for every gallon of gasoline consumed by road vehicles, 100 tonnes of prehistoric organic material was needed for its formation, and because we, burn almost  $10^{11}$  kg of carbon every year to maintain our current lifestyle, this is equivalent to 400 years of plant primary production annually (Stevens and Verhé, 2004). Clearly, such resource utilization is unsustainable. As words of Holmes and Jones (2003), “we now find only one barrel of oil for every four consumed” and an estimated 45% of the identified oil reserves have already been used. This has caused atmospheric carbon dioxide (CO<sub>2</sub>) to rise by 20% since the nineties, with a further projected increase of 20% by 2035 compared to 2014 (BP Global, 2015).

The U.S. Energy Information Administration estimated in 2009 that 86% of the 483 quadrillion BTU (British thermal unit) energy consumed in the world was derived from fossil fuel and its derivatives (Wei *et al.*, 2013). Fossil fuels produce heat-trapping CO<sub>2</sub> gas (Cho, 2010), and CO<sub>2</sub> emissions from energy sources make around two-thirds of all global man-made greenhouse gases (GHGs) (BP Global, 2015). These increases in CO<sub>2</sub> emissions from fossil fuel combustion has contributed greatly to GHGs in the atmosphere, producing what is known as ‘*global warming*’, a term associated with the effects of heat on climate change. It is projected that oil demand will outstrip supply by the year 2050 (Holmes and Jones, 2003), and still remains the world’s major fuel, accounting for 32.9%, of global consumption. This is growing by 1.9 million barrels per day (b/d), or 1.9% which is nearly double the historical average of +1% (BP Global, 2016). Consequently, numerous reports highlight the urgent and compelling need to

reduce GHG emissions rather than take the “*business as usual*” approach (Williamson, 1992; Stern, 2006). In the early 1900s at the UN Conference on Environment and Development in Rio de Janeiro, over 150 countries signed a document on Climate Convention, which strongly encouraged developed nations to limit their CO<sub>2</sub> and other GHGs with the goal of returning either individually or collectively to 1990 emission levels by the year 2000 (Williamson, 1992). In 2015, the UN conference on climate change – COP21, set the warming limit to 2 °C above the threshold level in order to limit the worst impacts of climate change (BP Global, 2015; UN, 2016; Kinley, 2017).

The solution to these environmental problems is to develop a sustainable energy based economy on different fuels that are environmentally benign and economically acceptable, and not limited in supply (Gao and McKinley, 1994; Redwood *et al.*, 2009). The use of marine biological resources, particularly macroalgae (seaweed) for solar energy conversion has been proposed as having the potential for mitigating global warming (Ritschard, 1992), or CO<sub>2</sub> fixing capability (Shobana *et al.*, 2017). Interest in the use of macroalgae as a source of bioenergy first received a major boost by the construction of marine farms for the cultivation of the giant kelp *Macrocystis* under the US Ocean Food and Energy farm project (Hughes *et al.*, 2012). As far back as 1974 the marine biomass program initiated and jointly sponsored by the America Gas Association (AGA) and US Energy Research and Development Administration (ERDA) spent nearly 20 million US dollars over a 10 year period to actualize the concept of growing macroalgae in open ocean farms for conversion by anaerobic digestion into methane and other by-products as such as feed supplements, fertilizers and chemicals (Ritschard, 1992).

It has been long recognised that both methane and hydrogen gas are suitable as alternative renewable energy substitutes for fossil fuels (Liu *et al.*, 2006). The world is continually confronted with evidence that fossil fuels are finite and an unsustainable resource due to continuous depletion (Demirbas, 2010), a constraint that results in volatility, geopolitical instability and uncertainty in global markets (Hinks *et al.*, 2013), environmental pollution of soil, water and air (Vergara-Fernández *et al.*, 2008), accumulation of greenhouse gasses and

threats posed by global climate change (Demirbas, 2010; Hinks *et al.*, 2013). These are pointers to an imminent near energy crisis which have resulted in increased interest and investment in applying and developing new technologies for the utilization of renewable biomass sources and their conversion to clean energy (Chynoweth *et al.*, 2001; Hinks *et al.*, 2013). Singh *et al.* (2011b), stated that of the various feedstocks which have been evaluated, macroalgae have the greatest potential for sustainable production and through anaerobic digestion (AD) can be converted to useful fuels such as methane and hydrogen (Vergara-Fernández *et al.*, 2008; Park *et al.*, 2009).

Biofuels from algae are known as third-generation biofuels (Allen *et al.*, 2013a), to differentiate them from the first and second generation which are produced from terrestrial biomass, which has negative implications for land-use and food production (Jung *et al.*, 2011). Macroalgae or microalgae are photosynthetic organisms that grow in aquatic environments (Demirbas, 2010), and their biomass can be degraded biologically (Park *et al.*, 2009). Whereas Microalgae, which are unicellular, have been the focus of intensive research in relation to their conversion to bioethanol (John *et al.*, 2011a), biodiesel (Chisti, 2007; Hughes *et al.*, 2012), methane gas (Ras *et al.*, 2011) and hydrogen gas (Melis and Happe, 2001). However, seaweed (marine macroalgae) has received relatively little attention as a prospective feedstock (Hinks *et al.*, 2013), consequently, their utilization globally is low (Vergara-Fernández *et al.*, 2008; Park *et al.*, 2009). Chen and Oswald (1998), considered algal biomass as a solar energy trap and referred to it as energy crops. This characteristic was also expressed by Demirbas (2010); who stated that photosynthetic aquatic organisms could convert water, sunlight and carbon-dioxide efficiently into algal biomass.

Many researchers have highlighted the inherent benefits seaweed has as a feedstock, these include avoidance of land mass utilisation for cultivation (Hansson, 1983; Park *et al.*, 2009), reducing competition with conventional agricultural resources (Schwede *et al.*, 2011), the possibility of large-scale mariculture (Titlyanov and Titlyanova, 2010), as commodity food and feeds (Buschmann *et al.*, 2017). Additionally, they also contain sulphated fucans and proteins (Kloareg *et al.*, 1986) and high carbohydrate content (the

polysaccharides of alginate, laminarin, and mannitol), with zero lignin and low cellulose content making them biodegradable to biofuels through anaerobic processes (Hansson, 1983; Vergara-Fernández *et al.*, 2008; Hinks *et al.*, 2013). For brown algae, alginates form the dominant cell wall/intercellular structural matrix making them a potential source of methane and hydrogen production as a result of the high easily fermentable carbohydrate content (Park *et al.*, 2009).

The process and application of anaerobic digestion is a simple and robust process that is well understood in relation to generating bioenergy as biogas (Hinks *et al.*, 2013). It has been identified as a viable means of producing carbon-neutral energy (Batstone *et al.*, 2002), while also reducing uncontrolled greenhouse emissions (Møller *et al.*, 2004). Other advantages are energy recovery, pollution control (Chen *et al.*, 2008), destruction of pathogens (Lo *et al.*, 1985), and the production of nutrient-rich sludge that can be used as a supplement for agricultural purposes. The acidogenic phase of an AD, using dark fermentation can be used to produce hydrogen from various biomass substrates with the effluent containing mainly volatile fatty acids VFAs which are then used in the methanogenic phase to produce methane gas (Guwy *et al.*, 2011). Recently, attention has shifted to hydrogen (H<sub>2</sub>) as the most promising transport fuel, and the production of bio-hydrogen is gaining an advantage over conventional methods because of its sustainable nature (Das and Veziroglu, 2008). Hydrogen is the only carbon-free fuel which upon combustion produces water alone (Das and Veziroglu, 2008) contributing to reduce greenhouse gas emission (Florin and Harris, 2007). Its energy density (142 kJ /g or 61000 Btu /lb) is the highest of any known fuel (Das and Veziroglu, 2008; Guwy *et al.*, 2011). Apart from the many highlighted advantages of using macroalgae feedstocks in combination with AD processes, there are some inherent drawbacks that have restricted their widespread application and limited scaling up to profitability/net energy gains.

## 1.2 The aim of the thesis

This research investigates some of the limitations in the use of macroalgae as a feedstock for AD, and its conversion to methane using approaches as co-

digestion, effect of temperature and optimisation process. Also explored were the thermal and biomaterial properties of the macroalgae using pyrolysis (Py-GC-MS), TGA and <sup>1</sup>H NMR.

Some of the themes to which this aim is targeted at includes;

- Can marine macro-algae be a viable feedstock in AD.?

Hierholtzer and Akunna (2012), stated that for AD systems to be economically and realistically viable, they must be able to produce sufficient biogas to maintain the reactor operating temperature and generate net energy output. This will require available and secure feedstocks (macroalgae) for an effective and sustained operation of the energy conversion systems. In most coastal regions there is a natural seasonal abundance of marine macrophytes, their production as a viable feedstock has generated interest in their biomass been used as a sole and co-substrate in AD systems (Hierholtzer and Akunna, 2012). An initial full life-cycle assessment of bio-methane production from offshore cultivated marine algae indicated 69% reduction in fossil fuels use compared to natural gas, and a 54% reduction in greenhouse gas emissions with an overall improvement in the marine eutrophication index (Hughes *et al.*, 2012).

- **Biodegradability of the Seaweed biomass (Cell disruption techniques).**

The mechanical resistance of the algae cell wall to disruption is generally a limiting factor in cell digestibility (Schwede *et al.*, 2011). Pre-treatment using cell-disruption techniques aids in the breakdown of tough algal cells (Bleakley and Hayes, 2017). It has been reported that the approximate quantity of energy in algae is about 6 calorie /g, of which only about 40% is actually released during mesophilic methane fermentation, the remaining 60% of the algal biomass being resistant to release through decomposition and unavailable for methane generation partly because many cells and cell walls remain intact throughout the fermentation process (Chen and Oswald, 1998). Evidently, higher methane yields could be achieved if the cells and cells walls could be rendered decomposable (Eisenberg DM *et al.*, 1981). Algae biomass are said to be resistant to degradation under anaerobic conditions due to cell walls which contains cellulose

and hemicellulose compounds (Dębowski *et al.*, 2013), some strains produce substances toxic to microorganism (Wu *et al.*, 2010), while some species are completely unsuitable for anaerobic digestion (McKennedy and Sherlock, 2015). For macroalgae, the lignin levels are low, making it suitable for AD (Ghadiryfar *et al.*, 2016), but they have tough and protective cell wall which makes them highly resistant to bacterial attack (Memere *et al.*, 2015). While, for instance, Derenne *et al.* (1992), reported that most green microalgae possess a thin trilaminar outer wall (TLS) that is highly resistant to both chemical and enzymatic degradation because it incorporates insoluble, non-hydrolysable aliphatic biomacromolecules called algeanans. Scott *et al.* (2010) stated that algal biomass is anticipated to comprise of about  $\geq 50\%$  lipid content by dry weight, leaving the remaining 50% as cultivated solid residues. These residues can be viewed as potential feedstock for energy recovery, and the associated nutrients, consisting of largely phosphorus and nitrogen are of potential benefit to agricultural production (Miao *et al.*, 2012).

- **Thermochemical conversion**

Understanding the chemical composition of macroalgae feedstock is essential for developing various biofuel processes and yield (Song *et al.*, 2015). Due to the low lipid content in macroalgae, production of oil based products as biodiesel or hydrocarbons are currently restricted, as biofuel and bioenergy from macroalgae is through conversion of their carbohydrates (Ghadiryfar *et al.*, 2016). Compared to terrestrial biomass, macroalgae has low heating value, high minerals and ash content hence conversion technologies tolerant to these like pyrolysis and anaerobic digestion have been investigated (Ghadiryfar *et al.*, 2016). Pyrolysis is a thermochemical conversion method that decompose biomass into char, pyrolytic bio-oil and gaseous fraction with a high fuel-to-feed ratio of 95.5% (Hong *et al.*, 2017), and has been used to study macroalgae (Adams *et al.*, 2011a). Other thermochemical processes used for energy conversion and production of fuels and chemicals from macroalgae include gasification, liquefaction and direct combustion (Ross *et al.*, 2008; Demirbas, 2010).

- **Quantifying Inhibitory factors**

Antimicrobial compounds: polyphenols, inhibitory conditions (low C: N, high salinity) and inhibitory agents of physio-chemical nature (ammonia, pH, volatile fatty acids (VFAs), sulphide, light /heavy metals, organics). Macroalgae are classified based on their pigmentation into three broad categories; Brown (*Phaeophyceae*), Red (*Rhodophyceae*) and Green (*Chlorophyceae*). Of these, the brown seaweed contains greater concentrations of phlorotannins, a polymerized form of polyphenol derived from phloroglucinol (1,3,5 trihydroxybenzene) units (Eom *et al.*, 2012; Hierholtzer *et al.*, 2013), and accounts for about 20% of the seaweed dry weight (Amsler and Fairhead, 2006). Phlorotannins are antimicrobial compounds produced by certain seaweed (Daglia, 2012), that may inhibit the anaerobic digestion process (Hierholtzer *et al.*, 2013; Hinks *et al.*, 2013). Both the hydrolysis and acetogenesis phase of AD can be inhibited by polyphenols (McKennedy and Sherlock, 2015). These are present in high quantity in the peripheral layer of an algae (Moen *et al.*, 1997), and has shown to cause decrease in methane production for *Laminaria Hyperborea* (Hinks *et al.*, 2013). Higher level of polyphenols present in algae results to lower methane yield (McKennedy and Sherlock, 2015). The red and green algae lack phlorotannins (Stern *et al.*, 1996b).

Both inhibitory conditions and agents have received quite a number of reviews which are very well established (Chen *et al.*, 2008; Hierholtzer and Akunna, 2012).

- **Co-digestion of Macroalgae with Organic Fraction of Municipal Solid Waste (OFMSW)**

Co-digestion has been shown to improve biogas productivity (Mata-Alvarez *et al.*, 2000; Xie *et al.*, 2017b), it has the ability to solve the problem of low C: N ratio (Yen and Brune, 2007b), and can dilute toxic compounds making them less toxic (Sialve *et al.*, 2009a). The need to develop renewable energy has seen a recent increase in the amount of research on the use of waste material for anaerobic digestion technologies. Food waste, biodegradable municipal waste fractions, energy crops, and potentially seaweed (macroalgae), are used as feedstocks for these systems. Research into the potential of mixed co-digestion feedstocks is

important as it can overcome some of the limitations of using single feedstocks (e.g. generation of high concentrations of toxic products like hydrogen sulphide) and extends access to greater quantities of potential feedstock material.

- **Trace metal supplementation**

Trace elements are necessary nutrients that support cell growth of the AD microbiome, and methanogens exhibit special requirements for some trace elements (Zhang *et al.*, 2012b). It has been shown that trace metal supplementation of AD reactors allows stable operation even at higher organic loading rate (OLR), and an enhanced performance efficiency (Banks *et al.*, 2012). According to Choong *et al.* (2016) they must be adequate in order to support the metabolism of microorganisms for an effective digestion process. Understanding the trace element dynamics in working AD reactors and their influence on reactor performance during the use of macroalgae feedstock will give an insight into optimal minimal dosages of these metals that can ensure maximum substrate conversion rates and to prevent perturbations in reactor performance during full-scale applications.

- **Hydrogen Sulphide toxicity control**

In anaerobic digesters in the absence of oxygen, sulphate is reduced to sulphide by sulphate-reducing bacteria (SRB) (Hilton and Oleszkiewicz, 1988; Madden *et al.*, 2014). Marine algae usually contain sulphated polysaccharides as structural components. These are converted to hydrogen sulphide (Briand and Morand, 1997), attaining potentially toxic level for microorganisms (Chen *et al.*, 2008). Biogas from AD using macroalgal feedstock must be desulphurised (both H<sub>2</sub>S and organic sulphur) before use to avoid corrosion (pipeworks) and toxic effects (Gayh, 2012). At concentrations above 250 ppm, treatment is recommended before combustion. When combusted H<sub>2</sub>S emits sulphur dioxide (SO<sub>2</sub>) and sulphur trioxide (SO<sub>3</sub>) which are even more severe pollutants than H<sub>2</sub>S. The mechanism of sulphide toxicity is said to be through the unionized or undissociated form of H<sub>2</sub>S which permeate into the cell membrane (Tursman and Cork, 1988). Once inside the cytoplasm it denatures native proteins through the formation of disulphide cross-links form in polypeptide chains of enzymes interfering with the metabolism (Chen *et al.*, 2008). Observed inhibitory levels for



most groups of bacteria range from 100-800 mg L<sup>-1</sup> for ionised sulphide (pH above 7.2) and 400 - 500 mg L<sup>-1</sup> (pH 6.8 - 7.2) for unionised H<sub>2</sub>S (Chen *et al.*, 2008). Ironically sulphur is a vital nutrient required by methanogens (O'Flaherty *et al.*, 1999) with optimal levels reported to be between 1-25 mg S L<sup>-1</sup> (Scherer and Sahm, 1981a). Several processes are used for sulphide control; adaptation of methanogens to free H<sub>2</sub>S in fixed biomass reactors (Chen *et al.*, 2008), physicochemical techniques (stripping), chemical reactions (coagulation, oxidation, precipitation, dissociation) and biological conversion through partial oxidation to elemental sulphur (Oude Elferink *et al.*, 1994), chemical adsorption / absorption, using molecular sieves or activated carbon, separation by membranes and most recently bio-scrubbers using a humic substance (Gayh, 2012).

- **Role of Temperature**

Temperature influences the rate of bacterial action (Demirbas, 2009a), and is one of the most significant parameters influencing AD because it not only influences the activity of enzymes and co-enzymes but also influences the methane yield and digestate quality (Zhang *et al.*, 2014). Understanding the relationship between maximum biogas production rates under different temperature conditions is directly linked to operational cost in pilot scale processes.

- **Mathematical models**

Mathematical models are used to demonstrate the effects of changing certain design parameters (Horton and Hawkes, 1981). They help to describe the kinetic behaviour of biologically mediated digesters. Models can be a useful tool for the prediction of optimal performance, and for a better understanding of the process (Manjusha and Beevi, 2016). To effectively operate an efficient anaerobic system in order to predict how the system will respond to changes in feed and other operating conditions, appropriate models need to be developed (Lyberatos and Skiadas, 1999). Various models have been used to estimate; first order hydrolysis constant  $k$  (Angelidaki *et al.*, 2009), maximum specific growth rate  $\mu_{max}$ , lag time  $\lambda$ , methane production time and rate (Zwietering *et al.*, 1990).

Anaerobic digestion of macroalgae could be examined in various ways with respect to experimental digestion techniques or algal specie(s). This study a combination of these will be applied.

### 1.3 Specific Objectives

To understand the technical feasibility of using brown seaweed (marine macroalgae) as a viable feedstock for the continuous generation of bio-energy via anaerobic digestion process, the following objectives were identified:

#### **Phase 1:**

- To carry out biological methane potential (BMP) tests on macroalgal feedstocks using batch reaction studies to determine biogas production potential.
- To estimate the yield and rate of methane production from macroalgae.
- To identify the optimal macroalgal substrate concentration for optimum biogas yield.
- To characterize the thermo- and physiochemical properties of brown seaweed, *Laminaria digitata* harvested from UK shores and the influence of seasonal effects on these parameters.

#### **Phase 2: Continuous performance and optimisation**

- To understand the performance of biogas production rate and yield using a continuous stirred tank reactor (CSTR) fed with macroalgae.
- To understand the influence of pre-treatment conditions (pre-treated cell, polyphenol extracted residual) on macroalgae solubilisation/digestibility and efficiency of biogas production.
- To understand the effect of temperature on biogas production.
- To understand the performance of the reactors with co-digestion of macroalgae and food waste.
- To understand the performance of the reactors with supplementation of trace metals.
- To understand under predefined reactor condition, factors inhibiting anaerobic digestion of macroalgae.

- To determine conversion efficiencies of the seaweed under a range of operational loading conditions.

#### **Phase 1 and 2:**

Use of mathematical models to validate experimental results. To determine the decay constant  $k$  ( $d^{-1}$ ), lag phase  $\lambda$  (days), growth rate  $\mu_{max}$ , regression coefficient ( $R^2$ ).

### **1.4 The thesis outline**

*Chapter one* gives an overview of the need for renewable energy research particularly with respect to using biomass feedstock. The aims and objectives of this study are stated with the limitations in the use of brown seaweed for bioenergy production. *Chapter two* is an overview of anaerobic digestion process together with a literature review on macroalgae. In *Chapter three* materials and methods used is given while *Chapter four* is a detailed study on the BMP prospectus of using *L. digitata* for methane production. *Chapter 5* the thermochemical characterization of *Laminaria digitata* was undertaken and pyrolysis products identified. The kinetics effect of temperature on anaerobic digestion of *L digitata* was studied in *Chapter 6* and *Chapter 7* gives a detailed insight in long-term continuous processes using macroalgae under different temperature conditions. *Chapter 8* examined process optimization using simple modelling techniques from results of the continuous digestion studies in Chapter 7. *Chapter 9* examined the anaerobic fermentation of mono and co-digestion of *L digitata* with a stimulated food waste. *Chapter 10* examined the effect of trace elements supplementation on anaerobic digestion of macroalgae while in *Chapter 11* is a general conclusion on the outcome of the study is given.

## Chapter 2. Literature Review

### 2.1 Marine biomass, Macroalgae as feedstock for bio-refinery

The world's population is projected to reach 8.5 billion by 2030 (UN, 2017), which is an additional 1.4 billion people compared to 2012 levels (Jones and Mayfield, 2012). This alarming rate of growth coupled with urbanisation, high standards of living in most parts of the world has put enormous pressure on fossil fuel-based resources, raising concerns over global energy security and the negative environmental impacts of their use.

Fossil fuels as depleting resources are now regarded as unsustainable and environmentally unfriendly. Considerable problems associated with their use include, but are not limited to, oil spills, acid rain, air quality deterioration and global warming (Kim and Lee, 2014). They are the greatest contributors to the build-up of greenhouse gases (GHGs) in the environment, which has been reported to exceed a dangerously high threshold of 450 ppm CO<sub>2</sub>-e (i.e. e=equivalent contribution of all greenhouse gases). Kraan (2013) reported that the GHGs, were around 350-380 ppm in 2010, with a potential to increase to 450 ppm by 2020 if mitigation action is not taken. Alternative sources of energy which are renewable, efficient, sustainable and cost-effective with lower emissions (Singh *et al.*, 2010; Nigam and Singh, 2011), such as tidal, wind, solar and liquid biofuels as a replacement for fossil fuels, has been researched extensively (Scott *et al.*, 2010; Demirbas and Fatih Demirbas, 2011). Biofuels have gained attention as an attractive alternative because they can blend with current transportation fuel technologies with minimal change, contribute to reductions in GHGs emissions and have considerable potential for sustainability (Carere *et al.*, 2008). Ragauskas *et al.* (2006), stated that from research and development (R&D) on energy alternatives, biorefinery is regarded as a potential pathway to break free from the fossil-based economy. The global demand for biofuels has continued unabated (Kraan, 2013). Biofuels are renewable fuels from biological sources (Singh *et al.*, 2011b), known as biomass which is carbon neutral (Ulgiati, 2001). Biomass can be used to produce biochemicals, fuel, electricity and heat, in addition, it can sequester carbon (Adams *et al.*, 2011b;

Singh *et al.*, 2011b). Unlike fossil fuels, use of renewable resources represents a closed carbon cycle (Wilkie, 2005). There has been a considerable advancement in biofuels research and technologies leading to first and second generation biofuels attaining economic and commercial productions (Nigam and Singh, 2011; Singh *et al.*, 2011b). The shortcomings associated with these biofuels which are well documented (Adams *et al.*, 2011a; Singh *et al.*, 2011b; Ward *et al.*, 2014; Montingelli *et al.*, 2015) include mainly the competition between food and fuel for land utilization and the logistics of competitive supply of biomass feedstock coupled with their conversion efficiency to reduce costs (Sims *et al.*, 2010; Singh *et al.*, 2011b), making the debate of their sustainability controversial (Goh and Lee, 2010). These limitations have driven the use and cultivation of marine biomass; algae from seawater and other sources as a possible and viable solution for this energy problem (Singh *et al.*, 2011b). Adams *et al.* (2011a) stated that the marine environment contributes over 50% of the global biomass production.

Marine biomass comprises of both micro and macroalgae. While the former is used mostly as a potential source for bio-oils, the latter is used as a carbohydrate source for fermentation to biogas and thermochemical-based conversions to heat and fuel gases (Demirbas, 2009b; Adams *et al.*, 2011a). Algae are regarded as the only substitute, to current biofuels crops such as wheat, soybean, sugarcane, corn and maize etc., because arable land is not required for their production (Chisti, 2007; Singh *et al.*, 2011a). They are recognised, as having a great potential for viable production and conversion to fuels (Singh *et al.*, 2011b). Attention has recently been paid to seaweed as a valuable biomass due to its high carbon dioxide absorption rate compared to terrestrial plants (Miyashita *et al.*, 2013), and its ability to generate and store carbon resources (Sambusiti *et al.*, 2015). Seaweed (or algae) is now known as third generation biofuels (Jung *et al.*, 2013; Allen *et al.*, 2015; Montingelli *et al.*, 2015). Macroalgae grows rapidly, yielding more kg of dry biomass m<sup>-2</sup> year<sup>-1</sup> than most quick growing terrestrial crop such as sugarcane (Gao and McKinley, 1994), switchgrass (Chung *et al.*, 2011) with a proven production potential of 2-20 times that of conventional energy crops (Bruhn *et al.*, 2011a; Chung *et al.*, 2011). Furthermore, the energy

potential estimates of aquatic biomass are greater than 100 EJ per year which is more than 22 EJ for land-based biomass (Chynoweth *et al.*, 2001).

## 2.2 Biomass a renewable energy resource.

Biomass is the name given to all earth's living matter (Liew *et al.*, 2014), and a term used to describe all biologically mediated matter (Demirbaş, 2001). Biomass is derived from plants as a result of photosynthesis (Schuck, 2006; Champagne, 2008). It is a major source of carbon often regarded as “renewable carbon source” with the characteristics to replace fossil carbon resource (Klass, 1998). Biomass feedstock includes a broad range of materials from agricultural crops and residue, trees and forestry products, biosolids, sludge, human sewage, and municipal solid, animal and green waste to purpose-grown energy crops and marine vegetation (Schuck, 2006; Champagne, 2008; Sillanpää and Ncibi, 2017). These feedstocks are converted by biological, chemical, mechanical and thermal methods into liquid or gaseous fuels, heat and power and other bioproducts (Champagne, 2008).

The energy and energy-related products recovered or derived from biomass through various processes are described by the term “*Bioenergy*” (Schuck, 2006), while the sustainable processing of the biomass into a range of different products and energy is called “*Biorefinery*”, Figure 2-1 (Pandey *et al.*, 2015).

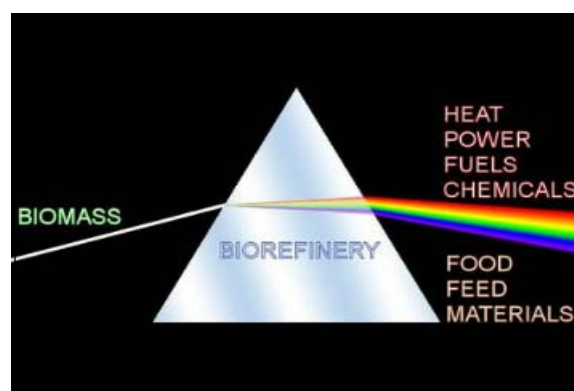
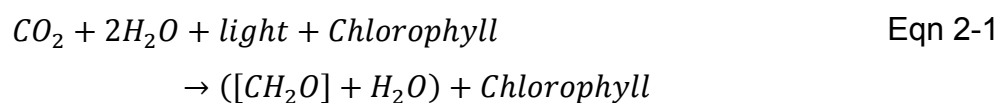


Figure 2-1: Biorefinery and its role in the transformation of biomass

(Pandey *et al.*, 2015)

The initial key step in the growth and formation of virgin biomass is depicted in Eqn 2-1;



In the presence of water, light and chlorophyll via photosynthesis, solar energy is captured within the fixed carbon of biomass when atmospheric carbon dioxide (CO<sub>2</sub>) is converted to organic compounds, producing oxygen (O<sub>2</sub>) in the process (Klass, 1998; Schuck, 2006). The building block (CH<sub>2</sub>O) represent the biomass as carbohydrates, the primary organic product (Klass, 1998). Photosynthesis as a carbon fixation process by CO<sub>2</sub> reduction is interconnected in a series oxidation-reduction reactions, where firstly oxygen is evolved from water followed by the transfer of hydrogen atoms to a primary hydrogen acceptor. The hydrogen acceptor then reduces CO<sub>2</sub> to carbohydrates using light energy to drive the flow of H atoms against the chemical energy gradient (Demirbas, 2009a).

Klass (1998), stated that the notion of biomass as a renewable energy source comprises the above process (Eqn 2-1), including transforming the derived biomass into various forms of fuels or using them as a source of thermal energy or hydrogen, and ultimately completing a cycle when the biomass or derived fuel is combusted (Kingsbury, 1984). The combustion process is akin to liberating the solar energy captured, and remitting the fixed carbon as CO<sub>2</sub> back to the atmosphere, making it essentially the reversal of photosynthesis (Demirbaş, 2001). When biomass is combusted the net energy available ranges from 8 MJ·kg<sup>-1</sup> for green wood, to 20 MJ·kg<sup>-1</sup> for a dry plant, to 55 MJ·kg<sup>-1</sup> for methane compared to 27 MJ·kg<sup>-1</sup> for coal (Demirbaş, 2001). Twidell and Weir (2015) stated that “*renewable energy*” is energy obtained from the local environment in naturally repetitive and persistent energy flows sources.

Globally, approximately 224 × 10<sup>9</sup> metric tonnes of dry biomass per annum is produced through photosynthesis (Champagne, 2008). This energy source is equivalent to almost 10 times the world’s primary energy usage (Schuck, 2006). Assuming, the average daily solar radiation hitting the earth’s surface is about 220 W/m<sup>2</sup> (1676 Btu/ft<sup>2</sup>), then about 0.01% of the annual earth’s insolation will

give approximately all the primary energy consumption required by human (Klass, 1998). Records from the United Nations shows in 1990, global biomass energy consumption was about 6.7% of the total consumed, and by 2000, the International Energy Agency (IEA) data showed renewable energy consumption has had increased to 13.8%, with 79.8% of it being biomass from waste or crop biomass (Klass, 1998). Currently, the dominant global energy supplies are fossil fuels ( $388 \text{ EJ}\cdot\text{a}^{-1}$ ), nuclear power ( $26 \text{ EJ}\cdot\text{a}^{-1}$ ), and hydropower ( $28 \text{ EJ}\cdot\text{a}^{-1}$ ), in comparison with biomass (approximate value of  $45 \pm 10 \text{ EJ}\cdot\text{a}^{-1}$ ) which contributes a significant renewable energy source (Champagne, 2008).

### *2.2.1 Classification of biomass feedstocks*

The use of renewable resources is becoming increasingly important in today's society. There are evidently significant environmental advantages for increased use and application of carbon-neutral and renewable bioresources (Stevens and Verhé, 2004). Research and development (R&D) on biofuels production from renewable biomass has been driven by favorable legislation and taxation (carbon taxes) and also societal appreciation of the gains made in GHG reduction and the production of sustainable biodegradable products (Stevens and Verhé, 2004). Biofuels come in various forms from biodiesel, bioethanol, biocrude, synthetic oil biochar, bio-hydrogen and biogas (Liew *et al.*, 2014). A great advantage that biorenewable feedstocks have over petroleum is oxygen content, ranging from 10 - 44% while petroleum has none (Demirbas, 2009a). This makes the chemical properties of biorenewable biomass quite dissimilar from petroleum, hence their products are more polar, some easily entrain water and are acidic (Demirbas, 2009a). Table 2-1, shows some major categorization of bioresources feedstocks.



Table 2-1: Categorization of biomass feedstock adapted from (Demirbas, 2009a)

Categorization of biomass feedstock			
1. Aquatic plants	2. Energy crops	3. Forest products	4. Food crops
Algae, kelps, lichens and mosses.	Short rotation woody crops	Wood Logging residues	Grains
Waterweed	Herbaceous woody crops	Trees	Oil Crops
Water hyacinth	Grasses	shrubs and wood residues	
Reed and rushes	Starch crops	Sawdust, bark, etc.	
5. Sugar crops	Sugar crops	7. Biorenewable wastes	
Sugarcane	Forage crops	Agricultural Wastes	
Sugar beets	Oilseed crops	Crop residues	
Molasses	6. Household and Industrial Waste	Mill wood wastes	
Sorghum	Landfill	Urban wood wastes	
	Industrial organic wastes	Urban organic wastes	

### 2.2.2 Biofuels

Biofuels are expected to contribute 6% of total fuels used by 2030 according to the International Energy Agency (Ayala-Parra *et al.*, 2017). Biofuels are in form of solid, liquid or gaseous fuels produced mainly from biomass feedstocks (Wei *et al.*, 2013), with the liquid biofuels playing an important role as future transport fuels by replacing petroleum (Demirbas, 2007). Biofuels are classified into 1<sup>st</sup> generation (conventional) and 2<sup>nd</sup>, 3<sup>rd</sup>, more recently 4<sup>th</sup> generation (advanced) biofuels (Janda *et al.*, 2012), based on their production technologies (Demirbas, 2009a). Figure 2-2 shows major potential pathways from marine algae to biofuels.

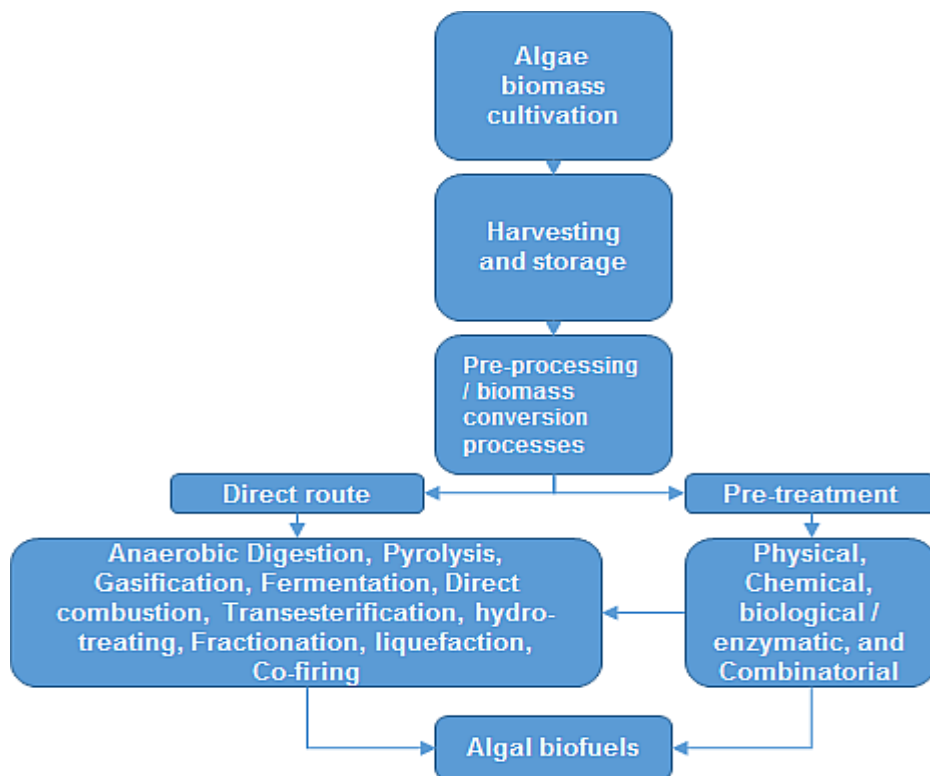


Figure 2-2: Potential pathways from marine algae to biofuels.

The first generation biofuels are fuels made from conventional technologies using food crops which are basic feedstocks usually seeds or grains converted to sugars, starch, vegetable oil and animal fats to produce the biofuels, for example wheat yields starch which can be converted into bioethanol while sunflower seeds are processed to produce vegetable oil which is used in biodiesel production (Demirbas 2009). Second generation biofuels are produced from non-food crops, mainly residuals from food crops, when the food has been extracted (Demirbas, 2009a; Liew *et al.*, 2014). The term ‘plant biomass’ refers to lignocellulose materials which makes up the majority of second generation feedstock, and as they are cheap and abundant (Naik *et al.*, 2010), for example wood, energy crops and corn whereas third generation biofuels, also known as “*oilgae*” are produced from marine based algae (Demirbas, 2009a). Emerging in recent years are the fourth generation biofuels based on the conversion of vegetable oil and biodiesel into “*biogasoline*” using more advanced technology (Demirbas and Demirbas, 2010). The 4<sup>th</sup> generation fuels are mostly in trial test phase, and not clearly defined. Some technologies in their production include genetic modification of organisms to secrete hydrocarbons, high-temperature

decomposition of biofuels and artificial photosynthesis reactions (Janda *et al.*, 2012) and petroleum-based processing (Liew *et al.*, 2014). Recently, 4<sup>th</sup> generation biofuels are produced from algae using metabolic engineering (Lü *et al.*, 2011; Daroch *et al.*, 2013). The benefits and shortcomings of the various classes have been highlighted in Table 2-2.

Table 2-2: Advantages and disadvantages of different generations of biofuels. (Liew *et al.*, 2014).

Fuel	Advantages	Disadvantages
Petroleum fuel	<ul style="list-style-type: none"> <li>• High availability.</li> <li>• Established technologies.</li> </ul>	<ul style="list-style-type: none"> <li>• Depletion of fossil fuel.</li> <li>• Causing climate change.</li> <li>• Fluctuation of fossil fuel price.</li> <li>• Higher carbon footprint than biofuel.</li> </ul>
First generation biofuel	<ul style="list-style-type: none"> <li>• Biodegradable.</li> <li>• Energy security.</li> </ul>	<ul style="list-style-type: none"> <li>• Competition of land use.</li> <li>• Blending with conventional fuel.</li> <li>• Highest carbon footprint compared with other generations of biofuel.</li> </ul>
Second generation biofuel	<ul style="list-style-type: none"> <li>• No food competition.</li> <li>• Production of high-value added products.</li> <li>• Energy security.</li> </ul>	<ul style="list-style-type: none"> <li>• Complex processes are required.</li> <li>• Conversion technologies are under development.</li> <li>• Low conversion as compared with petroleum fuel.</li> </ul>
Third generation biofuel	<ul style="list-style-type: none"> <li>• High oil yield.</li> <li>• No food and land competition.</li> <li>• No toxic content.</li> <li>• Energy security.</li> </ul>	<ul style="list-style-type: none"> <li>• High processing cost.</li> <li>• Production technology is under development.</li> <li>• Difficult to harvest and process</li> </ul>
Fourth generation biofuel	<ul style="list-style-type: none"> <li>• Carbon negative biofuel.</li> <li>• Energy security.</li> </ul>	<ul style="list-style-type: none"> <li>• Lack of study on its practical performance in terms of technical and economic aspects.</li> <li>• Still in research and development stage</li> </ul>

## 2.3 Overview of biofuels policy framework.

Policy plays an influential role in the commercialization and widespread acceptance of biofuels, and governments, industries, other relevant stakeholders have long been promoting use of renewable energies as a means to reduce CO<sub>2</sub> emission, our dependency on fossil fuels, energy security and economic sustainability (Schillo *et al.*, 2017). Renewable energies are the fastest growing energy source, are an important player in attaining lower-carbon economy and account for around 3% of global energy today, excluding large-scale hydroelectricity (BP Global, 2015). Their increasing competitive price sets them as an alternative substitute to replace fossil fuels (Liew *et al.*, 2014; Schillo *et al.*, 2017). The earth receives about 101,000 terawatts of sunlight power (Cho, 2010), which far exceed the 15 terawatts of energy utilized in the world, of which 7.8% is

derived from renewable energies sources (Jones and Mayfield, 2012).

Photosynthetic organisms like algae produce a range of organic molecules like carbohydrate, lipids and proteins (Naik *et al.*, 2010), and these '*biomolecules*' could, in turn, be used after modification to allow the ion, and extract biofuels (Jones and Mayfield, 2012).

In the US, the value of these biofuels, as a transportation fuel of the future was central in the formation of the policy on Renewable Fuels Standard in 2009 within the purview of the Federal Energy Policy Act of 2005. This mandated the production of 36 billion gallons of biofuels by 2022 to displace petroleum in fuel mix (Blanco and Isenhouer, 2010; Somma *et al.*, 2010). The US biofuels policies were originally initiated in the seventies, motivated by the need to reduce over-reliance on imported fossil fuels and to lower GHGs but to increase home-grown farm products serving as raw materials for biofuels (Janda *et al.*, 2012). The Energy Tax Act 1978 was introduced giving tax exemptions and subsidies for blending ethanol with gasoline while The Conservation Reauthorization Act 1998 gives subsidies for biodiesel (Janda *et al.*, 2012). Currently, the US biofuels policies are predicated on three instruments; Output-connected measures, support for input factors and consumption subsidies (Janda *et al.*, 2012). In the application of these instruments, producers of biofuels benefit through direct and indirect price support using tariffs (tax credit) as direct subsidies, while mandates are indirect subsidies (Janda *et al.*, 2012).

Within the European Union (EU), biofuels policy implemented under the EU Energy Directorate is based on obligations to Kyoto targets on GHG emissions and societal pressure to address environmental issues (Janda *et al.*, 2012). The policy is not captured in a single document but within various policy documents on biofuels within the EU governance structure (Janda *et al.*, 2012). For instance, The EU Biofuels Directive 2003/30 was introduced in 2003, setting a target of 2% biofuels in transport fuels by 2005, and 5.75% by 2010, while the EU Renewable Energy Directive 2009/29 established in 2009, formulated the "20-20-20" policy which set the total EU renewable energy consumption at 20% by 2020 and reduction of GHG emissions by 20% (Janda *et al.*, 2012).

Within South America, Brazil's renewable energy policies are mostly based on ethanol production as a government response to shortage in petroleum supply following the 1973 oil crisis (Goldemberg, 2006). The government framework was run on the proalcohol program started in 1975 for an increase of domestically produced ethanol-blended fuel but terminated in the 1990s with a transition to full liberalization in 2000 with no direct government control over ethanol production. The current blending ratio of ethanol is 18-25% for gasoline and 2% biodiesel in 2008 and increased to 5% in 2013 (Janda *et al.*, 2012).

## 2.4 Macroalgae biomass as third generation biofuels.

### 2.4.1 *Algae*

Algae has been described as a 'term' with no formal taxonomical standing but used routinely to describe polyphyletic organisms which do not share a common origin, they have evolved independently from multiple lines, are non-cohesive and an array of O<sub>2</sub> evolving, photosynthetic organisms with the exception of colourless members without pigmentation (Barsanti, 2006; Barsanti and Gualtieri, 2014). Algae are simple chlorophyll-containing organisms (Bold and Wynne, 1985), regarded as photoautotrophs which use sunlight as a source of energy and CO<sub>2</sub> as a carbon source to produce carbohydrates and adenosine triphosphate (ATP) (Barsanti and Gualtieri, 2014). They are composed of microscopic single cell, macroscopic multicellular loose or filmy groups, branched or matted colonies and complex blade or leafy forms (Barsanti and Gualtieri, 2014). Algae have a great diversity in size ranging from 0.2-2.0 µm for picoplankton to 2-8 µm for some species as *Chlorella* in range of bacterial size to kelps, which are considered the largest attaining lengths up to 60 or 70m (Bold and Wynne, 1985; Barsanti and Gualtieri, 2014), and growing up to 50 cm per day (Price, 1979). Algae are ubiquitous and can be aquatic or subaerial (Bold and Wynne, 1985; Kim, 2011; Barsanti and Gualtieri, 2014).

The term *algae* are used to classify and describe both *macroalgae* and *microalgae* (Wei *et al.*, 2013; Barsanti and Gualtieri, 2014). There are an estimated 32,260 identified species of algae as given in Algae Base with about 28,500 waiting to be identified.

## 2.4.2 Macroalgae

Macroalgae are a group of diverse eukaryotic, non-flowering, photosynthetic plant-like marine organisms (Roesijadi *et al.*, 2010; West *et al.*, 2016) which are biomass referred to as *Seaweed* (Chan *et al.*, 2006; Roesijadi *et al.*, 2010; Rocca *et al.*, 2015), and can be biologically degraded (Park *et al.*, 2009). Typically, they are comprised of a lamina (or blade), a stipe (or stem), and a holdfast for adhering to hard substrates in their environment and similar to land plants but contains a leaf-like thallus instead of roots, stems and leaves (Pandey *et al.*, 2015). In the open ocean, they occur in floating forms and are a constituent part of natural materials on the sea surface (Roesijadi *et al.*, 2010).

Seaweeds have complex methods of reproduction, forming different spores as well as asexual regeneration from fragments of the parent plant (Bunker, 2012). Collado-Vides (2001) pointed out that their life cycle is not consistent and complex having both sexual and asexual reproduction. Sexual reproduction uses either one multicellular phase or an alternation between haploid, a single set chromosome, and diploid phase with extensive multicellular interaction as shown in Figure 2-3. Asexual reproduction occurs possibly by parthenogenesis (haploid phase) or by spores production in the diploid phase.

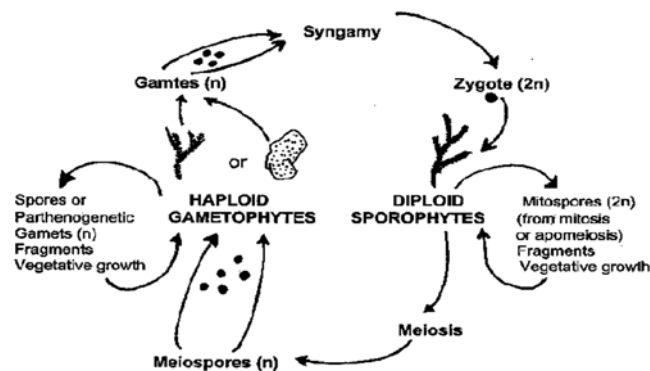


Figure 2-3 Generic representation of alternating life cycle of seaweeds

(Collado-Vides, 2001).

Currently, major products produced from macroalgae are popular food ingredients in the Asian countries of Japan, Korea and China (Kim and Chojnacka, 2015). In this sense Kim (2011) referred to them as “sea-vegetable”,

highlighting their importance to humans. They are also used in the food industries as fertilizers, thickeners, gelling agents and as ingredients in nutraceuticals and cosmetics (Kim, 2015). Marine algae are known to have various health benefits because of bioactive components in them and are rich in nutritional valuable components such as polysaccharides, minerals, vitamins (A, B, C, E), amino acids, lipids, proteins, dietary fibers, and polyphenols (Kim and Chojnacka, 2015).

Algae are regarded as a useful underestimated resources for biobased economy because their cells contain a range of beneficial compounds with high biological activity (Kim and Chojnacka, 2015), and macroalgae, in particular, have the potential of becoming viable aquatic energy crop (Chynoweth *et al.*, 2001; Bruhn *et al.*, 2011b; Costa *et al.*, 2012), but energy production from macroalgae is still limited due to economic viability (Jones and Mayfield, 2012).

Figure 2-4: illustrates current biofuels from algae.

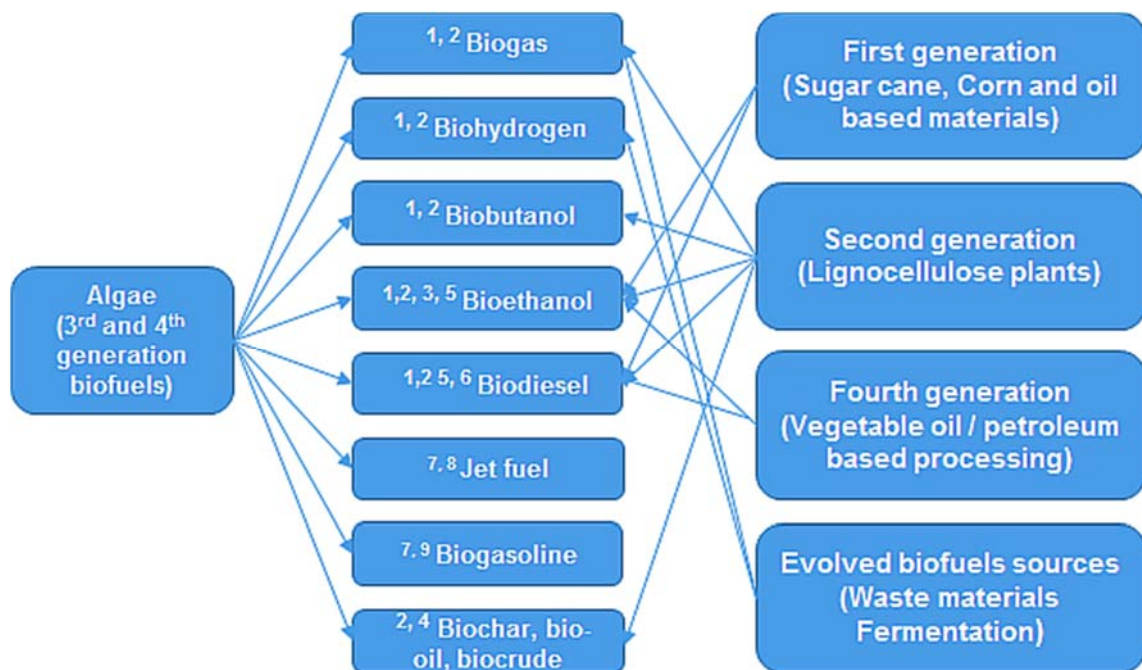


Figure 2-4: Renewable fuel sources and bioproducts from algae

(Takagi *et al.*, 1977; Demirbas, 2009a; Zhang *et al.*, 2010a; Lü *et al.*, 2011; Jones and Mayfield, 2012; Daroch *et al.*, 2013; Liew *et al.*, 2014; oilgae, 2014; Ullah *et al.*, 2014) <sup>3, 4, 5, 1, 6, 2, 7, 8, 9.</sup>

## 2.5 Macroalgae taxonomical and biochemical compositions

There are approximately 20,000 known seaweed species (Chung *et al.*, 2011) which are broadly classified into three main groups based on their thallus colour derived from natural pigment and chlorophylls into green (*Chlorophyceae*), red (*Rhodophyceae*) and brown (*Phaeophyceae*) algae (Sze, 1998; Chan *et al.*, 2006; Demirbas, 2010).

Within the chloroplasts of seaweed, storage carbohydrates are formed (Wiencke and Bischof, 2012) and Table 2-3, shows the major structural polysaccharides of macroalgae that can be used as substrate for liquid biofuels production. Some of these compounds are peculiar to a particular group, and their distribution differs across the major macroalgae taxonomic groups of brown, green, and red seaweeds (Roesijadi *et al.*, 2010; Wei *et al.*, 2013).

**Red algae** phylogenesis shows they can be regarded as the oldest division of marine macrophytes (Usov, 1998), and are suggested as the first eukaryotic organisms on earth (Stiller and Hall, 1997; Bojko *et al.*, 2002). They are the most diverse group with nearly all being marine with few in freshwater streams or in extreme environments as the edges of geothermal springs (Bunker, 2012). There are between 4000 - 7000 species in over 600 genera of the red algae which consist of two subclasses; *Bangiophycidae* and *Florideophycidae* (Bunker, 2012; Jung *et al.*, 2013). Their chemical composition is given in Table 2-3. The red seaweed has a unique cell wall composition made up of agar and carrageenans (Bunker, 2012).



Table 2-3: Approximate chemical composition of seaweeds  
 Readapted from (Jensen, 1993; Roesijadi *et al.*, 2010; Alves *et al.*, 2013; Wei *et al.*, 2013)

Component	Red	Green	Brown
Water	70-80%	70-80%	70-90%
Minerals	25-35%	10-25%	30-50%
Protein	7-15%	10-15%	7-15%
Lipids	1-5%	1-5%	2-5%
Cellulose	2-10%	20-40%	2-10%
Ash		50 - 53% (Ca,Cl,Fe,P)	
Carbohydrates	30-60%	25-50%	30-50%
	Carrageenan Agar Cellulose Lignin	Starch Cellulose	Laminarin Mannitol Alginate Fucoidin Cellulose

**Green algae** are often classified as plants primarily occurring in freshwater with a small proportion of the species found in marine and brackish environment (Bunker, 2012). Their similarities to plants are due to their colour having the same chlorophyll a and b pigments found in plants (Lobban and Wynne, 1981; Bunker, 2012). Although they are of the class of *Chlorophyceae*, due to their diversity, they are now divided into two phyla *Chlorophyta* and *Charophyta* and up to 17 classes (Guiry, 2017). The *Chlorophyta* are made up of about 4500 species with 3050 species of the class *Trebouxiophyceae* and *Chlorophyceae* as freshwater algae while the remaining 1500 species are seawater algae while the *Charophyta* have about 3500 species entirely as freshwater (Guiry, 2017). Green algae are entirely composed of 10% protein, 35% carbohydrate, and 50% ash (Ca, Cl, Fe, P) (Alves *et al.*, 2013).

**Brown algae** are physical the largest of all seaweed, found in shores and shallow seas in temperate regions all around the world, having their brown or olive- green colour due to pigments of chlorophyll 'a' and 'c',  $\beta$ -carotene and xanthophyll, fucoxanthin (Sze, 1998; Bunker, 2012; Guiry, 2017). Brown seaweed is used as food, and serve to provide a habitat for other organisms in the marine environment. There about 1500 - 2000 known species (Hoek *et al.*, 1995; Guiry, 2017). Typical they contain 30 - 50% carbohydrate and 70-90% water, Table 2-3.

## 2.6 Advantages of macroalgae as biomass feedstock

The life cycle assessment of terrestrial based biomass final products shows that it exacerbates climate change (Jung *et al.*, 2013), with direct and indirect land use for energy crop cultivation inducing both high carbon debt and water consumption significantly (Fargione *et al.*, 2008; Dominguez-Faus *et al.*, 2009). Although, currently food crops such as corn and sugarcane (ethanol), oil and soybeans (biodiesel) are widely used for large-scale biofuels production due to firmly established farming practices which are simple and cheap for starches, oil and sugar release (Wei *et al.*, 2013), there are concerns with respect to food scarcity, high prices for food commodities and land pollution (John *et al.*, 2011b). These concerns have led to research and use of non-food terrestrial lignocellulose biomass such as energy grasses, agricultural residues and wood waste to avoid undesirable competition between food and fuel (Wei *et al.*, 2013). But the drawback in their use is the lack of efficient chemical and biochemical processes for the release of fermentable sugars for large commercial scale production (Jones and Mayfield, 2012), due to technical, economic and commercial bottlenecks (Huang *et al.*, 2009). As a result, terrestrial based biomass for a biorefinery is not environmentally friendly, has economic impacts and hence is unsustainable (Jung *et al.*, 2013).

Macroalgae based biomass from marine resources has the potential to partially and fully displace this terrestrial based biomass for a sustainable biorefinery via bioenergy and biomaterials production (Jung *et al.*, 2013). Macroalgae mainly do not need land or freshwater for cultivation (Lobban *et al.*, 1985). They are characterized as having no lignin, low cellulose and lipid content (Jung *et al.*, 2013), although, recently the presence of secondary walls and lignin within the cells of red algae have been reported (Martone *et al.*, 2009). Seaweed can convert solar energy into chemical energy with photosynthetic efficiency up to 6 - 8% higher than terrestrial biomass 1.8 – 2.2% (FAO, 1997). As photoautotrophic plants, they produce and store organic carbon as resources needed for biorefinery (Gao and McKinley, 1994). Because seaweeds lack many of the distinct organs found in terrestrial plants, whole parts are available as a biomass source (Miyashita *et al.*, 2013). They have lower risk for competition for food and

energy than other land-based crops (McHugh *et al.*, 2003; Bixler and Porse, 2011). Growing and harvesting of macroalgae removes nutrients from water and hence, reduces eutrophication (Hughes *et al.*, 2013), with the potential for carbon sequestration during cultivation of seaweed (McHugh *et al.*, 2003). It has been estimated that their cultivation along coastlines could sequester about 1 billion tons of carbon annually (Chung *et al.*, 2011). A report shows mass cultivated seaweed as *Undaria*, *Hizikia*, *Laminaria* and *Porphyra spp.* etc in Japan absorbed about 32,000 tons of carbon annually, corresponding to 1.2% of the annual macrophyte production along the coastline (Muraoka, 2004). Seaweed aquaculture industry can be very useful within an integrated system for example together with fish farms (such as salmon) and renewable energy installations such as offshore wind farms and tidal turbines (McHugh *et al.*, 2003). Also, there is a potential for 3 to 10-fold increase in production of macroalgae with reduction in cultivation area to meet specified production goals with advances in cultivation technologies (Roesijadi *et al.*, 2010).

## 2.7 Macroalgae biomass cultivation and production

A number of interrelated factors are considered when seaweed species are chosen for cultivation according to their cost-effectiveness and to the end application of seaweeds, either food for human consumption or products for industrial use. All cultivation methods might be grouped into two; extensive and intensive cultivation (Titlyanov and Titlyanova, 2010), and can be generalized into either vegetative or separate reproductive cycle (McHugh *et al.*, 2003). Extensive cultivation involves growing seaweed in natural water areas using only naturally available light, heat, water motion energy, and nutrients. In contrast, intensive cultivation implies cultivation in tanks using natural or artificial light with nutrients and phytohormones, or in small natural water bodies like lagoons, ponds and lakes using organic and inorganic fertilizer, and applying agronomic techniques (Titlyanov and Titlyanova, 2010). Another segment in intensive cultivation which is developing rapidly is integrated seaweed-animal farming, or polyculture (Schneider *et al.*, 2005). World cultivation and production of seaweeds come from two sources; wild stocks harvesting and aquaculture including land-based culture, mariculture and farming (West *et al.*, 2016). Three options are available for

macroalgae farming: land-based ponds, nearshore coastal farms and offshore farms (Roesijadi *et al.*, 2010). Among the seaweed species only a few about 30-33 genera of seaweeds, mostly red and brown, are harvested and farmed commercially (McHugh *et al.*, 2003; Titlyanov and Titlyanova, 2010).

Mass cultivation of macroalgae is based on current farming technology (Jung *et al.*, 2013), but methods are greatly varied (Titlyanov and Titlyanova, 2010), and over the past 10 years production has continued to increase at an average of 10% per annum with the brown and red algae cultivated more than the green algae (Figure 2-5) (Jung *et al.*, 2013). Reports show production increased from approximately  $10 \times 10^6$  in 2001 to  $16 \times 10^6$  wet metric ton in 2010 (FAO, 2001; Lüning and Pang, 2003; FAO, 2010; Kraan, 2013). Currently, within the industry about 80-90% of the global value of seaweed is used directly for human consumption as food (Wei *et al.*, 2013; Kim and Lee, 2014; West *et al.*, 2016), while the remaining 20% is used for extraction of algal hydrocolloids or phycocolloids such as alginate, carrageenan, and agar for use in the cosmetic, industrial, medical and food industries (Roesijadi *et al.*, 2010; Wei *et al.*, 2013; West *et al.*, 2016). For instance in 2006 aquaculture production of macroalgae for these products accounted for about 3.1 million dry metric tonnes compared to 22 000 dry metric tons from wild stocks (Wei *et al.*, 2013). The FAO (2014) report suggests seaweed production from mariculture, reached 24.9 million tons in 2012, valued at about \$6 billion United States dollars.

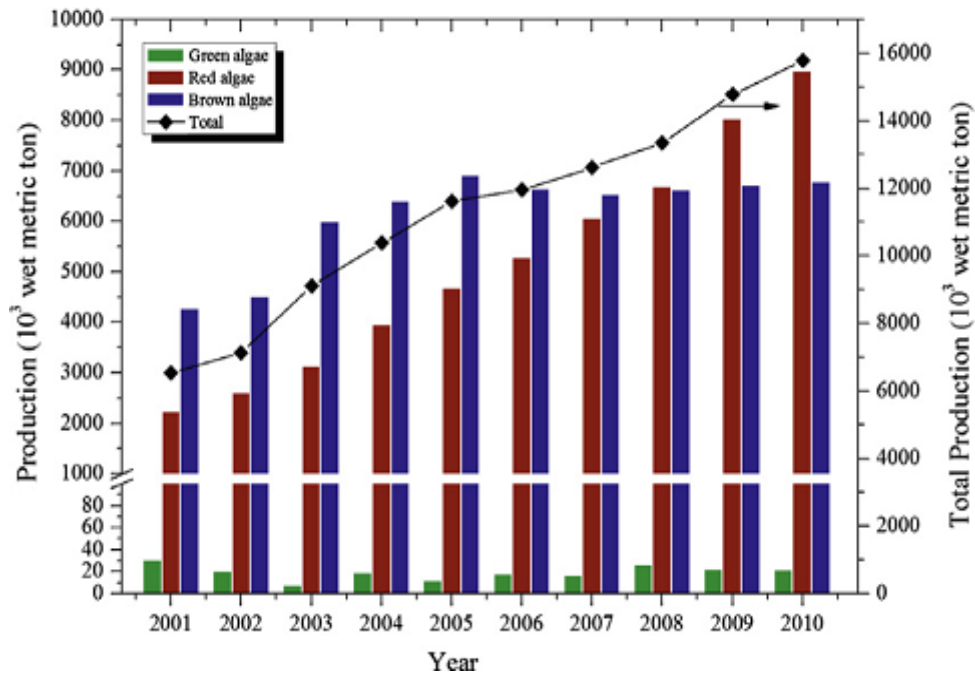


Figure 2-5: World production of farmed macroalgae from 2001 to 2010

(Jung *et al.*, 2013).

Jung *et al.* (2013) and Kim and Lee (2014), reported that mass-cultivated macroalgae are two orders of magnitude less than the energy crops but four and six orders of magnitude greater than microalgae and lignocellulose biomass, respectively. This demonstrates the advantage macroalgae has as a feedstock for bio refinery. Some problems associated with commercialization of seaweed cultivation to make it economically sustainable are algae fouling and epiphyte growth (Lüning and Pang, 2003).

Figure 2-6, shows coastline areas with potential for macroalgae culture for biogas. The Asian countries contribute over 80% of the world seaweed biomass global annual production with China contributing within 60 - 72% of this amount (Roesijadi *et al.*, 2010; Titlyanov and Titlyanova, 2010). In Europe, seaweeds cultivation is still in its early stage with a few commercial attempts totalling about 50-tonne wet weight combined, notably in Germany, France, and Ireland (Buck and Buchholz, 2004).

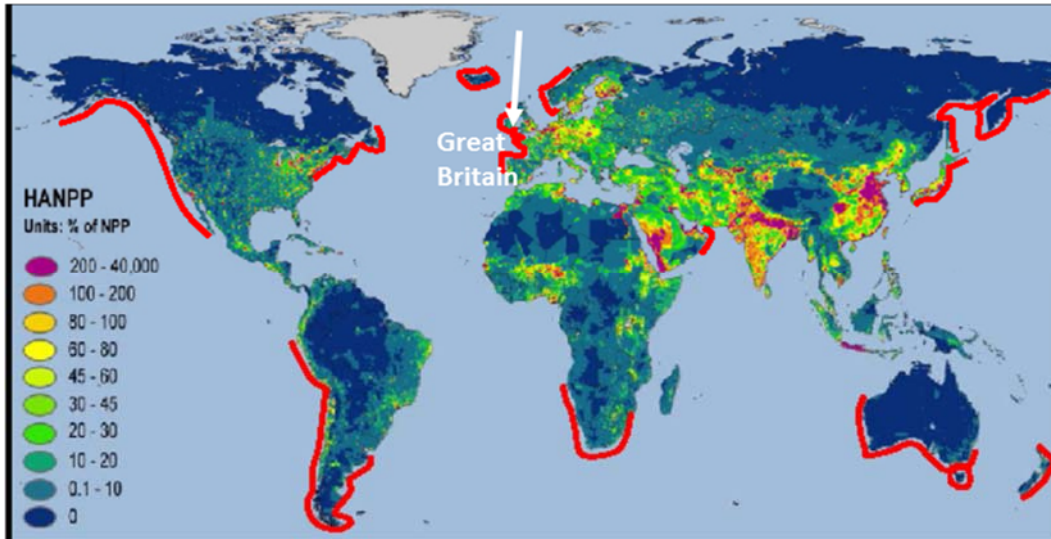


Figure 2-6: Redline indicates natural distribution of shallow water with potential for macroalgae cultivation

(Hughes et al., 2012)

## 2.8 Brown seaweed

The intertidal and shallow subtidal sea around Britain contain about 7% of the world's red, green and brown seaweeds (Brodie *et al.*, 2016). *Laminaria digitata* utilised in this work has been described as a widespread kelp growing off the coast of the UK, but is hardly considered as a potential source of biomass to date (Adams *et al.*, 2011b).

Figure 2-7 shows the distribution of *Laminariales* in Britain, dominating rocky shores at, or just below low water mark. Kelp is the common name for *Laminaria*, found typically at depths of 8 to 30m in the north Atlantic, and is considered a good candidate for bioconversion to energy (McHugh *et al.*, 2003). Within the *Phaeophyceae*, the kelps are primarily members of the *Laminariales* order which are the largest growing macroalgae species and in the Atlantic waters surrounding the UK, they grow up to 4 m in length (Adams *et al.*, 2011a).

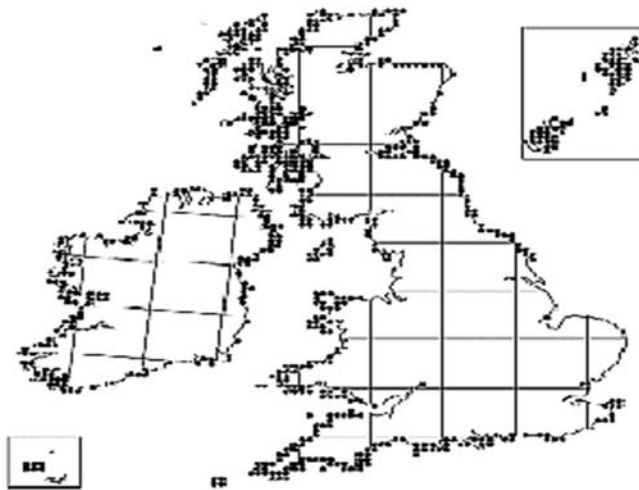


Figure 2-7: *Laminariales* distribution in UK, dominating rocky shores at, or just below low water mark

(Hardy *et al.*, 2006).

Brown seaweed species generally dominate the flora in temperate seas and their relative abundance on the sublittoral zone of the British coastline make them a substrate of choice for anaerobic digestion (Hierholtzer, 2013). It has been suggested there are approximately 100,000 hectares of kelp forests in UK waters which could be harvested commercially (McHugh *et al.*, 2003). The kelps are affected by rising water temperature because sexual reproduction, (gamete formation) in most kelps, will not occur above 20°C (West *et al.*, 2016). Within three European species of *Laminaria*, 15 °C has been reported as optimal growth temperature (Guiry and Blunden, 1991).

Figure 2-8, shows the life cycle of the *Laminariales*, the kelp plant is a diploid having a flat blade in all their morphology. An interesting feature is their fecundity which can be harnessed for mass cultivation because during their reproduction the zoospores formed are so small that 50 million spores can be produced per square centimetre of the blade (Guiry and Blunden, 1991).

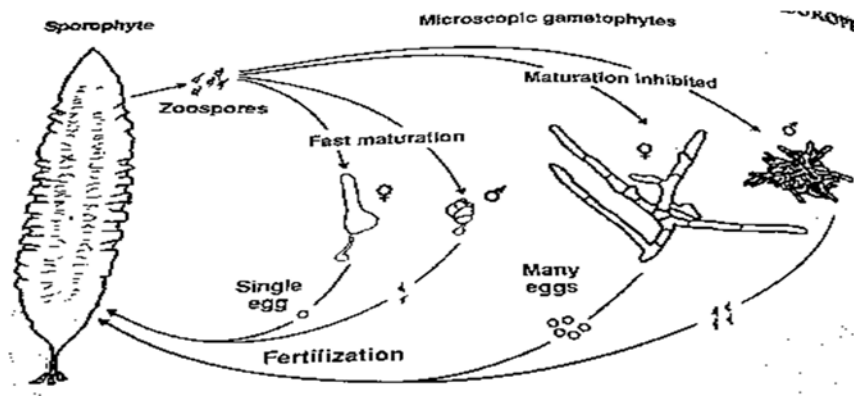


Figure 2-8: Life history of *Laminaria*

(Guiry and Blunden, 1991)

Among the seaweed species, brown seaweeds are considered the single largest macroalgae resource and are a likely candidate for energy processing (Burton *et al.*, 2009). The primary carbohydrates in brown seaweeds are alginate, laminarin, mannitol, fucoidans and cellulose (Kloareg *et al.*, 1986; Roesijadi *et al.*, 2010; Wei *et al.*, 2013). A semi-speculative or hypothetical model of the structure of cell wall of brown algae is presented in Figure 2-9 (Kloareg *et al.*, 1986; Michel *et al.*, 2010).

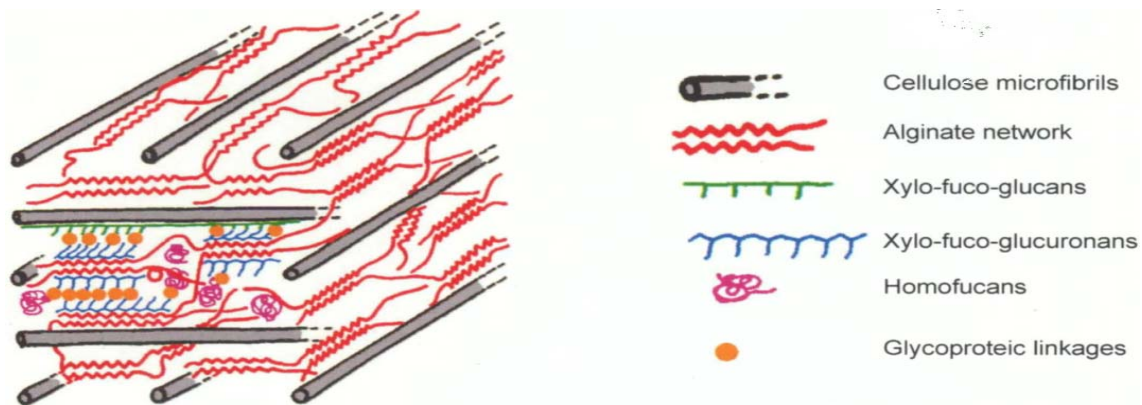


Figure 2-9: Hypothetical model of the biochemical organization of cell walls of brown algae

(Michel *et al.*, 2010).



### 2.8.1 Cellulose

Brown algae produce cellulose as crystalline microfibrils and account for between 1% and 8% of the dry weight of the thallus (Michel *et al.*, 2010). The cellulose is organized in crystalline parallel microfibrils arranged tangentially to the cell surface, and cross each other at definite angles, Figure 2-9 (Kloareg *et al.*, 1986). As a polysaccharide, it consists of a linear chain of several hundred to more than 10,000  $\beta$ -1, 4 linked D-glucose units as shown in Figure 2-10 (Ross *et al.*, 2009; Wei *et al.*, 2013).

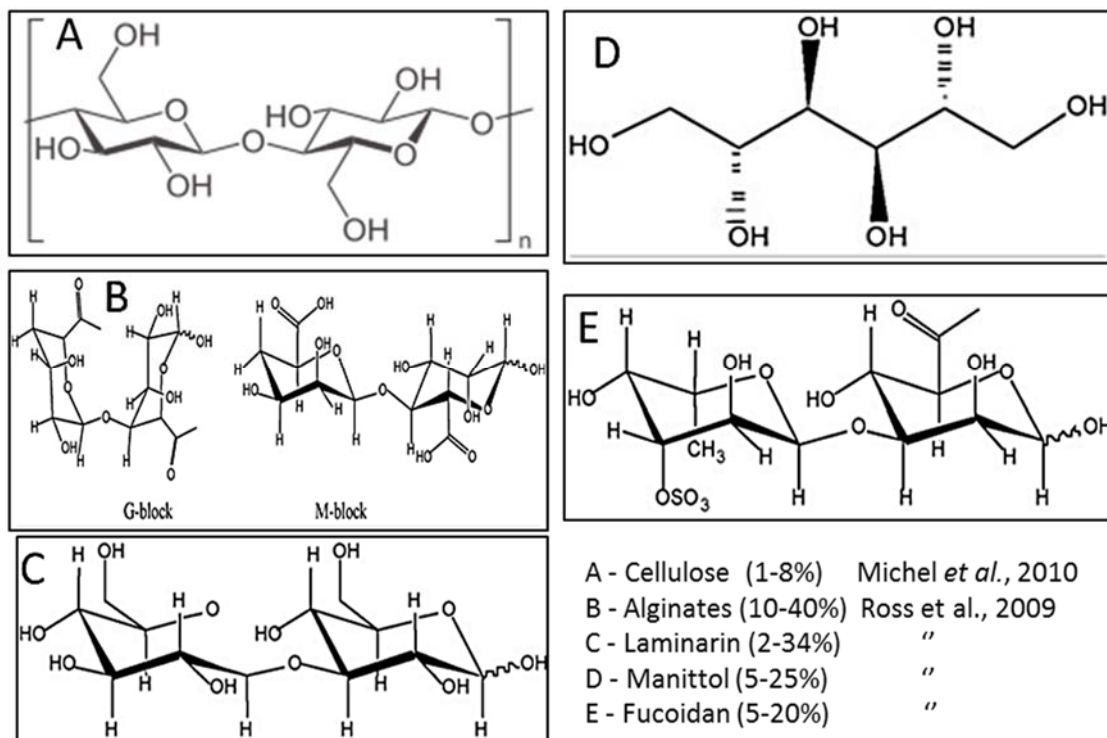


Figure 2-10: Structural presentation of polysaccharides abundant in seaweed biomass,

Adapted from Ross *et al.* (2009).

### 2.8.2 Alginate

Alginate is found in both large and smaller brown seaweeds and is naturally present in the cell walls (Kloareg and Quatrano, 1988). Alginate exists in brown algae as an anionic polysaccharide, comprising up to 40% of the dry matter (Michel *et al.*, 2010; Draget *et al.*, 2016). Alginate is a linear binary copolymer

consisting of two uronic acids, 1-4 linked  $\beta$ -D-mannuronic acid (M) and its C5 epimer,  $\alpha$  (1,4)- L-guluronic acid (G) in varying sequences (Kloareg *et al.*, 1986; Kim, 2011; Wei *et al.*, 2013; Draget *et al.*, 2016). It is located within the intercellular matrix as a gel containing sodium, calcium, magnesium, strontium, and barium ions and mainly functions to give both strength and flexibility to the algal tissue (Draget *et al.*, 2016). Alginate can be extracted, precipitated and quantified by weighing (Horn *et al.*, 1999). The average weight ratio of alginate, fucoidans and cellulose is 3:1:1 in mature intertidal brown algae (Michel *et al.*, 2010). Alginates are used as gelling agents, thickeners, emulsifiers, and stabilizers for frozen food, cosmetics and printing ink (Jard *et al.*, 2013).

### 2.8.3 *Laminarin*

Brown algae contain a storage laminarin ( $\beta$ -D- glucopyranose) which is a combination of soluble and insoluble chains of  $\beta$ -1,3 and  $\beta$ -1,6-D-glucans (Wiencke and Bischof, 2012). Typically, it is ~25 monomers chains which may be soluble or insoluble in cold water, depending on the proportion of branching and is hydrolysed to glucose by laminarinase, an endo-1,3 - $\beta$ - glucanase (Adams *et al.*, 2008).

### 2.8.4 *Fucoidans*

Fucans encompass a range of fucose-containing sulphated polysaccharides, divided into three main families: homofucans, xylofuco-glycuronans and glycuronofucoglycans (Kloareg *et al.*, 1986). In brown algae, the homofucans, or fucoidans, are heterogeneous polysaccharide primarily composed of  $\alpha$  (1, 2)-linked units of 4-sulphuryl-L-fucose, with very small proportions of D-xylose, D-galactose, D-mannose (Kloareg *et al.*, 1986; Wei *et al.*, 2013).

### 2.8.5 *Mannitol*

Mannitol is an alcohol form of the sugar mannose (Adams *et al.*, 2008), it is a C-2 epimer of glucose (Adams *et al.*, 2011a), that can be readily converted to fructose by mannitol dehydrogenase (Horn *et al.*, 2000b).

### 2.8.6 Brown Algae Phlorotannins

Tannins are water soluble polyphenols (Scalbert, 1991), produced as secondary metabolites by diverse plant species with an ability to bind and precipitate protein (Spencer *et al.*, 1988; Stern *et al.*, 1996a), a trait referred to as astringency (Scalbert, 1991; Arnold and Targett, 2000). They are divided into soluble tannins found in the cytoplasm or within cell wall, and an insoluble form bound to the cell wall (Strack *et al.*, 1988; Peng *et al.*, 1991). Phlorotannins are a subgroup of tannins produced wholly from polymerization of phloroglucinol (1,3,5 trihydroxybenzene) (Eom *et al.*, 2012), a product of the acetate-malonate pathway, also known as the polyketide pathway (Koivikko *et al.*, 2005). Phlorotannins are known only from brown algae (*Phaeophyceae*) (Van Alstyne *et al.*, 1999), and the soluble form accounts for about 20% of the seaweed dry weight (Amsler, 2006) or up to 25% dry weight (Targett *et al.*, 1992; Van Alstyne *et al.*, 1999). The phloroglucinol parent molecule (1,3,5 trihydroxybenzene) isolated from various natural sources is shown in Figure 2-11 (Jormalainen and Honkanen, 2008).

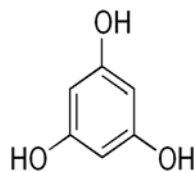


Figure 2-11 Phloroglucinol parent molecule (1, 3, 5 trihydroxybenzene)

Phlorotannins concentration is characterised by phenotypic plasticity showing intraspecific variation with respect to environmental conditions as nutrient, salinity, plant size, age, light availability, intensity of herbivory, ultraviolet irradiation and season (Pedersen, 1984; Denton *et al.*, 1990; Yates and Peckol, 1993; Steinberg, 1995). Such concentration variations suggest that the pool of phlorotannins are not stable but in a state of flux and their concentration is determined by a balance between rates of synthesis and turnover (Arnold and Targett, 2000). Soluble phlorotannins are stored in physodes (0.1-10µm in diameter), a subcellular body which aggregates around the nucleus (Schoenwaelder, 2002), and are highly mobile and reflective bodies observed in the cytoplasm of brown algae (Ragan and Glombitza, 1986). Phlorotannins are

antimicrobial compounds produced by certain seaweed that may inhibit sustained anaerobic digestion (Hierholtzer *et al.*, 2013; Hinks *et al.*, 2013). Both the red and green algae lack phlorotannins (Stern *et al.*, 1996a).

## 2.9 Anaerobic digestion process

Anaerobic digestion is a technology that has evolved over the past 200 years (Begum, 2014). It has been used for centuries to produce biogas (Dāsa, 2015). The technology was first demonstrated in 1859, in Bombay, India by building an anaerobic digester (Meynell, 1982), and the energy product now called “biogas” was commonly referred to as “gobar gas” after the Hindi word cattle dung which was the predominant feed for the digesters (Gunnerson and Stuckey, 1986). The term ‘anaerobic digestion’ describes the technology of accelerating naturally evolved bioprocesses in an artificial environment of a closed vessel (Luque *et al.*, 2011). It is an engineered methanogenic degradation of organic matter by mixed consortium of microorganism under oxygen-free conditions into biogas (Wilkie, 2005). During AD, the chemical environment in which the organism is maintained governs the rate and extent of substrate conversion to methane and carbon dioxide (Isaacson, 1991), and because little heat is generated unlike in aerobic decomposition, the energy which is chemically stored in the substrate, remains mainly as produced biogas, in the form of methane (Seadi Al Teodorita, 2008). Kim *et al.* (2017) stated that biogas production from AD processes is considered a practical approach for energy recovery. Anaerobic digestion process, ideally should function without molecular oxygen as its name implies but in reality except extreme measures are taken to exclude it, some oxygen will still get into the digesters, through water or occluded feedstock, but is utilized by the facultative anaerobes bringing the level of dissolved oxygen concentration lower and suitable for anaerobic organisms (Isaacson, 1991). Removal of the oxygen in the digesters is important because it provides a conducive environment for the anaerobes, oxygen is a thermodynamically better electron acceptor forming CO<sub>2</sub> instead of methane and oxygen, it is a contaminant in the produced gas which is a potential safety hazard (Isaacson, 1991). Water is prerequisite for AD, because it serves as a medium of transportation for the substrate to and waste products from the bacteria, with a water level of approximately 75%, below which microbial

activity is retarded (Wujcik and Jewell, 1980). Over the years AD is now very well established, reliable and a successful technology implemented worldwide (Luque *et al.*, 2011), with the chemistry well understood (Holm-Nielsen *et al.*, 2009). There are enormous advantages associated with the use of AD both as a waste treatment technology with environmental benefits and a sustainable energy producing technology (Wilkie, 2005).

## 2.10 The Fundamental biochemical AD process

AD, also known as biological gasification (biogasification) (Isaacson, 1991) is a natural microbiological process that converts organic matter through decomposition to biogas (mainly methane, its most reduced form and carbon dioxide, most oxidized form ) and digestate (Isaacson, 1991; Seadi Al Teodorita, 2008; Madsen *et al.*, 2011), in an environment devoid of dissolved oxygen or its precursors ( $H_2O_2$ ) (Khanal, 2011). In AD, the organic matter is initially catabolized by facultative anaerobes in the absence of external electron acceptor through a balance of oxidation-reduction reactions under dark conditions, with products generated serving as an electron acceptor while the organic matter is also the donor (Khanal, 2011). It is a complex process which requires strict anaerobic conditions, redox potential  $< -200mV$  to proceed (Appels *et al.*, 2008), and can occur in the temperature range from 10–71°C (Demirbas, 2009a). During the fermentation process, because the substrate is partially oxidized only a small amount of energy stored in the substrate is conserved, most of the energy or adenosine triphosphate (ATP) is generated by substrate-level phosphorylation, Figure 2-12 (Khanal, 2011; Madigan *et al.*, 2014).

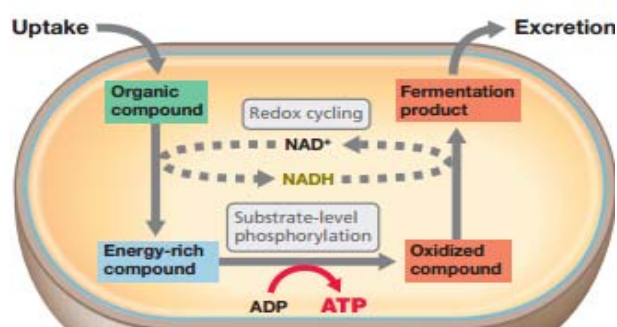


Figure 2-12: The essentials of fermentation.

The product is excreted from the cell, and only a relatively small amount of the original organic compound is used for biosynthesis (Madigan *et al.*, 2014).

The conversion process is carried out by the action of a consortium of bacteria working synergistically and the biogas formation is linked to distinct interconnected steps, 1-4 with specific groups of micro-organism as shown in Figure 2-13, which highlights the four main process steps: hydrolysis, acidogenesis, acetogenesis, and methanogens.

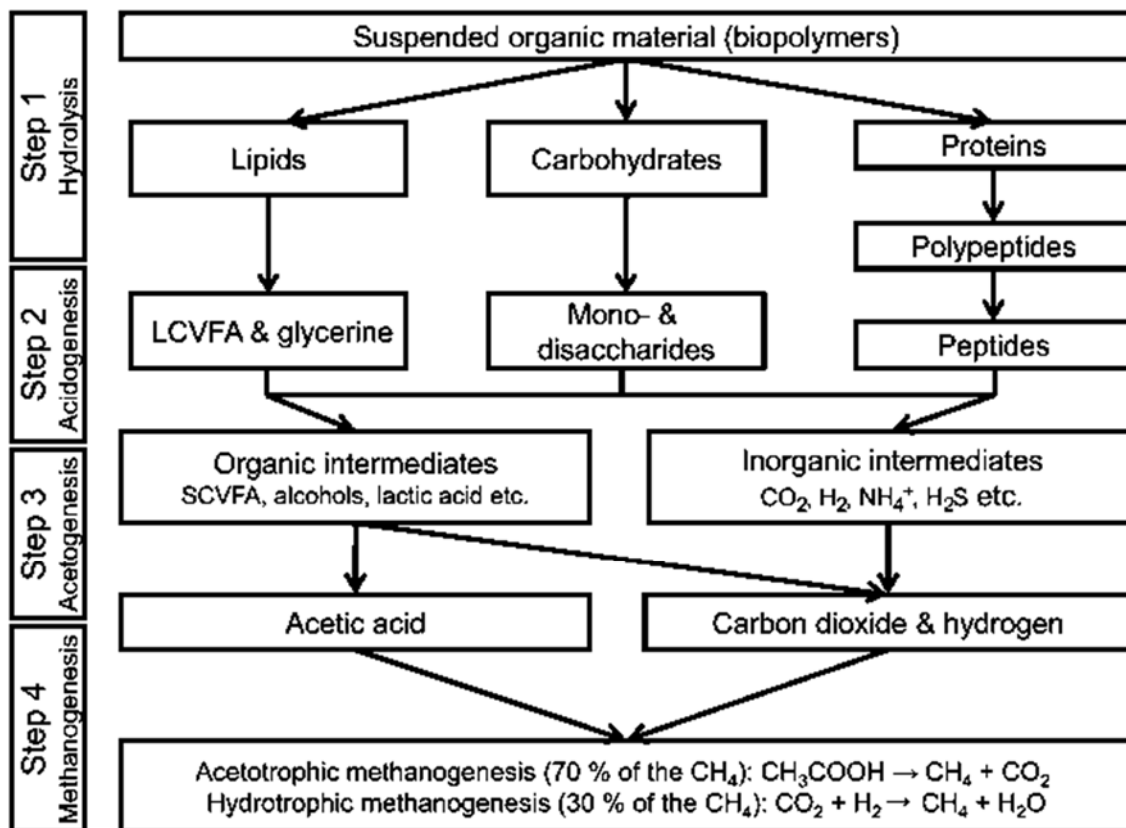


Figure 2-13 Overview of the four principle reaction steps of anaerobic digestion

(Madsen *et al.*, 2011)

### 2.10.1 Disintegration phase

The disintegration step is often not included in the four basic steps of anaerobic digestion but has been thought as preceding the more complex hydrolytic step (Pavlostathis and Gossett, 1986). There complex particulate waste first disintegrates to organic polymers such as carbohydrate, protein and lipids as well

as particulate and soluble inert compounds using an array of processes such as lysis, non-enzymatic decay, phase separation and shearing (physical breakdown) (Batstone *et al.*, 2002).

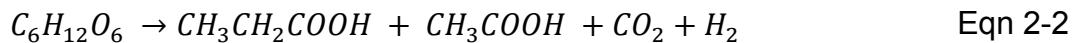
### 2.10.2 *Hydrolysis*

In anaerobic degradation of complex compounds, hydrolysis is theoretically regarded as the first step where compounds such as carbohydrates, proteins, and lipids are hydrolyzed into smaller units, such as sugars, amino acids, alcohols, and long-chain fatty acids (Demirbas, 2009a; Begum, 2014). Hydrolysis is not necessarily a strictly anaerobic process as studies showed that micro-oxygenation enhances the physiological metabolism of the facultative hydrolytic bacteria assisting substrate hydrolysis (Chen *et al.*, 2012). During the process, organic polymers are broken down to monomers and dimers through biological decomposition and solubilisation of insoluble particulate matter. Depending on the substrate various pretreatment processes have been used to enhance hydrolysis making the substrate more amenable to enzymatic attack (Müller *et al.*, 1998; Seadi Al Teodorita, 2008; Demirbas, 2009a). Pretreatment helps to break down the solids, facilitating the release of cell components and other organic matter. The hydrolysis process, is carried out by exoenzymes (extracellular enzymes), produced by hydrolytic microorganisms which decompose the undissolved particulate material (Seadi Al Teodorita, 2008), and also dissolved colloids and molecules which are too large to diffuse through cell walls and membranes (Wiesmann *et al.*, 2007), as compounds can only be transported, metabolized and assimilated into microbial cells in water-soluble state (Schieder *et al.*, 2000). This step is often considered the rate-limiting in the anaerobic digestion of organic wastes (Tiehm *et al.*, 2001; Appels *et al.*, 2008). It should be noted that under anaerobic conditions, the hydrolysis rate of carbohydrate is higher than that of protein (Demirbas, 2009a).

### 2.10.3 *Acidogenesis*

This step is also called fermentation or acid forming fermentation (Khanal *et al.*, 2010; Luque *et al.*, 2011). In acidogenesis, another group of microorganisms (acidogenic) ferments the broken down simple sugars, amino acids and fatty

acids into short chain organic acids (mainly Volatile fatty acids (VFAs)), C<sub>1</sub>–C<sub>5</sub> molecules (acetate, acetic acid, propionic and butyric acid), hydrogen (H<sub>2</sub>), carbon dioxide (CO<sub>2</sub>), nitrogen oxide, alcohols and hydrogen sulphide (H<sub>2</sub>S), (Deublein and Steinhauser, 2011). The lower weight simple alcohols and volatile organic acids like propionic and butyric acid, are in turn converted to acetic acid (Demirbas, 2009a). The growth rate of acidogens is quite high, they have a doubling time of the order of one hour or even less and can prevail under adverse condition as low as pH (5 – 6) (Luque *et al.*, 2011). As depicted in Eqn 2-2, glucose reduction for a typical acidogenic reaction, the concentration of the hydrogen ion formed affects the fermentation products, because of the higher the partial pressure of H<sub>2</sub> the fewer the reduced compounds such as acetate that is produced (Deublein and Steinhauser, 2011).



Because, the products of hydrolysis are converted into methanogenic substrates by acidogenesis bacteria (Seadi Al Teodorita, 2008), acetate, carbon dioxide, and molecular hydrogen can be directly utilized as a substrate by a group of obligate and facultative anaerobes called methanogens (Demirbas, 2009a).

#### 2.10.4 *Acetogenesis*

Acetogenesis is the third stage in AD process, where products that cannot be directly converted to methane in the acidogenesis phase by methanogenic bacteria, are converted into methanogenic substrates (Seadi Al Teodorita, 2008). Products like higher volatile fatty acids (propionate, butyrate, valerate etc.), and alcohols produced by acidogenesis are converted mainly into acetic acid, CO<sub>2</sub> and H<sub>2</sub> (Appels *et al.*, 2008; Khanal *et al.*, 2010; Luque *et al.*, 2011). Basically, VFAs with carbon chains longer than two units and alcohols, with carbon chains longer than one unit, are oxidized into acetate and hydrogen (Seadi Al Teodorita, 2008). The hydrogen produced during the formation of acetate depends on the oxidation state of the original organic compounds (if Ne<sup>-</sup> > 4, acetate and H<sub>2</sub> is formed and Ne<sup>-</sup> < 4, acetate and CO<sub>2</sub> are formed) (Van Haandel and Lettinga, 1994). The formation of acetate by oxidation of the VFAs runs on its own and is thermodynamically possible only with low hydrogen partial pressures because



acetogenic bacteria obtain their energy for growth at very low H<sub>2</sub> concentration (Deublein and Steinhauser, 2011). Since, the acetogenes are obligatory H<sub>2</sub> producers (Deublein and Steinhauser, 2011), increase in hydrogen production increases the hydrogen partial pressure which in turn inhibits metabolism of the acetogenic bacteria (Seadi Al Teodorita, 2008), hence, they enter into a symbiotic relationship with methanogens that can survive the high hydrogen partial pressure environment, converting the hydrogen into methane via CO<sub>2</sub> reduction, thus maintaining a low hydrogen partial pressure environment (Deublein and Steinhauser, 2011). It is important that H<sub>2</sub> produced is oxidized by other anaerobic bacteria otherwise the butyric, propionate, capronic, valeric acids and ethanol concentration will continue to increase (Wiesmann *et al.*, 2007; Deublein and Steinhauser, 2011). A number of different microbes carry out this conversion, notably e.g., *syntrophobacter wolinii*, a propionate decomposer and *syntrophomonos wolfei*, a butyrate decomposer both produces acetate and hydrogen from the VFAs while a group of bacteria called *homoacetogens* (*Acetobacterium woodi*, *Ruminococcus hydrogenotrophicus*) form acetate from hydrogen and carbon dioxide (Deublein and Steinhauser, 2011). Kotsyurbenko *et al.* (2001) stated that a high H<sub>2</sub> partial pressure (1 - 10 Pa) is required for homoacetogenesis to occur over methanogenesis.

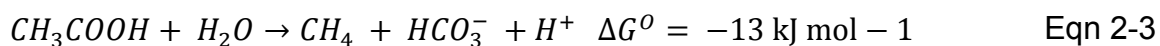
#### 2.10.5 Methanogenesis

The fourth (final) stage, is methanogenesis known as the formation of methane (Khanal *et al.*, 2010). Methane formation occurs strictly under anaerobic conditions (carbonate respiration) (Deublein and Steinhauser, 2011), by methanogenic bacteria belonging to *Archae*, a unique group of microorganisms, phylogenetically different from prokaryotic microorganisms (Wiesmann *et al.*, 2007; Demirbas, 2009a). They are distinguished from true bacteria by distinct ribosomal RNA (Khanal, 2009). The methanogenic bacteria exhibit two main products of catabolic metabolism where carbon is converted into methane, a water-insoluble gas of limited solubility forming biogas bubbles and CO<sub>2</sub> together with which is desorbed in water in equilibrium with HCO<sub>3</sub><sup>-</sup> and CO<sub>3</sub><sup>2-</sup> as function of pH (Wiesmann *et al.*, 2007; Deublein and Steinhauser, 2011). The methane content of the biogas depends on the oxidation state of the organic carbon in the

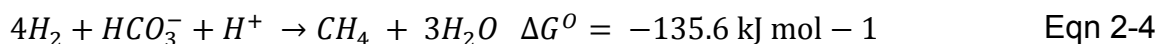
initial substrate (ranging from -4 for methane to +4 for carbon dioxide) (Luque *et al.*, 2011). The methanogens degrade only a limited number of substrates among these are acetate, H<sub>2</sub>/CO<sub>2</sub>, methanol, formate and methanol (Demirbas, 2009a).

Two distinct groups of microorganisms produce the methane and carbon dioxide: (1) *Acetoclastic methanogens* utilizing acetic acid produces approximately 60 - 70% of the methane in the biogas (Khanal, 2011). (2) *Hydrogenotrophic methanogenesis* that consumes hydrogen and carbon dioxide produces the remaining 30% (Mackie and Bryant, 1981; Seadi Al Teodorita, 2008), both the reactions are exergonic, Eqn 2-3 and Eqn 2-4 (Deublein and Steinhauser, 2011), but *hydrogenotrophic methanogenesis* is thermodynamically advantageous.

#### *Acetotrophic methanogenesis*



#### *Hydrogenotrophic methanogenesis*



(Henze and Harremoes, 1983; Seadi Al Teodorita, 2008).

## 2.11 Factors influencing digesters performance

Process control in AD system is often difficult, due to diverse interrelated conditions which are interdependent on each other, as changes in one condition may directly or indirectly affect the other (Gerardi, 2003). The efficiency of AD depends on a number of these interdependent conditions which must be satisfied (Speece, 1996a). These conditions determine the rate and extent of conversion of the substrate to methane and carbon dioxide (Isaacson, 1991). Since, the rate-limiting reaction in AD, is conversion of VFAs to methane, and because methane-forming bacteria obtain very little energy from the degradation of the VFAs, their growth rate is restricted implying substrate utilization per unit gram of organism is high, hence bacteria growth is low and optimum operational conditions must be maintained for satisfactory substrate degradation and methane production (Gerardi, 2003). Operational environmental conditions can be separated into two

general areas: physical (temperature, water, retention time, loading rate, mixing and particle surface area) and chemical (pH, alkalinity, substrate, nutrients, toxics and anaerobic conditions) (Isaacson, 1991; Luque *et al.*, 2011).

### 2.11.1 pH and Alkalinity

pH is a critical operating parameter in AD, because it affects the growth of microorganisms during all stages of the process (Korres *et al.*, 2013), as the optimal growth of microorganisms is under neutral pH conditions, their metabolism is impacted by acid or alkaline media (Pesta, 2007). Controlling the pH of digesters can significantly improve the overall performance of the system (Ravi *et al.*, 2018). Changes in pH alter the chemical equilibrium of enzymatic reactions or destroy enzymes (Burton and Turner, 2003). The pH affects the formation of undissociated acids and bases that easily penetrate the cellular membrane changing the internal pH of the cells (Luque *et al.*, 2011). The pH also influences the function of the extracellular enzymes and has an impact on the hydrolysis rate (Luque *et al.*, 2011). But it should be noted as stated by (Chae *et al.*, 2002) in a well-buffered substrates (e.g. swine manure), it can be a poor indicator of process performance. Sufficient alkalinity is essential for proper pH control because the methane-forming bacteria are strict anaerobes and are highly sensitive to pH variation and alkalinity (Grady, 1999; Gerardi, 2003). They perform optimally, within a pH range of 6.5 - 8.2 (Speece, 1996a; Gerardi, 2003) but are generally inhibited at pH below 6.6 (Isaacson, 1991). Dāsa (2015) stated that at pH 5.5 - 6.5 and pH 7.8 - 8.2 acidogens and methanogens exhibit their maximum activity respectively. At low pH, inhibition has been attributed to increase in unionised substrate acid, as the unionised acid penetrates the cells and disturbs the internal pH (Hobson, 1993), while above pH 8.0 a sharp drop in activity may be related to a shift in NH<sub>4</sub>-N to the toxic, unionized NH<sub>3</sub> form (Seagren *et al.*, 1991). In the AD process, accumulation of VFAs or excessive generation of CO<sub>2</sub> causes a drop in the pH (Khanal, 2009). One medium of CO<sub>2</sub> production can be attributed to the oxidation state of carbon in carbohydrates which makes the gas produced by fermentation contains 50% CO<sub>2</sub>, causing a high partial pressure in the gas phase which depresses the digester pH, requiring a high alkalinity to maintain a neutral pH (Isaacson, 1991). The CO<sub>2</sub> concentration of the gas phase

and  $\text{HCO}_3^-$  alkalinity in the liquid phase control the pH of the system (Appels *et al.*, 2008). In the destruction of an organic matter (COHNS), proteins releases ammonia-N, with each molecule of organic nitrogen theoretically generating one equivalent of alkalinity (Moosbrugger *et al.*, 1990), while a reduction in 1g of  $\text{SO}_4$  generates around 1.04g of alkalinity as  $\text{CaCO}_3$  (Greben *et al.*, 2000). Alkalinity ranges from 1.0 – 5.0 g L<sup>-1</sup> as  $\text{CaCO}_3$  in AD systems (Metcalf and Eddy, 2003; Dāsa, 2015).

### 2.11.2 Temperature

Temperature is possibly the most important environmental factor affecting the growth and survival of microorganism and affects them in two opposing ways (Madigan *et al.*, 2014). As temperature increases, chemical and enzymatic reactions within the cell takes place at rapid rates and growth becomes faster up to the point above a certain temperature where cell components (proteins, nucleic acids etc.) becomes irreversibly damaged, rendering them inactive, Figure 2-14 (Luque *et al.*, 2011; Madigan *et al.*, 2014).

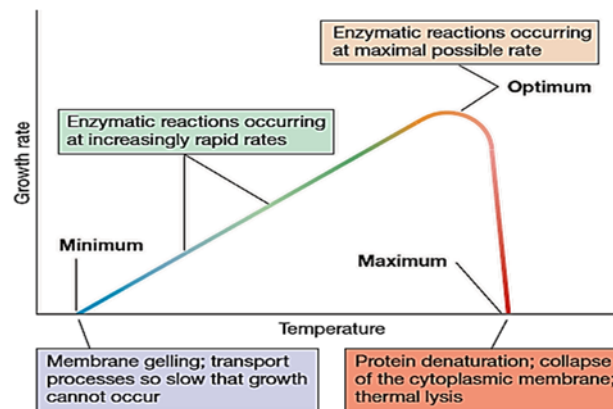


Figure 2-14: The Cardinal temperature: minimum, optimum and maximum

The mechanism governing an organism minimum growth temperature is not clear but thought to be stiffening of a semifluid cytoplasmic membrane to a point where it can no longer function properly in transport, develop or consume a proton motive force, the organism at that point cannot grow (Madigan *et al.*, 2014). In AD system, the microbial communities are affected by temperature in various ways, for example, metabolic rate controls, ionization equilibrium, solubility of substrate

and fat to bioavailability of iron (Speece, 1996a). Methanogenesis can occur over a temperature range of 4 – 100 °C (Speece, 1996a), and in the AD process, there exist three optimal temperature ranges for methanogenesis: psychrophilic, mesophilic, and thermophilic (Seadi Al Teodorita, 2008; Khanal, 2011). The conversion efficiency is highest between 5 – 15 °C (psychrophilic), 35 - 40 °C (mesophilic), and about 55 °C (thermophilic) with lower rates between these optima as shown in Figure 2-15 (Lettinga *et al.*, 2001).

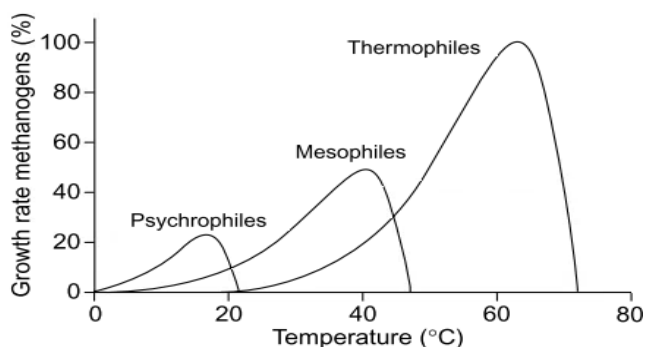


Figure 2-15: Relative growth rate of psychrophilic, mesophilic, and thermophilic

Temperature influences the rate of bacterial action (Demirbas, 2009a), and as a rule of thumb, the biological activity doubles for every 10 °C rise in temperature within the optimal temperature range (Khanal, 2011). It also influences quantity of moisture in the biogas as moisture content increases exponentially with temperature, also the quantity of gas and dissolved volatile organic compounds as well as the concentration of ammonia and hydrogen sulphide gas (Demirbas, 2009a).

### 2.11.3 Retention Times

The digestion process is described by two principal times: Hydraulic retention time (HRT), which defines the contact time for metabolism to occur and Solid retention time (SRT), determines organisms regeneration and accumulation within the system (Speece, 1996a). The HRT equals the volume of the tank divided by the daily flow ( $HRT = V/Q$ ) (usually expressed in days) whereas the SRT is amount of solids in a tank divided by the amount of solids degraded (washed out) each day  $SRT = (V)(C_S) / (Q_{SR})(C_{SE})$ , where V is the tank volume

( $m^3$ );  $C_S$  is the solids (sludge) concentration in the tank (mg /L);  $Q_{SR}$  is the sludge volume removal rate ( $m^3/d$ ) and  $C_{SE}$  is the solids concentration of the effluent (Burke, 2001) .

In many AD systems, both HRT and SRT are equal if there is no recycle but vary significantly if residues are recycled ( $SRT > HRT$ ) (Gerardi, 2003; Schnurer and Jarvis, 2010). Because methane-forming bacteria, have doubling times that are relatively long compared to facultative or aerobic bacteria, typical SRTs are  $> 12$  days for AD digesters, with SRTs  $< 10$  days resulting in to significant biomass wash-out, hence not recommended, this indicates SRT, not HRT as a more important retention time (Gerardi, 2003). The permissible organic loading rate is determined by SRT in the AD process (Khanal, 2011). HRT is determined by the average time it takes an organic substrate to completely digest, measured by the COD or BOD of the exiting effluents (Demirbas, 2009a), it depends on substrate digestibility and influences the effluent quality (Wellinger *et al.*, 2013). HRT is important because it indicates the time available for bacteria growth and conversion of the organic substrate to biogas (Korres *et al.*, 2013), and is specific for each type of bioreactor (Kispergher *et al.*, 2017). Burke (2001) stated a direct relationship exists between HRT and volatile solids converted to biogas. The conversion of the volatile solids to gas is controlled by the HRT and the HRT values affect the rate and extent of methane production (Gerardi, 2003).

The SRT or HRT retention time varies with different technologies, process temperature, and substrate composition (Khanal *et al.*, 2010) but basically mesophilic digester are operated in a greater number of SRT days (10 to 40 days) than thermophilic digesters (10 - 15) (Verma, 2002). In continuous stirred tank reactors (CSTRs) without solid separation and recycling, +10 long HRTs or SRTs should be maintained as they are prone to failure due to excessive biomass washout (Khanal, 2011).

#### 2.11.4 Organic Loading rate (OLR)

The OLR is the quantity of organic matter fed *per* unit volume of the digester *per* unit time (*e.g.*  $kg VS m^{-3} d^{-1}$ ) (Tiwari, 2005; Demirbas, 2009a). In AD processes, it serves as useful criteria for assessing performance of reactors and plays a critical

role in continuous systems (Parawira, 2004). The methane yield depends on the digester load, but with too high a solid content > 12% in the substrate impairs gas production (Deublein and Steinhauser, 2011). For instance, process failure may occur due to high organic loading rate where acidogenic bacteria doubles and produces acids rapidly (Demirbas, 2009a). A number of parameters such as reactor design, biomass activity and settlement and wastewater characteristics influence the maximum OLR for anaerobic digesters (Demirbas, 2009a).

#### 2.11.5 *Carbon to Nitrogen ratio (C: N)*

The C: N ratio is one operational parameter that influence the efficiency of an AD process (Mao *et al.*, 2017). Although the ratio of C: N is of greater significance for high growth mainly for aerobic degradation processes, anaerobic digestion process also depends on it to a certain degree (Pesta, 2007). One feasible means of increasing methane production efficiency is to optimize the carbon to nitrogen ratio of the feed (Hills and Roberts, 1981; Tiwari, 2005). The amount of carbon to nitrogen present in an organic substrate is the carbon-to-nitrogen (C: N) ratio (Verma, 2002). For AD process, the ideal C: N ratio should be between 25 – 35: 1 (Hills and Roberts, 1981). Micro-organisms utilization of carbon during AD is 20 to 30 times faster than nitrogen (Pesta, 2007). This predicts a feed substrates optimal ratio for C: N of 20 - 30: 1 for easily degradable carbons to meet the microbes requirement (Pesta, 2007; Demirbas, 2009a). Higher C: N ratio leads to a rapid consumption of nitrogen by the methanogenic consortium bacteria resulting in lower gas production rates, while lower C: N ratio causes ammonia accumulation and pH values exceeding 8.5, which is toxic to methanogenic bacteria (Tiwari, 2005; Demirbas, 2009a).

#### 2.11.6 *Mixing*

Mixing in AD process enhances the contact between the micro-organism and substrate, this helps to improve the microorganism ability to obtain nutrients (Monnet, 2003), and in efficient substrate conversion to biogas, also removal of the biogas from the mixture (Nandi *et al.*, 2017). Mixing brings about development of uniform temperature gradient within the reactors and prevents, in most cases, the formation of scums, improves mixing of fresh and degraded

substrate in order to inoculate the fresh substrate to the bacteria and effective removal of biogas formed, however high agitation has been known to disrupt the microorganism which is stress sensitive (Deublein and Steinhauser, 2011). Mixing helps to prevent stagnation zones which result from long solid retention where inorganic solids accumulate in these zones reducing effectively the digester volume (Isaacson, 1991).

## 2.12 Inhibition of AD process

Inhibitory substances are the leading cause of anaerobic reactor upset and failure when they are present in significant concentrations in sludge (Chen *et al.*, 2008). A broad variety of substances have been reported to be inhibitory to the anaerobic digestion process but manifest considerable variation in inhibition/toxicity levels (Chen *et al.*, 2008). These variations have been linked to mechanisms which influence the phenomenon of inhibition such as antagonism, synergism, complex formation and adaptation/acclimatisation (Chen *et al.*, 2008; Schnurer and Jarvis, 2010). A substance is considered inhibitory if it causes an adverse shift in the microbial population or inhibition of bacterial growth (Chen *et al.*, 2008), and inhibition is marked by a decrease in the steady-state rate of methane gas production and accumulation of organic acids (Kroeker *et al.*, 1979). Inhibition of the microbial community in AD process depends on the concentration of the inhibitors, the composition of the substrate and the adaption of the bacteria to the inhibitors (Deublein and Steinhauser, 2011).

Some of the inhibitory factors are listed below:

### 2.12.1 Oxygen

All bacteria contain enzymes that react with oxygen, producing toxic free radicals that destroy their vital cellular components. The removal of these radicals by other enzymes present determines their degree of tolerance to oxygen (Demirbas, 2009a). The vulnerability to oxygen varies widely among the strict anaerobes, although most acidifying bacteria are facultative anaerobes, as they can use oxygen for growth if available but does not require it (Demirbas, 2009a; Deublein and Steinhauser, 2011). Methane-forming bacteria are obligatory



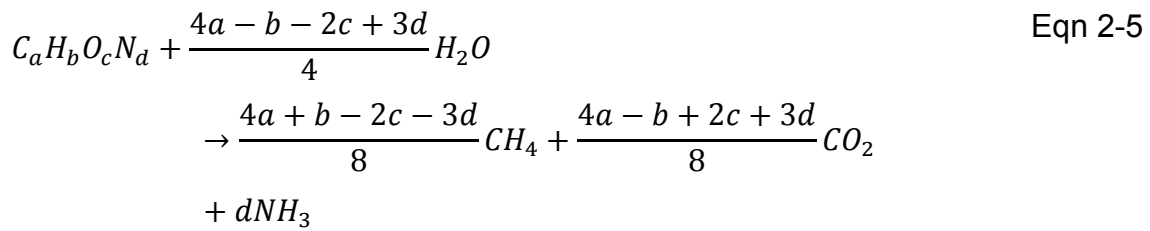
anaerobes, oxygen is toxic to them and can start to inhibit them at 0.1 mg/L O<sub>2</sub> (Deublein and Steinhauser, 2011). This is caused by an irreversible decomposition of F420 hydrogenase complex as a result of the lack of a protective superoxide dismutase (Garcia *et al.*, 2000).

During operational conditions, the synergy that operates among the microbes allow methanogens to grow because traces of oxygen are quickly taken up by facultative anaerobes of the media, decreasing the redox potential to acceptable levels (−400 mV) (Demirbas, 2009a). Aerobic conditions promote facultative which have a faster growth rate.

### 2.12.2 Ammonium (NH<sub>4</sub><sup>+</sup>) and Ammonia (NH<sub>3</sub>)

Biological degradation of nitrogenous compounds such as proteins and amino acids results in both ammonium (NH<sub>4</sub><sup>+</sup>) and ammonia (NH<sub>3</sub>) production (Deublein and Steinhauser, 2011). Nitrogen is an essential nutrient for anaerobic microbes digesting organic substrate (Kayhanian, 1999). The microbes require low levels of ammonia which is converted into organic nitrogen in the form of cellular protoplasm for growth and multiplication (Kayhanian, 1999). But in the presence of excess ammonia, inhibition of methanogenic process occurs, resulting in drop in methane production and pH (Parkin and Speece, 1982). Toxicity against methanogens has been noted during biogas formation from substrate containing high concentration of ammonia or organic nitrogen or protein (Sprott and Patel, 1986). Optimal ammonia concentration ensures sufficient buffer capacity of methanogenic medium in AD thus increasing the stability of the digestion process (Rajagopal *et al.*, 2013).

The theoretical basics for estimating the quantity of ammonia that can be generated from anaerobic biodegradation of an organic substrate is given by the following stoichiometric relationship (Tchobanoglous *et al.*, 1993).



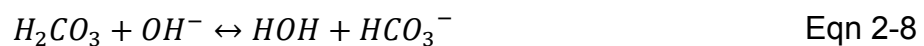
Where  $N_d$  is the amount of nitrogen in organic substrate and  $dNH_3$  is the amount of ammonia produced.

Ammonia as a product of anaerobic degradation of protein is essential for bacterial growth (Gallert *et al.*, 1998), and is released during the first stage of the bioconversion process, where hydrolyzing microorganisms deaminate nitrogenous compounds to produce ammonia (Kayhanian, 1999). The produced ammonia reacts with water to form ammonium and hydroxide ion depending on the process pH in an equilibrium relationship as shown below (Kayhanian, 1999; Rajagopal *et al.*, 2013):



The unionized specie is known as free ammonia (FAN)( $NH_3$ ) because it exists as a gas in solution and does not bind ionically to the water as the ionized ammonium ( $NH_4^+$ ) (Kayhanian, 1999). FAN has an inhibitory effect, becoming toxic at larger concentration whereas,  $NH_4^+$  is non-injurious (Demirbas, 2009a; Deublein and Steinhauser, 2011). FAN has been suggested as the main cause of nitrogen inhibition since it can freely permeate into the bacteria cell membrane (Müller *et al.*, 2006), and its toxicity is related to temperature and pH-dependent concentration of FAN (Gallert *et al.*, 1998).

The ionized ammonia ( $NH_4^+$ ) is more beneficial in AD than FAN because it produces hydroxide ( $OH^-$ ) from Eqn 2-6, which reacts with carbon dioxide produce from the AD process to form bicarbonate (Eqn 2-7 and Eqn 2-8) and gives buffering capacity to AD reactors (Kayhanian, 1999).



Several pathways have been suggested as the mechanism of ammonia inhibition such as a change in intracellular pH of methanogens, increase of maintenance energy requirement and inhibition of a specific enzyme reaction (Wittmann *et al.*, 1995; Rajagopal *et al.*, 2013). Knowledge of the mechanism of how ammonia toxicity occurs against methanogens is limited (Kayhanian, 1999; Rajagopal *et al.*, 2013). Few studies with pure cultures have shown two pathways of ammonia inhibition against methanogenic bacteria: (i) ammonium ion may inhibit the methane-producing enzymes directly and/or (ii) hydrophobic ammonia molecule may diffuse passively into bacterial cells, causing proton imbalance or potassium deficiency (Gallert *et al.*, 1998; Kayhanian, 1999; Rajagopal *et al.*, 2013). The physiology of methanogens determines the diffusion of ammonia molecules into cell wall (Rajagopal *et al.*, 2013). A mechanism of ammonia inhibition has been hypothesized using Figure 2-16, when a fraction of  $\text{NH}_3$  penetrate into the cell it is converted into  $\text{NH}_4^+$ , due to difference in intercellular pH and absorbs protons in the process. The cells then expend some energy in proton balancing, using a potassium ( $\text{K}^+$ ) antiporter to maintain the intracellular pH, thus increasing maintenance energy requirements and potentially causing inhibition of specific enzyme reactions (Sprott and Patel, 1986; Kayhanian, 1999).

Deublein and Steinhauser (2011) pointed out that  $\text{NH}_4^+$  inhibition increases with pH, for instance, the ammonium: ammonia ratio is 99: 1 at pH 7 and 70: 30 at pH 9. It leads to loss of potassium by methanogens and has a reciprocal effect with  $\text{Ca}^{2+}$  or  $\text{Na}^+$ .

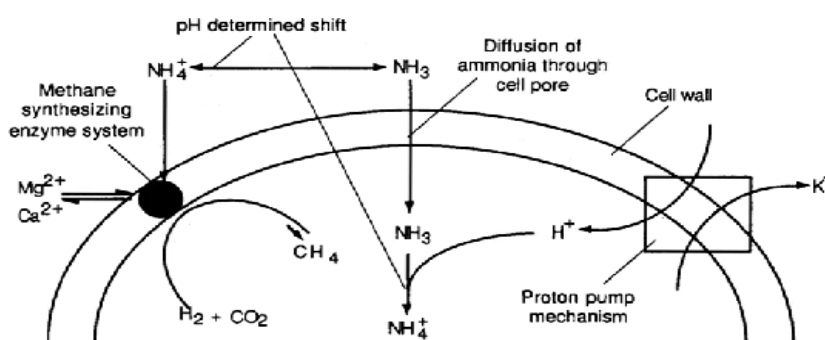


Figure 2-16: Proposed mechanism of ammonia inhibition in methanogenic bacteria

(Kayhanian, 1999)

Early research (Koster and Lettinga, 1984; Hashimoto, 1986; Sawyer and Carty, 1994) has also reported process inhibition due to total ammonia nitrogen (TAN) concentration. TAN is a combination of ammonium nitrogen ( $\text{NH}_4^+$ ) and free ammonia nitrogen ( $\text{NH}_3$ ) (Kayhanian, 1999).

The relationship between FAN, TAN with pH and temperature is given below:

$$NH_3 = \frac{TAN \times \frac{K_a}{[H]}}{\frac{K_a}{[H]} + 1} \quad \text{Eqn 2-9}$$

Where,  $\text{NH}_3$  = free ammonia nitrogen concentration,  $\text{mg l}^{-1}$ , TAN = total ammonia nitrogen concentration,  $\text{mg l}^{-1}$ ,  $K_a$  = temperature dependent dissociation constant ( $0.564 \times 10^{-9}$  at  $25^\circ\text{C}$ ,  $1.097 \times 10^{-9}$  at  $35^\circ\text{C}$ , and  $3.77 \times 10^{-9}$  at  $55^\circ\text{C}$ ,  $[H]$  = hydrogen ion concentration =  $10^{-\text{pH}}$

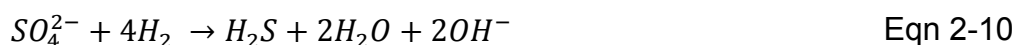
The FAN concentration is controlled by TAN, pH, dissociation constant  $K_a$  influence by temperature, hence to limit the inhibitory effect of FAN on anaerobic bacteria it is recommended to operate the digesters at pH around 7 (Kayhanian, 1999). From Eqn 2-9, the concentration of FAN at a given pH and temperature is six times higher for thermophilic than mesophilic digester (Kayhanian, 1999). The inhibitory levels of total ammonia concentration causing a 50% decrease in the methane production range from 1.7 to  $14 \text{ g L}^{-1}$  (Chen *et al.*, 2008).

### 2.12.3 Sulphur compounds

Sulphur is a nutrient required by methanogens (O'Flaherty and Colleran, 1999) and exist in various forms in AD system: sulphate ( $\text{SO}_4^{2-}$ ), sulfide ( $\text{S}^{2-}$ ), hydrogen sulfide in the gas and undissociated in the liquid phase ( $\text{H}_2\text{S}$ ) and hydrogen sulfide in dissociated form ( $\text{HS}^-$ ,  $\text{S}^-$ ) (Deublein and Steinhauser, 2011). In AD reactors, sulphate is reduced to sulfide by sulphate-reducing bacteria (SRB) (Chen *et al.*, 2008). The reduction is carried out by two main groups of SRB: incomplete oxidizers which reduce compounds to acetate and  $\text{CO}_2$  and complete oxidizers which convert the acetate completely to  $\text{CO}_2$  and  $\text{HCO}_3^-$  (Chen *et al.*, 2008). The SRB utilizes sulphate as terminal electron acceptor, competing with acetogens and methanogens for substrates such as propionate, butyrate,

ethanol, acetate, and H<sub>2</sub>/CO<sub>2</sub> (Oude Elferink *et al.*, 1994). The affinity of SRB for reduced substrates has been ranked in the order of H<sub>2</sub> > propionate > other organic electron donors (Laanbroek *et al.*, 1984). Both methanogenesis and sulphate reduction has been thought to occur simultaneously but the methanogens could not compete for H<sub>2</sub> in the presence of SRB (Oremland and Taylor, 1978). The SRB in the presence of excess sulphate is generally believed to outcompete other anaerobes because of their growth and thermodynamic properties (O'Flaherty *et al.*, 1998). In general, sulphate reducers have better growth kinetic properties than methanogens, other factors of importance in the competition are an affinity for sulphate of sulphate reducers, adherence properties, relative numbers of bacteria mixed substrate utilization, and reactor conditions such as pH, temperature, and sulfide concentration (Oude Elferink *et al.*, 1994). During sulphate reduction, two-phases of inhibition have been recognized: primary inhibition where there is a competition for organic and inorganic substrates form SRB, hence suppressing methane production (Harada *et al.*, 1994), and secondary inhibition, resulting from H<sub>2</sub>S toxicity to various bacteria groups (Colleran *et al.*, 1998). H<sub>2</sub>S is not only toxic to methanogens but also to the SRB (McCartney and Oleszkiewicz, 1991; Okabe *et al.*, 1995; Appels *et al.*, 2008; Luque *et al.*, 2011), thus the concentration of H<sub>2</sub>S is controlled by the competition between SRB and other anaerobes (Chen *et al.*, 2008).

Sulphate reduction is problematic because H<sub>2</sub>S which is inhibiting to the process develops in a stage before methane formation, Eqn 2-10 (Deublein and Steinhauser, 2011).



Sulphate might also inhibit methane-formation because the SRB require less energy than methane forming bacteria and don't need a symbiosis partner hence they dominate. Generally it is assumed the neutral undissociated H<sub>2</sub>S molecule is the agent of toxicity, since it is membrane permeable only in this form (Reis *et al.*, 1991; Speece, 1996a), causing denaturation of proteins and interfering with the assimilatory metabolism of sulphur (Boe, 2006; Chen *et al.*, 2008). H<sub>2</sub>S formed in

AD process escapes as a gas which equilibrates between undissociated and dissociated form in the substrate as weak acid depending on pH, Eqn 2-11. The pH of the system determines what fraction of the total sulphide concentration is present in the undissociated form (Okabe *et al.*, 1995; O'Flaherty *et al.*, 1998). At pH 8 most total sulfide is in the (HS<sup>-</sup>) form while at pH 6 most is in the H<sub>2</sub>S form (Okabe *et al.*, 1995). As the pH decreases dissolved H<sub>2</sub>S increases and act directly as cellular poison even at a concentration of 50 mg L<sup>-1</sup> (Deublein and Steinhauser, 2011). Concentrations as low as 0.003 – 0.006 mole/l total S or 0.002 – 0.003 mole/l H<sub>2</sub>S have been reported to be inhibitory to the micro-organism (Boe, 2006), although at a concentration of 150 mg/l sulphide possible stable methanogens has been stated to occur (Appels *et al.*, 2008)

H<sub>2</sub>S also cause inhibition by indirectly precipitating essential trace elements as insoluble sulfides and increases in toxicity strength as the temperature increases (Deublein and Steinhauser, 2011). The occurrence of sulphate reduction during AD process is unappealing because of reduction in methane yield and problems of corrosion, malodour, and toxicity caused by H<sub>2</sub>S, where the toxicity causes severe process disturbance and, in extreme cases, complete process failure (O'Flaherty and Colleran, 1999). The optimal level of sulphur reported in the literature varies from 1 to 25 mg S/L (Scherer and Sahm, 1981b) and the toxicity of H<sub>2</sub>S to anaerobic bacteria reported varies from of 50 – 125 mg H<sub>2</sub>S/L at pH 7 – 8 for suspended sludge and 250 mg H<sub>2</sub>S/L and 90 mg H<sub>2</sub>S/L at pH 6.4 – 7.2 and pH 7.8 – 8.0, respectively (Chen *et al.*, 2008).

#### 2.12.4 *Total Volatile fatty acids (TVFAs)*

For a long time, it has been recognized that the VFA concentration is one of the most important parameters for the accurate control of anaerobic digestion (Ahring *et al.*, 1995). Several authors (Hill *et al.*, 1987; Ahring *et al.*, 1995; Bjornsson *et al.*, 2000), have also shown, volatile fatty acids (VFAs) as a good control parameter/indicator of process imbalance in AD process, because they are indicative of the activity of the methanogenic consortia (Madsen *et al.*, 2011). Also as a product of fat degradation both VFAs and LCFAs have been noted as inhibitors of methanogenic activity, because they cause a decrease in pH (Demirbas, 2009a). VFAs are produced as intermediate compounds in an AD,

which are important in the metabolic pathway of methane fermentation and causes microbial stress if present at high concentrations, resulting in a reduction in pH and can lead ultimately to reactor failure (Buyukkamaci and Filibeli, 2004; Khanal *et al.*, 2010). The intermediate compounds produced are mainly acetic, propionic, butyric and valeric acids, with acetic and propionic acids being the main VFAs dominating (Buyukkamaci and Filibeli, 2004). The VFAs produced are degraded by proton-reducing acetogens in synergy with hydrogen-consuming methanogens (Mechichi and Sayadi, 2005). This is because, under anaerobic methanogenic conditions, VFA oxidation is thermodynamically unfavorable unless there is a coupling of the oxidation with consumption of reducing equivalents (hydrogen or and formate) (Schink, 1997). Accumulation of VFAs in the anaerobic digester reflects a kinetic uncoupling between the acid producers and consumers (Ahring *et al.*, 1995; Mechichi and Sayadi, 2005), sometimes interpreted as organic overload or inhibition of the methanogenic microbial communities (Madsen *et al.*, 2011), due to the influence of variation in temperature, organic loading rates, or the presence of toxic compounds (Mechichi and Sayadi, 2005).

VFAs exits partly in dissociated and undissociated forms, with the undissociated acids having an inhibiting effect, because they can penetrate as lipophilic into cells, denaturing the cell protein (Deublein and Steinhauser, 2011). Boe (2006) pointed out that VFAs toxicity is due to the undissociated form which can flow freely through the cell membrane where they dissociate, hence causing a pH reduction and a disruption of homoeostasis. A propionic acid concentration of 5 mg L<sup>-1</sup> is strongly inhibitory, this corresponds to about 700 mg l<sup>-1</sup> undissociated acids at pH 7 while isobutyric or isovaleric acid the inhibiting threshold is 50 mg l<sup>-1</sup> for undissociated acid (Deublein and Steinhauser, 2011).

During AD process, LCFAs which formed from the degradation of fat and lipids are reduced to acetate and hydrogen through  $\beta$ -oxidation by proton-reducing acetogens (Alves *et al.*, 2001; Boe, 2006). The LCFAs are inhibitory at low concentrations to Gram-positive bacteria but not Gram-negative bacteria (Chen *et al.*, 2008). LCFA toxicity results from its adsorption onto the cell wall or cell membrane where it interferes with transport and/or protective cells functions

(Alves *et al.*, 2001). When a layer of LCFA sorbs onto a biomass it leads to the flotation of sludge and sludge washout (Chen *et al.*, 2008).

The VFA/Alkalinity ratio is used to monitor the stability of the anaerobic process. It is a critical parameter and serves for fast evaluation of the digesters (Deublein and Steinhauser, 2011). It is also known as the FOS: TAC ratio and indicates the quantity of volatile organic acid (FOS) in relation to the buffer capacity of carbonate (i.e. total alkaline carbonate) (Deublein and Steinhauser, 2011). Stable processes have a ratio between 0.1 - 0.25 without acidification risk, beyond 0.3-0.4 indicates the digester is upset, due to hyperacidity in the digester (Deublein and Steinhauser, 2011) and a ratio of 0.8 and above, there is significant pH reductions and inhibition of methanogens, resulting in digester failures (Khanal, 2009).

#### 2.12.5 *Heavy metals*

Heavy metals are part of the essential enzymes that drive numerous anaerobic reactions (Chen *et al.*, 2008). Heavy metals can be stimulatory, inhibitory, or even toxic for biochemical reactions, depending on their concentrations (Li and Fang, 2007; Altaş, 2009), chemical forms of the metals, and process-related factors such as pH and redox potential (Lin and Chen, 1999; Zayed and Winter, 2000). An Analysis of ten methanogenic strains showed the following order of heavy metal composition in the cell:  $Fe \geq Zn \geq Ni > Co = Mo > Cu$  (Takashima and Speece, 1989). Generally, heavy metals are considered as toxic compounds that inhibit the growth of micro-organisms (Leduc *et al.*, 1997), even though their growth and cell synthesis are often stimulated by the presence of trace amounts of selected metals (Gikas and Romanos, 2006). Figure 2-17, by McCarthy, demonstrates the effect of these phenomena (stimulatory, inhibitory, toxic) beautifully into three zones (Gikas and Romanos, 2006).



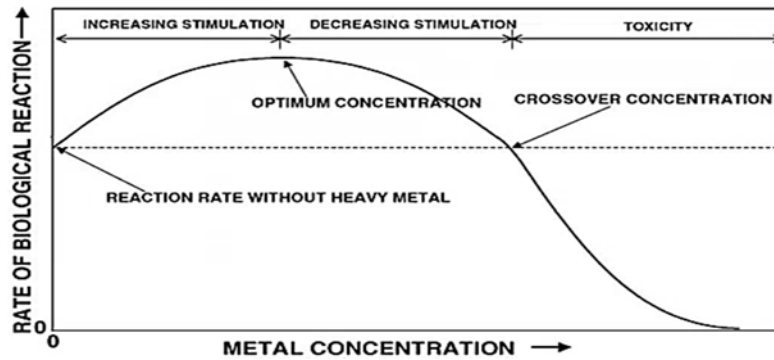


Figure 2-17: Effect of heavy metal concentration on biological reactions by McCarthy (Gikas and Romanos, 2006).

Certain minimal amount of trace metal is required by enzymes and co-enzymes for their activation and functioning but if present in large amounts, they lead to inhibition or toxicity of microorganism (Altaş, 2009). The inhibition is due to chemical binding of heavy metals to the enzymes and the subsequent disruption of the enzyme structure and activities (Li and Fang, 2007). A distinct characteristics feature of heavy metals is that, unlike many other toxic substances, they are not biodegradable and can accumulate to potentially toxic concentrations (Takashima and Speece, 1989). Critical inhibitory concentrations of metals have been listed by some authors (Turovskiĭ, 2006; Appels *et al.*, 2008).

### 2.12.6 Light metals

The most common salts of light metal ions found in the AD process are sodium, potassium, calcium, and magnesium (Turovskiĭ, 2006; Chen *et al.*, 2008). These are cations of the salts in solution which determines predominately the toxicity of salts (Chen *et al.*, 2008). They are released in AD digesters by the breakdown of organic biomass or added as chemicals for pH adjustment (Grady Jr *et al.*, 2011). Salt toxicity is well studied in biological systems, with high salt level causing bacterial cells to dehydrate due to osmotic pressure (de Baere *et al.*, 1984). While they are needed for microbial growth and, consequently, affect specific growth rate like any other nutrient, concentrations that are moderate stimulate microbial growth, excessive amounts retard growth, and even higher

concentrations can cause severe inhibition or toxicity (Appels *et al.*, 2008; Chen *et al.*, 2008).

#### 2.12.7 Sodium

Sodium (Na<sup>+</sup>) is essential for methanogens at low concentration, probably because of its role in the formation of adenosine triphosphate or in the oxidation of NADH (Dimroth and Thomer, 1989; Appels *et al.*, 2008), but at a high concentrations it inhibits the activity of the micro-organisms and interferes with their metabolism (Feijoo *et al.*, 1995; Mendez *et al.*, 1995). In literature, reported sodium concentrations range of 100 – 200 mg L<sup>-1</sup> is said to be beneficial for the growth of mesophilic anaerobes (Chen *et al.*, 2008). Compared to other metal cations, sodium proved to be the strongest inhibitor on a molar basis (de Baere *et al.*, 1984). Sodium shows moderate inhibition at 3.5 - 5.5 g L<sup>-1</sup> and strong inhibition at 8 g L<sup>-1</sup> (de Baere *et al.*, 1984; Turovskii, 2006; Appels *et al.*, 2008; Chen *et al.*, 2008). Sodium concentration of 6.3, 11.3, and 18.7 g L<sup>-1</sup>, respectively, have been shown to cause inhibition of 10%, 50%, and 90% during anaerobic digestion of *Sargassum sp.* (Zhang *et al.*, 2017b).

#### 2.12.8 Potassium

K<sup>+</sup> toxicity is due to high concentrations of extracellular potassium which leads to the passive influx of K<sup>+</sup> ions in a cell where it neutralizes the membrane potential (Chen *et al.*, 2008). The concentration of K<sup>+</sup> below 400 mg L<sup>-1</sup> has been reported to enhance both mesophilic and thermophilic digesters (Chen *et al.*, 2008). Potassium shows moderate inhibition at 2.5 - 4.5 g L<sup>-1</sup> and strong inhibition at 12 g L<sup>-1</sup> concentration levels respectively (Turovskii, 2006).

### 2.13 Anaerobic digestion of macroalgae biomass for biogas production.

Macroalgae can be converted to biofuels from thermal, fermentation and various other processes (Montingelli *et al.*, 2015). Anaerobic digestion is the most direct route to obtaining biofuels from macroalgae (Hughes *et al.*, 2012). Jung *et al.* (2013) stated that biogas specifically methane has been produced from AD.

Knowledge of the chemical composition of an algal biomass enables calculations of the methane potential and ammonium yields that can be obtained from AD processes (Angelidaki and Sanders, 2004). The use of algal biomass as feedstock for biogas production has certain limitations which must be taken into account during anaerobic digestion. These are mostly feedstock-related obstacles (Montingelli *et al.*, 2015). For instance, algae have higher water content compared to terrestrial energy crops, hence suitable for wet AD process (Burton *et al.*, 2009; Chen *et al.*, 2015), but the elevated moisture content can result to the use of low organic loading rate (OLR) and short-term storage of the biomass (Bruhn *et al.*, 2011b; Nielsen and Heiske, 2011). Factors such as slow rate of conversion (10 - 30 days), incomplete digestion of algal cells, high sensitivity to fluctuations of operational and environmental conditions in AD process has also been pointed out (Dāsa, 2015). Yet, the need to breakdown the cells walls through pre-treatment (physical and chemical) for easier digestibility, inhibition as a result of inherent metal content (Chen *et al.*, 2015), which causes reactor fouling (Teh *et al.*, 2017), has also been highlighted. Algal biomass is rich in nutrient such as carbon, nitrogen, and phosphorus (Montingelli *et al.*, 2015), but affected by wide variation in nutrient content as a result of environmental factors such as seasonal or ecological changes (Marinho-Soriano *et al.*, 2006; Jung *et al.*, 2013). These seasonal variations in their composition have an impact on the potential of macroalgae as a biofuel feedstock (Adams *et al.*, 2011a; Bruhn *et al.*, 2011a). Another, drawback from this variation is the low C: N ratio which is regarded as an important limitation in AD process (Yen and Brune, 2007a). This has been earlier highlighted in section 2.11.5. The effect of low C: N ratio from mono-digestion of macroalgae such as accumulation of high VFA, and chloride (Tabassum *et al.*, 2017), is overcome by co-digestion with other feedstocks to improve the C:N ratio. Various feedstocks (glycerol, cattle manure, dairy slurry, bovine slurry, waste frying oil, and wheat straw) has been used in co-digestion studies with macroalgae (Tabassum *et al.*, 2017).

Other factors identified that affects algal biomass for biogas production include carbohydrate, lipids and protein, ash and lignin content (Montingelli *et al.*, 2015). Brown algae, for instance, lack easily fermentable sugars (Burton *et al.*, 2009), hence pretreatment is needed in order to break the polysaccharides into

monomers to enhance hydrolysis in the AD process (Montingelli *et al.*, 2015). Both the red and green seaweeds have high levels of easily fermentable sugars.

The degradation pathway of algae biomass component to biogas during AD process is influenced by difference in species but primarily since cellulose hydrolysis which is a common component among the species is slow, and inhibited by other associated structural constituent (alginate, fucoidan, proteins), for macroalgae, digestibility is determined by specific carboxylated, sulphonated and methylated polysaccharides, lipids, mannitol and proteins (Dāsa, 2015).

Dāsa (2015) stated that among the four major components (Alginate, laminarin, fucoidan and mannitol) found in brown seaweed, the final products of alginate degradation during AD is glyceraldehyde-3-phosphate and pyruvate, while laminarin is the formation of butyrate and other VFA, mannitol is the formation of hydrogen and acetate as the major products, with ethanol, formate, lactate and succinate as minor products whereas there is no clear cut products reported for fucoidan as the molecular structure of particular strains makes the AD of fucans difficult.

Energy returns with respect to methane yield per mass of macroalgae feedstock has been previously reported as are low compared to terrestrial crops (Nallathambi Gunaseelan, 1997; Nielsen and Heiske, 2011). Reports by Jung *et al.* (2013) shows macroalgae ( $0.31 - 0.48 \text{ m}^3 \text{ CH}_4 \text{ kg}^{-1}$ ) digestion per volatile solid exhibited higher methane yield compared to land-based biomass such as wood ( $0.32 - 0.42 \text{ m}^3 \text{ CH}_4 \text{ kg}^{-1}$ ) and grass ( $0.34 - 0.42 \text{ m}^3 \text{ CH}_4 \text{ kg}^{-1}$ ). Factors such as unsuitable C: N ratio and inhibitory high salt, heavy metal and sulphate content bioaccumulated in the macroalgae often breed conditions leading to low methane yields obtained from AD processes (Peu *et al.*, 2011; Hughes *et al.*, 2012; Migliore *et al.*, 2012). The higher methane yield exhibited by the macroalgae is partly due to the low lignin content (Shobana *et al.*, 2017), which is as low as 0.03 g/kg dry weight and in some instance pre-treatment (Chen *et al.*, 2015), makes it easier for fermentation to biogas. Since, the cellulose, protein and intracellular polysaccharides of the macroalgae are not freely available for use by the microorganism during AD, pre-treatment helps to release these sugars, reduce inhibitory substances and enhance the access of the microorganisms to the

sugars leading to increased biogas yield (Radha and Murugesan, 2017). This results in accelerated hydrolysis which is the rate limiting step (Bux and Chisti, 2016).

## 2.14 Toxicity to macroalgae digestion

### 2.14.1 Polyphenols

Phlorotannins are antimicrobial compounds produced by certain seaweed that may inhibit sustained anaerobic digestion (Hierholtzer *et al.*, 2013; Hinks *et al.*, 2013). The successful anaerobic degradation of brown seaweed has been found to be dependent on the concentration of phenolic compounds present and their bactericidal effect on micro-organism (Hierholtzer *et al.*, 2013). The degradation pathway of phloroglucinol under anaerobic conditions is assumed to be the formation of phenol intermediate by the removal of a ring substituent, followed by ring fission and formation of cyclohexanol and cyclohexanone (Hierholtzer *et al.*, 2013), yielding organic acids metabolites that are converted to methane (Young and Rivera, 1985). High polyphenol content is associated with low decay and biodegradability index values (Tabassum *et al.*, 2017). It has been reported that there is variation in polyphenol content in seaweed within a year (Apostolidis *et al.*, 2011; Tabassum *et al.*, 2016c), which depends on the location, harvesting time, temperature, light intensity, and nutrients (Parys *et al.*, 2009). The concentration of polyphenol in *L. digitata* has been reported as 11 mg g<sup>-1</sup> and at a concentration of 1.0 g L<sup>-1</sup>, 20% methane inhibition has been observed (Hierholtzer *et al.*, 2013). Values between 30.2 – 49.4 mg g TS<sup>-1</sup> and inhibitory range of 0.2 – 1.3 g L<sup>-1</sup> reported for *Ascophyllum nodosum* (Tabassum *et al.*, 2016c).

### 2.14.2 NaCl toxicity

The effect of Na<sup>+</sup> on AD process has earlier been stated in Section 2.12.7. Salinity particularly due to sodium divalent cations impacts negatively on microorganism in AD process (Ward *et al.*, 2014). For seaweed AD, chloride concentration is of interest in mono-digestion processes (Tabassum *et al.*, 2016a), as studies have shown the concentration of chloride in the digesters

increase with increase in digestion time (Allen *et al.*, 2014; Tabassum *et al.*, 2016a; Tabassum *et al.*, 2017). One route through which Na inhibition occurs is via gradual increase and accumulation of propionate acid which causes pH imbalance and eventual digester failure (Zhang *et al.*, 2012a). There are a wide disparity in reported chloride inhibition ( $5 - 20 \text{ g L}^{-1}$ ) levels for AD due to the variable substrate type (Lefebvre *et al.*, 2007). For mono-digestion of *L. digitata*,  $11 \text{ g L}^{-1}$  has been reported as inhibitory whereas  $> 14 \text{ g L}^{-1}$  in an acclimatization inoculum experienced stable gas production for mono-cultivated *S. latissima* (Tabassum *et al.*, 2016a). Methanogens have been found to acclimatise to salinity concentration up to  $15 \text{ g L}^{-1}$  (Mottet *et al.*, 2014). Low OLR and ammonia concentration have been reported as conditions factorable to higher salt tolerance for AD process (Lefebvre *et al.*, 2007; Hierholtzer and Akunna, 2012).

## 2.15 Organic fraction of municipal solid waste (OFMSW)

One of the direct results of increased population and urbanization is a high solid waste generation. On the average, the rate of solid waste generation is  $0.77 \text{ kg/person/day}$  in 23 developing countries and is still increasing. In 2006, the worldwide municipal solid waste generation was about 2 billion tons per year, projected to increase by 51% to about 3 billion tons by 2025 (Charles *et al.*, 2009). In Europe, an estimated 3,000 million tons of waste are generated annually (European Environment Agency., 2003). Out of this number, 60 million tons of recyclable organic waste is collected separately from households and food industries (Nayono *et al.*, 2009). Organic waste from mainly food waste is a very attractive and potential feedstock for anaerobic digestion due to its high fraction in waste generation (Khairuddin *et al.*, 2016). Anaerobic digestion (AD) of the organic fraction of municipal solid waste (OFMSW) offers the advantage of both a net energy gain by producing methane as well as the production of a fertilizer from the residuals (Hartmann and Ahring, 2005). One of the biotechnologies developed in the last years to utilize municipal solid wastes (MSW) for useful energy and materials recovery is anaerobic digestion (Sans *et al.*, 1993). Anaerobic digestion is widely applied to treat these diverse ranges of organic waste promoting better landfill management and produces a potential renewable energy source. The EU directives are geared towards diverting

organic waste from landfill with energy consumption targeted from renewable energy (Cogan and Antizar-Ladislao, 2016). The European landfill directive requires member state to take steps required to reduce the quantities of biodegradable municipal waste going to landfill from 75 to 50 and to 35% of the total amount of biodegradable waste produced in 1995 by weight, in periods of 5, 8 and 15 years after 2001 respectively (Luning *et al.*, 2003). Food waste is a highly desirable substrate for anaerobic digestion with regards to its high biodegradability and methane yield (Zhang *et al.*, 2012b). Food waste is defined as materials that result from the processing, storage, preparation, cooking, handling, or food residual (Zhang *et al.*, 2007), from residences, commercial and industrial institutions. The characteristics of food waste that makes it a good co-substrate has been highlighted by Nayono *et al.* (2009): 1) The concentration of the organic substances should be comparable with biowaste, so that addition will not change significantly loading and hydraulic retention time, 2) The waste should consist of easily degradable organics with a high biogas production potential, 3) it should not contain any dangerous or poisonous substances, which hinder anaerobic digestion 4) it must be available in sufficient quantities at a reasonable price and should be storable 5) it should be pumpable without danger of clogging.

The typical food waste contained 69 - 93% moisture, 7 – 31 wt% of total solids (TS), volatile solids to total solids ratio (VS/TS) of 85 - 96%, and carbon to nitrogen ratio (C: N) of 14.7 – 36.4: 1 (Zhang *et al.*, 2007; Zhang *et al.*, 2011).

## 2.16 Co-digestion of Macroalgae with OFMSW.

Anaerobic co-digestion is regarded as a more favourable option for increasing biogas production because of balanced nutrients and improved efficiency (Mao *et al.*, 2017). In anaerobic digestion, co-digestion or co-fermentation is a term used to describe waste treatment techniques in which different wastes with complementary characteristics are mixed and treated together (Ağdağ and Sponza, 2007; Khalid *et al.*, 2011). Co-digestion of several wastes has been increasingly applied in an effort to boost plant profitability (Angelidaki *et al.*, 1999). Macroalgae have been identified as feedstock with sustainable potential for co-digestion with food waste having positive environmental and health

benefits (Cogan and Antizar-Ladislao, 2016). Generally, OFMSW is a very attractive waste for the biogas plants as they are dependent on the addition of organic waste with a high biogas potential (Hartmann and Ahring, 2005). Khalid *et al.* (2011) stated that co-digestion is preferably used for improving yields of anaerobic digestion of solid organic wastes due to its numeral benefits: dilution of toxic compounds, increased load of biodegradable organic matter, improved balance of nutrients, synergistic effect of microorganisms and better biogas yield are the potential benefits that are achieved in a co-digestion process. It improves the C: N ratio and decreases the concentration of nitrogen. While dedicated digesters using macroalgae for biogas production are scarce and practically non-existent in the UK, there is a steady growth of industrial-scale anaerobic digesters using food waste as part or mono-feedstock (Cogan and Antizar-Ladislao, 2016). These infrastructures can be leveraged upon for co-fermentation as digestion of either macroalgae or food waste alone has certain inherent disadvantages that often leads to process instability and or reactor failure. However, co-digestion of their feedstocks can overcome these interferences which causes inhibition of biogas production. For macroalgae which were once regarded as a “silver bullet” with potential as an alternative to fossil fuels (Aitken and Antizar-Ladislao, 2012), large-scale cultivation can offer positive energy returns when juxtaposed with other biofuel processes (Aitken *et al.*, 2014). Methane production rate has been improved up to 26% by co-digesting macroalgae *Ulva spp.* with manure and waste activated sludge (Costa *et al.*, 2012)

Food waste has been used as a co-substrate in a biowaste digester for equilibration of biogas production because of its steady availability, similar biodegradability and high methane potential (Nayono *et al.*, 2009). Several studies have reported co-digestion of the organic fraction of municipal solid waste with other feedstocks, such as sewage sludge (Xie *et al.*, 2017a), grease trap sludge (Grosser *et al.*, 2017), swine manure (Vallejo *et al.*, 2017), energy crops manure (Nordberg and Edstroem, 2005). Work carried out by Hartmann and Ahring (2005) investigated thermophilic anaerobic co-digestion of the organic fraction of municipal solid waste (OFMSW) with manure, achieving VS reduction of 69 – 74% when treating 100% OFMSW and all other co-digestion experiments,



none of the processes showed signs of inhibition at the free ammonia concentration of 0.45 – 0.62 g N L<sup>-1</sup>.

## 2.17 Nutrient requirement for anaerobic digestion.

Nutrients are needed for all forms of life for their preservation and growth (Zandvoort *et al.*, 2006). In anaerobic digestion processes, the nutrients required by various methane-forming bacteria are classified into macronutrients and micronutrients. Whereas the macronutrients such as carbon, nitrogen, phosphorus, and sulphur are required in large quantity, micronutrients are also known as trace elements, for example, cobalt, molybdenum, nickel, iron tungsten, and selenium are required in relatively small quantities by most bacteria (Gerardi, 2003). Trace metals (elements) are a necessary nutrient for all microorganism and important for optimal cell metabolism (Speece, 1996a; Zhang *et al.*, 2012b; Bohutskyi and Bouwer, 2013). A trace element is defined as “any chemical element that occurs in very small amounts in organisms but is essential for many physiological and biochemical processes” (Zandvoort *et al.*, 2006). These essential trace elements are mostly metals and are often present in the enzyme system as part of a cofactor or they are of vital importance for the enzyme system (Newman and Kolter, 2000). On non-enzymatic forms, metals are involved in microbial respiration processes either with an electron transfer bound to the cell wall or extracellular electron acceptors (Newman and Kolter, 2000). The incorporation of micronutrients in enzyme systems is essential to ensure not only proper degradation of a substrate but also an efficient operation of the digester (Gerardi, 2003). Anaerobic digestion and microbial growth depend on the availability and/or optimal supply of these nutrients (Demirel and Scherer, 2011).

The coenzymes are metal-laden organic acids that are incorporated into enzymes and allow the enzymes to work more efficiently. Coenzymes that are unique to methane-forming bacteria are coenzyme M and the nickel-containing coenzymes F420 and F430. Coenzyme M is used to reduce carbon dioxide to methane. The nickel-containing coenzymes are only found in methanogenic bacteria (Bohutskyi and Bouwer, 2013), and are important hydrogen carriers (Gerardi, 2003). Copper and cobalt are constituents of B<sub>12</sub>-enzyme which

catalyses the methanogens and molybdenum and selenium are subcomponents of formate dehydrogenase (Bohutskyi and Bouwer, 2013). The coenzymes are components of energy-producing electron transfer systems that obtain energy for the bacterial cell and remove electrons from degraded substrate (Gerardi, 2003).

Macro and micronutrients are required for the stable growth of anaerobic microorganisms (Gerardi, 2003). For the macronutrients, the approximate ratio of carbon to nitrogen and phosphate should be in the range of 75:5:1 to 125:5:1 (Lee, 2013). Trace metals such as iron, nickel, cobalt, molybdenum, zinc, selenium, copper, boron, manganese and tungsten have been shown to be stimulatory to methanogens (Speece, 1996a), and are necessary for stable AD in the mg/L level (Kida *et al.*, 2001). A literature survey about the stimulatory ranges of trace metals for anaerobic digestion of biomass for Co, Fe, Mo, Ni, and Se was reported to be 0.05-0.19, 0-0.39, 0.16-0.3, 0.11-0.25, and 0.062 mg kg<sup>-1</sup>, respectively (Demirel and Scherer, 2011). It has been reported Fe, Co and Ni are required at the rates of 0.02, 0.04 and 0.003 mg/gm acetate respectively (Speece, 1996a). The unavailability of these elements in biogas digesters is probably the first reason of poor process efficiency without any other obvious reason (Demirel and Scherer, 2011). Methane-forming bacteria are able to easily remove or “harvest” micronutrients from bulk of a solution through the production and excretion of extracellular “slime” that chelates and transports the nutrients into the cell. The use of extracellular slime permits “luxury” uptake of micronutrients, that is, the removal and storage of nutrients beyond the quantity that is needed (Gerardi, 2003).

Various researchers have studied the effect of trace metals on AD process. In their work on mesophilic digestion of *Napiergrass*, Wilkie *et al.* (1986) reported a 40% increase methane production and a significant decreased in the VFA concentration by daily addition of micronutrients (nickel, cobalt, molybdenum, selenium, and sulphate). The addition of both macro (N, K, P, and S) and micronutrients (Co, Cu, Fe, Mo, Ni, Se, W and Zn) during thermophilic pilot-scale digestion of the OFMSW helped to elevate the gas production rate by 30% and increase the stability of the digesters (Kayhanian and Rich, 1995). Zhang *et al.* (2010b) stated that selenium, molybdenum, and tungsten are essential trace

elements for certain enzyme catalysing reactions, such as formate dehydrogenase (FDH) which is crucial for propionate oxidation, hence important for AD process.

## 2.18 Kinetic Models for biogas production

Kinetic analysis is an effective way in determining the key steps in anaerobic digestion process (Fang, 2010), which helps in pilot plants to provide insight for reactor designs and operations leading to more efficient process performance and reduce reliance on skilled operators (Page *et al.*, 2008). Kinetic models are divided into two classes; structural and un-structural models (Page *et al.*, 2008) whereas the former considers metabolic pathways making it generally complicated, the latter is simpler (Mu *et al.*, 2007b). The application of the un-structural models such as the first order, Monod and Gompertz equation on anaerobic digestion of macroalgae and food waste is presented in this work.

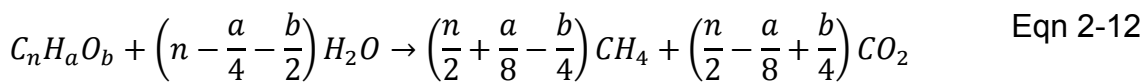
### 2.18.1 *Mathematical models*

Mathematical modeling of anaerobic digestion process was motivated by the need for efficient operation of AD systems in the early 70's (Donoso-Bravo *et al.*, 2011). Models using the kinetics of microorganisms growth and chemical reactions to predict the behavior of system have long been reported (Kythreotou *et al.*, 2014). Currently a variety of scientific models have been developed as a result of the complexity of AD process designed for different purposes. One common feature among the models is they predict and calculate biogas and methane production rate, which are both very important parameters for design of an efficient biogas plant (Kythreotou *et al.*, 2014). Some of the most applied models are presented below.

### 2.18.2 *Theoretical biogas yield*

This model is used to estimate the potential theoretical biogas yield from the chemical composition of a feedstock. The model uses the basic elements or components of an organic matter in estimating only the production of methane and carbon dioxide (Kythreotou *et al.*, 2014). According to Buswell and Mueller

(1952), using Eqn 2-12, if the chemical composition of the organic matter is known, methane and carbon dioxide can be calculated with an uncertainty of about 5%. This does not take into consideration the breakdown of the organic matter for bacteria metabolism including synthesis of cell mass, energy for growth and maintenance (Kythreotou *et al.*, 2014). Fully degraded glucose ( $C_6H_{12}O_6 \rightarrow 3CH_4 + CO_2$ ) gives about 50% methane (by weight at STP) from this relationship (Kythreotou *et al.*, 2014).



### 2.18.3 Reaction kinetics model

Processes can be distinguished into continuous and discontinuous (batch) based on substrate load to the reactors. In continuous process, substrate continuously flows in and out of a system resulting in a constant gas production (steady state), where microorganism growth requirement becomes constant over time whereas the discontinuous process, the system is feed once, subsequently substrate degradation and gas production change over the retention time whereby the requirement of microorganisms change permanently (Kythreotou *et al.*, 2014). During batch anaerobic digestion bacteria goes through different phases (Figure 2-18), due to changing concentrations of nutrients and inhibitors. In batch discontinuous process these changing continuous adaption by the bacteria causes the occurrences of small-time lags which corresponds to measurable deviations in kinetic parameters (Yano *et al.*, 1966), hence kinetic parameters describing the growth of bacteria in batch process cannot be applied to continuous processes (Kythreotou *et al.*, 2014).

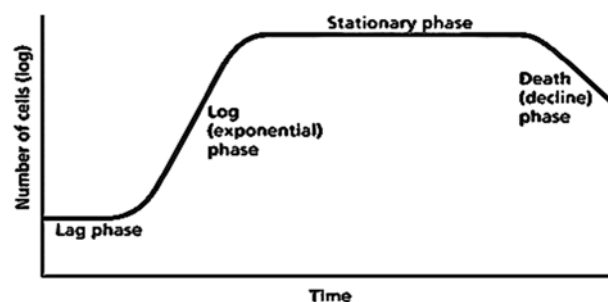


Figure 2-18: Phases of bacteria growth curve

### *Continuous State Model*

The model considers the various reactors as single completely stirred mixed (CSTR), constant volume reactors. In continuous cultures, equations for microorganism growth is well developed and understood (Pretorius, 1969; Metcalf and Eddy, 2003). Applying these equations to the CSTR, a material balance can be written for both the microorganism and substrate as follows;

Material balance for microorganism growth,

$$\begin{aligned} \Delta \text{Change in concentration of cell number in reactor} \\ = \text{cell in influent feed} + \text{growth} - \text{cells in effluent} \end{aligned}$$

This can be rewritten as;

$$V * \frac{dC}{dt} = C_o F + \mu C_t V - C_t F \quad \text{Eqn 2-13}$$

Where  $V$  = reactor volume,  $C_o$  = concentration of microorganism in influent, mass/vol.,  $C_t$  = concentration of microorganism in reactor, mass/vol.,  $F$  = reactor flow rate, vol/time,  $\mu$  is specific growth rate  $\text{time}^{-1}$ .

Since the hydraulic retention can be written as  $\theta = V/F$ , then Eqn 2-13 can be written as;

$$\frac{dC_t}{dt} = \left[ \mu - \frac{1}{\theta} \right] C_t + \frac{C_o}{\theta} \quad \text{Eqn 2-14}$$

Assuming  $C_o = 0$  (there are no organism in the influent), then Eqn 2-14 can also be written as;

$$\frac{dC_t}{dt} = \left[ \mu - \frac{1}{\theta} \right] C_t \quad \text{Eqn 2-15}$$

In steady state conditions  $dC_t/dt = 0$ , then the specific growth rate is equal to the reciprocal of the hydraulic retention time,  $\mu = 1/\theta$  (this control control the growth-rate by varying flow rate).

Relating this to substrate degradation;

$$\begin{aligned} \Delta \text{Change in mass of substrate in reactor} \\ = \text{influent} - \text{consumption} - \text{effluent} \end{aligned}$$

Rewriting this as;

$$V \frac{dS_t}{dt} = S_o F - \frac{\mu C_t V}{Y} - S_t F \quad \text{Eqn 2-16}$$

Where  $V$  = reactor volume,  $S_o$  = concentration of substrate in influent, mass/vol.,  $S_t$  = concentration of substrate in reactor, mass/vol.,  $Y$  = growth yield, Substrate consumed by organisms =  $(\mu C_t V) / Y$ .

For steady state operation, it possible to show by algebraic computation that; (Pretorius, 1969; Metcalf and Eddy, 2003)

$$C_t = Y (S_o - S_t) \text{ and } S_t = \frac{K_s}{\mu\theta - 1}$$

$S_t$  is derived from the relationship of the Michaelis-Menten equation,  $K_s$  is its constant. Calculating  $\mu$ ,  $\theta$  and  $K_s$ , both organism and substrate concentration in the reactor for any value of the residence time  $\theta$  or concentration of the influent substrate  $S_o$  can be evaluated.

### *First order model (discontinues)*

The apparent microbial growth rate can be described using the first –order equation as (Fang, 2010):

$$\frac{dX}{dt} = \mu X \quad \text{Eqn 2-17}$$

This can be rewritten in terms of substrate degradation in exponential form as (Gunaseelan, 2004; Angelidaki *et al.*, 2009) :

$$B = B_o \cdot [1 - \exp(-k \cdot t)] \quad \text{Eqn 2-18}$$

Where  $B$  ( $mL CH_4 g^{-1} VS$ ) is the cumulative methane yield,  $B_o$  ( $mL CH_4 g^{-1} VS$ ) is the ultimate methane yield,  $k$  ( $day^{-1}$ ) is the first order rate constant and  $t$  (d) is the time.

The equation is a linear regression model based on empirical relationship and is used to determine the rate and extent of degradation where the value of  $k$  (*slope of the linear curve*) is the characteristics of a given substrate which gives the time required to generate a ratio of the ultimate methane potential (Angelidaki *et al.*, 2009)

### *The Gompertz model*

The modified Gompertz model have been used to describe microbial growth, substrate degradation and product formation (Zwietering *et al.*, 1990).

$$B = B_0 \cdot \exp \left\{ -\exp \left[ \frac{\mu_{max} e}{B_0} (\lambda - t) + 1 \right] \right\} \quad \text{Eqn 2-19}$$

Where  $B$  ( $mL CH_4g^{-1}VS$ ) is the cumulative methane yield,  $B_0$  ( $mL CH_4g^{-1}VS$ ) is the ultimate methane yield,  $t$  ( $d$ ) is the time,  $\lambda$  is the lag phase and  $\mu_{max}$  is the maximum methane production rate.

The modified Gompertz equation is a non-linear equation, mostly used to account for the lag phase ( $\lambda$ ) duration and the  $\mu_{max}$  biogas production rate (Nopharatana *et al.*, 2007; Angelidaki *et al.*, 2009; Allen *et al.*, 2013a).

### *The Monod model*

Monod (1949) equation is used to express the non-linear relationship between microbial growth and limited substrate concentration. It proposes that the specific growth rate is inversely proportional to substrate concentration, Eqn 2-20 (Kythreotou *et al.*, 2014).

$$\mu = \mu_{max} * \frac{S}{K_S + S} \quad \text{Eqn 2-20}$$

$\mu_{max}$  is the maximum specific growth rate,  $K_s$  is half saturation constant, substrate concentration at 50%  $\mu_{max}$  ( $\mu_{max} / 2$ ).

The Monod model is a bacterial growth model frequently used for biogas production (Kythreotou *et al.*, 2014). Several authors have modified the Monod equation as shown Table 2-4 (Kythreotou *et al.*, 2014), and used it for batch

(Bryers, 1985), batch, steady-state and dynamic processes (Mu *et al.*, 2007a; Lauwers *et al.*, 2013).

Table 2-4: Modified models for bacterial growth

Author	Model
[50]	$\mu = \mu_{\max} \cdot \frac{S}{K_s + S} \cdot \frac{K_p}{K_p + P} \quad (22)$
Holzberg <i>et al.</i> [48]	$\mu = \mu_{\max} - K_1 \cdot (P - K_2) \quad (23)$
Aiba <i>et al.</i> [4]	$\mu = \mu_{\max} \cdot \frac{S}{K_s + S} \cdot \exp(-K \cdot P) \quad (24)$
Bazua and Wilke [15]	$\mu = \frac{S}{K_s + S} \cdot \left( \mu_{\max, P=0} - \frac{a \cdot P}{b - P} \right) \quad (25)$
Ghose and Tyagi [38]	$\mu = \mu_{\max} \cdot \left( 1 - \frac{P}{P^*} \right) \cdot \frac{S}{S + K_s + S^2/K_1} \quad (26)$
Moser [68] and Bergter [17]	$\mu = \mu_{\max} \cdot \frac{S^n}{K_s + S^n} \cdot \frac{K_p}{K_p + P^m} \quad (27)$
Dagley and Hinshelwood [29]	$\mu = \frac{S}{K_s + S} \cdot (1 - K \cdot P) \quad (28)$
Han and Levenspiel [42]	$\mu = \mu_{\max} \cdot \left( 1 - \frac{P}{P^*} \right)^n \cdot \frac{S}{S + K_s \cdot (1 - P/P^*)^m} \quad (29)$

## 2.19 Anaerobic biodegradability assessment

Anaerobic biodegradability (AB) is a terminology now used to describe Biochemical methane potential (BMP) (Guwy, 2004; Rozzi and Remigi, 2004; Raposo *et al.*, 2011a). It is defined as the fraction of compound(s) converted to biogas (methane and carbon dioxide) under oxygen-free conditions mediated by a diverse mixture of microorganisms for an indefinite degradation time. But in practice the degradation time is definite and methane potential estimated from extrapolation of the experimented degradation curve (Angelidaki and Sanders, 2004). AB can be determined by the volume of biogas produced, or the amount of substrate depleted or the formation of intermediates and end products (Guwy, 2004). The biochemical methane potential (BMP) test is the procedure developed to measure the volume of methane produced (Angelidaki *et al.*, 2009; Raposo *et al.*, 2011a). The assay was developed as a standardized method to determine the ultimate biodegradability (Nizami *et al.*) and associated methane yield during the anaerobic methanogenic fermentation of organic substrates (Raposo *et al.*, 2008). It is a proven and reliable method to obtain the extent and rate of organic



matter conversion to methane (Chynoweth *et al.*, 1993). The parameter, ultimate methane potential ( $\lambda_{max}$ ) from the BMP assay is regarded to a great extent as the determining factor for both design and economic details of a biogas plant (Angelidaki *et al.*, 2009). The experimental BMP approach is simple; a characterized (Bird *et al.*, 1990) and quantified organic substrate is mixed with a known anaerobic inoculum in a suitable medium (minerals and water) under defined operating conditions where the gas evolved is quantified by a specified measurement system until gas production virtually ceases (Raposo *et al.*, 2011b). Mixtures of nitrogen (N<sub>2</sub>) 70 - 80% and carbon dioxide (CO<sub>2</sub>) 20 - 30% are used as headspace gas to create anaerobic conditions, these prevent pH - change in the water phase due to CO<sub>2</sub> from the headspace of the reactors (Hansen *et al.*, 2004), pure N<sub>2</sub> alone has been also used (Raposo *et al.*, 2011b). Blank controls are included to account for the biogas produced from the inoculum alone, these are termed endogenous tests (Raposo *et al.*, 2011a). The blank control gives an idea of the volume of biogas produced by the substrate alone (Angelidaki *et al.*, 2009). Glass bottles with rubber septums as closed vessels are normally used (Figure 2-19). The volume of the bottles ranges between 0.1 L - 2 L (Angelidaki *et al.*, 2009) to 0.1 - 120 L (Raposo *et al.*, 2011a), all depending on the homogeneity of the substrate used. It is recommended that samples and blank assay should be carried out in triplicate for statistical significance (Angelidaki *et al.*, 2009) because the BMP assay uses inoculum from different sources with varying quality and these can be relatively heterogeneous (Hansen *et al.*, 2004; Raposo *et al.*, 2011b). Furthermore, the biological approach in determining methane potential leads to substantial uncertainty hence triplicate samples should be used as a minimum (Hansen *et al.*, 2004).

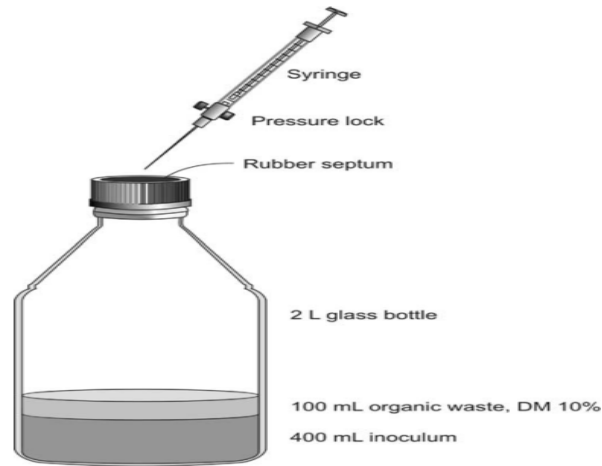


Figure 2-19. Bio-methane potential reactor and sampling illustration (Hansen *et al.*, 2004).

Generally, the anaerobic biodegradability assay is used in triplicate (Angelidaki and Sanders, 2004); to establish biodegradability of substrate for products (biogas /intermediates) formation, determination of the ultimate biogas potential and rate of biodegradation. In the first category, most methods are based on monitoring biogas using gasometric techniques (Angelidaki and Sanders, 2004; Guwy, 2004; Hansen *et al.*, 2004; Angelidaki *et al.*, 2009; Raposo *et al.*, 2011a) while different chemical analysis techniques are used to quantify formation of intermediates or substrate depletion (Guwy, 2004). In the gasometric methods, biogas is quantified either manometrically, by measuring pressure increase in constant volume or volumetrically as volume increase under constant pressure (Guwy, 2004; Angelidaki *et al.*, 2009; Raposo *et al.*, 2011a), and also by gas chromatography (Rozzi and Remigi, 2004; Raposo *et al.*, 2011a).

Volumetric methods comprise three approaches; displacement of a piston of a glass syringe inserted into the reactor, liquid displacement method using an alkaline solution for washing the biogas, or absorbing CO<sub>2</sub> and collection of the biogas in a gas sampling bag with low permeability (Raposo *et al.*, 2011a), e.g. aluminium foil bags (Parawira *et al.*, 2004). During the manometric method, biogas produced in the reactors creates a proportional overpressure which is measured by pressure transducers of various kinds (Guwy, 2004). Both methods require a complementary gas analyser to obtain percentage composition of methane in the biogas (Membere *et al.*, 2015).

## 2.20 Thermochemical processes for biomass conversion

Various technologies are continuously being investigated for conversion of biomass into energy products (biofuels, power and chemical commodities). In the UK for instance as reported by Ross *et al.* (2008) legislation supporting renewable obligatory credit has been a vehicle for increased utilization of biomass in the energy sector. Thermal decomposition reactions play an increasingly vital role during several of the biomass utilization processes (Várhegyi *et al.*, 2011). The two main thermochemical processes for converting biomass into energy and chemical products are gasification and pyrolysis (Cherubini, 2010). Biomass fuels contain a wide range of pyrolyzing species (Várhegyi *et al.*, 2011) and thermochemical conversion methods such as pyrolysis have been used to produce bio-oil as replacement for fossil fuel-based diesel (Adams *et al.*, 2011a). The potential for the production of valuable chemicals and fuels by pyrolysis of macroalgae has been studied (Ross *et al.*, 2009; Rowbotham *et al.*, 2013). Other studies on thermal behaviour of marine macroalgae have also been carried out (Wang *et al.*, 2006; Ross *et al.*, 2008). Until recently, attention has rarely been paid to thermochemical conversion of kelp (Ross *et al.*, 2008). Recently, a sizeable number of studies has demonstrated the potential of algae as a renewable energy resource using pyrolysis (Kositkanawuth *et al.*, 2017). The thermochemical conversion of biomass into fuels; charcoal, bio-oil and gaseous products by heat under anaerobic conditions is known as pyrolysis (Demirbas and Arin, 2002; Hong *et al.*, 2017). Pyrolysis is regarded as an effective method to produce fuel from dry biomass (Demirbas and Arin, 2002). TGA is often employed in pyrolysis studies to examine biomass thermal characteristics by measuring changes in mass as a function temperature and time when biomass volatilizes under a controlled atmosphere (Kositkanawuth *et al.*, 2017). The thermal conversion of brown algae using pyrolysis-gas chromatography/mass spectrometry (Py-GC/MS) and thermogravimetry (TGA) has been studied and their reactions products identified (Choi *et al.*, 2015). Their identification is through the detection of 'fingerprint' compounds by Py-GC/MS which has been used to determine the presence of certain carbohydrates in the seaweeds (Anastasakis *et al.*, 2011). During the

pyrolysis characterization of carbohydrates components (alginic acid, mannitol, laminarin and fucoidan) of brown macroalgae using py-GC/MS predominantly furfural, 5-methyl 2-furancarbox-aldehyde and 2-methoxy-5-methyl thiophene, 1-(2-furanyl) ethanone and dianhydromannitol and 1,2-cyclopentadiene, 2-hydroxy-3-methyl 2-cyclopenten-1-one and acetic acid were identified (Anastasakis *et al.*, 2011). In other studies ten consistent compounds; ethanone, pyrrole toluene; furfural; 1-(2-furanyl); furfural, dianhydromannitol; 5-methyl; 3-methyl; phenol; indole; 3, 7, 11, 15-tetramethyl-2-hexadecen-1-ol, 1, 2-cyclopentadi-one were previously identified from pyrolysis of *Laminaria digitata* (Ross *et al.*, 2008; Adams *et al.*, 2011a). In brown algae, the kelps, alginate is the largest organic fraction and extracted for the production of alginate on an industrial scale (Horn *et al.*, 2000a). They contain natural occurring biopolymers (Brus *et al.*, 2017). Alginate is a term used to describe the salts of alginic acid (Ross *et al.*, 2011), and has been extracted from wracks such as *Laminaria digitata* and *Hyperborea*, *Macrocystis pyrifera*, *Ascophyllum nodosum* and *Saccharina latisima* (McHugh *et al.*, 2003; Pathak *et al.*, 2010). The residues from such extraction processes also represent a raw material for renewable energy (Milledge *et al.*, 2014). The majority of the polysaccharide in brown algae is alginic acid which is a polymer of 5-carbon acids, D-mannuronic (M-block) and L-guluronic acid (G-block) with the formula  $(C_6H_8O_6)_n$  (Anastasakis *et al.*, 2011). The M and G monomers constitute M-, G-, and MG- sequential block structures (Pathak *et al.*, 2010), with a  ${}^4C_1$  and  ${}^1C_4$  conformation giving generally three types of glycosidic linkages (diequatorial (MM), diaxial (GG), and equatorial-axial (MG) in the block structure (Funami *et al.*, 2009). The alginate is present as a salt form of the alginic acid (sodium, calcium and magnesium salts) and their extraction process is geared towards obtaining filtered and dried sodium alginate powder since both calcium and magnesium salts do not dissolve in water (Ross *et al.*, 2011; Venkatesan *et al.*, 2017). The alginate structure, composition and distribution sequence of the two uronic acids can be characterized by  ${}^1H$  NMR spectroscopy (Subramanian and Dakshinamoorthy, 2015). Extracted alginate fraction can be used in the production of gels (Wong *et al.*, 2002; Fertah *et al.*, 2014), thickeners, stabilizers and colloids (Kirk and Othmer, 1997; Venkatesan *et al.*, 2017). The pyrolytic behaviour of alginate acid and its salt (Na alginate) has been previously studied using TGA in an inert atmosphere (Soares *et al.*, 2004).

From the result of their TGA curve both the alginic acid and its salt shows two decomposition steps which are attributed to loss of water (hydration) and polymer (decomposition), and for Na alginate formation of carbonaceous residue and  $\text{Na}_2\text{CO}_3$  (Soares *et al.*, 2004). The decomposition temperature of the biopolymer (alginate) takes place at 240-260 °C represented by an exothermic peak (rapid devolatilization) while carbonaceous material occurs around 300 °C and above (Soares *et al.*, 2004). Study on the thermal behaviour of *L. digitata* biomass by Rowbotham *et al.* (2013), a sharp exothermic event (peak) in the thermogram around 235 °C was assigned to the degradation of alginate. Figure 2-20 is an example of the thermal degradation profile of alginate in three forms. The pyrolysis temperature is characterized by initial weight loss due to dehydration followed by initiation of the devolatilisation region described by two-decomposition step between 200 - 545 °C. The first step occurs within the range 200 - 270 °C at which the weight loss rate peaks and for Na-alginate was reported as 245 °C (Ross *et al.*, 2011). The second phase of the degradation occurred at 545 °C which signify the end of the main devolatilisation process and after 500 °C the overall mass loss corresponds to increase in char yields obtained (Ross *et al.*, 2011). The gases evolved include both  $\text{CO}_2$  (220 - 330 °C) and  $\text{CO}$  (600 - 800 °C) and at higher temperature >900 °C char decomposition continued further (Ross *et al.*, 2011).

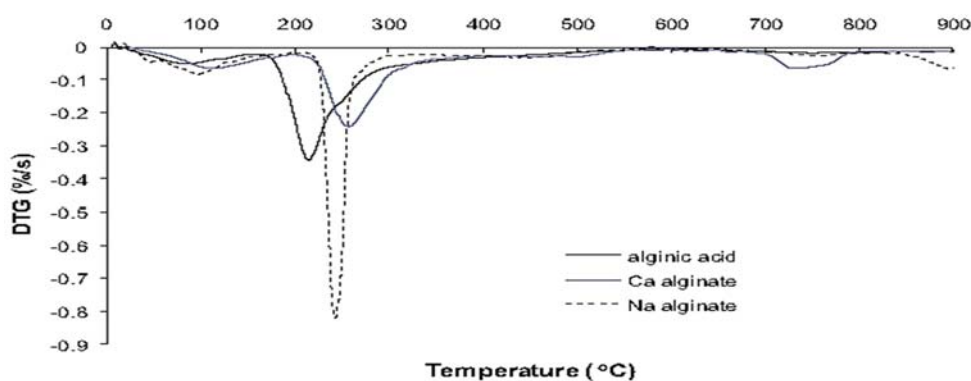


Figure 2-20 An example of a DTG profile of alginic acid, Na and Ca-alginate in an inert ( $\text{N}_2$ ) atmosphere (Ross *et al.*, 2011).

Then it could be argued that thermal behaviour of a compound using TGA / Py-GC/MS can provide considerable insight into decomposition data of the biopolymers present and in this instance alginate while NMR analysis helps in identification of the composition and distribution sequence of alginate molecules. Although current commercial cultivation of macroalgae is mainly for products other than fuel, their exploitation also for biofuels alone may not be profitable (Milledge *et al.*, 2014). Hence, in commercialisation of macroalgae, it may be beneficial in terms “biorefinery” where a variety of bio-based products (high values chemicals and materials) is co-produced with energy products (fuels, power, heat) (Cherubini, 2010; González-Delgado and Kafarov, 2011).

## Chapter 3. Materials and Methods

### 3.1 Collection, pre-treatment, and storage

Algal biomass *Laminaria digitata* (LD) used in the both the batch and continuous reactor experiments were collected from shallow water during low tide at Culler coats Bay, 55.0342° N, 1.4309° W ,Tyne and Wear (NZ3572) in December, 2013 and Seaton sluice, 55.0836° N, 1.4744 ° W, Northumberland UK (NZ 3350) in January, July and December, 2015. The seaweeds were transported in 30 liter bags and were immediately washed to remove marine salts and sediments which can cause mechanical problems in digesters. Sand is known to be abrasive to moving parts such as mixers and pumps while salt removal leads to more stable digestion (Allen et al., 2013). The reactors feedstocks were prepared using only the frond; the stipe and holdfast were discarded. This has an inherent advantage of scalable mariculture for biomass regrowth and production (Hinks et al., 2013). The fronds were roughly chopped by hand to particle size of about 10 mm using knife, approximately 250 g were then macerated with 250 ml of distilled water using a kitchen blender to give a consistent slurry (particles generally < 2 mm) to obtained fresh substrate. To obtain the dry algal substrate the roughly chopped frond were oven dried at 70 °C for 24 - 48 hrs. This was then pulverized with a Kenwood 100 coffee blender to particle size generally < 1mm. All samples were stored at 4 °C in an airtight gas bag until required.

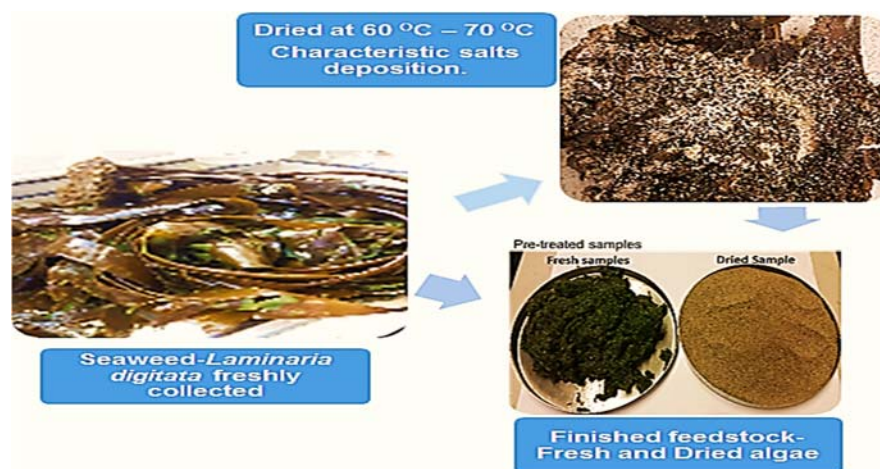


Figure 3-1 *Laminaria digitata* feedstock preparation process

### 3.1.1 *Experimental design/reactor system*

The setup of the CSTR as described by Hinks et al. (2013) but modified; the continuous study were performed in 1 L Quick fit® reactor vessels (800 ml working volume) with wide ground-glass necks, Figure 3-2. A multi-port head plate Quickfit® flanged was fitted to the reactor vessel with a spring clamp. Five, 19/26 ground sockets on the head plate allowed gas lines to be fitted, and the impeller drive shaft to pass into the reactor through a Quickfit glass stirrer gland with a water-seal to ensure the reactor remained gas-tight. In order to ensure complete anaerobic conditions a feeding / sampling port was fitted with a PVC tube (12 mm in diameter, 80 cm long) into the reactor vessel through one 19/26 sockets on the head plate to reach below the liquid level. Vacuum grease (Dow Corning, USA) was used to maintain the integrity of all ground glass seals and sockets pots not used were sealed with glass 19/26 stoppers. Mixing was achieved with a 40 × 80mm rectangular impeller rotating at 90 rpm.



Figure 3-2 Continuous reactor set up and design

### 3.1.2 *Inoculum and operation*

The reactors were inoculated with a mixed methanogenic sludge from a full-scale running anaerobic digester (Cockle Park Farm, Newcastle) operating on grass silage. It had following characteristics; pH 7.50, 21.2% TS, 60% VS (%TS), 0.019 Sulphur and C: N of 0.061.



The CSTRs were operated in semi-continuous batch mode, with daily feeding event being initiated by the removal of an appropriate volume (Reactor Volume/hydraulic residence) of mixed liquors from the feeding/sampling point on the head plate of the reactor using a 100 ml plastic syringe. Stirring continued during sampling to prevent settling and fractionation of the reactor solids (Hinks et al., 2013), and the importance of mixing the reactors for efficient substrate conversion has been reported by many researchers (Nandi *et al.*, 2017). An experimentally determined quantity (expressed as dry weight (g VS / L) was made up to a specified volume of water (water volume dependent on hydraulic residence), to replace exactly the sample volume that had been removed from the reactor, and added manually through a head plate port. All samples were carried out in duplicate and standard deviation (SD) of the data shown in parenthesis.

## 3.2 Laboratory analytical methods

### 3.2.1 *pH and Solids*

The pH was measured daily from the removed liquors (reactor effluent) at each feeding event using a Jenway 3010 pH meter. The total solids (TS) and volatile solids were determined gravimetrically using methods described in (APHA, 2005). %TS was obtained by placing the sample (20 - 30 mL) in triplicate into an oven for 24hrs at 104 °C and subsequently placed in a furnace at 550 °C between 1 - 2 hrs to obtain the volatile solids content. (APHA, 2005).

### 3.2.2 *Chemical oxygen demand (COD)*

Chemical oxygen demand (COD) analysis was carried out using commercially available COD kits (Merck, UK). Diluted sample were centrifuged at 3600g for five minutes, and supernatant were then filtered through a 0.20 µm syringe filter (VWR, UK). 3ml of this filtered sample was added to COD tubes and digested at 150 °C for 2 hrs. The COD values were determined by spectroscopic absorbance using a Spectroquant Nova 60 (VWR, UK) colorimeter.

### 3.2.3 Ammonical nitrogen ( $\text{NH}_3$ -N)

Ammonical nitrogen ( $\text{NH}_3$  -N) was determined using a Vapodest 30S steam distillation apparatus (C Gerhardt Lab Supplies, UK). Fifty milliliters of sample was placed in a Kjeldahl digestion tube, with few drops of phenolphthalein indicator and adjusted to pH above 8.3 using NaOH where necessary. Borate buffer solution (3 ml) was added to the mixture and distilled into 50 ml of boric acid indicator. The distillate was titrated with 0.02 N  $\text{H}_2\text{SO}_4$  to a pale lavender endpoint. A reagent blank was distilled and titrated in the same way and subtracted from the sample titer to calculate the  $\text{NH}_3$ -N of the sample (APHA, 2005).

### 3.2.4 Total Kjeldahl Nitrogen (TKN)

Total Kjeldahl Nitrogen (TKN) was determined using Turbotherm acid digestion and Vapodest 30S steam distillation apparatus (C Gerhardt Lab Supplies, UK). Ten milliliters of the samples were digested by the Turbotherm in Kjeldahl tubes with  $\text{H}_2\text{SO}_4$  and a  $\text{K}_2\text{SO}_4/\text{CuSO}_4$  Kjeltab tablet. The digestate was then neutralised and steam distilled as described for ammonia nitrogen analysis (APHA, 2005). The Total protein content was estimated by multiplying the TKN value by 6.25. All reagents both  $\text{NH}_3$ -N and TKN were prepared to the manufacturer's specification.

### 3.2.5 Total organic carbon (TOC)

Total organic carbon (TOC) was analysed with Shimadzu 5050A total organic carbon analyser, with an ASI-5000A autosampler. The carrier gas is zero grade air, and the inorganic catalyst solution is 25% phosphoric acid.

### 3.2.6 Elemental Composition (CNS) analysis

Samples (dried, powdered; ca. 50 mg) were weighed accurately into ceramic crucibles and analysed for carbon, nitrogen and sulphur content using an Elementar VarioMAX CNS analyser. The analysis involves combustion at  $1145^\circ\text{C}$  in an oxygen-enriched helium atmosphere. Sulfadiazine (%N = 22.37; %C = 47.99; %S = 12.81) was used as the calibration standard and was analysed at

the start and end of the sample sequence and after every 5 - 10 samples. Raw data were corrected for analytical drift (based on the calibration standard data) during the analysis using the Elementar software.

### 3.2.7 Sulphate ( $SO_4^{2-}$ )

Sulphate ( $SO_4^{2-}$ ) was determined on a Dionex ICS-1000 Ion Chromatograph system with an AS40 autosampler. The column is an Ionpac AS14A, 4x250mm analytical column. Flow rate is  $1\text{ ml min}^{-1}$ , eluent a  $8.0\text{ mM Na}_2\text{CO}_3/1.0\text{ mM NaHCO}_3$  solution. Injection loop was 25ul.

### 3.2.8 Volatile fatty acids (VFAs)

Volatile fatty acids (VFAs) was analysed on a Dionex ICS 1000 with an AS40 autosampler (Dionex, USA). Separation was carried out on an ionpac ICE-AS1 4 × 250 mm analytical column with a flow rate  $16\text{ ml min}^{-1}$ ;  $1.0\text{ mM}$  heptafluorobutyric acid eluent;  $5\text{ mM}$  tetrabutylammonium hydroxide suppressant regenerant; and a 10ul injection loop. Supernatant of centrifuged samples liquors were filtered through a  $0.20\text{ }\mu\text{l}$  syringe filter (VWR, UK),  $0.4\text{ ml}$  of filtered samples were then diluted 1:1 with octanesulfonic acid, and sonicated (FS200B Sonic Bath, Decon Laboratories, Sussex, UK) for 40 mins to remove carbonate, which caused interference. The prepared samples were then transferred to  $1\text{ ml}$  tubes with filter caps (Dionex, USA) before analysis.

### 3.2.9 Biogas and methane measurement

The percentage (%) methane from the biogas content was determined using a GC-FID analyser (Carlo-Erba 5160 GC) in split mode with the injector at  $150^\circ\text{C}$  and FID at  $300^\circ\text{C}$ . Using a  $100\text{ }\mu\text{l}$  sample Lock syringe (Hamilton, USA), duplicate headspace samples ( $100\text{ ul}$ ) were injected manually every 2 minutes into the GC with the split open 5 turns ( $100\text{ mls min}^{-1}$ ). After the initial injection, the GC temperature programme and data acquisition commenced. Separation was performed on an HP-PLOT-Q capillary column ( $30\text{ m} \times 0.32\text{ mm id}$ ) packed with  $20\text{ }\mu\text{m}$  Q phase. The GC was held isothermally at  $35^\circ\text{C}$  for 90min and heated to  $250^\circ\text{C}$  at  $10^\circ\text{C min}^{-1}$  and held at final temperature for 10 minutes with Helium as

the carrier gas (flow 1ml min<sup>-1</sup>, pressure of 50kPa, split at 100mls min<sup>-1</sup>. The acquisition was stored on an Atlas laboratory data system. Methane standard were prepared prior to each analysis from 100% analytical grade CH<sub>4</sub> (BOC Gases, UK) by injecting duplicate sample to make a five–point standard curve in the range 20 - 100% CH<sub>4</sub>. The volume of biogas produced was measured using a 100 ml BD Plastipak syringe from the gas bags. The % methane calculated was multiplied by the measured biogas volume giving the volume of methane produced.

Total volume of methane (*V*) produced daily was calculated by using Eqn 3-1 **Error! Reference source not found.** and corrected to STP with Eqn 3-2**Error! Reference source not found.;** (VDI, 2006)

$$V = X_1 + X_2 - X_3 \quad \text{Eqn 3-1}$$

Where; *X*<sub>1</sub> = daily calculated headspace methane volume, *X*<sub>2</sub> = daily measured volume of methane in gas bags, *X*<sub>3</sub> = previous day headspace methane volume.

$$V_d = V \cdot \frac{(p - p_w) \cdot T_o}{p_o \cdot T} \quad \text{Eqn 3-2}$$

Where *V*<sub>*d*</sub> = volume of dry gas in normal state, in mL<sub>N</sub>; *V* = volume of gas as read off, in ml; *p* = pressure of gas at time of reading, in hPa; *p*<sub>*w*</sub> = vapour pressure of water as a function of temperature of the ambient space, in hPa; *T*<sub>*o*</sub> = normal temperature, 273 K; *p*<sub>*o*</sub> = normal pressure, 1013 hPa ; *T* = temperature of the gas or ambient, K.

### 3.2.10 Hydrogen sulphide and CO<sub>2</sub> gas measurement.

Gas chromatography-Mass spectroscopy (GC-MS) analysis of hydrogen sulphide from the biogas gas was performed on a Fisons 8060 GC using split injection (150 °C) linked to a Fisons MD800 MS (electron voltage 70eV, filament current 4A, source current 800uA, source temperature 200 °C, multiplier voltage 300V, interface temperature 150 °C). The acquisition was controlled by a compaq

deskpro computer using xcalibur software; in full scan mode (1.0 - 151.0 amu / sec) or sim mode (7 ions 100ms). The headspace sample (100ul) was injected in split mode and the GC programme and MS data acquisition commenced. Separation was performed on an HP-PLOT-Q capillary column (30m x 0.32mm id) packed with 20um Q phase. The GC was held isothermally at 100°C with Helium as the carrier gas (flow 1ml min<sup>-1</sup>, pressure of 65kPa, split at 100 mls min<sup>-1</sup>). The chromatograms of the separated gas (H<sub>2</sub>S) were integrated and quantified. The acquired data was stored on DVD for any further data processing, integration, and printing.

### 3.2.11 *Trace metals extraction*

Trace metal extraction were carried out by (APHA, 2005) 3030G method, briefly explained: 5 ml of HNO<sub>3</sub> acid was added to 1g of biomass sample and heated, then 5 ml HNO<sub>3</sub> + 10 ml HCl was added to the sample and continued heating to evaporation until a dense white fume is seen. If the solution is not clear a further addition of 10 ml HNO<sub>3</sub> were carried out and heated to drive off all NO<sub>3</sub><sup>-</sup> until a white fume SO<sub>3</sub> is seen. The sample is cooled and diluted to 50 ml with H<sub>2</sub>O before reheating it to almost boiling point to dissolve slowly soluble salt.

### 3.2.12 *Trace metals analysis by inductively coupled plasma optical emission spectrometry (ICP-OES).*

This was carried out according to (ISO, 2009), in the ICP-OES laboratory, Newcastle University. The basis of the method is the measurement of emission of light by an optical spectroscopic technique. Prepared standard samples and extracted metal samples are nebulized and the aerosol that is produced is transported to the plasma torch where excitation occurs. Characteristic emission spectra are produced by a radio-frequency inductively coupled plasma (ICP). The spectra are dispersed by a grating spectrometer and the intensities of the lines are monitored by a detector. The signals from the detector(s) are processed and controlled by a computer system. The metal content is calculated from the standard concentrations.

## Chapter 4. Bio-methane Potential Test (BMP) using inert gas sampling bags with macroalgae feedstock.

### *Abstract*

An approach to Bio-methane potential test (BMP) was carried out at mesophilic temperature of 35 °C with Supel™ inert gas sampling bags as biogas collection and storage bags, using selected seaweed (macroalgae) as substrate. Samples were given a range of pre-treatment from washing, drying and macerating. Dried *Laminaria digitata* (DD) with 68.14 VS (%TS) produced the highest BMP of  $141 \pm 5.77$  L CH<sub>4</sub> kg VS<sup>-1</sup>, with methane content increasing to about 70%, while the lowest BMP of  $93 \pm 5.03$  L CH<sub>4</sub> kg VS<sup>-1</sup> with methane content of about 65% was obtained for fresh *Laminaria digitata* (FD) with 72.03 %VS (%TS). Methane yields of 97.66 and 67.24 m<sup>3</sup> CH<sub>4</sub> t<sup>-1</sup> wet weight based on BMP results were obtained for DD and FD respectively. Both DD and FD achieved within 28% and 38% of the theoretical BMP value based on the Buswell equation, respectively. The total methane (*V*) produced was computed based on;

$$V = X_1 + X_2 - X_3 \text{ corrected to Standard temperature and pressure (STP)}$$

Where  $X_1$  = daily calculated headspace methane volume,  $X_2$  = daily measured volume of methane in gas bags,  $X_3$  = previous day headspace methane volume. An advantage of this approach is the volumetric measurement of gas produced directly from the gas bags, hence it does not require liquid displacement or pressure transducers. Results from the second set of freshly collected seaweed sample showed it was in agreement with published BMP values. All analysis was carried out without mineral supplementation.

## 4.1 Introduction

This chapter explains analysis of BMP of macroalgae using a modified approach. An introduction has been given in Section 2.17 on anaerobic biodegradability assessment.

## 4.2 Materials and Methods

### 4.2.1 *Collection, pretreatment, and storage*

This is in accordance with Section 3.1.

### 4.2.2 *Inoculum*

The specific methanogenic activity test (SMA) is normally used to check the quality of inoculum in anaerobic digesters. It is an indication of the efficiency of anaerobic treatment process because it measures the rate of the methanogenic activity under defined substrate conditions (Dolfing and Bloeman, 1985). The SMA test is a quick and simple way to get information about the percentage of active methanogenic microorganism in a sludge, and also estimate the rate of maximum methane production of a reactor at a particular sludge density (Valcke and Verstraete, 1983), or capability (Souto *et al.*, 2010) to convert volatile fatty acids into methane under ideal conditions (Souto *et al.*, 2010). The test is performed with acetate, or acetic acid, or mixture of acetic, propionic and butyric acids (Raposo *et al.*, 2006), because in non-gastrointestinal environments like anaerobic digesters, acetate is one of the major intermediates of fermentation (Valcke and Verstraete, 1983) and is regarded as the principal precursor of about 70% of methane produced under typical operating conditions (Kaspar and Wuhrmann, 1978). The inoculum used was collected from laboratory scale mesophilic anaerobic digesters running in the environmental engineering laboratory, Newcastle University. It had been stored at 4°C for between 1 - 4 weeks before use, and had the following characteristics; pH 7.33, 13.95% TS and 58.77% VS (%TS). The inoculum was pre-incubated using 2L reactor bottles at 35 °C for 3 days with waste beer COD concentration 117 g L<sup>-1</sup> to restore/reactivate the methanogenic activity. Active biomass was confirmed by

good biogas production (1L biogas / L reactor / d) with 50 – 70% methane content in the biogas (Figure 4-1).

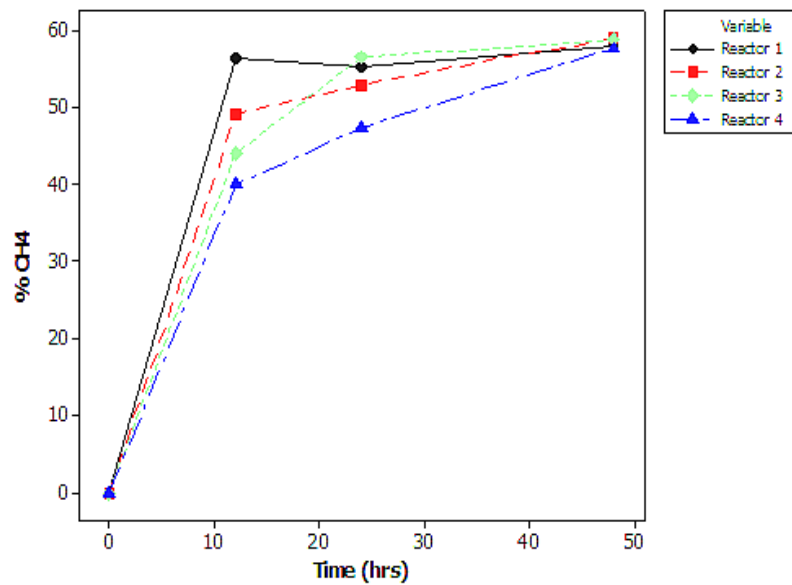


Figure 4-1. % Methane composition in biogas using waste beer as substrate

Before using the pre-incubated inoculum for both SMA and BMP tests it was de-gassed between 3-5 days until biogas production was negligible. The SMA test was carried out by adding different amounts of sodium acetate (NaAc) (1g HAc = 1.37 g NaAc) to 98 ml of inoculum (2 g VS L<sup>-1</sup>) in 0.5 L reactor bottles and the volume made up to 400 mL with de-ionised water. Then the procedure described for the BMP assay (Valcke and Verstraete, 1983) was used to carry out the SMA test. Acetate (0.5 - 2.0 g L<sup>-1</sup>) was used as substrate since approximately 72% of methane formed during anaerobic digestion is from acetic acid (McCarty, 1964).

#### 4.2.3 Characterization of the sample

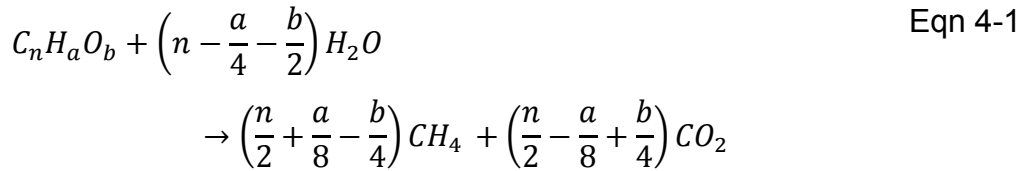
pH was measured on the prepared substrate prior to digestion using a Jenway 3010 pH meter. The total solids (TS) and volatile solid (Laurinovic *et al.*) as %TS, were determined gravimetrically using methods described in (APHA, 2005). VS was obtained by placing the sample in triplicate into an oven for 24hrs at 104 °C, and these solids subsequently placed in a furnace at 550°C for 1 - 2 hrs to obtain the volatile solids content as a fraction of the total solid (%TS) (APHA, 2005). Total Kjeldahl Nitrogen (TKN) was determined using Turbotherm acid



digestion and Vapodest 30S steam distillation apparatus (C Gerhardt Lab Supplies, UK). 10 ml of the samples were digested by the Turbotherm in Kjeldahl tubes with H<sub>2</sub>SO<sub>4</sub> and a K<sub>2</sub>SO<sub>4</sub>/CuSO<sub>4</sub> Kjeltab tablet. The digestate was then neutralised and steam distilled as described for ammonical nitrogen analysis (APHA, 2005). The total protein content was estimated by multiplying the TKN value by 6.25 (Allen, 1974; Raposo *et al.*, 2008). To obtain the percentages of carbon, hydrogen, and nitrogen for the generation of stoichiometric description of biomass, the fresh slurry samples were firstly oven dried at 70°C for multiple 30 minutes periods until constant weight obtained to remove moisture content, and passed through 1 mm sieve before CHN analysis. Each pre-treated substrate stock was sampled and tested in triplicate for total carbon (C), hydrogen (H) and nitrogen (N) on a total solid basis. The ultimate analysis of the fresh samples was carried out by Micro elemental Ltd, UK using a CE Instruments (now Thermo) elemental analyser model EA1110 for CHN and a Fisons instrument (now Thermo) elemental analyser model NA2000 for oxygen and sulphur. The Instruments were calibrated and verified using certified reference chemical, acetanilide 141 d traceable to NIST primary standards (ASTM 2005). A confirmation analysis was done for CHN using (Carlo Erba 1108 Elemental Analyser, confidence limit <0.3%) by the Chemistry Department at Newcastle University Upon Tyne.

#### *4.2.4 Assessment of Bio-methane potential energy from the Buswell equation*

When the atomic or organic fraction composition of a compound is known, it is possible to calculate the theoretical bio-methane potential ( $BMP_{theo}$ ) (Angelidaki and Sanders, 2004). From the experimental elemental analysis determination, the empirical formulae (C<sub>a</sub>H<sub>b</sub>O<sub>c</sub>N<sub>d</sub>S<sub>e</sub>) can be calculated (Raposo *et al.*, 2011b). A stoichiometric equation can be developed using the Buswell equation (Eqn 4-1) (Allen *et al.*, 2013a) to obtain the  $BMP_{theo}$  and Carbon dioxide (CO<sub>2</sub>) volumes produced when a substrate is broken down by a consortium of micro-organisms present in a digester.



Assuming a total stoichiometric conversion of the organic compounds to methane and carbon dioxide, the methane yield ( $BMP_{theo}$ ) from the Buswell equation can be calculated from Eqn 4-2 ; (Raposo *et al.*, 2011b).

$$BMP_{theo} \text{ yield} = \frac{\left(\frac{n}{2} + \frac{a}{8} - \frac{b}{4}\right) 22.4}{12n + a + 16b} \left(STP \frac{lCh_4}{g - VS}\right) \quad \text{Eqn 4-2}$$

#### 4.2.5 Modified Bio-methane potential assessment of pre-treated Substrate.

The modified assessment was carried out in a water bath at mesophilic temperature of 35°C. The batch reactors consisted of 500 ml Duran bottles (actual internal volume 580 ml) fitted with rubber stoppers (Fisher brand Height 30 mm, bottom 29 mm) with a 4 mm diameter stainless steel tube (45 mm long) inserted to serve as an outlet port for biogas collection in gas bags and as a purging port for Nitrogen flushing of the headspace. The plastic bottle caps were used to hold the stoppers in place (Figure 4-2) preventing any frictional movement of the stoppers as a result of biogas pressure build-up in the reactors and preventing loss and oxygen penetration into the reactors. A flexible PVC (non- oxygen/methane permeable) tubing connector 0.5 cm long was attached to the stainless; and a tube clip was used to close the tube (Figure 4-2). Before starting the BMP test all reactor bottles were pressure tested for air leakage, and once the experiment has commenced, nitrogen or methane leakage using a thermo-scientific GLD ProLeak detector used to check any CO<sub>2</sub>, NO<sub>2</sub>, and CH<sub>4</sub> leaks. The required amount of inoculum and substrate was evaluated for each reactor on a VS basis using a ratio of 3:1 (6 g VS / L: 2 g VS / L). This was to ensure adequate destruction of the volatile solids and overcome possible VFA inhibition (Raposo *et al.*, 2006; Angelidaki *et al.*, 2009). The inoculum and substrate were then placed inside the reactor and the solution was made up to 400 ml with of de-ionised water. The rubber stoppers were then used to closed

the bottles, and the headspace (approx. 160 ml) was flushed for 5 minutes with pure (99.99%) N<sub>2</sub> gas to establish anaerobic conditions. The tube clamp was used to close the PVC tube ensuring all the bottles were gas-tight without the gas bags. Triplicates samples were used to overcome inoculum variability, sample heterogeneity and allow statistical significance (Hansen *et al.*, 2004; Angelidaki *et al.*, 2009)



Figure 4-2. Modified BMP reactor and gas collection bag

#### 4.2.6 *Biogas collection*

Biogas collection started after 24 hrs of digestion. Any biogas production was initially contained within the headspace of the closed reactor and caused a proportional pressure increase within the reactors. Supel™ inert gas sampling bags were attached to the PVC tubing connectors daily for collection of biogas. This was achieved by releasing the clamps allowing the biogas to flow into the bags after which they are resealed before removal, ensuring no air penetration into the reactor bottles. The collected biogas was allowed to equilibrate at room temperature  $22 \pm 3$  °C before compositional analysis and volume determination. The gasbags contained septa from which the gas was collected by gas syringe for analysis. It is assumed that composition of the gas bag is proportional to the headspace of the reactors.

#### 4.2.7 Biogas and methane measurement

The methane composition in the biogas was determined using a GC-FID instrument (Carlo-Erba 5160 GC) in split mode with the injector at 150 °C and FID at 300 °C. Hydrogen was used as carrier gas at a flow rate through the column of 1 ml/min. Using a 100 µl sample Lock syringe (Hamilton, USA), duplicate headspace samples (100 µl) were taken from the sample bags and injected manually into the GC with the inlet in a split mode (flow rate 100 mls/min giving a split ratio of 100:1). After the initial injection, the GC temperature programme and data acquisition commenced. Separation was performed on an HP-PLOT-Q capillary column (30 m x 0.32 mm i.d) packed with 20 µm Q phase. The GC was held isothermally at 35 °C for 90min and heated to 250°C at 10 °C / min and held at final temperature for 10 minutes. Methane standards were prepared prior to each analysis from 100 % analytical grade CH<sub>4</sub> (BOC Gases, UK) by injecting duplicate samples to make a five-point standard curve in the range 20 - 100% CH<sub>4</sub>. The volume of biogas produced was measured at room temperature 22 ± 3 °C using a 100 mL BD Plastipak syringe to remove all biogas from the gas bags. The methane composition (%) calculated was multiplied by the measured biogas volume giving the volume of methane produced at room temperature. The measurement was carried out daily for the first 10 days, as between 80 and 90% of methane production is normally achieved within 8 - 10 days (Hansen *et al.*, 2004), thereafter it was sufficient to measure twice week.

#### 4.2.8 Determination of the kinetic decay constant and lag phase.

Although the  $BMP_{theo}$  gives a rough idea of the strength of a substrate's biogas potential, experimental assays must be used to ascertain the actual potential. Raposo *et al.* (2011b) stated that two experimental methods can be used; the  $B_{o-experimental}$  (calculated by dividing the net methane production by weight of sample on (VS or COD basis) at STP conditions and  $B_{o-kinetic}$  (derived from ultimate methane yield at infinite digestion time). The latter method is mainly used.

The  $B_{o-kinetic}$  is assumed to follow a first-order degradation rate (Gunaseelan, 2004; Angelidaki *et al.*, 2009; Raposo *et al.*, 2011b);

$$B = B_o \cdot [1 - \exp(-k \cdot t)] \quad \text{Eqn 4-3}$$

Where  $B$  ( $mL CH_4 gVS^{-1}$ ) is the cumulative methane yield,  $B_o$  ( $mL CH_4 gVS^{-1}$ ) is the ultimate methane yield,  $k$  ( $day^{-1}$ ) is the first order rate constant and  $t$  (d) is the time.

The equation is a linear regression model based on the empirical relationship, and is used to determine the rate and extent of degradation, where the value of  $k$  (*slope of the linear plot*) shows the characteristics for a given substrate, and gives the time required to generate a ratio of the ultimate methane potential (Angelidaki *et al.*, 2009). It should be noted that, if  $B_{o-kinetic}$  differs from  $B_{o-experimental}$  by more than 10%, then  $k$  is not valid because the kinetic model cannot be used to explain data obtained as the experimental data does not fit the proposed model Eqn 4-3 (Raposo *et al.*, 2011b).

#### 4.2.9 Validation samples

In order to check and validate the proposed batch method, a second set of seaweed samples was collected during low tide at Seaton Sluice, Whitley Bay (NE26) on 29<sup>th</sup> August 2014. Samples were subjected to the same pre-treatment described in Section 3.1. The prepared feedstocks were: *Fresh Laminaria Hyperborea Frond (FHL)*, *Fresh Laminaria Hyperborea Stipe (FHS)*, *Dried Laminaria Hyperborea Frond (DHL)*, *Dried Laminaria Hyperborea Stipe (DHS)* and *Fresh Laminaria Digitata Frond (FDL)*, *Fresh Laminaria Digitata Stipe (FDS)*, *Dried Laminaria Digitata Frond (DDL)*, *Dried Laminaria Digitata Stipe (DDS)*. Table 4-1 shows the characteristics of the samples.

Table 4-1: Characteristics of macroalgal samples

Sample	%Moisture	% TS	%VS (%TS)
Fresh Lam. Digitata Fond (FDL)	91.48	8.52	70.80
Fresh Lam. Digitata Stem (FDS)	92.47	7.53	54.85
Dried Lam. Digitata Fond (DDL)	7.41	92.59	70.55
Dried Lam. Digitata Stem (DDS)	22.14	77.86	64.97
Fresh Lam. Hyperborea Fond (FHL)	92.70	7.30	77.28
Fresh Lam. Hyperbola Stem (FHS)	92.97	7.03	60.94
Dried Lam.Hyperbola Fond (DHL)	4.86	95.14	69.95
Dried Lam.Hyperbola Stem (DHS)	11.32	88.68	61.84

## 4.3 Results and discussion

### 4.3.1 Inoculum

The SMA was carried out at four different acetate concentrations (0.5 g, 1.0 g, 1.5 g and 2.0 g L<sup>-1</sup>) each combined with 2 g VS L<sup>-1</sup> of inoculum to ensure substrate limitation did not occur (Ince *et al.*, 2001). Figure 4-3 shows that the higher acetate concentrations (1.0, 1.5, and 2.0) gave higher cumulative methane production rates. The daily methane production ranged between 14 ± 0.11 mL CH<sub>4</sub> g HAC<sup>-1</sup> d<sup>-1</sup> on day 2 to 81 ± 0.16 mL CH<sub>4</sub> g HAC<sup>-1</sup> d<sup>-1</sup> on day 8 (data not shown), while the lowest acetate concentration of 0.5 g produced between 5 ± 0.19 mL CH<sub>4</sub> g HAC<sup>-1</sup> d<sup>-1</sup> – 27 ± 0.13 mL CH<sub>4</sub> g HAC<sup>-1</sup> d<sup>-1</sup> on day 8. These values show a low methanogenic yield of the inoculum compared to typical values of 350 mL CH<sub>4</sub> gVS<sup>-1</sup> d<sup>-1</sup> obtained for granular sludge with acetate as substrate (Raposo *et al.*, 2006) and 1000 mL CH<sub>4</sub> gVS<sup>-1</sup> d<sup>-1</sup> for acetoclastic methanogens (Ince *et al.*, 2001). The final methane composition was around 70% for all acetate concentration obtained, except 0.5 g (50% methane).

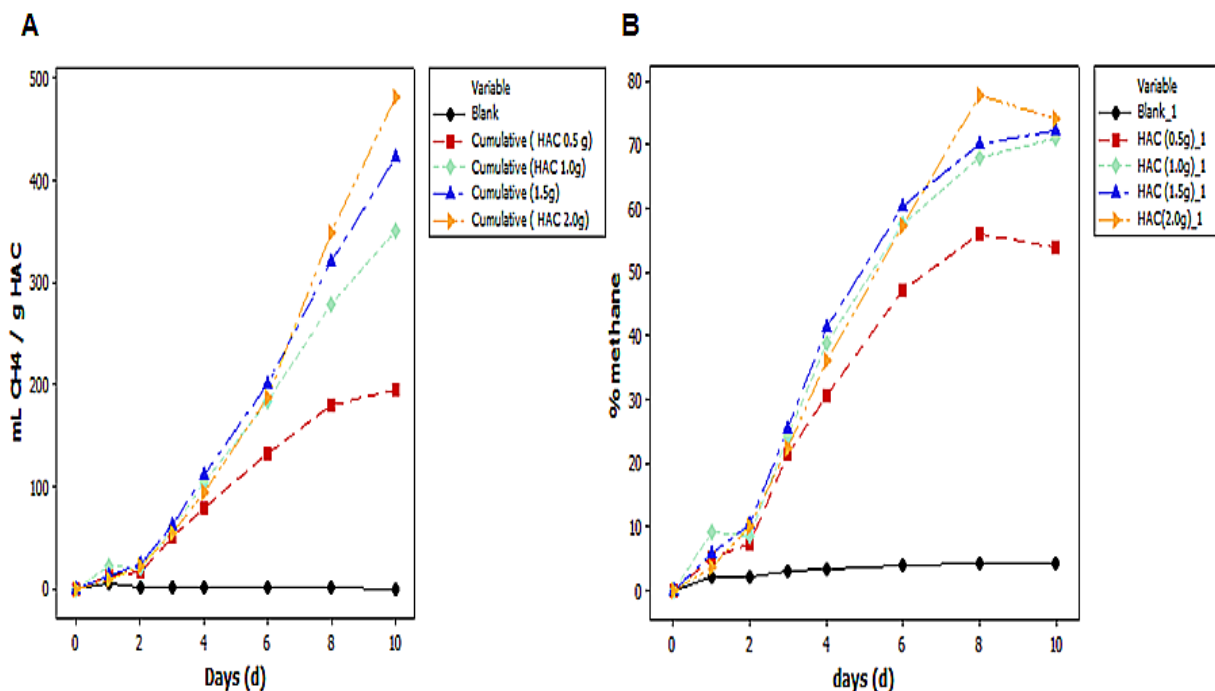


Figure 4-3 a) Plot of cumulative methane at different HAC concentration b) methane composition obtained at different concentrations HAC concentration.

### 4.3.2 Characterisation of macroalgal substrates

The physiochemical properties of the samples and inoculum were measured in terms of pH, TS, VS, TKN and elemental analysis as shown in Table 4-2.

Table 4-2: Elemental and physical analysis of macroalgal samples

Macroalgal sample	%C	%H	%O	%N	% moisture	%TS	VS (%TS)	TKN (g/Kg)	Protein (%TS Kg)	pH
Fresh Laminaria. Digitata (FD)	27.28	3.77	37.54	3.17	92.22	7.78	72.03	1.76	0.14	7.10
Fresh Laminaria. Hyperborea (FHY)	25.62	3.58	35.16	1.30	93.84	6.16	69.08	0.98	0.09	7.15
Dried Laminaria Digitata (DD)	30.11	4.73	37.54	2.16	1.29	98.71	69.04	29.40	0.19	7.18
Dried Laminaria Hyperborea (DHY)	28.67	4.26	35.16	1.02	2.08	97.92	63.19	16.33	0.10	7.14
Inoculum						13.95	58.77			7.33

Table 4-3: Elemental components for generation of the stoichiometric equation for macroalgal samples.

Macroalgal sample	Component	Number of atoms per mole of algae biomass	Atomic Weight	Weight Contribution (Kg/t)	%
Fresh Laminaria Digitata (FD)	Carbon	22.73 (10.06)	12	272.8	27.28
	Hydrogen	37.70 (16.68)	1	37.7	3.77
	Oxygen	23.46 (10.38)	16	375.4	37.54
	Nitrogen	2.26	14	31.7	3.17
Fresh Laminaria Hyperborea (FHY)	Carbon	21.35 (22.96)	12	256.2	25.62
	Hydrogen	35.8 (38.49)	1	35.8	3.58
	Oxygen	21.98 (23.67)	16	351.6	35.16
	Nitrogen	0.93	14	13	1.3
Dried Laminaria Digitata (DD)	Carbon	25.09 (16.29)	12	301.1	30.11
	Hydrogen	47.30 (30.71)	1	47.3	4.73
	Oxygen	23.46 (15.23)	16	375.4	37.54
	Nitrogen	1.54	14	21.6	2.16
Dried Laminaria Hyperborea (DHY)	Carbon	23.89 (32.73)	12	286.7	28.67
	Hydrogen	42.60 (58.36)	1	42.6	4.26
	Oxygen	21.98 (30.11)	16	351.6	35.16
	Nitrogen	0.73	14	10.2	1.02

Refer to Table 4-4

Results showed that VS constitute a major part of the macroalgal biomass, ranging from 63% in *DHY* to 72% of TS in *FD*. pH was in the range of 7.0 - 7.18

in all the reactor bottles before commencing digestion, which is ideal for methanogenic bacteria (Angelidaki and Sanders, 2004). Table 4-3 outlines the stoichiometric equation of the pre-treated algal samples while the analysis in Table 4-4 shows that fresh *Laminaria digitata* (FD) with 5.6% VS should give the maximum theoretical yield of 335 L CH<sub>4</sub> kg VS<sup>-1</sup>. Using this methodology, the theoretical maximum methane composition (% methane in biogas) and the maximum biogas attainable from each sample is shown in Table 4-5.

Table 4-4: Theoretical prediction of biogas production from macroalgal samples using the Buswell Equation.

Biogas production assessment using Buswell equation			
Fresh Laminaria. Digitata (FD)	C <sub>10.05</sub> H <sub>16.68</sub> O <sub>10.38</sub>	+	0.69 H <sub>2</sub> O → 4.52 CH <sub>4</sub> + 5.54 CO <sub>2</sub>
Fresh Laminaria. Hyperborea (FHY)	C <sub>22.96</sub> H <sub>38.49</sub> O <sub>23.63</sub>	+	1.52 H <sub>2</sub> O → 10.38 CH <sub>4</sub> + 12.78 CO <sub>2</sub>
Dried Laminaria Digitata (DD)	C <sub>16.29</sub> H <sub>30.71</sub> O <sub>15.23</sub>	+	1.0 H <sub>2</sub> O → 8.18 CH <sub>4</sub> + 8.12 CO <sub>2</sub>
Dried Laminaria Hyperborea (DHY)	C <sub>32.73</sub> H <sub>58.36</sub> O <sub>30.11</sub>	+	3.08 H <sub>2</sub> O → 16.13 CH <sub>4</sub> + 16.60 CO <sub>2</sub>
Example biogas estimation for Fresh Laminaria Digitata (FD) ( 5.6% VS )			
	C <sub>10.05</sub> H <sub>16.68</sub> O <sub>10.38</sub>	+	0.69 H <sub>2</sub> O → 4.52 CH <sub>4</sub> + 5.54 CO <sub>2</sub>
	56 kg VS + 2.66 H <sub>2</sub> O → 13.41 kg CH <sub>4</sub> + 45.25 kg CO <sub>2</sub>		
	Density of CH <sub>4</sub> = 0.714 kg m <sup>-3</sup> , Density of CO <sub>2</sub> = 1.96 kg m <sup>-3</sup>		
	Gas by volume → 18.78 m <sup>3</sup> CH <sub>4</sub> + 23.09 m <sup>3</sup> CO <sub>2</sub> = 41.87 m <sup>3</sup> biogas @ %44.9 CH <sub>4</sub>		
Theoretical Maximum methane production for FD	18.78 m <sup>3</sup> / 56 kg VS : 335 L CH <sub>4</sub> / kg VS		

Table 4-5: Theoretical methane yields for pre-treated macroalgal samples

Substrates	LCH <sub>4</sub> / kg VS	L Biogas / kg VS	% CH <sub>4</sub>
Fresh Laminaria. Digitata (FD)	335.36	747.68	44.90
Fresh Laminaria. Hyperborea (FHY)	334.74	747.65	44.82
Dried Laminaria Digitata (DD)	393.73	784.28	50.2
Dried Laminaria Hyperborea (DHY)	384.16	784.00	49.00



### 4.3.3 CH<sub>4</sub> production

Bio-methane production potential was measured under controlled conditions (35 °C) for 32 days. The cumulative and daily methane production profile is shown in Figure 4-4 A and Figure 4-4 B respectively. Contribution from background CH<sub>4</sub> produced by the inoculum was deducted from the cumulative yield in evaluating the data. The appearance of the graph (Figure 4-4 a) conforms with the typical assay (Angelidaki *et al.*, 2009).

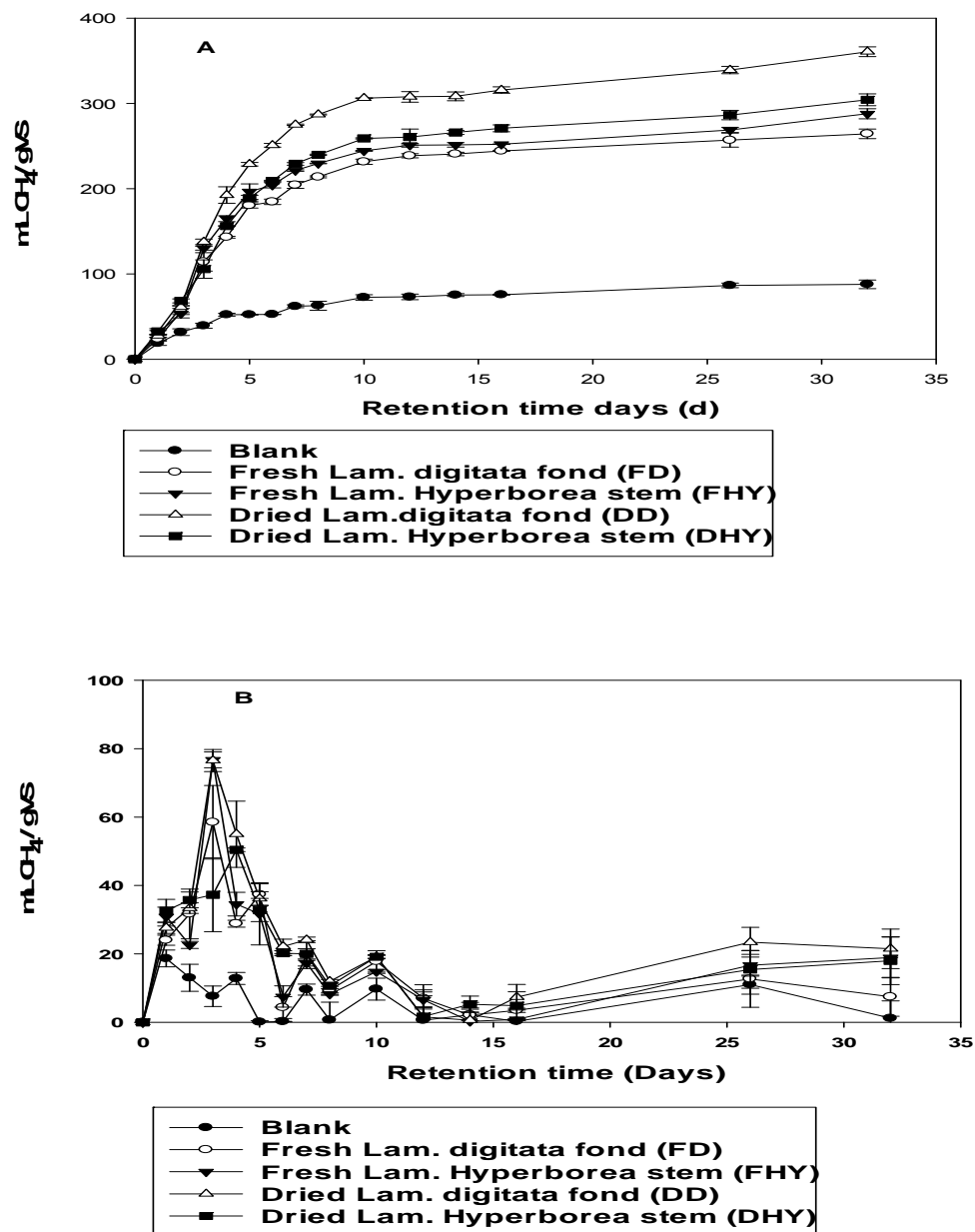


Figure 4-4: A), Cumulative; and B), Daily BMP for macroalgal samples; FD, FHY, DD, DHY.

Samples of *L. digitata* and *Hyperborea* were subjected to a range of pre-treatment from washing, drying and macerating. Cumulative CH<sub>4</sub> yield obtained was the highest for washed and dried *L. digitata*, with a value of 141 ± 5.77 L CH<sub>4</sub> kg VS<sup>-1</sup>, with methane content increasing to about 70% (Figure 4-5), while fresh *L. digitata* gave the lowest cumulative yield of 100 ± 5.03 L CH<sub>4</sub> kg VS<sup>-1</sup>, attaining 65% methane content. Chynoweth *et al.* (1993) have documented values up to 280 L CH<sub>4</sub> kg VS<sup>-1</sup> for the brown seaweed *Laminaria*, and between 126 - 174 L CH<sub>4</sub> kg VS<sup>-1</sup> for the fresh green seaweed *Ulva* (Allen *et al.*, 2013a). Analysis of Figure 4-4 A indicates that there is no linearity of methane production rate over the time period of maximum biogas production. Figure 4-4 A shows that methane production quality increased within the first 72 hrs, followed by a decline in production to a basal level, then a transient recovery on day 26 based on this BMP method (after 10 days of biogas accumulation in the reactor headspace before measurement).

Biogas production started with an almost negligible lag time in all experimental bottles, which confirms good microbial activity of the inoculum (as a result of pre-incubation), and rapid digestibility of some macroalgal components as a result of cell wall disruption from the pre-treatment. Macroalgal cells have a tough and protective cell wall which makes them highly resistant to bacterial attack (Mussgnug *et al.*, 2010), producing low methane yields during the fermentation process. The pre-treatment process can aid the decomposition of the cells and improve methane production (Chen and Oswald, 1998). From Figure 4-4, the steep initial curve for all macroalgal substrates is indicative of fast degradation rates (*k*), with values ranging from 0.33 – 0.36 /day (Table 4-6). This suggests that basic pre-treatments can improve hydrolysis rates (Costa *et al.*, 2012) and enhance biogas production and yield (Bruhn *et al.*, 2011b; Allen *et al.*, 2013a). The values are comparable to (0.23 / d) obtained for dried *Ulva*, (0.433 / d) food waste and (0.239 / d) for grass silage (Allen *et al.*, 2013a). The R<sup>2</sup> values (Figure 4-5 B) indicate a good fit of the first order rate model,  $\log(\ln((B_0 - B) / B_0))$  against time. Of all the substrates, FD had the lowest C: N ratio at 8.61:1 (Table 4-2) while the other substrates were in the range 15 - 30: 1 which has been proposed as being optimum for anaerobic digestion (Xu *et al.*, 2013).

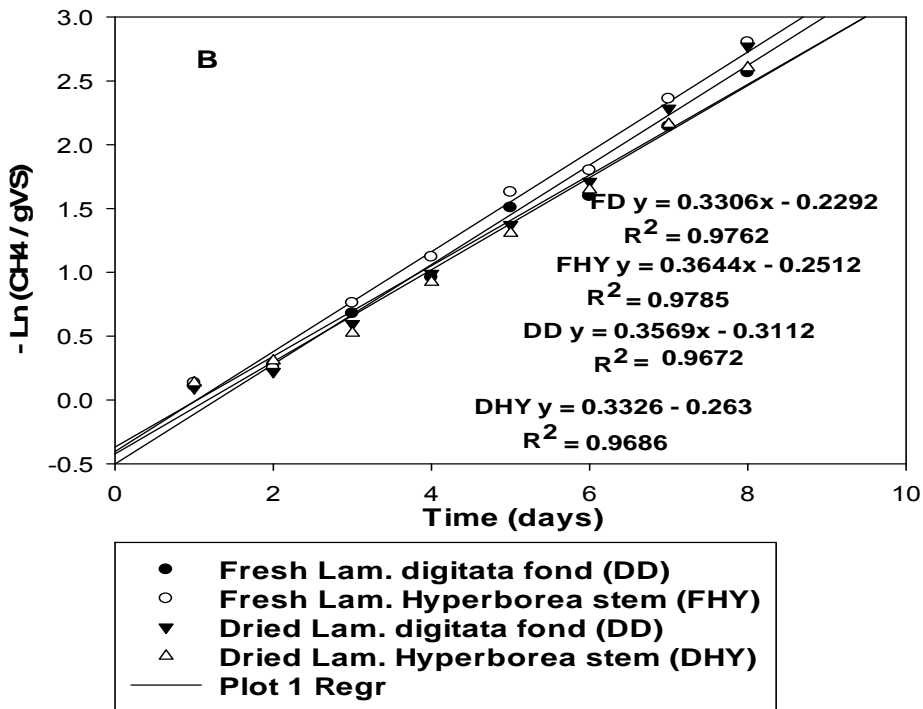
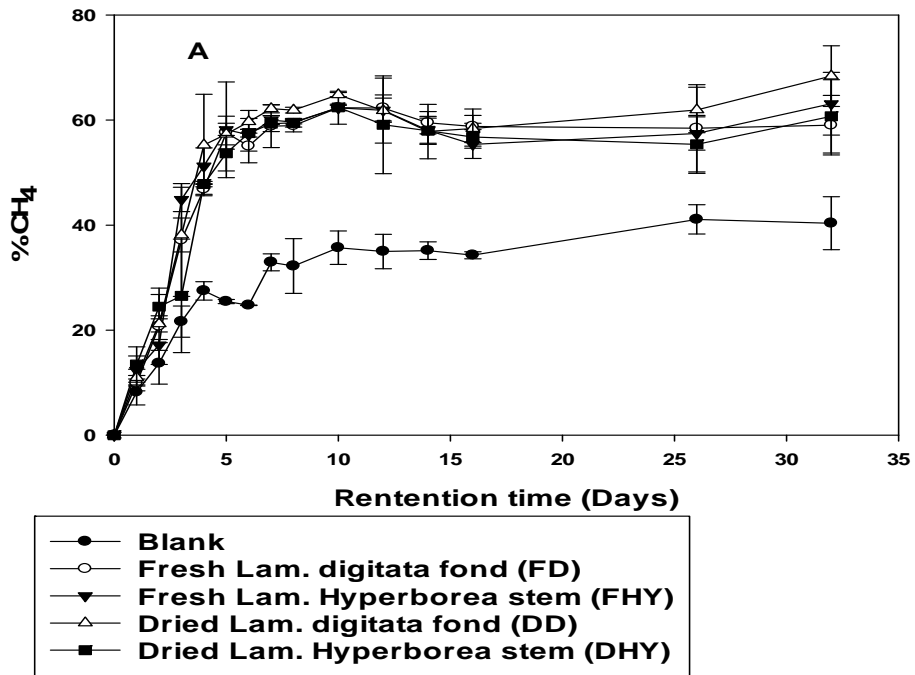


Figure 4-5: A) Macroalgal methane composition and, b) First order plot of the cumulative methane production of pre-treated macroalgal samples FD, FHY, DD and DHY.

Although there was no apparent inhibition of methane production when the C: N ratio was less than 20: 1, it is assumed that the imbalance between carbon and nitrogen requirements of the anaerobic microflora (Speece, 1996b) could eventually lead to elevated ammonia levels in the bioreactors, leading to failure (Chen *et al.*, 2008; Nielsen and Angelidaki, 2008). Ammonia toxicity is due to the accumulation of total ammonia nitrogen (TAN), but specifically, it is mainly from free ammonia (NH<sub>3</sub>) which inhibits methanogens, leading to the accumulation of volatile fatty acids (VFAs) (Astals *et al.*, 2013). The selection of an appropriate inoculum to substrate ratio is one way of overcoming VFA toxicity, allowing continued biogas production as the sludge (inoculum) acclimatizes to the substrate content or any inhibitory substances present (Muruganandam *et al.*, 2008). The inoculum to substrate ratio of 3:1 used in this research has been recommended by various authors (Raposo *et al.*, 2006; Angelidaki *et al.*, 2009), and as a result, inhibition from known inhibitory compounds such as sulphide and phlorotannins, which are well-described components of brown algae (*Phaeophytes*) (Connan *et al.*, 2006), did not occur in these batch tests.

Table 4-6 compares the BMP results with the theoretical methane potential estimated from Eqn 4-1. The fresh (FD) and dried (DD) samples achieved 28% and 36% of their theoretical values respectively. Allen (Allen *et al.*, 2013a) reported between 36% to 42% of the theoretical value achieved for pre-treated *Ulva* samples. The estimated methane yield was 103.56 m<sup>3</sup> CH<sub>4</sub> / t wet for DD and 72 m<sup>3</sup> CH<sub>4</sub> / t for FD, confirming that dried samples generated higher volumes of methane than the fresh samples.

#### 4.3.4 Methane Production (Validation samples)

The BMP results (cumulative methane production) is shown in Figure 4-6. The appearance of the graph for all samples agrees with typical example proposed by Angelidaki (Angelidaki *et al.*, 2009). Interestingly, both FDL (161 ± 1.44 L CH<sub>4</sub> kg VS<sup>-1</sup>) and FDS (161 ± 2.68 L CH<sub>4</sub> kg VS<sup>-1</sup>) achieved the highest BMP followed by DDL (150 ± 0.78 L CH<sub>4</sub> kg VS<sup>-1</sup>), while FHL (108 ± 3.16 L CH<sub>4</sub> kg VS<sup>-1</sup>) showed the lowest BMP after 38 days incubation at 35 °C.

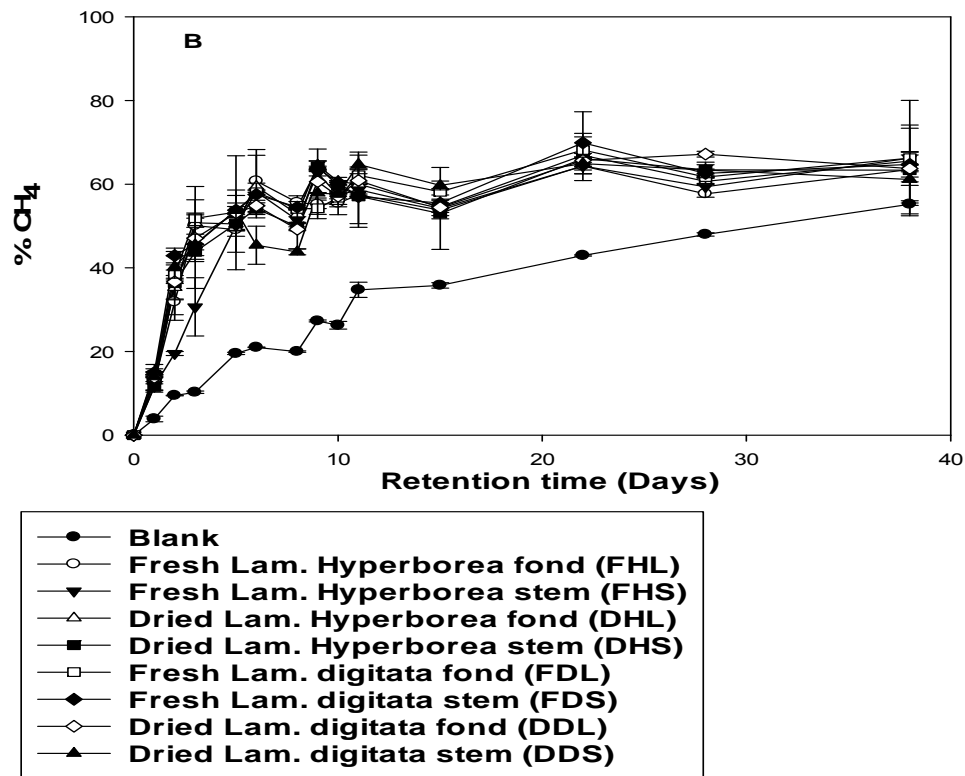
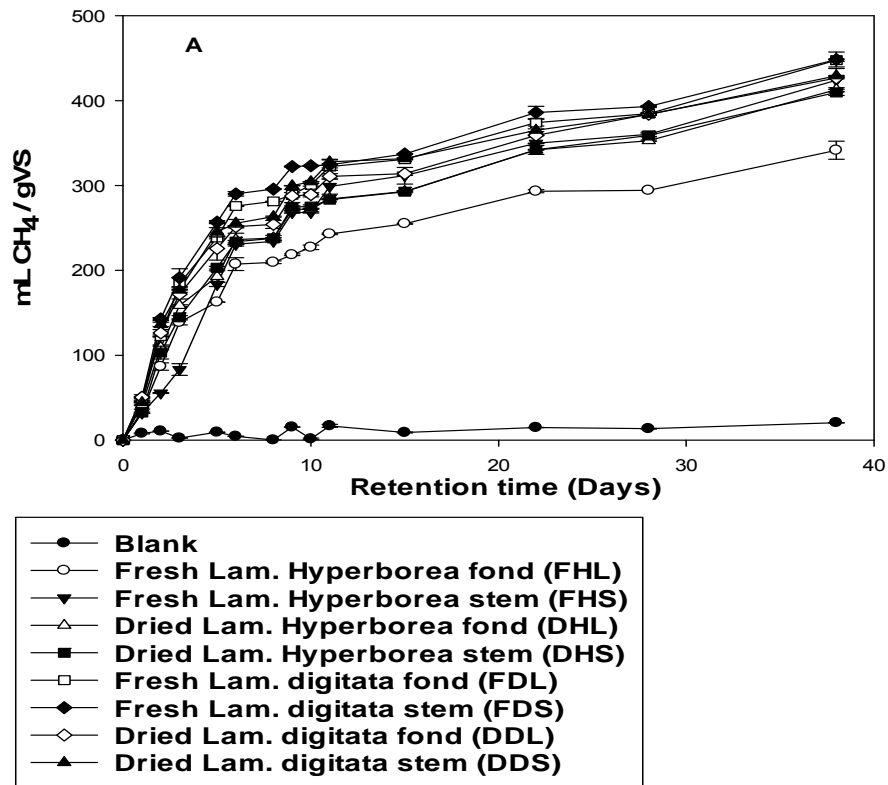


Figure 4-6: A) Cumulative BMP and, B) Percentage of methane in biogas from the BMP test for the second sample of seaweeds.

The values obtained for FDL differ from the first BMP results (Figure 4-4 A) supporting the fact that both seasonal and compositional variation of macroalgae can affect BMP values (Adams *et al.*, 2011b). Comparing the steeper curve between Figure 4-4 and Figure 4-6, the degradation rate (k) was slightly lower for second seaweed samples with values ranging from 0.22 - 0.34 (Figure 4-7). The maximum percentage of methane obtained in all reactors was above 60%, Figure 4-6 B.

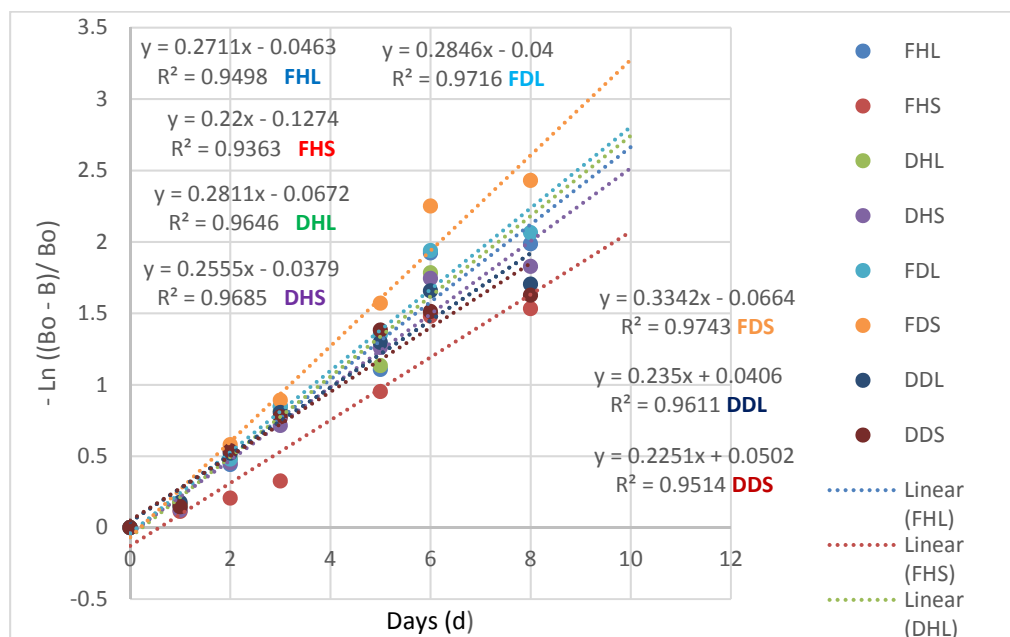


Figure 4-7: First order plot of cumulative methane production for Figure 4-6.

Table 4-6: BMP results compared to theoretical yield.

Algae substrates	Methane yield (BMP) L CH <sub>4</sub> /kg VS	*Theoretical methane yield L CH <sub>4</sub> / kg Vs	Wet yield m <sup>3</sup> CH <sub>4</sub> /t wet based on BMP	Degradation rate K (d <sup>-1</sup> )	R <sup>2</sup> (%)
Fresh Laminaria. Digitata (FD)	93.35 ± 5.77	335.36	67.24	0.33	0.98
Fresh Laminaria. Hyperborea (FHY)	105.06 ± 5.03	334.74	72.57	0.36	0.98
Dried Laminaria Digitata (DD)	141.45 ± 5.77	393.73	97.66	0.36	0.97
Dried Laminaria Hyperborea (DHY)	113.28 ± 5.97	384.16	71.58	0.33	0.97

\*By Buswell Equation (Eqn 4-1)

## 4.4 Conclusion

A proposed modified new BMP method using Supel™ inert gas sampling bags as biogas collection and storage system on all reactors were studied with macroalgae as substrate. Pre-treatment processes of washing, macerating and drying were undertaken to assess the algae strain with higher bio-methane potential. Washed and dried *Laminaria digitata* produced the highest BMP of  $141 \pm 5.77 \text{ L CH}_4 \text{ kg VS}^{-1}$  with  $k$  ( $0.36 \text{ d}^{-1}$ ) and methane content of about 70% during the period of experimentation. This yield compared to the theoretical methane yield ( $394 \text{ L CH}_4 \text{ kg VS}^{-1}$ ) is about %64 of the fermentable energy in the macroalgae. It can be concluded that both pre-treatment of the algae and pre-incubation of the inoculum aided in the faster degradation rate observed in all the substrate. The results shows as reported by (Allen *et al.*, 2015) that macroalgae has the potential to be a viable source of generation of gaseous biofuels which are now known as third generation biofuel (Jones and Mayfield, 2012) to differentiate first and second generation from terrestrial biomass which has significant negative opinion to limit their production (Smyth *et al.*, 2010; Jung *et al.*, 2011). Results, as shown from experiment two (Figure 4-6), proved the method is in agreement with a typical BMP test appearance (Angelidaki *et al.*, 2009).

The proposed modified BMP approach has certain inherent advantage over current methods in use;

- I. Gas measurement converted to STP is carried out directly from the gasbags at ambient conditions, so do not require liquid displacement or pressure transducers.
- II. The volume of methane produced is also directly measured from the gas bags.
- III. Larger volume of reactor and substrate of heterogeneous nature can be added/used.
- IV. Room for easy modification and adaptability to suite specific BMP process.
- V. Easy application.

A disadvantage to this method could be the cost of the gas bags. It is highly recommended that in applying this approach the duration of experimentation should exceed the typical 30 day period for batch assay depending on substrate used as evident in observed gas production after day 30 in this work. Hansen *et al.* (2004) has proposed a 50 day period in their approach. Care should be taken not to have too large a headspace in the reactor bottle leading to erroneous biogas and methane estimation.



## Chapter 5. Thermochemical characterization of brown seaweed, *Laminaria digitata* from UK shores.

### *Abstract*

Brown algae, *Laminaria digitata* (LD) samples were collected at six-month intervals within a year (January, July and December 2015), and assessed for a range of thermochemical properties. Initial pyrolysis rates using thermogravimetric analysis (TGA) were carried out to assess their proximate characteristics, ranging from moisture content (MC) (3.48% - 4.10%), volatile content (VC) (56.64 - 56.23%), char (11.80 - 12.76%) and ash (27.87 - 29.95%). Analysis by pyrolysis gas chromatography–mass spectrometry (Py-GC/MS) identified sixty-four compounds present in all samples, twenty of which have been reported previously as major pyrolysis products of *Laminaria digitata*. <sup>1</sup>H NMR analysis of sodium alginate fractions extracted from the samples was used to characterise the monad, diad, triad frequencies and average block length of the alginate. Results of the monad frequencies which ranging from  $F_M$  (0.36 - 0.46) and  $F_G$  (0.54 - 0.64) are consistent with reported values in literature. The *Laminaria digitata* alginate also showed values that are in agreement with most reported literature for both diad frequencies, homopolymeric mannuronic ( $F_{GG} = 0.19 - 0.25$ ) and guluronic ( $F_{MM} = 0.33 - 0.47$ ) blocks with alternating block fractions of ( $F_{GM} = 0.17 - 0.21$ ) and ( $F_{MG} = 0.17 - 0.21$ ), respectively. The M/G ratio value of 1.18 - 1.79 has been stated for alginates that can be used to produce soft and elastic gels rather than brittle ones. Furthermore, the computed triad frequencies results are ( $F_{GGG} = 0.14 - 0.17$ ,  $F_{MGM} = 0.11 - 0.13$ ,  $F_{GGM} = F_{MGG} = 0.05 - 0.09$ ) and the average block lengths are ( $N_G = 2.15 - 2.22$  and  $N_M = 2.61 - 3.85$ ). To the author's knowledge, this is the first report to evaluate triad frequencies and average block length on *Laminaria digitata* collected from UK shores.

## 5.1 Introduction

An introduction to this chapter has been given in Section 2. 20. In this study the pyrolytic characteristics of a representative sample of brown seaweed, *L. digitata* was studied using Py-GC/MS and the different degradation pathways of the characteristic volatile compounds present in the seaweed using TGA. <sup>1</sup>H NMR analysis of the alginate fraction extracted from the seaweed is given. A margin of errors  $< \pm 0 - 0.2\%$  was taken into consideration during integration of peak areas on the NMR spectrum.

## 5.2 Material and Methods

### 5.2.1 Collection, pretreatment, and storage

Algal biomass *L. digitata* used in this study were collected from shallow water during low tide at Seaton Sluice, 55.0836° N, 1.4744° W, Northumberland UK (NZ 3350) in January, July and December 2015 and pre-treated in accordance with Section 3.1.

### 5.2.2 Thermal Analysis

The samples were analysed using thermogravimetry (TGA) and differential scanning calorimetry (DSC), combined with quadrupole mass spectrometry (QMS) for analysis of the gas evolved during thermal decomposition. A subsample (ca.30 mg) of the finely disseminated sample was accurately weighed into an alumina crucible and analysed using a Netzsch Jupiter STA 449C TG-DSC (thermogravimetry-differential scanning calorimetry) system connected to a Netzsch Aeolos 403C quadrupole mass spectrometer (QMS). Samples were heated from 25 °C to 900 °C at a rate of 10 °C min<sup>-1</sup> in an atmosphere of helium (purge gas, flow rate 30 ml min<sup>-1</sup>). The protective gas was helium (flow rate 30 ml min<sup>-1</sup>). Adapter heads and transfer lines (between the Jupiter and Aeolos) were at 150 °C. TG and DSC data were acquired and processed using Netzsch Proteus 61 software. The QMS was operated in full scan mode over the range m/z 10 - 300, and mass spectrometric data were acquired and processed using Aeolos

software. The main ions of interest in the QMS analysis were:  $m/z$  12, (carbon);  $m/z$  18 (water) and  $m/z$  44, (carbon dioxide). Quantitative data for the abundance of selected ions in the evolved gas during heating were converted into ASCII format and subsequently into Excel format for further processing.

### 5.2.3 *Pyrolysis-gas chromatography-mass spectrometry analysis (Py-GC-MS)*

Py-GC-MS analysis was performed on a CDS Pyroprobe 1000 linked via a CDS1500 valve interface (320 °C) and a Hewlett-Packard 6890GC split injector (320 °C) linked to a Hewlett-Packard 5973MSD (electron voltage 70 eV, emission current 35  $\mu$ A, source temperature 230 °C, quadrupole temperature 150 °C, multiplier voltage 2200 V, interface temperature 320 °C). The acquisition was controlled by an HP Kayakxa Chemstation computer, in full scan mode (50 – 650 amu). The sample approximately 1mg, which was prepared as described in Section 5.2.1, was weighed into a quartz tube with glass wool end plugs. The tube was then placed into a pyro probe platinum heating coil and then sealed into the valve interface. The run was then started with the sample being pyrolyzed at 610 °C for 10 seconds with the split open. At the same time, the GC temperature programme and data acquisition commenced. Separation was performed on a fused silica capillary column (60 m x 0.25 mm i.d) coated with 0.25  $\mu$ m 5% phenyl methyl silicone (HP - 5MS). Initially the GC was held at 50 °C for 5 minutes and then the temperature programmed from 50 °C - 320 °C at 5 °C min and held at final temperature for 30 minutes, total 90 minutes, with Helium as the carrier gas (constant flow 1ml min<sup>-1</sup>, initial pressure of 120kPa, split at 30 mls min<sup>-1</sup>). Each acquired data run was stored on DVD for later data processing, integration, and printing.

### 5.2.4 *Alginate extraction*

Alginate extracted from the three algae samples (January, July, and December) and the analysis was conducted based on (Calumpong *et al.*, 1999) and (Torres *et al.*, 2007). Fifty grams of each dried samples were soaked overnight in a 2% formaldehyde solution (500 mL) to eliminate pigments, then washed with distilled water and added to a 0.2 M HCl solution (500 mL) before being set aside for 24 h. Samples were washed again with distilled water before being extracted with

2% sodium carbonate solution for 5 hrs (Torres *et al.*, 2007). The supernatants were collected after extraction by centrifugation and sodium alginate was precipitated with ethanol. Finally, sodium alginate was purified twice with ethanol, then with methanol and acetone before being dried at room temperature (Fertah *et al.*, 2014).

### 5.2.5 Proton Nuclear Magnetic Resonance ( $^1\text{H NMR}$ ) Analysis

The samples were run on a Bruker Avance III HD 700 MHz NMR spectrometer with a TCI cryoprobe. Samples were run in  $\text{D}_2\text{O}$  at 353 K and referenced to TSP. M/G ratios were calculated as described in the protocol (ASTM F2259., 2012). Sample preparation procedure was according to ASTM F2259. (2012). 100 mL of a 0.1% (w/v) alginate solution was prepared and the pH adjusted with HCl (1 M, 0.1 M) to pH 5.6, and the alginate sample was put in a water bath at 100 °C for 1hr. The pH of the sample solution was readjusted with HCl (1 M, 0.1 M) to pH 3.8, and the alginate sample put back to the water bath at 100°C for 30min. Thereafter, the pH was adjusted with NaOH (1 M, 0.1 M) to pH 7 - 8, and the sample was freeze-dried overnight. The alginate sample was then dissolved in 5 mL 99 - 99.9%  $\text{D}_2\text{O}$ , and freeze-dried again. 10 to 12 mg of the sample was then dissolved in 1 mL 99.9%  $\text{D}_2\text{O}$ . 0.7 mL of the alginate solution was then added to an NMR tube, and then 20  $\mu\text{L}$  0.3 M TTHA (triethylenetetraminehexaacetic acid) was added to the same tube. This analysis was carried out in the School of Chemistry, Newcastle University, UK.

## 5.3 Results and Discussion

### 5.3.1 Thermal Gravimetric Analysis (TGA)

The TGA represents an initial pyrolysis step with differences in mass loss at set temperatures indicating a difference in pyrolysis behaviour (Adams *et al.*, 2011a). Algae exhibit a stepwise degradation pathway corresponding to the thermal decomposition of the different biopolymers present, and the degradation can be observed using TGA under an inert atmosphere. (Ross *et al.*, 2009).

The TGA results are shown in Figure 5-1, for dried *L digitata* collected in January as a sample graph. The TGA profiles show the rate of change during heating and

were similar for all the dried samples collected in January, July and December. The different peaks in the DTG curve shown in Figure 5-1, indicate three main decomposition steps: The first step is the dehydration step (25 °C -105 °C), followed by the devolatilization region (105 °C - 499 °C) and the decomposing region (500 °C – 900 °C). The devolatilization is characterised by stepwise decomposition of the different biopolymers fractions (Ross *et al.*, 2009). The samples exhibited a typical decomposition profile with the largest decrease in sample weight (DT<sub>max</sub>) occurring at ~ 250 °C, followed by a second phase of decomposition around ~ 280 °C – 300 °C in all the samples, and a continual reduction in weight throughout the TGA process. The decomposition at ~ 250 °C which has the highest point of inflection from the thermogram peaks can be assigned to the Na-alginate biopolymer (Ross *et al.*, 2011; Rowbotham *et al.*, 2013), while at ~ 280 °C - 300 °C the peaks can be regarded as volatilization of carbonaceous material (Soares *et al.*, 2004). This is similar to values of ~ 250 °C and ~ 300 °C reported in literature for *L digitata* (Adams *et al.*, 2011a). The range ≤ 105 °C is considered as moisture content (MC), between 105 °C ≤ x ≤ 500 °C is the volatile content (VC) and 500 °C ≤ x ≤ 900 °C is char and materials still remaining at 900 °C are ash (Adams *et al.*, 2011a). These values from the TGA profiles indicating change in percentage mass are shown in Table 5-1.

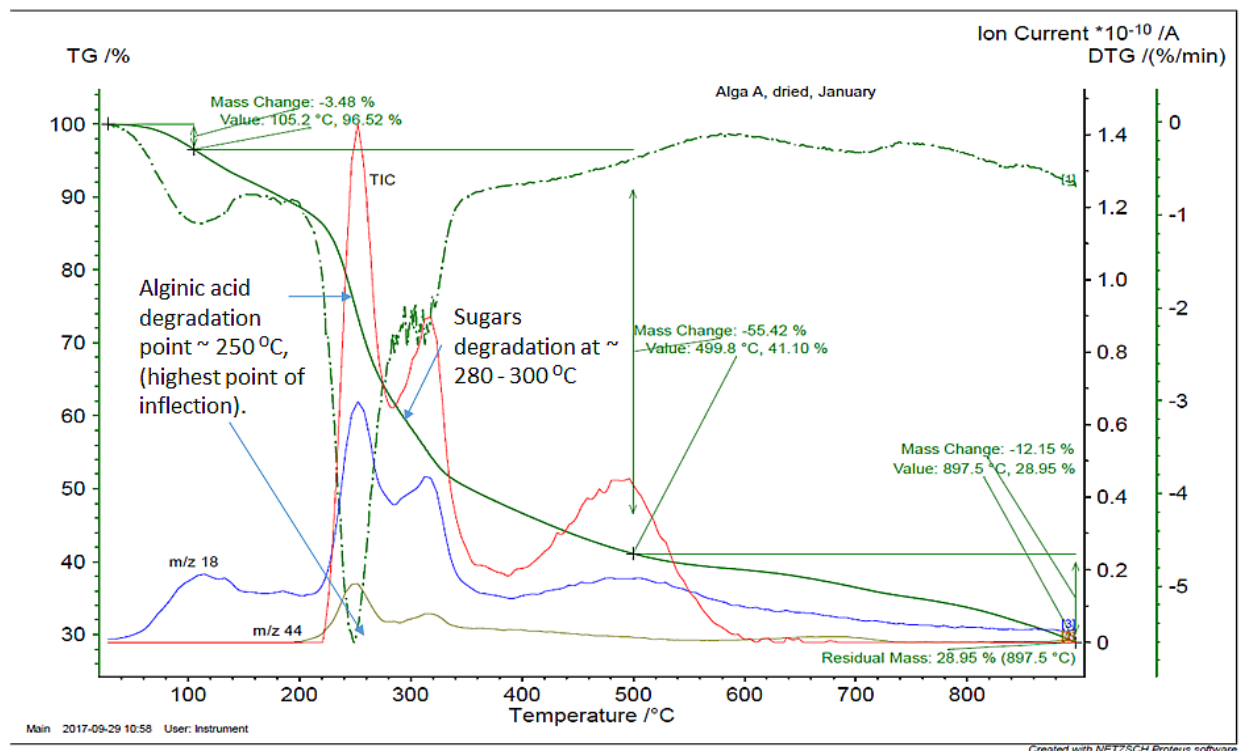
Table 5-1 TGA and elemental analysis results for algae samples

Algae	January	July	December		January	July	December
	TGA analysis				Elemental analysis		
Moisture content	3.48% (0.18)	3.02% (0.36)	4.10% (0.22)	Carbon (C)	28.93% (0.33)	30.83% (0.14)	29.44% (0.17)
Volatile content	55.42% (0.23)	54.64% (1.55)	56.23% (0.88)	Hydrogen (H)	5.22% (0.21)	4.98% (0.10)	4.99% (0.06)
Char	12.15% (1.25)	12.76% (1.97)	11.80% (0.38)	Nitrogen (N)	2.55% (0.11)	1.43% (0.08)	1.10% (0.18)
Ash	28.95% (1.19)	29.59% (2.12)	27.87% (1.11)	Oxygen (O)	37.54% (0.15)	37.56% (0.20)	37.59% (0.11)
				Sulphur (S)	0.35% (0.09)	0.26% (0.19)	0.33% (0.16)

SD is shown in parenthesis

The MC ranges between 3.48% - 4.10%, VC is within 56.64 - 56.23%, the char is 11.80 - 12.76% and ash is between 27.87 - 29.95%. This demonstrates the algae sample collected in different months had only minor difference and are relatively

constant in the parameters assessed. *L. digitata* has been reported to have an MC of ~3.5 - 6.1%, VC ~ 50 - 65%, char ~14% and ash ~ 22.5 - 33.2% (Adams *et al.*, 2011a). Assessing the different peaks in the DTG curve from Figure 5-1, using the m/z 44 ion shows that at the temperature region of between 200 °C - 300 °C some readily destroyed organic carbon were volatilized producing CO<sub>2</sub>, this was followed by the region between 400 °C - 500 °C where further volatilisation of heavier fraction took place producing more CO<sub>2</sub>. Also from Figure 5-1, assuming that char is thermally stable under inert conditions (He atmosphere), then the slight increase in abundance of the m/z 44 ion and decrease in the DTG curve in the range 600-750 °C could be due to the thermal decomposition of carbonates, producing CO<sub>2</sub>. The gradual loss of mass > 600 °C can be ascribed to the decomposition of mineral components of the algae (Ross *et al.*, 2009) which play an important role in the amount of char produced (Nowakowski and Jones, 2008). It should be noted that cations present in the biopolymer molecules (for instance in alginate structure) help to stabilise it during thermal decomposition, influencing the decomposition pathway, hence the extent of char formation (Ross *et al.*, 2009).



TIC – Total ion content, m/z 18 – mass to charge ratio for H<sub>2</sub>O, m/z 44 – mass to charge ratio for CO<sub>2</sub>

Figure 5-1: TGA profile for *Laminaria digitata* collected in January 2015.

### 5.3.2 Pyrolysis-gas chromatography-mass spectrometry analysis

Pyrolysis technique has been used to study and characterise behaviour of a number of brown macroalgae (seaweeds) collected in the UK (Ross *et al.*, 2009). Adams *et al.* (2011a), carried out Py-GC-MS at 500 °C on *L. digitata*, and identified 29 peaks as consistently present in the sample spectra of which 12 (toluene; pyrrole; furfural; ethanone, 1-(2-furanyl); furfural, 5-methyl; 1,2-cyclopentanedione, 3-methyl; phenol; dianhydromannitol; indole; 3,7,11,15-tetramethyl-2-hexadecen-1-ol) were selected as key marker compounds, used to screen for compositional changes over time.

In the current study, Py-GC-MS was carried at 610 °C on duplicate samples of the algae collected in January, July and December. A total of 64 peaks were identified, which were consistently present in all of the three sample spectra as shown in Figure 5-2, with an extended spectrum of January thermogram given in Appendix A, Figure (A-D). The peaks (compounds) were identified using a combination of a mass spectral database and retention data for standard components (Ross *et al.*, 2009). The identified peaks are listed in Table 5-2. Twenty of the compounds (2, 3 butanedione, 2-Propanone, 1-hydroxy-, Furfural, Ethanone, 1-(2-furanyl)-, 2-Furan carboxaldehyde, 5-methyl-, 1, 2-Cyclopentanedione, 3 methyl, 2-Cyclopenten-1-one, 2-hydroxy-3-methyl-, Dianhydromannitol, Acetic acid, 2-Butanone -3- hydroxyl, Pyrrole, Toluene, Furan-2,5 dihydro, 2- Cyclopenten-1-one-2- hydroxy, Phenol, Phenol, 4- methyl, 2-3 (H) Furanone, 5 acetylhydro, Isosorbide) have been previously identified as major pyrolysis products of *L. digitata* (Ross *et al.*, 2009; Adams *et al.*, 2011a). These compounds are derived from the pyrolytic degradation of the biopolymers present in the macroalgae which have been classified into the polysaccharide (carbohydrates) origin and those of protein, lipid and phenolic origin (Adams *et al.*, 2011a). Depending on the brown algae specie the carbohydrate fractions are dominated by alginates, laminarin, mannitol, and fucoidan. While several other compounds have been identified and listed, the major pyrolysis product from alginate is furfural (Ross *et al.*, 2009; de Wild, 2015) and a sizeable range of cyclopentenones (Ross *et al.*, 2011), while laminarin is mainly 1,2-cyclopentanedione, mannitol is isomannide, and fucoidian is dominantly 2-furancarboxaldehyde (Ross *et al.*, 2009). Pyrolysis of biomass is a complex

process (Adams *et al.*, 2011a) and variability in products could arise as a result of biomass composition, presence of inorganic material and heating rate (Nowakowski and Jones, 2008).

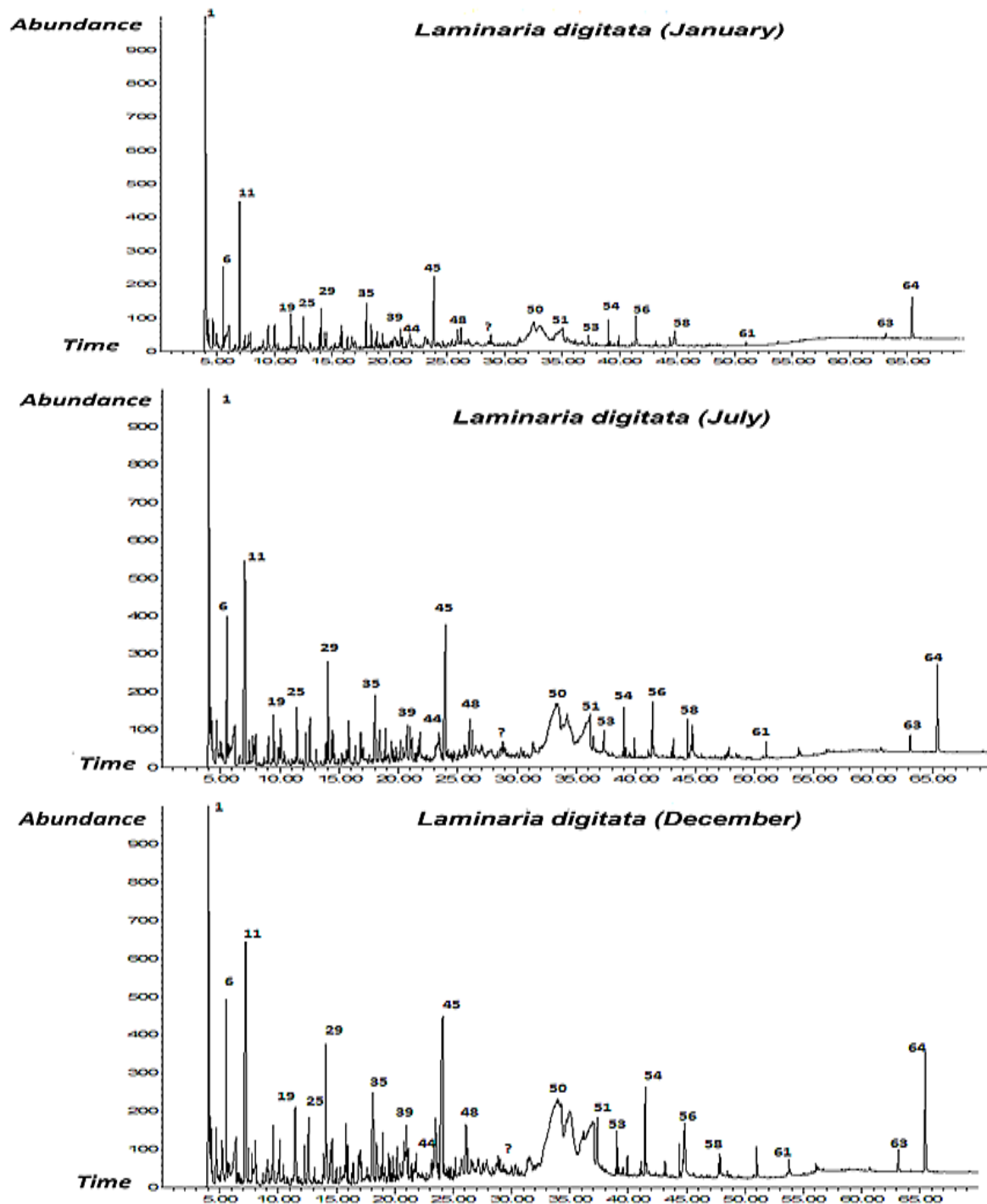


Figure 5-2 Py-GC/MS profile at 610°C for *Laminaria digitata* collected in January, July, December (identified compounds are listed in Table 5-2).



Table 5-2 Compounds identified in pyrograms from Py-GC/MS of *Laminaria digitata*.

No	Compounds	No	Compounds	No	Compounds
1	CO <sub>2</sub>	22	2-Propanone -1- acetyloxy	43	Cyclohexanol, 5-methyl-2-(1-methylethyl)-, (1 $\alpha$ ,2 $\beta$ ,3 $\alpha$ )
2	Acetaldehyde	23	2- Cyclopentene-1,4 dione	44	1,2 Benzenediol
3	Methanethiol	24	2- Cyclopentene-1-one 2 methyl	45	Dianhyromannitol
4	Acetone	25	Ethanone, 1-(2-furanyl)-	46	2,6,10 Dodecatrien-1-ol,3,7,11 trimethyl
5	Formic acid	26	Furan-2,5 dihydro	47	Isosorbide
6	2,3 Butanedione	27	2-Furancarboxaldehyde -5-methyl	48	Dianhyromannitol
7	2-Butanone	28	2- Cyclopenten-1-one,2-hydroxy	49	1H indole -3 methyl
8	Acetic acid + Furan 2 me	29	2-Furan carboxaldehyde, 5-methyl-	50	d-Mannitol-1,4 - Anhydro
9	Acetic acid	30	2- Cyclopenten-1-one-3 Methyl	51	d-Mannitol-1,5- Anhydro
10	Butenal + unknown	31	Phenol	52	Mannitol
11	2-Propanone, 1-hydroxy-	32	3-Amino-1,2,4-triazole	53	C14 Fatty acid
12	2,3 Pentanedione	33	Cyclopenten-1-one-2,3 dimethyl	54	1,19 Eicosadiene
13	2-Butanone -3-hydroxyl	34	2- Cyclopenten-1-one-3,4 dimethyl	55	Tetramethyl -2 hexadecenol
14	Pyrrrole- 1- methyl	35	1,2-Cyclopentanedione, 3 methyl	56	C16 Fatty acid
15	Pyrrrole	36	Thiophene-2-methoxy -5-methyl	57	Eicosapentaenoic acid methyl ester
16	Toluene + Alkane	37	3-4 Dimethyl- 2-hydroxycyclopent-2-en-1-one	58	C18 Fatty acid ( 9-octadecanoic acid)
17	Propanoic acid -2-oxo-methyl ester	38	Phenol, 4- methyl	59	C16 Diacid
18	Cyclopentanone	39	2-Cyclopenten-1-one, 2-hydroxy-3-methyl-	60	Pyrrrolopyrazine-dione-hexahydro
19	Furfural	40	2-3(H) Furanone , 5 acetyl hydro	61	2-hydroxy - hexadecanoic acid ethyl ester
20	2 Methyl Cyclopentanone	41	Benzo nitrile	62	9-Octadecenoic acid ethyl ester
21	2 Furanmethanol	42	Pyranones	63	Ergosta-5,24-dien-3,ol(3 beta) (Sitosterol)
				64	Fucosterol (Sterol)

Pyrolysis is an alternative thermolytic technique for the conversion of biomass to fuel and is classified by temperature and process time into slow ( $\leq 400$  °C, from minutes to days for solids), fast and flash process ( $\geq 500$  °C, short vapour residence times of a few seconds or less) (Milledge *et al.*, 2014). The technique employed here is fast  $> 500$  °C (610 °C for 10mins) and has the potential for the

commercial production of biofuel from biomass (Brennan and Owende, 2010; Li *et al.*, 2013b), however needs to get rid of water. Compared to other conversion technologies, research on the pyrolysis of algal biomass is quite extensive, and has achieved reliable and promising outcomes that could lead to commercial exploitation (Brennan and Owende, 2010). Information on the potential use of macroalgae for thermochemical conversion can be provided by Py-GC/MS (Adams *et al.*, 2011a). The brown algae studied produce pyrograms containing 1,4-5 dianhydro-D-mannitol (peaks 10 - 13) presumably from the dehydration of mannitol (hexane-1,2,3,4,5,6-hexol) (Ross *et al.*, 2009). The compounds, 2, 3 butanedione, 2-Propanone, 1-hydroxy-, Ethanone, 1-(2-furanyl)-, Dianhyromannitol, Fucosterol (Sterol) are the dominant products in all the *L. digitata* samples.

### 5.3.3 <sup>1</sup>H NMR Analysis

Information on the sequential structures of alginates were first given by the works of Haug and coworkers (Haug *et al.*, 1963; Haug *et al.*, 1967) where alginates were separated by partial acidic hydrolysis and fractionation into three fractions with differing composition: Two homopolymeric molecules of guluronic (G) and mannuronic (M) acid and equal proportions of both monomers containing large number of MG dimer residues (Stephen and Phillips, 2016). Now detailed chemical composition and sequential structure of alginate can be determined by <sup>1</sup>H- and <sup>13</sup>C-nuclear magnetic resonance spectroscopy (NMR) (ASTM F2259., 2012). <sup>1</sup>H NMR spectroscopy is regarded as the main technique used to investigate alginate composition and structural patterns (Grasdalen, 1983; Torres *et al.*, 2007). The <sup>1</sup>H NMR data are calculated from a set of equations relations which utilise numeric integration of the relevant signal (labelled as A, B<sub>1</sub>-B<sub>4</sub>, C) from the NMR spectrum as shown in Figure 5-3, from where both the chemical composition and sequence of the alginate are determined (ASTM F2259., 2012). The labelled signal is assigned or represented by signal A = G (Proton 1), B<sub>1</sub> = GGM (proton 5), B<sub>2</sub> = MGM (proton 5), B<sub>3</sub> = MG (proton 1), B<sub>4</sub> = MM (proton 1), C = GG (proton 1).

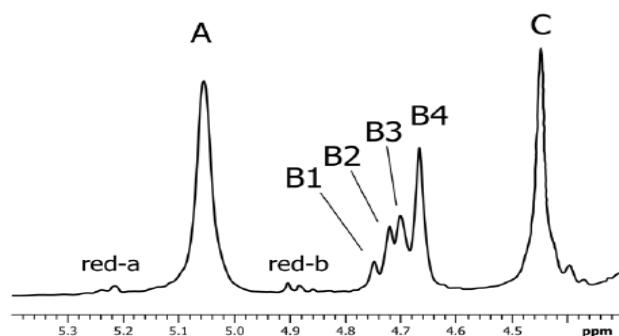


Figure 5-3 The region of the  $^1\text{H}$  NMR spectrum of alginate used for quantitative analysis .

A = G (Proton 1), B<sub>1</sub> = GGM (proton 5), B<sub>2</sub> = MGM (proton 5), B<sub>3</sub> = MG (proton 1), B<sub>4</sub> = MM (proton 1), C = GG (proton 1). (ASTM F2259., 2012)

Figure 5-4 shows examples of some typical  $^1\text{H}$ -NMR spectra from brown algae.

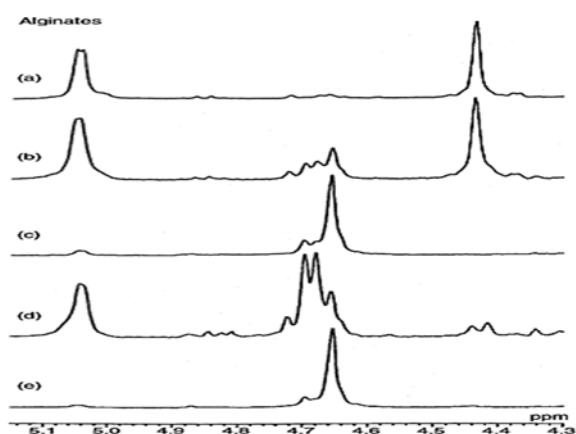


Figure 5-4 Some examples of typical  $^1\text{H}$ -NMR spectra of some alginates.

(a) G-block fraction from *L. hyperborea* stipes. (b) High-G alginate from *L. hyperborea* stipes. (c) Bacterial alginate from *Pseudomonas* spp. (d) MG-block fraction from *A. nodosum*. (e) M-block fraction from *A. nodosum* fruiting bodies

(Stephen and Phillips, 2016)

Figure 5-5 shows the  $^1\text{H}$  NMR spectra for *Laminaria digitata* sodium alginate samples (January, July, and December) from this study. These spectra show characteristics similar to the anomeric regions in Figure 5-3, with specific peaks of guluronic acid anomeric proton (G-1) at peak 5.05 ppm (peak A); guluronic acid H-5 (G-5) at 4.45 (peak C) and mannuronic acid anomeric proton (M-1) at

4.64 (peak B<sub>4</sub>) and the C-5 alternating block (G-M<sub>5</sub>) at 4.7 (peak B<sub>1</sub>-B<sub>2</sub>). This is in agreement with results observed for Moroccan *L. digitata* (G-1 5.17, G-5 4.56, M-1 4.76 and G-5 4.82) (Fertah *et al.*, 2014).

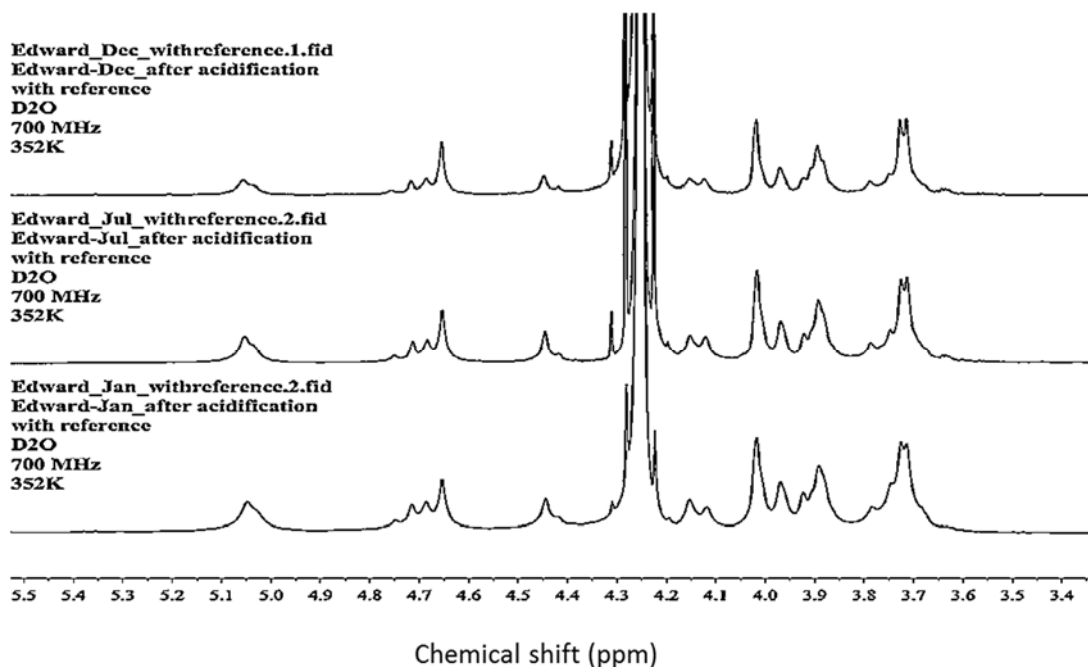


Figure 5-5: <sup>1</sup>H NMR spectra for solution of alginate from *Laminaria digitata* in D<sub>2</sub>O. 1. January 2. July 3. December, 2015.

The composition and block structure of the alginate molecules have also been reliably determined by <sup>1</sup>H NMR spectroscopy (Larsen *et al.*, 2003; Torres *et al.*, 2007; ASTM F2259., 2012). The NMR technique enables the determinations of monad frequencies F<sub>M</sub> (fraction of mannuronate units) and F<sub>G</sub> (fraction of guluronate units) and also both the nearest four diad (in form of F<sub>XX</sub>) and nearest eight triad (in form of F<sub>XXX</sub>) frequencies (ASTM F2259., 2012; Draget *et al.*, 2016). Grasdalen (1983) and Grasdalen *et al.* (1981) have proposed a method to calculate the block structure and M/G ratio.

There the individual, monad guluronic acid (F<sub>G</sub>), diad G-G (F<sub>GG</sub>) and triad (F<sub>GGG</sub>) is quantitatively calculated from relative area under peak (A, B<sub>1</sub>-B<sub>4</sub>, C) using the relations and equations below: (ASTM F2259., 2012).

The Monad frequencies

$$F_G = \frac{G}{M + G} , F_M = \frac{M}{M + G} \quad \text{Eqn 5-1}$$

The Diad (Doublet *et al.*) frequencies

$$F_{GG} = \frac{GG}{M + G} , F_{MM} = \frac{MM}{M + G}, F_{GM} = F_{MG} = \frac{G}{M + G} \quad \text{Eqn 5-2}$$

The Triad frequencies

$$F_{GGG} = \frac{GGG}{M + G}, F_{MGM} = \frac{MGM}{M + G}, F_{GGM} = F_{MGG} = \frac{GGM}{M + G} \quad \text{Eqn 5-3}$$

The Average block length is given as

$$N_G = \frac{F_G}{F_{GM}}, N_M = \frac{F_M}{F_{MG}}, N_{G>1} = \frac{F_G - F_{MGM}}{F_{GGM}} \quad \text{Eqn 5-4}$$

The M/G ratio was derived from the relations:

$$M/G = \frac{B_4 + 0.5 * (B_1 + B_2 + B_3)}{0.5 * (A + C + 0.5 * (B_1 + B_2 + B_3))} \quad \text{Eqn 5-5}$$

The computed values for monad, diad and triad frequencies, together with the average block length and M/G ratio of the alginate extracted in this study was compared to other reported *Laminaria* species (Table 5-3).

Fertah *et al.* (2014) stated that the three types of blocks present in a copolymer determine the physical properties of alginates. The uronic acid composition, *i.e* mannuronic (M) and guluronic (G) acid and M/G ratio influence the gelling properties of alginate (Penman and Sanderson, 1972). The value gives important information about the nature of the gel formed (Fertah *et al.*, 2014), and the gel strength depends on  $F_G$  and an average number of consecutive guluronate groups in the G-block structures ( $N_{G>1}$ ) (ASTM F2259., 2012). Alginates with high M/G ratios give elastic gels while low M/G ratios are an indication of a brittle gel (Penman and Sanderson, 1972). The results of the M/G ratio in this study for sodium alginate extract from *L. digitata* collected January (1.18), July (1.27) and December (1.79) compares closely with brown algae samples, *L. digitata* (1.56),

*Laminaria trabeculata* from Chapaco, Chile (1.73) (Torres *et al.*, 2007), *Laminaria digitata* from Morocco (1.12) (Fertah *et al.*, 2014), and others, as shown in Table 5-3. From the M/G ratios obtained in this study, it appears that *Laminaria digitata* from UK shores can be a good source of raw material to produce soft and elastic gels rather than brittle gels based on the report of (Penman and Sanderson, 1972) and the work of (Fertah *et al.*, 2014). It should be noted that the location of algae collection, and the extraction procedure used, influences the results of M/G ratio reported in literature (Torres *et al.*, 2007). The results of doublet fractions which are the homopolymeric block structure of mannuronic acid blocks ( $F_{MM}$ ), guluronic acid blocks ( $F_{GG}$ ) and alternating blocks ( $F_{MG=GM}$ ) are also shown in Table 5-3.

Table 5-3: Compositional data of alginate extracted from *Laminaria digitata* compared to other *Laminaries* species

		Calculated Peak Areas from Figure 5-5															
Algae collected (2015)	A	B1	B2	B3	B4	C	B1+B2+B3	G =	M =	M/G ratio	GG	MG =MG	MM	GGM = MGG	MGM	GGG	
January	1 (0.09)	0.23 (0.11)	0.32 (0.08)	0.382 (0.19)	0.75 (0.07)	0.60 (0.20)	0.932	1.0345	1.219	1.18 (0.69)	0.569	0.47	0.75	0.195	0.2711	0.37	
July	1 (0.05)	0.16 (0.06)	0.28 (0.33)	0.44 (0.23)	0.80 (0.17)	0.52 (0.06)	0.88	0.98	1.24	1.27 (0.22)	0.54	0.44	0.80	0.16	0.28	0.38	
December	1 (0.03)	0.17 (0.04)	0.37 (0.45)	0.43 (0.21)	1.38 (0.09)	0.60 (0.08)	0.97	1.0425	1.865	1.79 (0.80)	0.56	0.49	1.38	0.15	0.33	0.40	
Results compared with other compositional data of alginates extracted from <i>Laminaries</i> species.																	
		Monad frequencies		Diad frequencies					Triad frequencies				Avera block length				
Species	Origin	FG	FM	M/G ratio	FMM	FGG	FGM	FMG	FGGG	FMGM	FGGM	FMGG	NG	NM	NG>1	NM>1	Ref
<i>Laminaria digitata</i>	Morocco	0.47	0.53	1.12	0.47	0.41	0.06	0.06									Fertah et al., 2014
<i>Laminaria digitata</i>	Norway	0.41	0.59	1.44	0.43	0.25	0.16	0.16									Smidsrod and Draget 1996
<i>Laminaria digitata</i>	France Atlantic ocean	0.40	0.6	1.5	-	-	-	-									Parageorgiou at al.,2006
<i>Laminaria japonica</i>	China	0.35	0.65	1.86	0.48	0.18	0.17	0.17									Nai-yu et.al., 1994
brown algae, <i>Sargassum. vulgare</i>	Brazil	0.44	0.56	1.27	0.55	0.43	0.01	0.01									Torres et al., 2007
<i>Laminaria Digitata</i> January	UK	0.46	0.54	1.18	0.33	0.25	0.21	0.21	0.166	0.12	0.09	0.09	2.22	2.61	3.91	Not analysed	This study
<i>Laminaria Digitata</i> July	UK	0.44	0.56	1.27	0.36	0.24	0.20	0.2	0.17	0.13	0.07	0.07	2.22	2.82	4.38		This study
<i>Laminaria Digitata</i> December	UK	0.36	0.64	1.79	0.47	0.19	0.17	0.17	0.14	0.11	0.05	0.05	2.15	3.85	4.65		This study

SD is in parenthesis

The samples have slightly lower values for  $F_{MM}$  (0.33 - 0.47) and  $F_{GG}$  (0.19 - 0.25) compared to reported literature on *L. digitata*, and hence a slightly higher alternating block fractions  $F_{MG=GM}$  (0.17 - 0.21) except for the sample collected in December which compares very well with other *L. digitata* results. This could be attributed to method of calculation used, location of algae collection and the extraction procedure (Fertah *et al.*, 2014), or seasonal and growth conditions (Draget *et al.*, 2016). The alginate extracted from *L. digitata* collected from Florida has been reported to have a high alternating block fraction (0.24) which is closely related to this study. The calculated triad frequencies are the homopolymeric block structure of guluronic acid blocks ( $F_{GGG}$ ) and the alternating blocks of ( $F_{MGM}$ ,  $F_{GGM} = F_{MGG}$ ,) based on given relationships (ASTM F2259., 2012), as shown also in Table 5-3. The range of values for  $F_{GGM} = F_{MGG}$  (0.05 - 0.09) reported here is close to  $\approx 0.03$  reported for brown algae, *Macrocystis alginates* (Stephen and Phillips, 2016). Based on these frequencies, values for the average number of blocks lengths ( $N_G$ ) were determined (ASTM F2259., 2012).  $N_{G>1}$  is the average length of G-blocks after removal of singlets (-MGM-)(ASTM F2259., 2012). The results ( $N_G$ ) computed for the sodium alginate extracted from brown algae collected in January, July and December are also tabulated in Table 5-3, for the  $N_G$  guluronate units is (2.22, 2.22, 2.15) and  $N_M$  mannuronate units (2.61, 2.82, 3.85) respectively. From the above, it can be postulated that the range of average length of the G-blocks is between (2.15 - 2.22) and M-blocks (2.61 - 3.85) while the average length of the conservative G monomers ( $N_{G>1}$ ) is (3.91 - 4.65) for *L. digitata* collected from Whitney Bay off the UK in 2015. The M-entered triads and  $N_{M>1}$  were not assessed in this work as they are normally analysed using  $^{13}C$  NMR (ASTM F2259., 2012).

## 5.4 Conclusion

The brown algae samples exhibited a stepwise degradation pathway corresponding to the thermal decomposition of the different biopolymers which were observed using TGA under an inert atmosphere. Identification of the seaweed carbohydrates was carried out by detection of 'fingerprint' compounds by Py-GC/MS (Anastasakis *et al.*, 2011). The pyrograms obtained from Py-GC/MS of the samples at 610 °C include a range of interesting compounds



(fucoïdan, mannitol, Fatty acid, Sterol etc) identified against reference standards. From the alginate extracts, the monad frequencies ( $F_M$ , fraction of mannuronate units and  $F_G$ , fraction of guluronate units), diad frequencies ( $F_{MM}$ ,  $F_{GG}$  and alternating blocks  $F_{GM} = F_{MG}$ ) were evaluated. The values of the M/G ratio indicates *Laminaria digitata* from UK shore is a viable resource that could be used for the production of soft and elastic gels.

Therefore, the use of several analytical techniques; thermogravimetric analysis (TGA), pyrolysis gas chromatography-mass spectrometry (Py-GC/MS), and  $^1\text{H}$  NMR analysis helps to obtain a more thorough characterization of the *L. digitata* feedstock, which gives a better understanding of the general physicochemical and molecular properties of *L. digitata* tissue. The samples from *L. digitata* taken at different months of the year did not present significant differences in their properties, suggesting that *L. digitata* used in this study does not change considerably in its composition throughout the year. Knowledge of the results gives an insight and aid in the application of the feedstock for anaerobic digestion purposes. For instance, alginate which constitutes about 10 – 40% of brown algae component (Ross *et al.*, 2009), degrades to glyceraldehyde-3-phosphate and pyruvate during anaerobic digestion (Dāsa, 2015). The pyruvate formed is an important intermediate product that is easily oxidized to acetyl-CoA (Wang *et al.*, 2014), and are further converted by various enzymatic action to produce acetate and butyrate (Chen *et al.*, 2013). Moen *et al.* (1997) showed that during alginate degradation 13 – 15 % of the alginate remained insoluble. This presumably can amount to within 1.3 – 6% of the macroalgae feedstock that remain as particulate matter in solution during digestion. Alginates solubilisation is hindered by calcium ca-crosslinkage of guluronate residues and complexation with polyphenols (Moen *et al.*, 1997), and is influence by pH (Draget *et al.*, 2005). Rehm and Moradali (2017) has reported that accumulation of alginate in the periplasm of cells during degradation has a lethal effect on the cells. Processes that will limit this hindrances and help in solubilisation of the alginate components will make it beneficial to use the macroalage as feedstock for anaerobic digestion. Biological degradation of alginate is possible and catalysed by alginate lyases (Moen *et al.*, 1997). These are a group of alginate degrading enzymes utilizing it as a carbon source (Rehm and Moradali, 2017).

## Chapter 6. Effect of temperature on kinetics of biogas production from macroalgae.

### *Abstract*

An assessment was carried out on the effect of temperature on the anaerobic digestion of *Laminaria digitata* biomass, in batch reactors with a hydraulic retention time of 40 days. The reactors were set at 10 °C intervals (25, 35, 45 and 55 °C), operated with a volatile solid content of 65% and C: N ratio of 21.56. A first order regression model was used to calculate the degradation constant  $K$ . The modified Gompertz and logistics models were then used to obtain the kinetic parameters of the biogas production process. Furthermore, the chemical composition, biodegradability index, theoretical and experimental methane yield of the algae were all evaluated for the reactors. Results indicated that the chemical composition of the algae substrate could be written as  $C_{316.21}H_{612.92}O_{288.92}N_{12.57}S_1$ , with a theoretical methane yield of  $336 \pm 0.86$  L  $CH_4$  kg VS<sup>-1</sup>. Experimental results showed the cumulative biogas yield obtained in the reactors for 25, 35, 45, and 55 °C were  $559 \pm 0.10$ ,  $639 \pm 0.19$ ,  $558 \pm 0.06$  and  $501 \pm 0.11$  mL biogas / gVS respectively over the 40 days of operation. This results shows a trend of 35 °C > 25 °C > 45 °C > 55 °C. The lowest  $K$  (0.31) and lag time of between 9.3 - 11.7 days were obtained for 55 °C, indicating acclimatization and slow degradation rate at the start of the experiment from both models. The methane yield obtained from the biogas yield shows a different trend of 55 °C > 25 °C > 35 °C > 45 °C. The biodegradability index was highest for 55 °C (0.96), showing that as the experimental run progressed the thermophilic reactor gave a better overall degradation of the substrate. This indicates that methane yield potential is not directly proportional to biogas yield but rather can be influenced by other factors such as the methane content (%) produced by the methanogenic microorganisms, and the acclimatization period, both of which play a critical role in determining the methane potential of a substrate from AD.

## 6.2 Materials and methods

### 6.2.1 Algae collection, pretreatment, and storage

Algal biomass *Laminaria digitata* (LD) used in the batch reactor experiments were collected from shallow water during low tide at Seaton Sluice, Northumberland UK (NZ 3350) on 5<sup>th</sup> July, 2015 and treated in accordance with Section 3.1. The inoculum used has been described in Section 3.12.

### 6.2.2 Substrate characterization and analysis

Characterization of the macroalgae feedstock used in this study are summarized in Table 6-1. (See Section 3.2 for analysis methods).

Table 6-1: Physiochemical characteristics of *Laminaria digitata* of macroalgal feedstock

% Moisture	6.30%	Carbon ©	30.83%
%TS	93.70%	Hydrogen (H)	4.98%
%VS	65.00%	Nitrogen (N)	1.43%
TOC	36.11%	Oxygen (O)	37.56%
C/N RATIO	21.56	Sulphur (S)	0.26%
Neutral Detergent Fibre	7.00%	Acid Detergent Lignin	0.67%
Oil A (Ether Extract)	0.50%	Acid Detergent Fibre	20.32%
Total Oil (Oil B)	1.43%		

The dried macroalgae prepared as described in Section 3.1 had a TS content of approximately 94%, and a VS content of about 65%, giving a fairly high VS/TS ratio of 0.69, indicating mostly organic digestible matter in the feed. The C: N ratio was 21.56:1 which is within the optimal range (25 - 30:1) for stable anaerobic digestion (Kafle and Kim, 2013; Xu *et al.*, 2013). C: N values as high as 27.45:1 (Tabassum *et al.*, 2016a), and 22.3:1 (Allen *et al.*, 2015) have been reported for *L. digitata*. It has a very low lignin content (0.67%), indicating the storage carbohydrates should be accessible to fermentation since a high lignin content results in reduced biodegradability of the biomass by microbial processes, hence limiting digestibility and gas production (Ward *et al.*, 2014). Both the pH and TS was measured as described in Section 3.2.1.

## 6.3 BMP studies at different temperatures

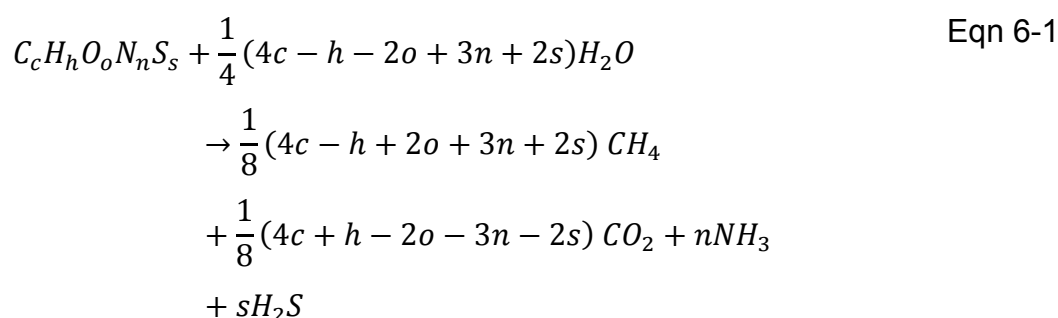
### 6.3.1 Batch studies

The batch test was divided into four different temperatures range and carried out according to (Membere *et al.*, 2015), briefly described below; The incubation was carried out in a water bath at temperatures of 25 °C, 35 °C, 45 °C, 55 °C. The batch reactors consisted of 500 mL Duran bottles (actual internal volume 580 ml) fitted with rubber stoppers inserted to serve as an outlet port for biogas collection in gas bags and as a purging port for nitrogen flushing of the headspace. Before starting the BMP test, all reactor bottles were pressure tested for air leakage, and once the experiment has commenced, for nitrogen or methane leakage using a Thermo-scientific GLD ProLeak detector used to check any CO<sub>2</sub>, NO<sub>2</sub>, and CH<sub>4</sub> leaks. The required amount of inoculum and substrate was evaluated for each reactor on a VS basis using a ratio of 3:1 (3g VS<sub>i</sub> / L: 1g VS<sub>f</sub> / L). This was to ensure adequate destruction of the volatile solids and overcome possible VFA inhibition (Raposo *et al.*, 2006; Angelidaki *et al.*, 2009). The inoculum and substrate were then placed inside the reactor and the solution was made up to 500 mL with deionized water. The rubber stoppers were then used to close the bottles, and the headspace (approx. 80 ml) was flushed for 5 minutes with pure (99.99%) N<sub>2</sub> gas to establish anaerobic conditions. The tube clamp was used to close the PVC tube ensuring all the bottles were gas-tight without the gas bags. Triplicates reactors were used to overcome inoculum variability, sample heterogeneity and allow statistical significance (Hansen *et al.*, 2004; Angelidaki *et al.*, 2009). Each digester was mixed manually by shaking for 15 - 30s once a day.

Biogas collection and methane measurement were done every day as described in (Membere *et al.*, 2015). The methane potential and production rate from biogas production were studied in this experiment. Assays with inoculum alone were used as controls and the methane produced from this inoculum were subtracted from the sample assays (Liu *et al.*, 2009; Kaparaju *et al.*, 2010).

### 6.3.2 Kinetic study on batch experiment

From the experimental elemental analysis determination, the empirical formulae ( $C_aH_bO_cN_dS_e$ ) of the macroalgae composition was calculated (Raposo *et al.*, 2011b). This was used to develop a stoichiometric equation using the Buswell Equation, Eqn 6-1 (Allen *et al.*, 2013b), to obtain the theoretical methane potential ( $BMP_{theo}$ ), ammonium yields and carbon dioxide ( $CO_2$ ) volumes that can be produced when the macroalgae feedstock is broken down by a consortium of microorganisms present in a batch reactor (Sialve *et al.*, 2009a; Montingelli *et al.*, 2015).



Using the calculated ( $BMP_{theo}$ ), the biodegradability index was determined. The biodegradability index is defined as the ratio of the observed BMP to the Buswell theoretical methane yield ( $BMP_{theo}$ ) (Allen *et al.*, 2013b; Tabassum *et al.*, 2016a).

Although the ( $BMP_{theo}$ ) gives a rough idea of the strength of a substrate's biogas potential, experimental assays must be used to ascertain the actual potential (Membere *et al.*, 2015). The degradation kinetics (derived from ultimate methane yield at infinite digestion time) was used in this study.

The degradation kinetics were assumed to follow a first-order degradation rate, Eqn 6-2 (Gunaseelan, 2004; Angelidaki *et al.*, 2009; Raposo *et al.*, 2011b);

$$B = B_o \cdot [1 - \exp(-k \cdot t)] \qquad \text{Eqn 6-2}$$

Where B (mL  $CH_4$  gVS<sup>-1</sup>) is the cumulative methane yield,  $B_o$  (mL  $CH_4$  gVS<sup>-1</sup>) is the ultimate methane yield, k (day<sup>-1</sup>) is the first-order rate constant and t (d) is the time.

The first order kinetics for hydrolysis of particulate organic matter used a linear regression model based on the empirical relationship (Eqn 6-2), and is used to determine the rate and extent of degradation, where the value of k (slope of the linear plot) represents the characteristics of a given substrate, and gives the time required to generate a ratio of the ultimate methane potential (Angelidaki *et al.*, 2009).

But the linear form of the first-order model which is in an exponential form cannot be used to adequately account and predict the cumulative methane production through the entire process particularly after the exponential phase (Li *et al.*, 2011). A nonlinear regression model, the modified Gompertz equation (Eqn 6-3), is mostly used to account for the lag phase ( $\lambda$ ) duration, biomethane potential ( $B_0$ ) and the  $\mu_{max}$  biogas production rate (Nopharatana *et al.*, 2007; Lo *et al.*, 2010; Allen *et al.*, 2013a) ;

$$B = B_0 \cdot \exp \left\{ -\exp \left[ \frac{\mu_{max} e}{B_0} (\lambda - t) + 1 \right] \right\} \quad \text{Eqn 6-3}$$

Several authors have further modified the Gompertz equation to estimate the cumulative biogas production (Ginkel *et al.*, 2001; Lay, 2001), and also applied in this study is the modified logistics model (Eqn 6-4).

$$B = \frac{B_0}{\left\{ 1 + \exp \left[ 4\mu_{max} \frac{\lambda - t}{B_0} + 2 \right] \right\}} \quad \text{Eqn 6-4}$$

Where  $B$  ( $mL CH_4g^{-1}VS$ ),  $B_0$  ( $mL CH_4g^{-1}VS$ ),  $t$  ( $d$ ),  $\lambda$ , and  $\mu_{max}$  is as defined in Section 2.18.3 for the Gompertz model.

Using both models, the kinetic parameters ( $\lambda$ ,  $\mu_{max}$ ,  $B_0$ ) of each reactor were estimated using nonlinear least-square regression analysis in MATLAB<sup>®</sup>(R2016a) software. The statistical indicators  $R^2$  (correlation coefficient) and root mean square error (RMSE) were calculated (Kafle and Kim, 2013; Deepanraj *et al.*, 2015b). The RMSE is a standard statistical metric used to measure model performance (Chai and Draxler, 2014). Both the  $R^2$  and RMSE (lowest value) were used to access best-fitted model (Jahedsaravani *et al.*, 2014).

$$RMSE = \left[ \frac{1}{m} \sum_{j=1}^m (d_j)^2 \right]^{1/2} \quad \text{Eqn 6-5}$$

Where 'm' is the number of data pairs; j is the jth values; Y is measured methane yield; 'd' is the difference between experimental and predicted methane yield.

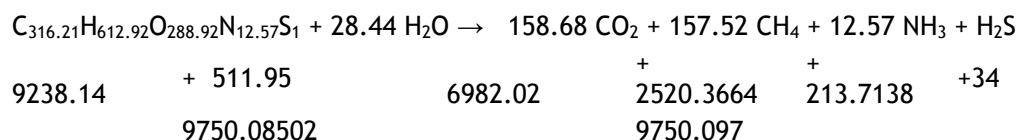
## 6.4 Results and Discussion

### 6.4.1 Experimental batch study

The characteristics of the substrate, ultimate analysis and inoculum are given in Table 6-1. From the atomic weight of the elements, the stoichiometric description of the algae is derived as  $C_{316.21}H_{612.92}O_{288.92}N_{12.57}S_1$ . Theoretical biomethane and ammonium yield, calculated using the Buswell equation for the algae (*L. digitata*) using the VS (65%) per kg of the algae weight contribution is shown in Table 6-2. The  $BMP_{theo}$  obtained was  $366 \pm 0.08 \text{ L CH}_4 \text{ kg VS}^{-1}$  which is similar to  $368 \text{ L CH}_4 \text{ kg VS}^{-1}$  (Tabassum *et al.*, 2016a), and  $335 \text{ L CH}_4 \text{ kg VS}^{-1}$  (Membere *et al.*, 2015), but lower than  $479 \text{ L CH}_4 \text{ kg VS}^{-1}$  (Allen *et al.*, 2015) reported for *L. digitata*. *L. species* are known to exhibit variation in biomass composition across the year (seasonal variation) which can alter the carbohydrate concentrations composition dramatically (Adams *et al.*, 2011a), and probably explains the difference in reported gas production yields above. The biodegradability index was highest at 55 °C (0.96), while the value obtained at 35 °C (0.80), Table 6-3, compares very well to (0.78) reported for *L. digitata* (Tabassum *et al.*, 2016a) and (0.81) for *S. latissimi* (Allen *et al.*, 2015). This gives an indication of how well the substrate was degraded and how the BMP yield compared to the theoretical biomethane yield (Allen *et al.*, 2013b). Higher biodegradability indices corresponded to higher digestion efficiencies (Tabassum *et al.*, 2016a).

Table 6-2 Generation of the stoichiometric equation and theoretical assessment of biogas production from macroalgae (collected in July 2015).

Component	Number of atoms per mole of algal biomass	Atomic weight	Weight contribution (Kg/t)	%
Carbon	25.69 (316.21)	12	369.96	36.996
Hydrogen	49.8 (612.92)	1	4.98	0.498
Nitrogen	1.02 (12.57)	14	20.02	2.002
Oxygen	23.48 (288.92)	16	600.96	60.096
Sulphur	0.08 (1)	32	8.32	0.832



0.65 kg + 308.65 H<sub>2</sub>O → 171.30 kg CO<sub>2</sub> + 170.05 kg CH<sub>4</sub> (algae is 65% VS dry wt)

Density of CH<sub>4</sub> = 0.714 kg m<sup>-3</sup>, Density of CO<sub>2</sub> = 1.96 kg m<sup>-3</sup>

Gas by volume → 238.17 m<sup>3</sup> CH<sub>4</sub> + 87.40 m<sup>3</sup> CO<sub>2</sub> = 325.565 m<sup>3</sup> biogas @ 47.77% CH<sub>4</sub>

Theoretical maximum methane production: 238.17 m<sup>3</sup> CH<sub>4</sub>/ 650 kg VS: 366.42 L CH<sub>4</sub>/kg VS

%CH<sub>4</sub> = 47.77 %, CO<sub>2</sub> = 48.11 %, NH<sub>3</sub> = 3.81%, H<sub>2</sub>S = 0.303 %

Table 6-3 Bio-methane production for macroalgae using results of BMP and theoretical analysis.

Reactors	Theoretical yield (L CH <sub>4</sub> kg VS-1)	BMP yield (L CH <sub>4</sub> kg VS-1)	Biodegradability index	K (d-1)
Algae (L. digitata)	366.42 ± 0.86			
25 °C		317.60 ± 1.58	0.87	0.69
35 °C		292.78 ± 1.11	0.80	0.45
45 °C		271.07 ± 0.98	0.73	0.54
55 °C		352.0 ± 0.63	0.96	0.31

The cumulative biogas and methane production, daily methane production, and % methane content, with respect to the retention time of 40 days for all the reactors is shown in Figure 6-1 and Figure 6-2. The cumulative biogas production obtained in the reactors for 25 °C, 35 °C, 45 °C, and 55 °C are 559 ± 1.23, 639 ± 0.96, 558 ± 1.10 and 501 ± 0.18 ml respectively. These results show a trend of 35 °C > 25 °C > 45 °C > 55 °C, Figure 6-1 A. The cumulative biogas produced by the reactor with a temperature of 35 °C is 14.5%, 14.5%,



and 27.5% higher than the yield of the reactors which are 25 °C, 45 °C and 55 °C.

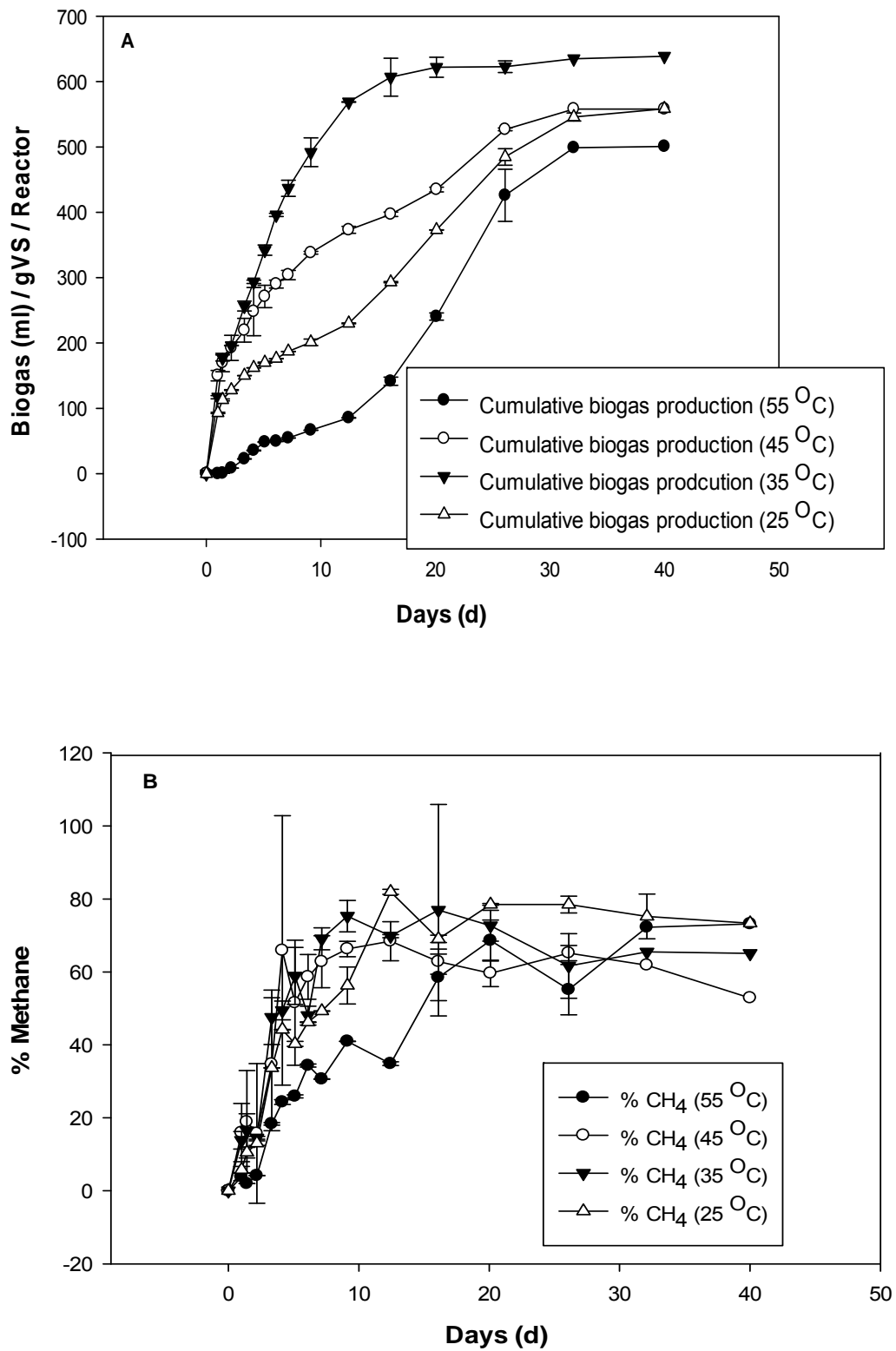


Figure 6-1 A) Cumulative biogas production B), % Methane

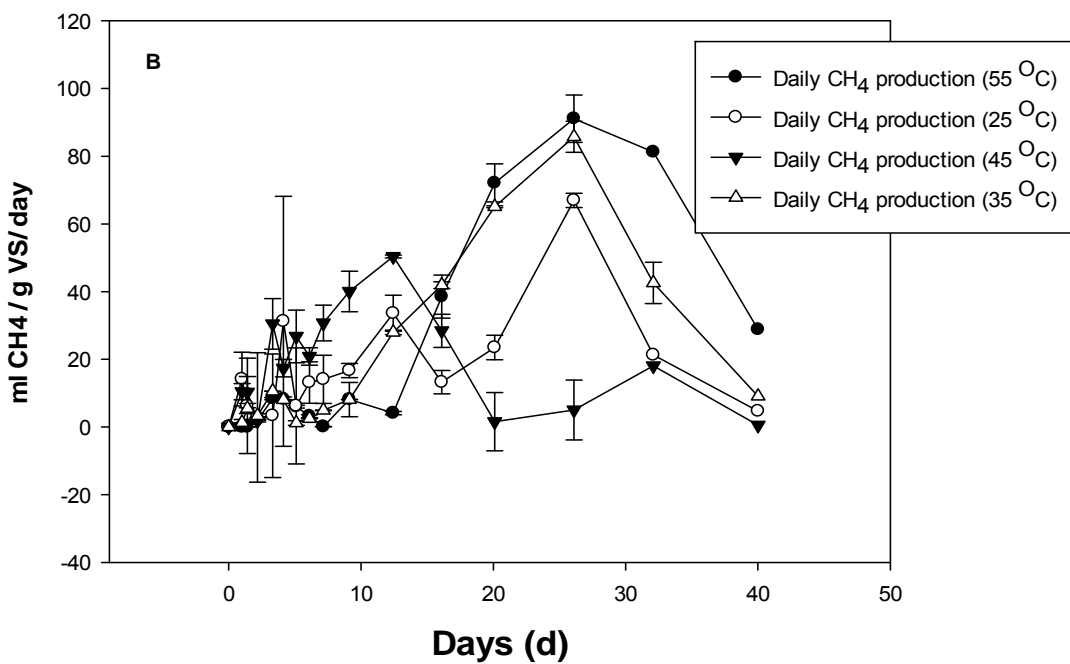
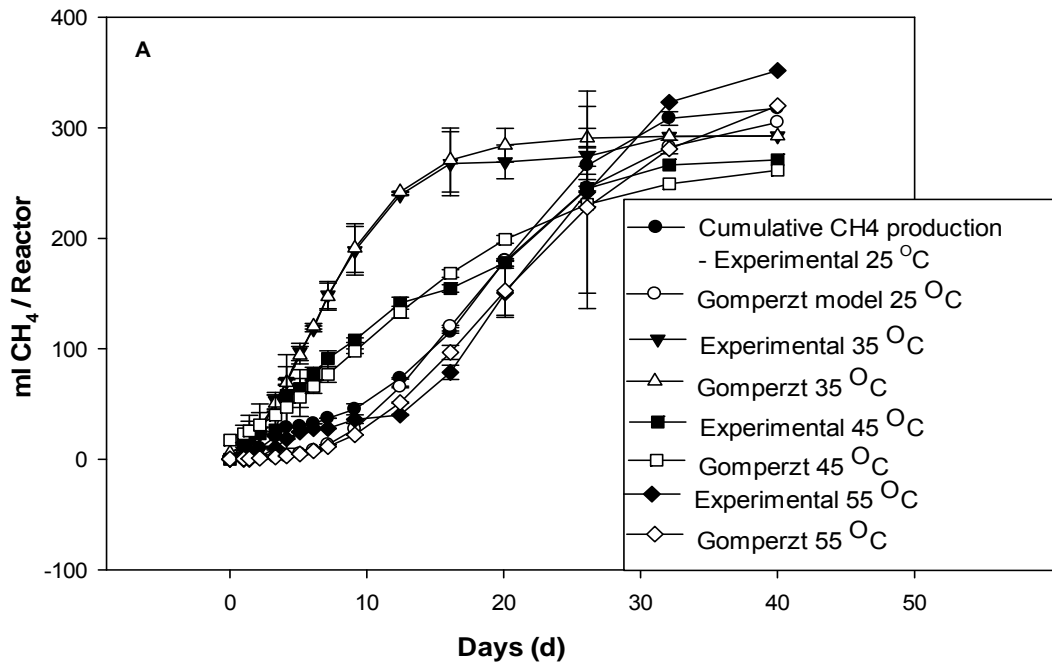


Figure 6-2 A) Cumulative methane production B) Daily methane production (mL CH<sub>4</sub> / gVS).

A similar trend has been observed by Vanegas and Bartlett (2013a), on the effect of temperature on anaerobic digestion of *L. digitata*, using three different temperatures (20 °C, 35 °C, and 45 °C), with reactors incubated at 35 °C producing the highest biogas. This trend was also reported by Varel *et al.* (1988), with *Spirulina maxima*, biogas production was higher at the mesophilic (35 °C) temperature than thermophilic temperature (55 °C). The methane yield obtained shows a different trend of 55 °C > 25 °C > 35 °C > 45 °C, Figure 6-2 A. This trend indicates that acclimatisation plays a critical for the thermophilic temperature (55 °C) which began to work best after day 20 - 30 (see steep slope in Figure 6-2 A). The results suggest the activity of the methanogenic bacteria (Deepanraj *et al.*, 2015b), process of adaptation of the inoculum to the various temperatures, the inoculum ability to produce a number of specific enzymes capable of hydrolysing the main polysaccharides of *L. digitata* (cellulose, laminarin, fucoidan and mannitol) to biogas (Vanegas and Bartlett, 2013a), and the degradation rate (K) (Membere *et al.*, 2015), depend on the reactors operation temperatures, which in turn influences the rate of biogas production as the solubility of both of CH<sub>4</sub> and CO<sub>2</sub> decreases with increase in temperature (Patel *et al.*, 2012), at 20 °C, 40 °C and 60 °C is approximately 0.023, 0.152 and 0.012 g CH<sub>4</sub> /kg water at one atmosphere, respectively (Engineering ToolBox., 2008). Therefore, in batch reactors operating under different temperature conditions, using unacclimatised inoculum, the mesophilic temperature 35 °C seems more effective for biogas production than thermophilic 55 °C for macroalgae but as the experimental run progresses, acclimatisation of the inoculum takes place and thermophilic fermentation may be the preferred temperature for methane production for *L. species*. The kinetic parameter (K) was calculated for each set of temperature conditions by the procedure described in Section 4.2.8 elsewhere (Angelidaki *et al.*, 2009) and shown in Figure 6-3 and Table 6-3. The K values varied from 0.31, 0.45, 0.54 to 0.69 (d<sup>-1</sup>) in increasing order for 55, 35, 45 and 25 °C. K values of 0.33 - 0.36 (Membere *et al.*, 2015) and 0.19 – 0.22 (Allen *et al.*, 2015), 0.08 - 0.21 (Tabassum *et al.*, 2016b) for the mesophilic temperature of 35 °C has been previously reported for *Laminaria species*. Various values of k has reported for other substares, Ulva (0.08 – 0.23), dairy slurry (0.06) (Allen *et al.*, 2013a), maize silage (0.03), cattle slurry (0.05) (Mähner and Linke, 2009), sugarcane waste 0.09 – 0.4 (Janke *et al.*, 2015). The higher the K values mean the shorter

the degradation time and can display a huge variability which is site- specific (Palmeri *et al.*, 2013). The thermophilic reactor at 55 °C indicate it was more inhibited than the other reactors, Figure 6-1 A, as it has been previously reported, K is a kinetic parameter that increases as the degradation rate increases (Nedwell *et al.*, 1999; Xie, 2016) The R<sup>2</sup> values, (Figure 6-3) indicate a good fit of the first order rate model.

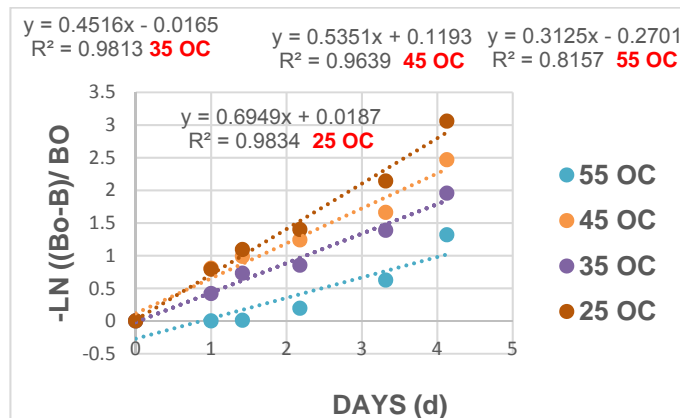


Figure 6-3 First order plot of cumulative methane production of *Laminaria digitata* at various temperature range.

The methane composition in the biogas was determined using a GC-FID instrument as described by Membere *et al.* (2015). The % methane evaluated was multiplied by the daily measured biogas volume from the gas bags giving the volume of methane produced at room temperature. The total volume of methane produced daily was calculated by using **Error! Reference source not found.**, as described by (Membere *et al.*, 2015), and the volume normalised to dry gas at STP (Angelidaki and Sanders, 2004; VDI, 2006). The measurement was carried out daily for the first 10 days, thereafter between once or twice a week, as between 80 and 90% of methane production is normally achieved within 8-10 days (Hansen *et al.*, 2004).

Biomethane potential and daily methane volume measured is shown in Figure 6-2 A and B. The cumulative methane (CH<sub>4</sub>) produced was highest for 55 °C with a value of 352 ± 0.63 ml CH<sub>4</sub> g VS<sup>-1</sup> with methane content increasing from 3% on day 1 to about 68% by day 21, Figure 6-1 B. The cumulative methane production for 25, 35 and 45 °C are 318 ± 1.58, 293 ± 1.11 and 271 ± 0.98 ml CH<sub>4</sub> g VS<sup>-1</sup>. These are similar to results obtained (267 - 288 L CH<sub>4</sub> kg VS<sup>-1</sup>) for mono-digestion of natural *L. digitata* and (258 - 296 L CH<sub>4</sub> kg VS<sup>-1</sup>) for cultivated

*S. latissimi*, at 37 °C (Tabassum *et al.*, 2016a), and documented values of up to 280 L CH<sub>4</sub> kg<sup>-1</sup> VS<sup>-1</sup> for the brown seaweed *Laminaria* (Chynoweth *et al.*, 1993). Allen *et al.* (2015), reported the highest BMP yield 342 L CH<sub>4</sub> kg VS<sup>-1</sup> for *Saccharina latissima* among 10 species of seaweed, with 218 ± 4.1 L CH<sub>4</sub> kg VS<sup>-1</sup> for *L. digitata* at 37 °C with a C: N ratio of 22.5. The % methane for 25 °C reactor increased from 5% on day 1 to about 78% on day 21 while the 35 °C reactor increased from 13% methane content on day 1 to 75% on day 10 and the 45 °C reactor increased from 15% on day 1 to 68% by day 13. The percentage of CH<sub>4</sub> in the biogas was higher for the 25, 35 and 45 °C digesters (81, 69, 68% at t = 13 days) than the 55 °C digesters (34% at t = 13 days). This suggests that some acclimatization of the inoculum was occurring in the 55 °C reactor between day 1 and day 13.

#### 6.4.2 Kinetic study using modified Gompertz and logistics model

The modified Gompertz equation was used to fit the cumulative methane data obtained from the batch reactors. Table 6-4 shows the results of the estimated kinetic parameters based on the Gompertz model, which indicates that it can be used to predict the methane yield potential, maximum methane production rate and duration of the lag phase (Zwietering *et al.*, 1990).

Table 6-4 Results of kinetics study (Modified Gompertz and Logistics model)

Parameter	Modified Gompertz				Logistic Model			
	25 °C	35 °C	45 °C	55 °C	25 °C	35 °C	45 °C	55 °C
Cumulative methane produced - Experimental (ml CH <sub>4</sub> /reactor/gVS)	317.6	292.78	271.07	352.01	317.6	292.78	271.07	352.01
Cumulative methane produced - predicted (ml CH <sub>4</sub> /reactor/gVS)	333.58	284.95	271.904	366.04	323.27	279	267.55	355.8
Biomethane potential - predicted (ml CH <sub>4</sub> /gVS)	371.8	285	283.8	441.6	329.4	279	270.8	369.4
Max biomethane potential - predicted (ml CH <sub>4</sub> /gVS)	414.9	291	315.6	518.4	342.9	289.2	301.3	390.2
μ <sub>max</sub> (ml/day)	12.93	26.3	10.86	14.13	15.51	28.36	11.18	17.14
Lag phase (λ)	5.936	1.524	0.1087	9.279	8.34	2.114	1.182	11.65
R <sup>2</sup>	0.99	0.9976	0.9816	0.9899	0.9967	0.9928	0.9649	0.9961
RMSE	11.25	5.454	13.37	12.78	6.47	10.23	17.19	7.909

The soundness of the model results was evaluated by plotting the predicted cumulative methane values against experimental values as shown in Figure 6-4. The max predictable biomethane potential of the algae is shown in Table 6-4, with batch reactors operating temperatures of 25, 35, 45 and 55 °C, found to be 415, 291, 351 and 518.4 mL CH<sub>4</sub>/ gVS respectively. This shows the reactor with operating temperature of 55 °C should have a maximum methane yield followed by 25 °C. This trend seemed to follow the cumulative experimental values, as shown in Figure 6-2 A. The lag phase was found to be in between 0.11 – 9.28 d. Reactor 45 °C (0.11 d) and 35 °C (1.52 d) shows faster degradation, this could be as a result of the acclimatization of the inoculum at this temperature with a proportional growth of methanogenic bacteria whereas reactor 55 °C (9.28 d), showed there was initial inhibition of the anaerobic biomass as depicted in Figure 6-2 A. Inhibition can be attributed to several factors, apart from non-acclimatization of the inoculum at 55 °C to the substrate as shown in this study, drop in pH to about 5.5 -5.9 after 1 - 2 days, has been identified as one factor that causes a reduction in biogas production in anaerobic digestion of *L. digitata* (Hanssen *et al.*, 1987; Vanegas and Bartlett, 2013a).

The R<sup>2</sup> values which are the coefficient of determination, for reactors 25, 35, 45 and 55 °C were 0.99, 0.99, 0.98 and 0.99. This shows the predicted values give a good fit to experimental values. The RMSE values were between 5.5 -13.3 L CH<sub>4</sub> kg VS<sup>-1</sup>. Figure 6-4 A shows the comparison of experimental and predicted cumulative methane production, the R<sup>2</sup> values agree with kinetic results in Table 6-4. This shows that the modified Gompertz equation fitted the data from the kinetics study of methane production from *Laminaria* predicting reliably both the lag time and maximum methane potential. Using the logistics model, the estimated kinetic parameters are also shown in Table 6-4. To evaluate the robustness of model results from the logistic model, the predicted cumulative methane production was plotted against the measured values, as shown in Figure 6-4 B. The max predictable biomethane potential of the algae substrate from the logistic model with operating temperatures of 25, 35, 45, and 55 °C are 343, 289, 301 and 390 mL CH<sub>4</sub> g VS<sup>-1</sup>, respectively. The lag time was between 1.2 – 11.7 days with R<sup>2</sup> values of 0.99, 0.99, 0.97, and 0.99 in order of increasing temperature. The RMSE values were between 6.5 - 17.2 L CH<sub>4</sub> kg

VS<sup>-1</sup>. Similar results (9.7 - 13.9 L CH<sub>4</sub> kg VS<sup>-1</sup>) has been reported by researchers studying kinetics using the logistics model (Deepanraj *et al.*, 2015b). Comparison of the predicted logistics models with experimental cumulative methane production for all the reactors is shown in Figure 6-4 B. The R<sup>2</sup> obtained from Figure 6-4 A (0.99, 0.99, 0.98, 0.99) and B (0.99, 0.99, 0.97, 0.91) for 25 °C, 35 °C, 45 °C and 55 °C are similar to the predicted values in Table 6-4, indicating the Gompertz and logistics model fits well for the kinetics of methane production, lag time determination and maximum methane potential. From the RMSE values (Table 6-4), the Gompertz model appears to be better suited than the logistics model with a good fit and indicating, for instance at 55 °C the typical point was 13.34 ml compared to 17.19 ml using the logistics model which is a deviation of about 22% compared to the Gompertz model.

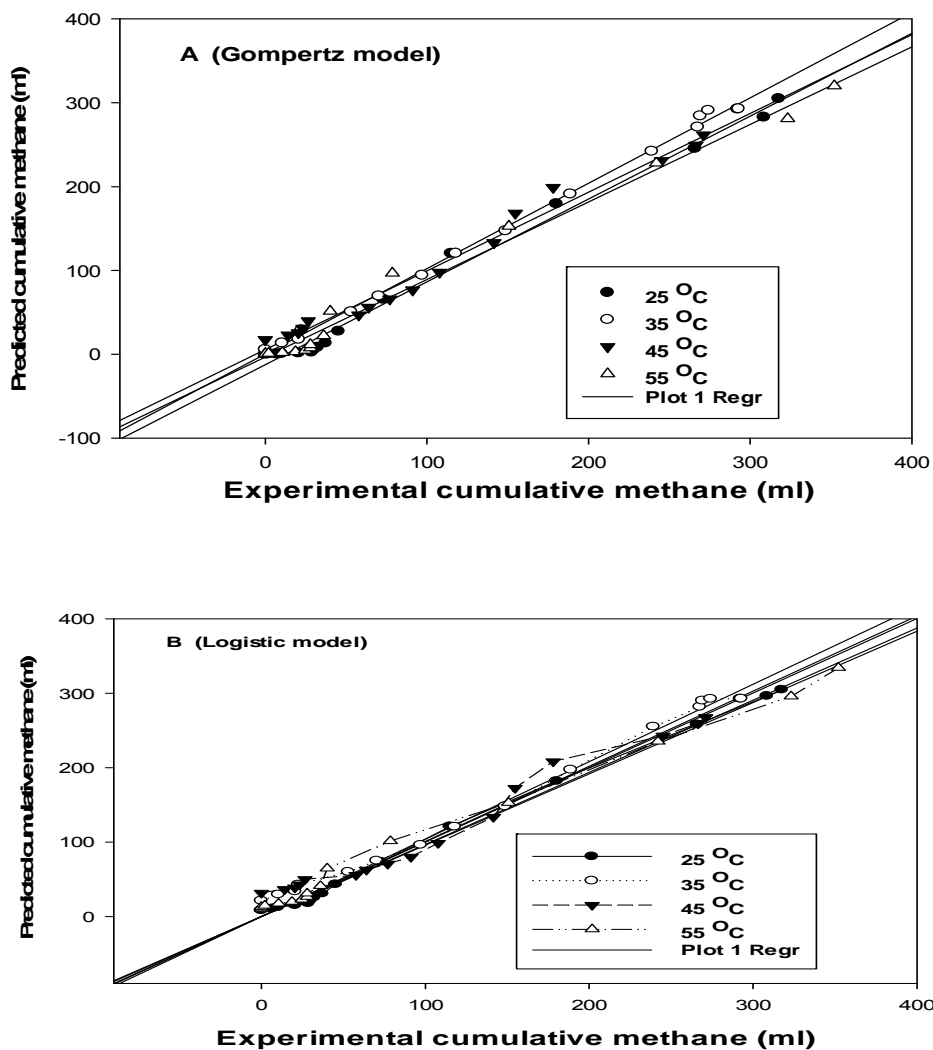


Figure 6-4 Comparison of predicted A), modified Gompertz; and B), logistics models with experimental cumulative methane production.

## 6.5 Conclusion

A batch experimental study on the effect of temperature on biogas and methane yield from macroalgae, *L. digitata* was investigated in 500 mL reactors running at 25, 35, 45 and 55 °C. The results demonstrated the feasibility of producing biogas at all the digestion temperatures, and this parameter had an influence on cumulative gas production. The theoretical methane yield, biodegradability index, modelled biogas and methane production rates were all assessed for the reactors. First order rate model was used to calculate the degradation constant  $K$ . The modified Gompertz and logistics model were then used to obtain and evaluate the kinetic parameters of the reactor's digestion process. This enabled the prediction of the cumulative biogas production, methane yield, lag time and maximum methane potential of all the reactors. These results were then compared with the experimentally obtained values. From the results the cumulative biogas production was best at 35 °C, while the overall methane yield potential computed from the % methane in the biogas produced, was best for 55 °C, with an initial lag phase of between 9.3 - 11.65 days, and a lowest  $K$  (0.31) value compared to all the other reactors, indicating inhibition and slower degradation from both models at higher temperature of 55 °C. These results show the critical role the dynamics of the methanogenic microorganisms play within reactors when evaluating the response of operating temperature on biogas production from AD of *L. digitata*.



## Chapter 7. Continuous reactor study of macroalgae feedstock under mesophilic and thermophilic conditions

### *Abstract*

Six laboratory-scale continuous stirred tank reactors (CSTR) were used to investigate the anaerobic digestion of *Laminaria digitata* (LD) feedstock under mesophilic (35 °C) and thermophilic (55 °C) conditions. The reactors were fed once a day, and mixed continuously with an HRT of 25 days, and their contents sampled for physiochemical analysis. The methane yields obtained were  $350 \pm 1.23$  and  $360 \pm 0.98$  mL CH<sub>4</sub> g VS<sup>-1</sup> for the control mesophilic reactor (MR 1) and control thermophilic reactor (TR 1) reactors respectively, but the performance differed as the OLR was increased. The total cumulative methane production after 127 days of incubation was 91.8 and 88.3 L CH<sub>4</sub> / reactor for MR 1 and TR 1, respectively. Reactors, MR 3 and TR3, where FePO<sub>4</sub> was added as buffer respectively, showed overall higher cumulative methane production (93.6 and 93.8 L CH<sub>4</sub> / reactor). Reactors MR 2 and MR 3 where NaHCO<sub>3</sub> was added as buffer produced 91.7 and 90.4 L CH<sub>4</sub> / reactor, respectively. Statistical analysis of the control reactors showed the means for the two conditions were not significantly different ( $p = 0.27$ ). Results from two-way ANOVA showed that the main effect of the temperature on the reactors was not significant ( $p = 0.07$ ). The % methane in MR 1 and TR 1, averaged around 65 and 68 %, while the H<sub>2</sub>S content was similar in both reactors, ranging between 0.04 - 0.33% (v/v). The total volatile fatty acid (tVFA) concentration ranged from 5.2 - 9.1 g L<sup>-1</sup> for reactors MR 1 - 3, compared to 2.2 - 8.4 g L<sup>-1</sup> for TR 1 - 3. Total alkalinity (TA) content was between 10 g to 15 g CaCO<sub>3</sub> L<sup>-1</sup> in all six reactors, indicating well-buffered systems. The free ammonia nitrogen (FAN) concentration in MR 1, peaked at 187 mg NH<sub>3</sub>-N/L before decreasing to a final value 22 mg NH<sub>3</sub>-N/L while for TR 1, it peaked at 278 mg NH<sub>3</sub>-N/L before decreasing to 14 mg NH<sub>3</sub>-N/L. The cumulative sulphate (SO<sub>4</sub><sup>2-</sup>) produced for MR 1 and TR 1 was 2.90 g L<sup>-1</sup> and 2.96 g L<sup>-1</sup>, with the highest value of 3.4 g L<sup>-1</sup> observed for MR 3 where FePO<sub>4</sub> was added. Chloride concentration in the reactors continued to show an increasing trend with increases in OLR, indicating the macroalgae was the source of the chloride. The final chloride

concentration reached 27.9 g L<sup>-1</sup> for MR 1 and 28.7 g L<sup>-1</sup> for TR 1. These results show the biomass of LD is a promising feedstock for methane production at mesophilic and thermophilic temperatures. However, the methane production rates are influenced by certain factors which cause instability, and the digestion process should be closely monitored to avoid reactor failure.

## 7.2 Materials and methods

### 7.2.1 *Experimental procedure*

This continuous reactor study comprised a series of 6 identical, 1-litre continuous stirred tank reactors (CSTR) operating simultaneously for 127 days under different reactor conditions, but with the same daily feeding regime (seaweed feedstock). The 6 CSTRs were run as 3 sets of reactors, at mesophilic 35 °C (MR 1 - 3) and thermophilic 55 °C (TR1 - 3) conditions, with a hydraulic residence time of 25 days. For both the MR and TR reactors, the conditions were; Reactor group 1 (algae only - control), Reactor 2 (algae + NaHCO<sub>3</sub>), and Reactor 3 (algae + FePO<sub>4</sub>). Details of reactor systems are given in Section 3.1.1, and analytical methods are described in Section 3.2.

The initial inoculum concentration was 10 gVS.L<sup>-1</sup> and the organic loading rate (g VS L<sup>-1</sup> d<sup>-1</sup>) was increased stepwise after acclimatization from 1 g VS L<sup>-1</sup> d<sup>-1</sup> on day 1 of the experiment to 2 g VS L<sup>-1</sup> d<sup>-1</sup> on day 15, thereafter, to 3 g VS L<sup>-1</sup> d<sup>-1</sup> on day 70, 4 g VS L<sup>-1</sup> d<sup>-1</sup> on day 90 and, finally to 5 g VS L<sup>-1</sup> d<sup>-1</sup> on day 98, till the end of the experiment in both temperature conditions. Biogas production rate was measured daily for the first 40 days, after which it was measured every 2 days.

### 7.2.2 *Algae collection, pretreatment, and storage*

In accordance with Section 6.2.1

## 7.3 Results and discussion

### 7.3.1 *Methane production profiles: Mesophilic and thermophilic digesters*

The cumulative methane production (mL/g VS<sub>added</sub>), daily methane production rate (mL. g VS<sup>-1</sup>.d<sup>-1</sup>), methane content and H<sub>2</sub>S concentration in the biogas produced during digestion of the macroalgae feedstock under mesophilic and thermophilic conditions are shown in Figure 7-1-Figure 7-3 A and B. The experiment lasted for 127 days and results reported here represent the daily value of data obtained. Biogas production started immediately, on the first day of the digestion in all the reactors, which can be attributed to pre-incubation (acclimatisation) of the inoculum with the algal feedstock and rapid digestability

of some macroalgae components as a result of cell wall disruption from pre-treatment (Membere *et al.*, 2015). Pretreatment has been reported to improve the efficiency of methane fermentation of algal biomass (Chen and Oswald, 1998). The initial inoculum concentration, HRT and OLR were standardized in all reactors, to allow for direct evaluation of the effect of temperature on biogas production (Li *et al.*, 2013a). The methane yields obtained from average data for between 5 - 15 consecutive days of stable and pseudo-steady gas production, regarded as when the deviation was less than 5 - 10% for at least five consecutive days (Li *et al.*, 2013a), are shown in Table 7-1.

Table 7-1 Methane yields (mL CH<sub>4</sub>/ g VS) of seaweed fermentation at mesophilic and thermophilic temperature at five OLR.

Reactors	Reactor Feedstock	Operating Temperature	OLR (gVS L <sup>-1</sup> d <sup>-1</sup> )				
			1	2	3	4	5
MR 1	Algae only	35 °C	350.45 (± 1.23)	320.66 (± 0.69)	334.79 (± 2.05)	319.26 (± 1.11)	318.23 (± 1.48)
TR 1	Algae only	55 °C	361.50 (± 0.98)	316.23 (± 0.87)	314.83 (± 1.65)	251.02 (± 1.33)	301.42 (± 1.79)
MR 2	Algae and NaHCO <sub>3</sub>	35 °C	443.55 (± 0.28)	285.44 (± 0.88)	368.61 (± 0.26)	358.11 (± 0.18)	323.63 (± 0.17)
TR 2	Algae and NaHCO <sub>3</sub>	55 °C	438.93 (± 0.18)	315.79 (± 0.19)	364.98 (± 0.22)	251.50 (± 0.11)	283.46 (± 0.24)
MR 3	Algae and FePO <sub>4</sub>	35 °C	369.15 (± 0.41)	334.44 (± 0.32)	324.55 (± 0.16)	331.25 (± 0.68)	322.14 (± 0.66)
TR 3	Algae and FePO <sub>4</sub>	55 °C	352.90 (± 0.08)	313.81 (± 0.19)	349.20 (± 0.75)	304.61 (± 0.55)	302.87 (± 0.14)

The values of methane obtained at OLR of 1 gVS L<sup>-1</sup> d<sup>-1</sup> are comparable to 359 ± 5.1 mL CH<sub>4</sub> gVS<sup>-1</sup> for *L. digitata* (D'Este *et al.*, 2017), and to those reported by Hinks *et al.* (2013) of 0.25 and 0.41 L CH<sub>4</sub> gTS<sup>-1</sup>, and Montingelli *et al.* (2015) of 280 mL CH<sub>4</sub> gVS<sup>-1</sup> for *Laminaria spp.*. It is also similar to 353 mL CH<sub>4</sub> g VS<sup>-1</sup> obtained for algae biomass, *Spirulina maxima* (Samson and Leduyt, 1986), but higher than the 209 ± 7.50 – 254 ± 6.21 mL CH<sub>4</sub> g VS<sup>-1</sup> for *L. digitata* obtained from a batch experiment (Adams *et al.*, 2011b). In comparison to other energy crops it is greater than 211 ± 6 mL CH<sub>4</sub> g VS<sup>-1</sup> reported for maize (Raposo *et al.*, 2006) but less than 450 mL CH<sub>4</sub> g VS<sup>-1</sup> obtained for rapeseed (Antonopoulou *et al.*, 2010).

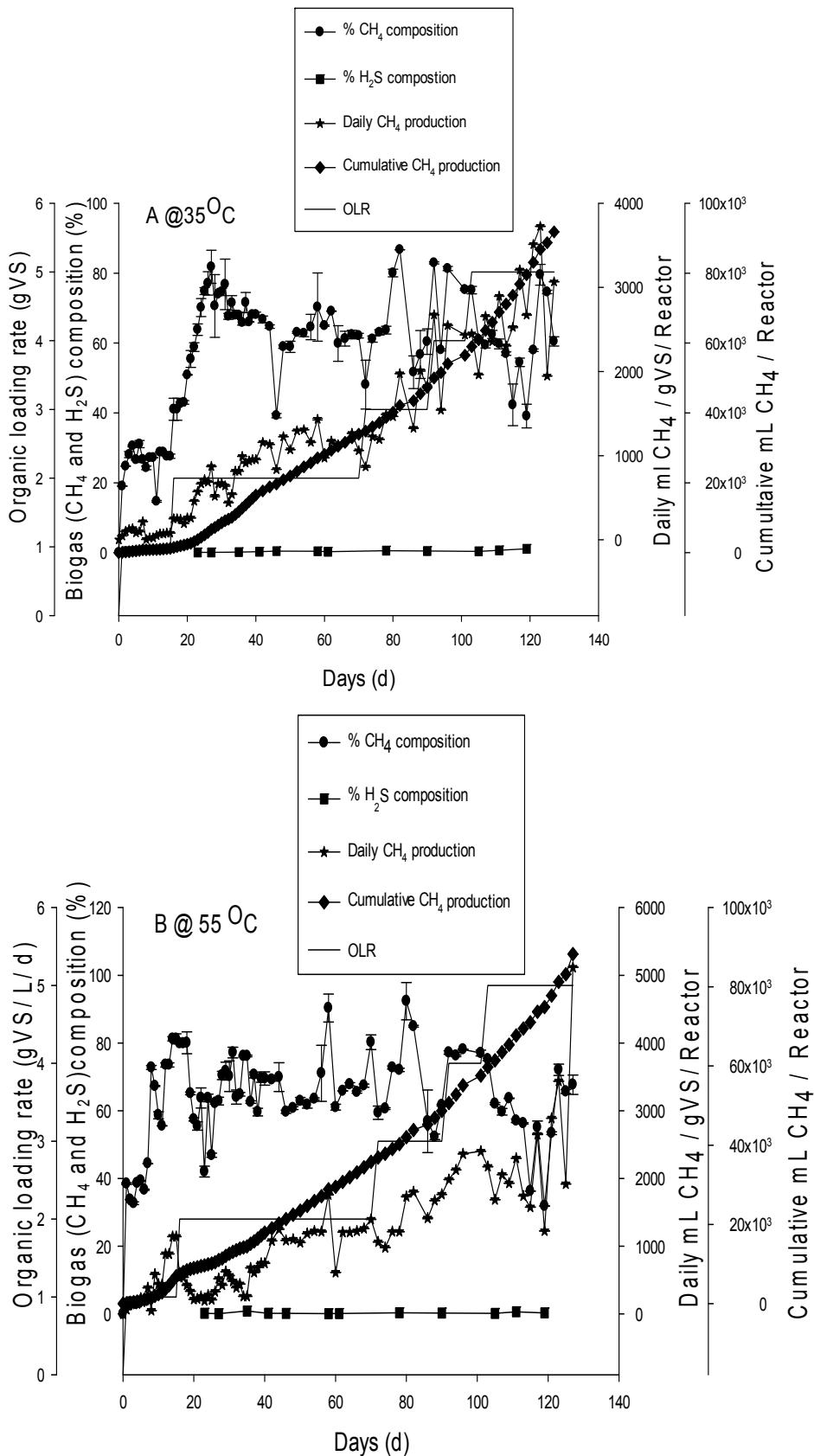


Figure 7-1 Daily and cumulative CH<sub>4</sub> production, % CH<sub>4</sub> and H<sub>2</sub>S composition and organic loading rate (OLR) for; A), MR 1, Control (algae only) at 35 °C; B), TR 1, Control (algae only) at 55 °C.

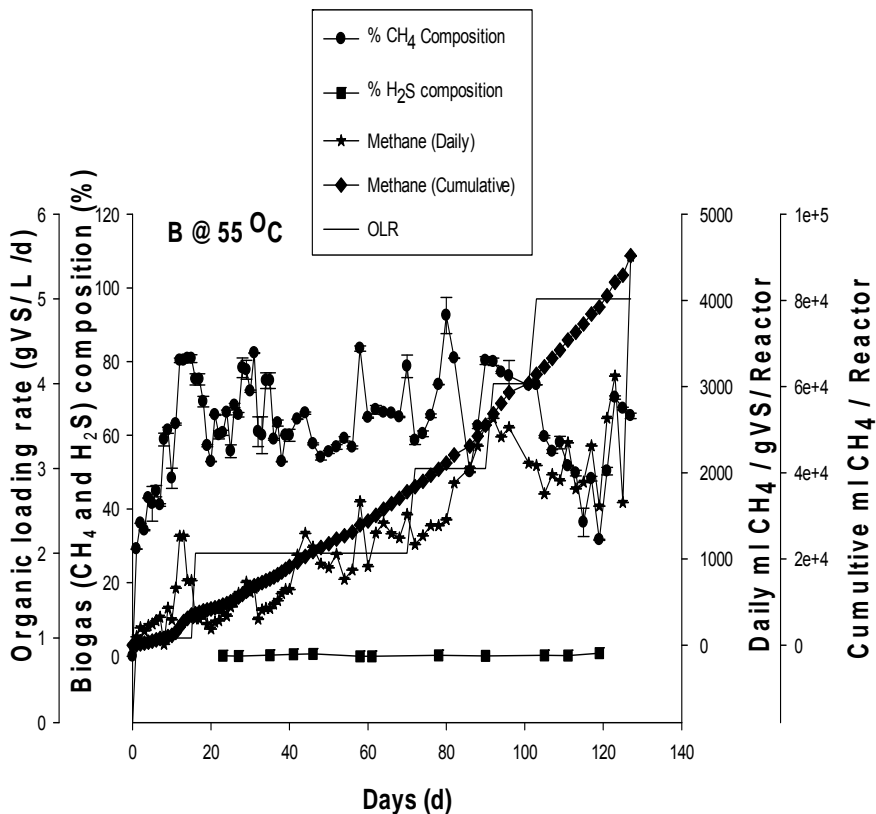
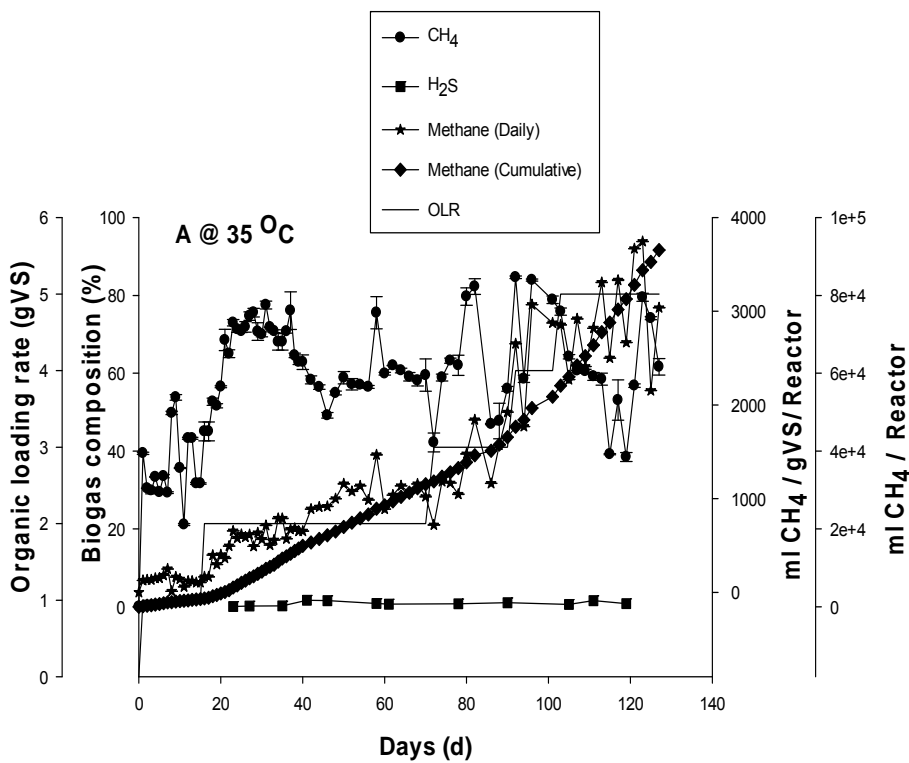


Figure 7-2 Daily and cumulative CH<sub>4</sub> production, % CH<sub>4</sub> and H<sub>2</sub>S composition and organic loading rate (OLR) for; A), MR 2, Algae + NaHCO<sub>3</sub> addition at 35 °C; B), TR 2, Algae + NaHCO<sub>3</sub> addition at 55 °C.

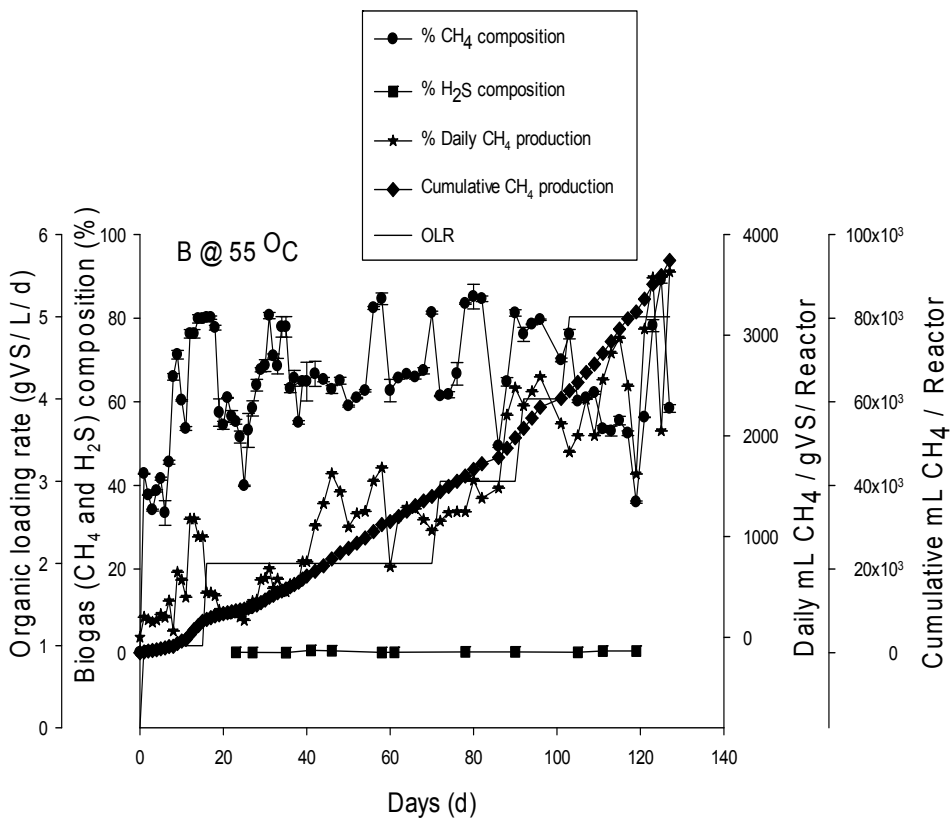
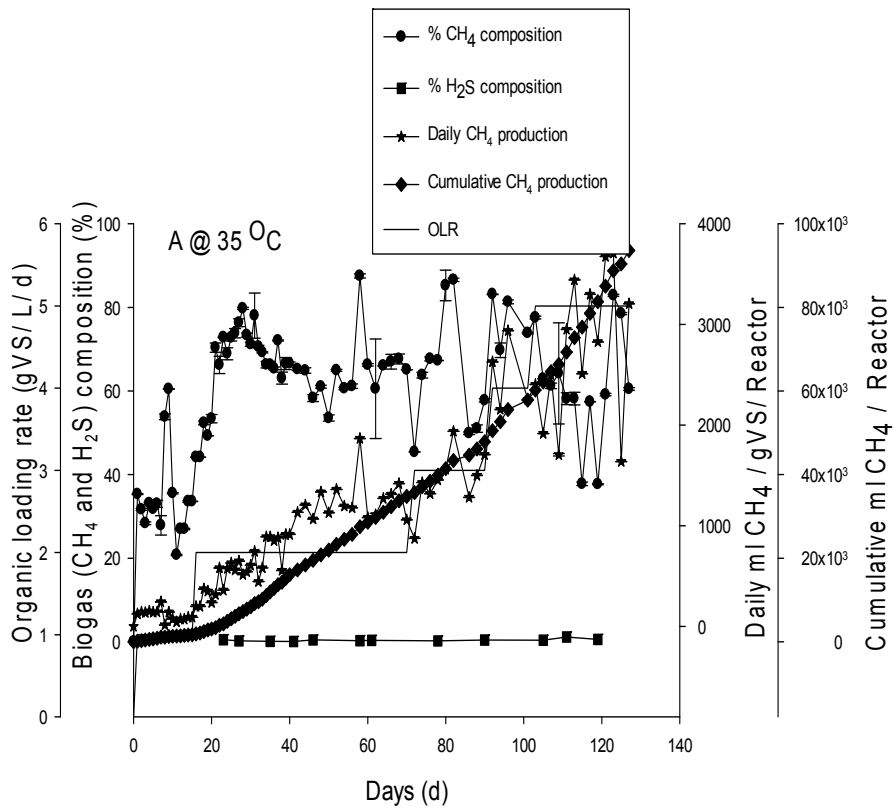


Figure 7-3 Daily and cumulative CH<sub>4</sub> production, % CH<sub>4</sub> and H<sub>2</sub>S composition and organic loading rate (OLR) for; A), MR 3, Algae + FePO<sub>4</sub> addition at 35 °C; B), TR 3, Algae + FePO<sub>4</sub> addition at 55 °C.

In the 6 reactors MR 1 - 3 and TR 1 - 3, shortly after start-up, biogas was produced soon after feeding and was assumed to have reached steady state at 3 hydraulic residence times when the biomass in the reactors would have been replaced entirely by new biomass, as a result of growth/biomass wash out (Hinks *et al.*, 2013).

The total cumulative methane production for the reactors over the 127 days was 91.8 and 88.3 L CH<sub>4</sub>/ reactor for MR 1 (Figure 7-1 A at 35 °C) and TR 1 (Figure 7-1 B at 55 °C), respectively. Expressing the cumulative methane production, as a function of the hydraulic residence time ( $\theta$ ), the total mass of seaweed which has been feed to each reactor after  $5\theta$  was equivalent to 362 g VS. This was delivered stepwise according to the following regime; day 1 - 15 (15g), day 15 - 70 (110g), day 70 - 90 (60g), day 90 - 98 (32g) and day 98 - 127 (145g), giving an average methane yield of  $254 \pm 1.21$  mL CH<sub>4</sub> g VS<sup>-1</sup> and  $244 \pm 1.09$  mL CH<sub>4</sub> g VS<sup>-1</sup>, under mesophilic and thermophilic conditions, respectively. This shows the slightly higher rates of hydrolysis and fermentation expected from thermophilic considerations under thermophilic conditions did not necessarily lead to overall higher methane yield (Vindis *et al.*, 2009). In batch experiment Vanegas and Bartlett (2013a) reported that thermophilic temperature at 45 °C produced 30% less biogas and 23% less CH<sub>4</sub>, while Hashimoto *et al.* (1981), reported no significant change in methane yield on fermentation of beef cattle manure between the temperature range 30 °C and 60 °C. It suggests that cumulative biogas production is influenced by the 24-hour biogas production cycle rather than hydraulic residence time (Hinks *et al.*, 2013). The specific methane yield was higher for MR 1 than TR 1, in all the OLRs applied within a residence time (Table 7-1), except 1  $\theta$ , where the specific methane yield was higher for TR 1. This can be attributed to the higher rate of hydrolysis achieved by TR 1, during the start of the experiment (day 1 - day 15) as evident in Figure 7-1 B, showing higher rate of gas production was achieved before declining on day 16. From Table 7-1, it is evident that as the OLR is increased from 1 - 5 gVS L<sup>-1</sup> d<sup>-1</sup> there was a corresponding marginal decrease in methane yield per gram of VS in both MR 1 and TR 1, with MR 1 having a slightly higher rate. Methane yield among the six reactors shows close proximity in rate and similarity as the OLR was increased. The highest methane yield of 369 mL CH<sub>4</sub> gVS<sup>-1</sup> was achieved in MR 2 followed by 365 mL CH<sub>4</sub> gVS<sup>-1</sup> for TR 2 at OLR 3



gVS L<sup>-1</sup> d<sup>-1</sup> where the reactors seem steadier in gas production patterns. Since the SRT is equal to HRT in this study, it can be deduced that biogas yield was related to the reactors exposure to the seaweed and its breakdown products (Hinks *et al.*, 2013). Consequently, factors such as biomass washout (dilution rates) and length of time of exposure of microbial community to the feedstock governed the performances of reactors (Hinks *et al.*, 2013). Inhibitory component of the seaweed feedstock such as polyphenols might have caused greater negative effects on the biogas yield during longer exposure time that was linked to the greater number of HRT (Adams *et al.*, 2011b).

Figure 7-1 - Figure 7-3 A and B, also shows the pattern of methane and H<sub>2</sub>S in the biogas produced in all the reactors. The methane content from MR 1 digester was 19% on day 1, and increased to about 27% on day 3, remaining relatively constant until day 16, when it increased to approximately 41%, before continuing on an upward trend until day 27 achieving 80%. It then declined to an average value of about 65% and peaked again on day 82, with maximum value of 82%. For TR 1, the methane content reflected the initial higher rate of hydrolysis for the thermophilic system, it increased rapidly from 40% on day 1 to about 72% on day 8 and 81% by day 15 before declining, averaging about 60%, then attained its maximum value of 82% on day 80. The H<sub>2</sub>S concentration was similar for both control reactors MR 1 and TR 1 ranging from a minimum of 0.04% (v/v) on day 3 to 0.6% (v/v) on day 111 and to a maximum of 1.10% (v/v) on day 119 for MR 1, while it increased from a minimum 0.19% (v/v) on day 3, peaked at 0.89% (v/v) on day 35 before declining to about 0.33% (v/v) on day 119 for TR 1. From Henry's relationship, Eqn 7-1, the undissociated H<sub>2</sub>S in solution was calculated to be 0.7 g L<sup>-1</sup> on day 23, increased to about 10.98 g L<sup>-1</sup> on day 111 for MR 1.

$$[H_2S]_s = \alpha [H_2S]_g \quad \text{Eqn 7-1}$$

Where  $\alpha$  is the absorption coefficient (1.83 at 35 °C).

Inhibitory levels of H<sub>2</sub>S reported in the literature for AD process, range from 50 - 400 mg L<sup>-1</sup> for undissociated H<sub>2</sub>S, to about 100 - 800 mg L<sup>-1</sup> for dissolved sulphide (Chen *et al.*, 2008). The values obtained in this study did not cause any significant inhibitory effect on biogas production for either temperature condition, which seems to agree with Vanegas and Bartlett (2013a), who found

values > 200 mg/l had no inhibitory effect. However, both pH and H<sub>2</sub>S concentration have been identified as factors contributing to reactor failures during AD of *L. digitata* (Vanegas and Bartlett, 2013a; Montingelli *et al.*, 2015). In order to evaluate the effect of pH and H<sub>2</sub>S on the digestion process, NaHCO<sub>3</sub> was added as a buffering agent to reactors MR 2 and TR 2, while FePO<sub>4</sub> was added to reactors MR 3 and TR 3 in order to control H<sub>2</sub>S production, once or twice weekly. NaHCO<sub>3</sub> has been used previously to stabilise the pH of reactors (Rao and Singh, 2004), and CaCO<sub>3</sub>, NaHCO<sub>2</sub>, or NH<sub>4</sub>HCO<sub>3</sub> can also be used as an acid neutralizing agent (Chang *et al.*, 2010). Kispergher *et al.* (2017) recommended the addition of alkaline agents (NH<sub>4</sub>HCO<sub>3</sub>, NaOH, CaOH or lime) to aid in continuous biomethane production; because, they have the capacity to neutralise tVFAs production (Deublein and Steinhauser, 2011) whereas FePO<sub>4</sub> is used as a reductive solubilisation compound which helps in the removal of inhibitory soluble sulphide via FeS(s) precipitation (McFarland and Jewell, 1989). Reductive solubilisation is a process where Fe<sup>2+</sup> becomes available in solution from an insoluble Fe<sup>3+</sup> compound (McFarland and Jewell, 1989). Since, H<sub>2</sub>S in biogas causes corrosion of engines and boilers, during the digestion of macroalgae, which contains high levels of sulphur compounds, it is suggested that biogas treatment is not only given after digestion but also during digestion to limit H<sub>2</sub>S production (Peu *et al.*, 2011). From Table 7-1, in terms of OLR, reactor MR 2 and TR 2 with NaHCO<sub>3</sub> supplementation produced the highest CH<sub>4</sub> yield /g VS at 35 °C (444), followed by 55 °C (439), although this trend was not obtained in all the different loading rates that were applied. This is an indication that the methanogenic populations were not significantly affected although well supported in the buffered environment, as the production of tVFAs was not sufficiently high to cause toxicity. Without any buffer adjustment, pH changes are based on the reactions occurring in the reactors (Migliore *et al.*, 2012). A well-buffered system maintains the pH values of the process (Montingelli *et al.*, 2015), preventing inhibition of methanogenic bacteria. At an OLR of 1 gVS.d<sup>-1</sup> the specific methane yield for MR 2 at 35 °C was 444 mL CH<sub>4</sub> g VS.d<sup>-1</sup> compared to 351 mL CH<sub>4</sub> g VS.d<sup>-1</sup> obtained for MR 1 at 35 °C without NaHCO<sub>3</sub> addition. This represents a 26.6% increase in biogas produced which was not sustained as the OLR was increased but shows the possible synergetic and stimulatory role a well-buffered process can play in AD of macroalgae substrates. For optimal biogas production, it has been suggested that suitable

OLR and HRT should be chosen (Montingelli *et al.*, 2015), as studies have shown an HRT > 20 days could achieve steady state gas production in a continuous digestion process (Li *et al.*, 2013a). The profile of MR 2 shows that H<sub>2</sub>S increased from a minimum of 0.06% (v/v) on day 1 to a maximum of 1.6% (v/v) on day 41 compared to TR 2 which increased from 0.16% (v/v) on day 1 and peaked at 0.88% (v/v) on day 119. Vergara-Fernández *et al.* (2008), reported H<sub>2</sub>S at 0.1% (v/v) in biogas, and values as high as 3.5% (v/v) H<sub>2</sub>S have been reported during the digestion of *Ulva sp.* of seaweed (Peu *et al.*, 2011). From Table 7-1, with respect to reactor MR 3 and TR 3 with FePO<sub>4</sub> supplementation produced CH<sub>4</sub> yield /g VS of (369) at 35 ° C and (353) at 55 ° C respectively, but as the OLR is increased from 1 - 5 gVS.d<sup>-1</sup> there was marginal decrease in methane yield per gram of VS in both reactors with MR 3 having a slightly higher rates. Comparing MR 3 (369 mL CH<sub>4</sub> /g VS) to MR 1 (351 mL CH<sub>4</sub> /g VS) without FePO<sub>4</sub> addition, this represent an increase of about 5% whereas TR 3 (353 mL CH<sub>4</sub> /g VS) to TR 1 (353 mL CH<sub>4</sub> /g VS) without also FePO<sub>4</sub> addition gave a decrease of about 2.5% in methane production. This indicates that the addition of FePO<sub>4</sub> did not significantly improve methane yield, even as the OLR was increased as shown from Table 7-1. From an operational standpoint, removal of aqueous sulphide through iron precipitation should relieve not only sulphide inhibition but also reduce gaseous sulphide levels (McFarland and Jewell, 1989), and hence better digester performance which was not observed in the reactors added with FePO<sub>4</sub>. The profile of MR 3 shows that H<sub>2</sub>S increased from a minimum of 0.48% (v/v) on day 1 to a maximum of 1.1% (v/v) on day 111 compared to TR 3 which increased from 0.09% (v/v) on day 1 and peaked at 0.56% (v/v) on day 41 before reducing to 0.38% (v/v) on day 111.

## 7.4 Process performance indicators

### 7.4.1 pH, VFAs, and alkalinity

The characteristic profile of the digesters content pH, volatile fatty acids VFA / total alkalinity TA (FOS: TAC), total volatile fatty acids (TVFA) and alkalinity, are shown in Figure 7-5 and Figure 7-6. An initial decrease in pH (8.15 to 7.11) was observed in all the reactors, during first few days of acclimatization (data not shown). This might be attributed to the initial specific loading rate of 2 gVS L<sup>-1</sup> d<sup>-1</sup>

<sup>1</sup> which was found to be too high causing an increase in VFAs production and reduction in pH, but was not sufficient to cause reduction in biogas production. Subsequently, at the start of the experiment on day 1 the OLR was reduced to 1 gVS L<sup>-1</sup> d<sup>-1</sup> and the reactors started to recover to pH of about 8.0 by day 10 (Figure 7-5 A). Another factor that could have been responsible for the drop in pH is the VS content (69%) of the substrates, leading to high rate of hydrolysis (Michele *et al.*, 2015). The hydrolysis step is also enhanced by the pretreated macroalgal feedstock, which breaks down the cell wall rigidity, and is considered a key factor in biogas production (Jung *et al.*, 2011). Hence, the OLR was applied as a stepwise loading, starting from 1 gVS L<sup>-1</sup> d<sup>-1</sup>. Thereafter, the pH was stable between 7.70 and 7.20 throughout the duration of the experiment, which is within the optimal pH values for AD, assumed to be between 6.8 – 7.5 (Jabłoński *et al.*, 2015b). The tVFAs concentration ranged from 5.2 - 9.1 g L<sup>-1</sup> for MR 1 compared to 2.2 - 8.4 g L<sup>-1</sup> for TR 1, with a decreasing trend from day 20 - 80, before increasing again from day 98 till the end of the experiments, in all the reactors. This trend can be attributed to increases in the OLR within the 4 - 5 HRT loading regime. The OLR is a critical factor causing accumulation of excessive VFAs (Montingelli *et al.*, 2015). During anaerobic digestion of *Laminaria spp.* in a fermentation tank, Matsui and Koike (2010), reported acetic and propionic acid concentrations between 2.0 to 6.0 g L<sup>-1</sup>. VFAs values between 8.3 - 12.2 g L<sup>-1</sup> have been reported for *L. japonica* (Pham *et al.*, 2013b). Using glucose as a fermentation feedstock, the inhibitory level of VFAs for AD process is reported to be above 6.0 g L<sup>-1</sup> (Siegert and Banks, 2005). Stable digestion conditions have been observed when the VFAs concentration was below 4.0 g L<sup>-1</sup>, and inhibitory conditions when the concentration increased to 7.0 g L<sup>-1</sup> (Llaneza Coalla *et al.*, 2009). This was similar to digester instability observed when tVFAs concentration was higher than 5.0 g L<sup>-1</sup> (Ehimen *et al.*, 2011). Accumulation of tVFAs results in AD instability with a concomitant decrease in methane gas production (Rajagopal *et al.*, 2013). The trend observed in this study among the six reactors was particularly not pronounced at OLR of 4 and 5 gVS L<sup>-1</sup> d<sup>-1</sup> compared to OLR 3 gVS.d<sup>-1</sup>, as shown in Table 7-1, with a corresponding gradual increase in tVFAs accumulation, Figure 7-4 B. During the digestion of microalgae substrate (*Chlorella spp.*), tVFA accumulation was observed at OLR above 40 kg VS.m<sup>-3</sup>.d<sup>-1</sup> leading to reduced CH<sub>4</sub> production (Raposo *et al.*, 2008).

The FOS: TAC ratio followed the pattern of VFA production. For reactor MR 1, between day 1 - 20, the ratio was 0.8, when the VFAs concentration increased to  $> 8.0 \text{ g L}^{-1}$ , indicating instability in the reactor, hence the lower gas production observed as compared to TR 1, where higher rate of biogas production was achieved within the same period and FOS: TOC ratio was lower at  $< 0.4$  and VFAs  $< 2.0 \text{ g L}^{-1}$ . The FOS: TOC ratio in all other reactors fluctuated between 0.33 - 1 but increased to between 1 - 2.0 in all the six reactors when the OLR was increased up to  $4 \text{ gVS L}^{-1} \text{ d}^{-1}$ , indicating the digestion processes becoming unstable for biogas production. Increase in FOS: TAC ratio above 0.5 showed a corresponding increase in tVFA on days 19 (for Reactors 1, 2, 3), 56 (Reactor 2), and more pronounced within days 92 - 126 for the thermophilic reactors as shown in Figure 7-5 B. While low FOS:TAC ratio indicates a digestion systems that is still below optimal OLR (Jabłoński *et al.*, 2015a), stable digestion has been observed in the range 0.30 - 0.40, and when above 0.70 instability results in the digesters (Raposo *et al.*, 2009). At tVFA concentration close to  $1.0 \text{ g L}$ , digester stability was always observed when FOS: TAC ratio was less than 1.0 (Kafle and Kim, 2011).

The total alkalinity (TA) values in the reactors ranged between  $10.0$  to  $15.0 \text{ g CaCO}_3 / \text{L}$  indicating well-buffered conditions, which was sufficient to maintain the pH in the reactors above 7.0, hence the high tVFA levels observed in this study were not considered to be toxic to methane formation. Migliore *et al.* (2012) stated that inhibition of methanogens occurs when the buffer capacity is not able to prevent the drop in pH. Since the TA is a non-specific determination which measures all the basic components present in a media, evaluation of the TA yield showed a decreasing trend with VS loading from  $6.9 \text{ g CaCO}_3 \text{ g}^{-1} \text{ VS}_{\text{added}}$  to  $3.0 \text{ g CaCO}_3 \text{ g}^{-1} \text{ VS}_{\text{added}}$  (MR 1) and from  $7.5 \text{ g CaCO}_3 \text{ g}^{-1} \text{ VS}_{\text{added}}$  to  $2.5 \text{ g CaCO}_3 \text{ g}^{-1} \text{ VS}_{\text{added}}$  (TR 1), Figure 7-5 A, which is not an unexpected result, as TA was consumed in the neutralization the TVFAs generated (Raposo *et al.*, 2008).

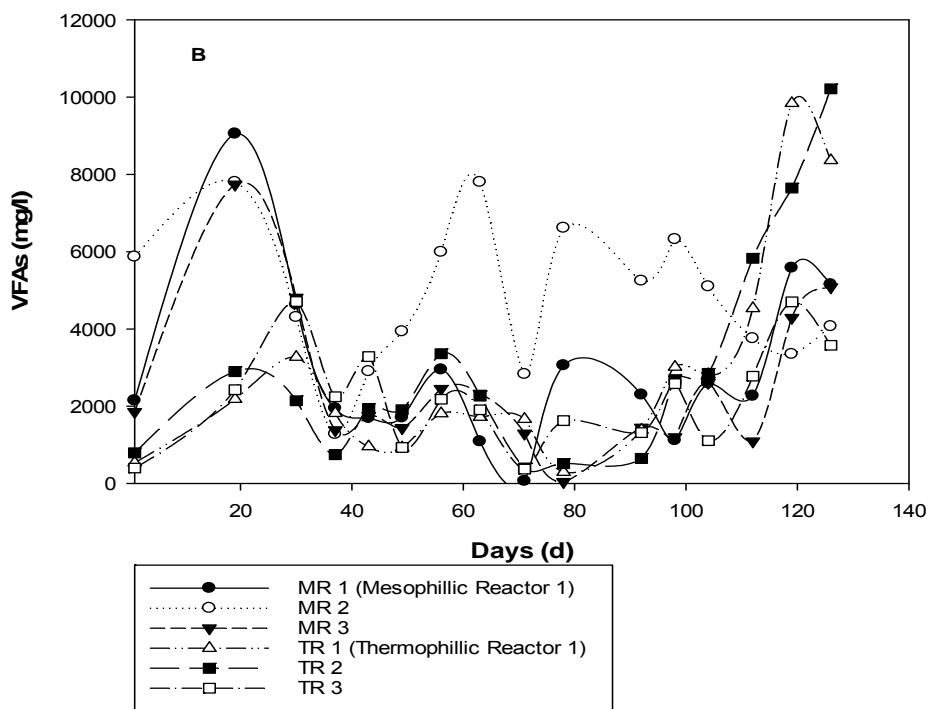
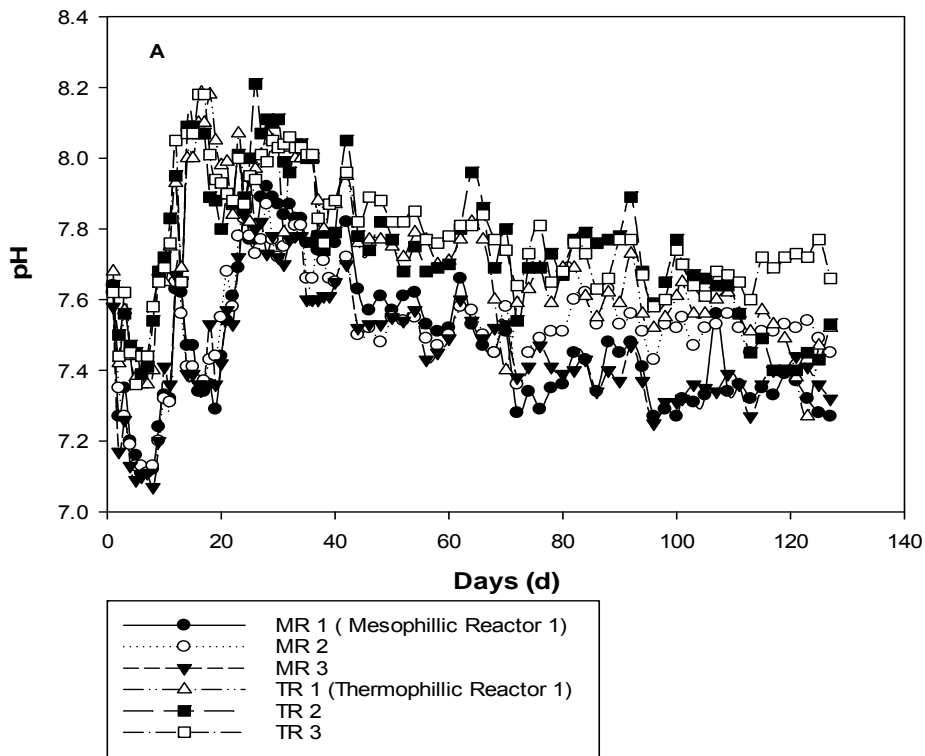


Figure 7-4 A), Variations in pH, B), VFAs, of both mesophilic (MR 1, 2, 3) and thermophilic (TR 1, 2, 3) digesters.

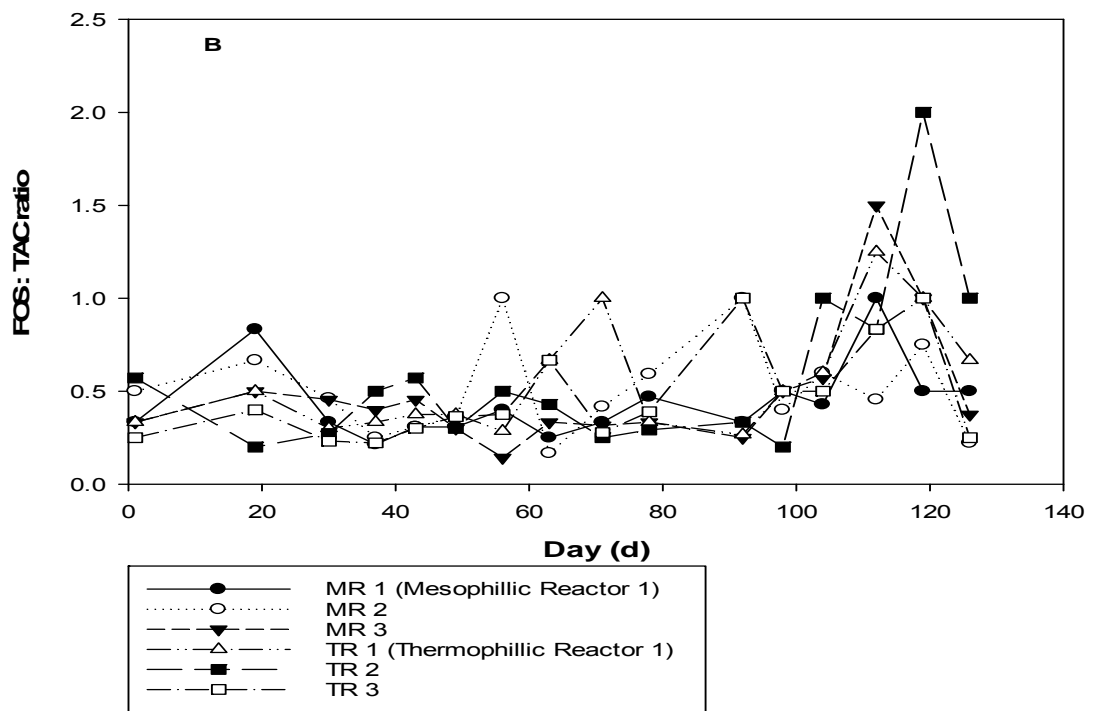
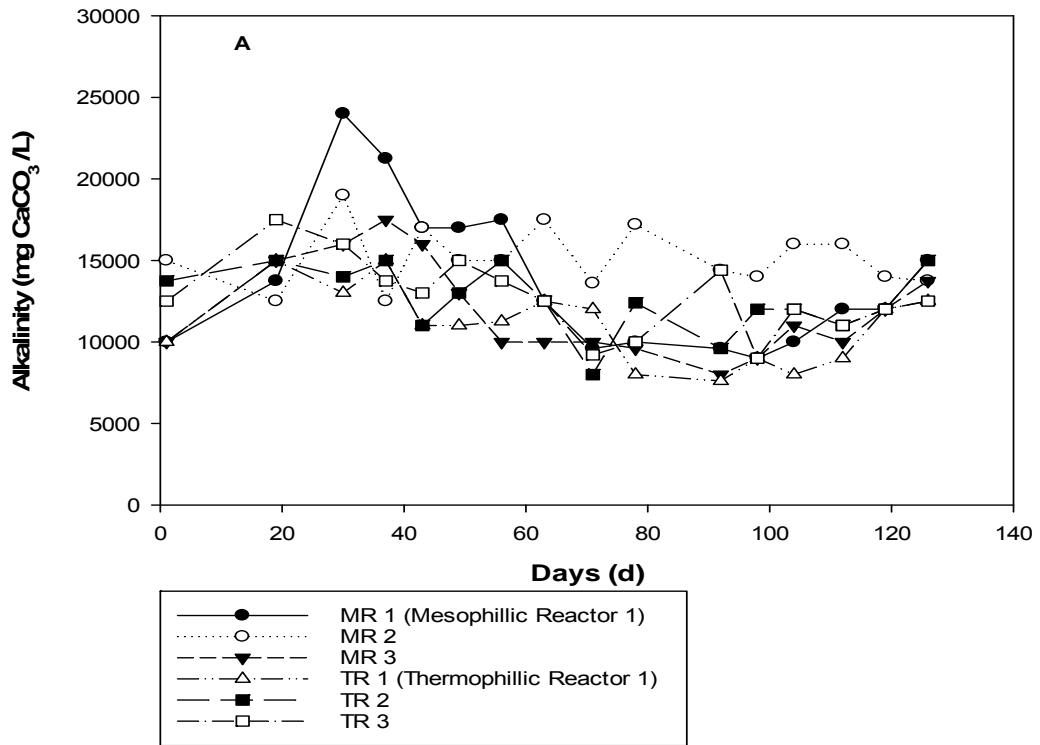


Figure 7-5 A), Variations in Alkalinity; and B), FOS: TAC ratio of both mesophilic (MR 1, 2, 3) and thermophilic (TR 1, 2, 3) digesters.

The identification of individual tVFAs formed is important as it can provide useful information on the metabolic pathways involved in AD processes (Raposo *et al.*, 2008). The chemical composition of various type of VFAs such as acetic, propionic, butyric, and lactic acid that can be produced from macroalgae using anaerobic digestion (Jung *et al.*, 2013), for both MR 1 and TR 1, are shown in Figure 7-6. During the first HRT (1 - 25 days), predominately acetic and propionic acid were produced accounting for about 60 - 70% of the tVFAs produced at both temperature conditions. This was followed by additional production of butyric acid in high concentration which declined as the reactor run time progressed. In AD of cellulose by rumen microorganisms acetic and propionic, followed by butyric acid were the two major aqueous products of fermentation reported by the study (Raposo *et al.*, 2008). Both acetic and propionic acid are regarded as the main precursors to methane in AD (Li *et al.*, 2013a; Zhang *et al.*, 2013), and their concentration can be used as indicator of process performance (Buyukkamaci and Filibeli, 2004). Short-chain fatty acids are composed mainly of acetate and butyrate which can be produced by compounds with low lignin content (i.e macroalgae) (Jung *et al.*, 2013).

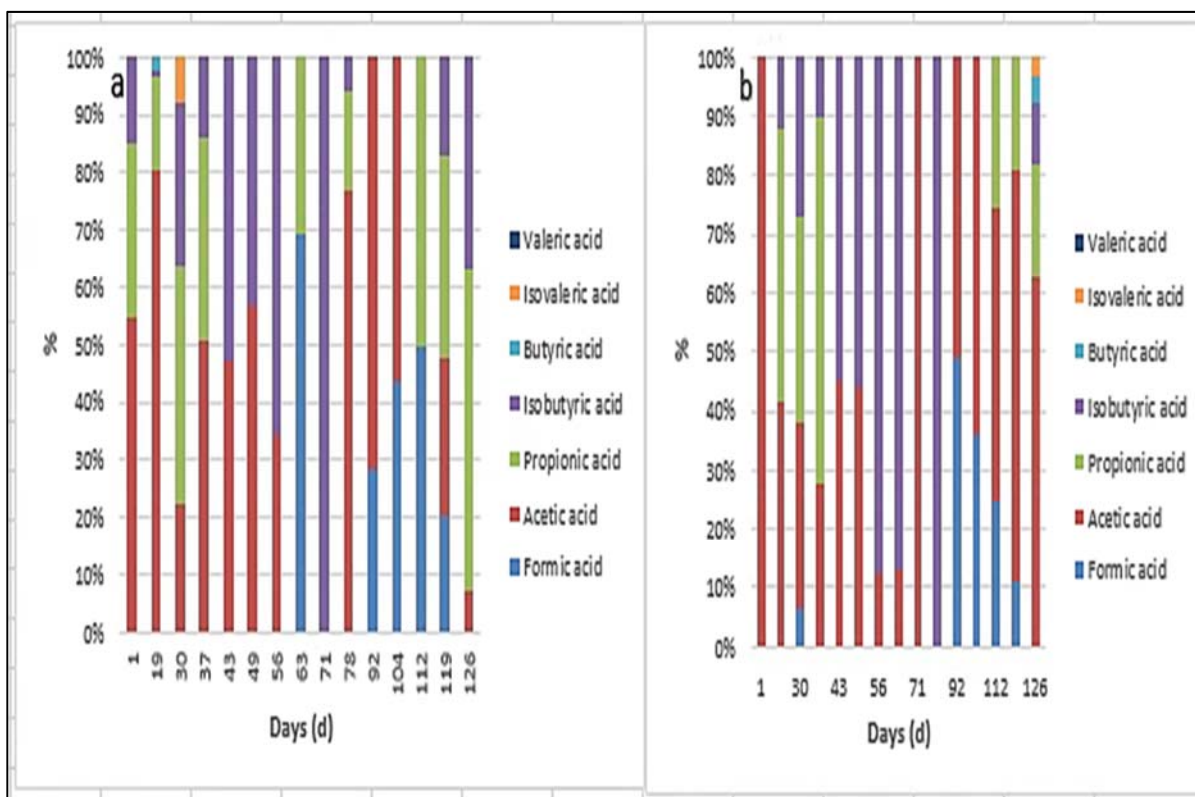


Figure 7-6 Volatile fatty acids speciation from macroalgae during AD, a) Mesophilic (MR 1) and, b) thermophilic temperature (TR 1).



### 7.4.2 Ammonium ion ( $\text{NH}_4^+$ ) and free ammonia ( $\text{NH}_3$ ) nitrogen

Figure 7-7 and Figure 7-8 shows the net concentration profile for total Kjeldahl nitrogen (TKN), total ammonia nitrogen (TAN), ammonium ion ( $\text{NH}_4^+$ ) and free ammonia ( $\text{NH}_3$ ) nitrogen (FAN) in the mesophilic and thermophilic digesters.

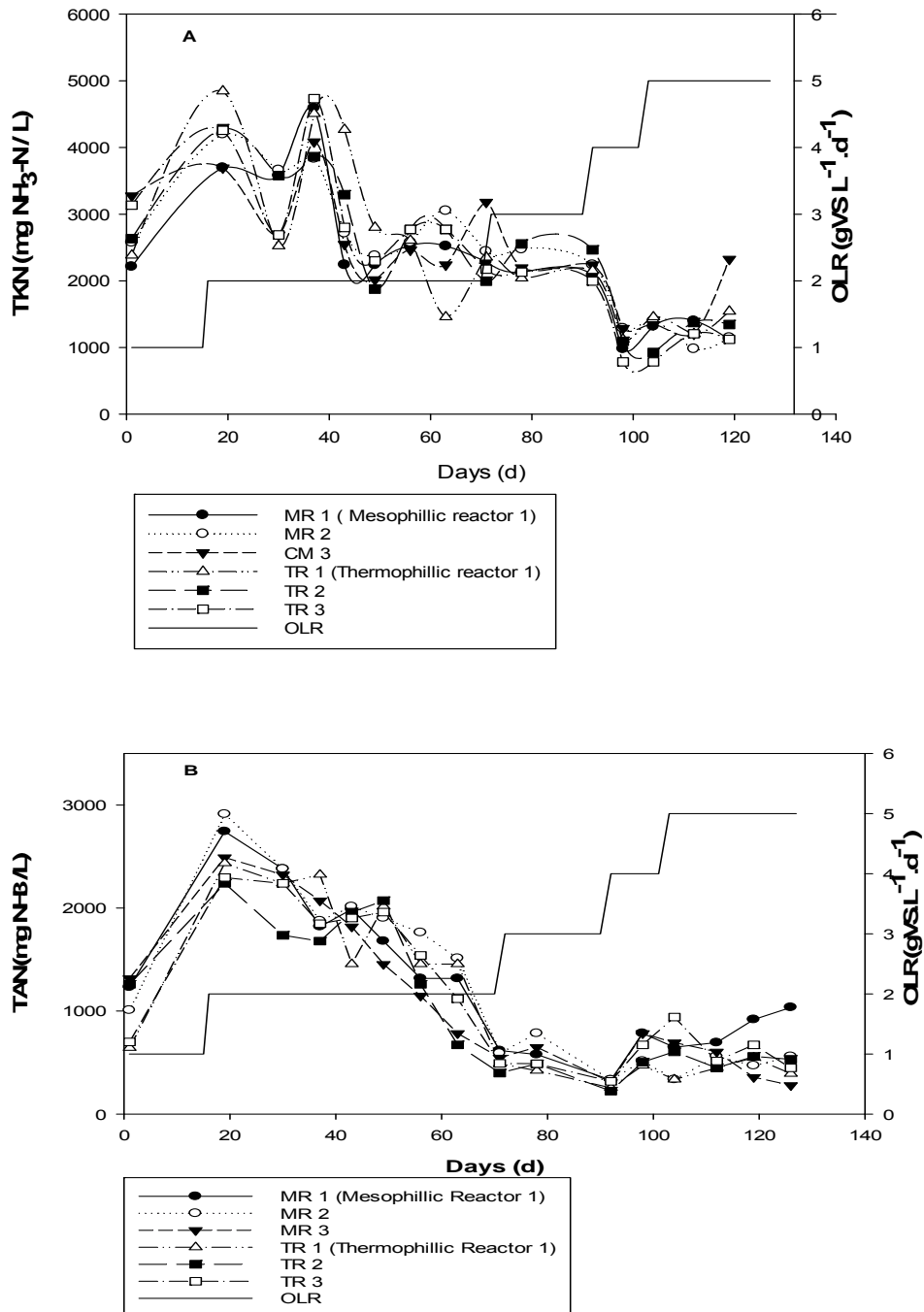


Figure 7-7 A), Concentration profile for Total Kjeldahl (TKN); B), Total ammonia nitrogen (TAN) in mesophilic (MR 1, 2, 3) and thermophilic (TR 1, 2, 3) digesters.

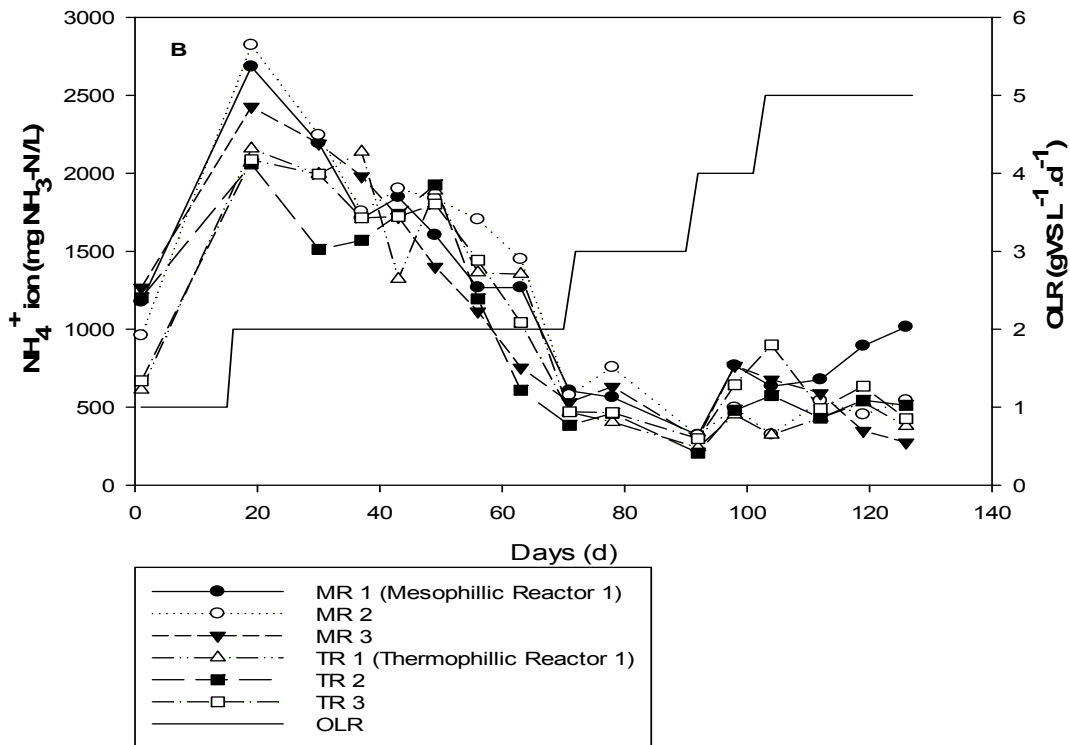
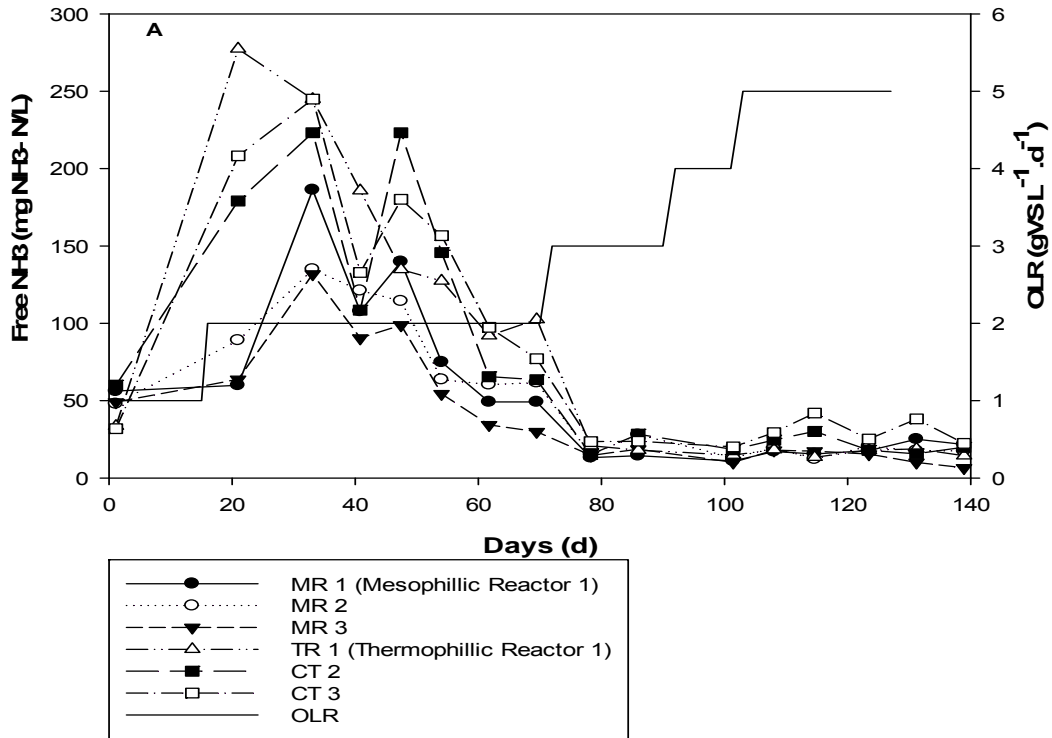


Figure 7-8 A), Concentration profile for free ammonia ( $\text{NH}_3$ ) nitrogen (FAN); B), ammonium ion ( $\text{NH}_4^+$ ) in mesophilic (MR 1, 2, 3) and thermophilic (TR 1, 2, 3) digesters.

The concentration of the TKN, which gives an indication of the amount of protein present in the substrate (Galí *et al.*, 2009), continued to decrease as the reaction progressed from day 1 to 127, ranging from 2.2 – 1.1 and 2.4 - 1.5 g NH<sub>3</sub>-N/L for the mesophilic and thermophilic reactors respectively, Figure 7-7 A. TKN which is degraded to ammonia, its determinations helps to evaluate nitrogen availability for growth of anaerobic bacteria and in estimating reactors nitrogen concentrations (Wellinger *et al.*, 2013). Ammonia is the end product of protein, urea and nucleic acid degradation (Chen *et al.*, 2008; Rajagopal *et al.*, 2013), although TAN inhibitory concentration for AD varies between 1.7 to 14 g L<sup>-1</sup> (Chen *et al.*, 2008), and depends on pH, it is generally reported that a concentration close to 200 mg L<sup>-1</sup> is beneficial to AD processes, because ammonia is a nutrient required by anaerobic microbes (Liu and Sung, 2002). The inhibitory level for TKN is rarely reported as it is not inhibitory directly, but leads to TAN formation which can be toxic. An increase in TKN concentration could minimise instability in reactors by preventing the risk of ammonium–nitrogen limitation for methanogens (Li *et al.*, 2013a). The Ammonia nitrogen is present mainly as inorganic NH<sub>4</sub><sup>+</sup> ions and undissociated NH<sub>3</sub> (Appels *et al.*, 2008; Montingelli *et al.*, 2015). Both forms have been reported as inhibitory to methanogens with the free NH<sub>3</sub> ion being more toxic (Astals *et al.*, 2013), as it can penetrate the cell wall reaching the cytoplasm, and interrupt the metabolism of the microorganism (Angelidaki and Ahring, 1993). The average daily free NH<sub>3</sub> concentrations were estimated on the basis of the TAN concentration, temperature and pH value, according to Eqn 2-9 and shown in Figure 7-8 A. For the mesophilic reactor MR 1, free NH<sub>3</sub> concentration (mg NH<sub>3</sub>-N/L) increased from 56 mg NH<sub>3</sub>-N/ on day 1 to 187 mg NH<sub>3</sub>-N/L by day 30 before a continuous steady decline to a value of 22 mg NH<sub>3</sub>-N/L on day 119. In the thermophilic reactor TR 1, it increased from 33 mg NH<sub>3</sub>-N/ on day 1 to 277 mg NH<sub>3</sub>-N/ on day 19 before decreasing to a value of 14 mg NH<sub>3</sub>-N/L on day 119.

The reported minimum inhibitory value for FAN is 80 mg N/L (Montingelli *et al.*, 2015). Studies by Vanegas and Bartlett (2013b) and Peu *et al.* (2011) on *Laminaria digitata* and other macroalgae species, FAN concentrations between 68 - 350 mg L<sup>-1</sup> did not result in any inhibition of biogas formation. The NH<sub>4</sub><sup>+</sup> ion concentrations (mg NH<sub>3</sub>-N/L) in the current study, which was computed from the difference between TAN and FAN in the reactors, are also shown in Figure 7-8

B. For MR 1,  $\text{NH}_4^+$  concentration increased from 1.2 g  $\text{NH}_3\text{-N/L}$  on day 1 to 2.7 g  $\text{NH}_3\text{-N/L}$  by day 19 before decreasing to a value of 0.89 g  $\text{NH}_3\text{-N/L}$  on day 119, while in the thermophilic reactor TR 1, it increased from 0.6 mg  $\text{NH}_3\text{-N/L}$  on day 1 to 2.2 g  $\text{NH}_3\text{-N/L}$  on day 19 before decreasing to a value of 0.5 mg  $\text{NH}_3\text{-N/L}$  on day 119.  $\text{NH}_4^+$  ions concentrations up to 1.5 g  $\text{L}^{-1}$  have no substantial effects on the methanogens but can lead to significant toxicity above that threshold (Costa *et al.*, 2012). Using *Laminaria sp.* and *Ulva sp.* as fermentation materials,  $\text{NH}_4^+$  ions concentration of up to 1.2 g  $\text{L}^{-1}$  did not have any effect on methane production (Montingelli *et al.*, 2015). The results obtained for both  $\text{NH}_4^+$  and  $\text{NH}_3$  follow the pattern of protein degradation via the TKN profile with higher TAN corresponding to higher free  $\text{NH}_3$ , because the  $\text{NH}_3$  concentration depends on TAN, temperature, and pH (Astals *et al.*, 2013). The increase in ammonia concentration within the ideal range could support stability in AD process by improving N availability as a nutrient (Li *et al.*, 2013a). In the current study, the  $\text{NH}_4^+$  increased up until day 19 when it exceeded 2000 mg  $\text{NH}_3\text{-N/L}$  in both the thermophilic and mesophilic reactors, while the FAN concentration for all the thermophilic reactors peaked above 150 mg  $\text{NH}_3\text{-N/L}$ , the mesophilic reactors were always below < 100 mg  $\text{NH}_3\text{-N/L}$ . It has been shown that FAN concentration under the same pH values is expected to be six times higher under thermophilic (55 °C) than mesophilic conditions due to the chemical equilibria effects (Kayhanian, 1999). Within this same period (Day 1 -19), these inhibitory levels coincided with a decline in pH and high VFAs accumulation, but this does not necessary lead to process instability, as has been stated, the interaction between the  $\text{NH}_3$ , VFA and pH can lead to an inhibited steady-state in reactors (Astals *et al.*, 2013). This inhibited steady-state is a condition where the biogas production is low under relatively stable conditions (Hansen *et al.*, 1999). Angelidaki and Ahring (1993) reported ammonium nitrogen tolerance level of up to 3.0 – 4. g  $\text{NH}_4\text{-N/L}$ . Specifically, with respect to the inhibitory effect of ammonia on methanogens, it causes an increase in VFAs concentration which decreases the pH, which in turn lowers the inhibitory FAN concentration (Astals *et al.*, 2013), promoting a mechanism referred to as “inhibition relief” which helps to stabilise the process at certain VFA concentrations and pH levels (Angelidaki *et al.*, 1993). This phenomenon was observed in this study, as stated earlier, in all the reactors as the OLR was increased up to 4 gVS.L<sup>-1</sup> d<sup>-1</sup>,

there was increase in the tVFAs concentration with a continuous but reduced yield in biogas production.

### 7.4.3 Solids, COD, and Anions

The results of total and soluble COD are shown in Figure 7-9.

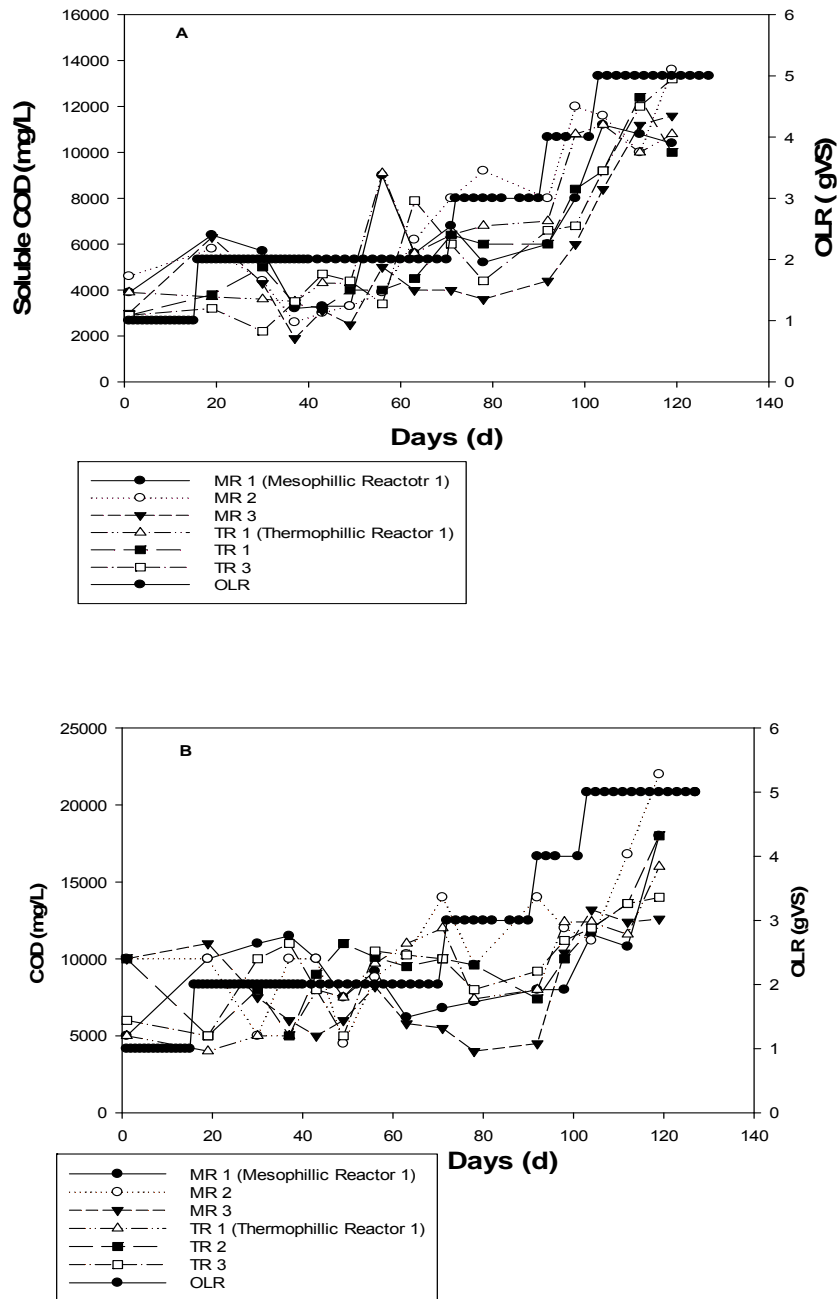


Figure 7-9 A), Concentration profile of soluble COD; B), Total COD in mesophilic (MR 1, 2, 3) and thermophilic (TR 1, 2, 3) reactors.

The COD concentration profile at 3 cycles of HRT can be used as an indication of achieving a steady state process in AD (González-Fernández *et al.*, 2013). The maximum chemical energy stored in a feedstock which can be recovered as biogas by microbes is represented by the COD (Wellinger *et al.*, 2013). Both the total COD (tCOD) and soluble COD (sCOD) concentration in the thermophilic reactor (TR 1) decreased slightly, tCOD, decreasing from 5.0 g L<sup>-1</sup> on day 1 to 4.0 g L<sup>-1</sup> by day 19, and sCOD decreasing from 3.9 to 3.7 g L<sup>-1</sup> in the same period. This period (Day 1 - 19) was characterised by increased biogas production and low VFAs production. The tCOD increased to 7.50 g L<sup>-1</sup> by day 49 and increased further at an OLR of 3 gVS.L<sup>-1</sup>.d<sup>-1</sup> to 9.7 g L<sup>-1</sup> by day 56 before remaining relatively stable till day 98 at OLR 4 gVS.L<sup>-1</sup>.d<sup>-1</sup>, where it increased to 12.4 g L<sup>-1</sup> and continued in that trend till day 119 to 16.0 g L<sup>-1</sup>. In the same period the sCOD increased to 4.3 g L<sup>-1</sup> by day 49, to 9.1 g L<sup>-1</sup> by day 56, 10.8 g L<sup>-1</sup> on day 98 and to 11.0 g L<sup>-1</sup> by day 119. As the COD levels continued to rise as a result of the increase in OLR, the process was characterised by a declining pH and increasing VFA concentration. This trend (increase in COD with accumulation of VFA) with digestion time as been described as a stress situation which reflects the kinetic uncoupling of acid consumers and formers (Switzenbaum *et al.*, 1990), and implies the satisfactory working of the hydrolytic – acidogenic phase but an imbalance in the methanogenic phase due to stress on the methanogenic microbes (Raposo *et al.*, 2008). The extent of solubilisation is represented by the COD parameter (Raposo *et al.*, 2008). Since, the COD measurement of heterogeneous samples like macroalgae is fraught with high error (Wellinger *et al.*, 2013), the difference (tCOD – sCOD) then represents the unsolubilised COD, i.e. fragments of algae that are not broken down, which shows to an extent how the hydrolysis phase is working. The sCOD shows how much possible COD is there as VFA and other soluble organics, that might be converted to methane but are actually not being converted. This is because soluble organic compounds produced in the hydrolytic phase are transformed into short chain volatile fatty acids in the acidogenic phase (Bolzonella *et al.*, 2005). In thermophilic reactor TR 1, tCOD – sCOD on day 1 is 1.10 g L<sup>-1</sup> which is about 22.0% of the tCOD and 28.2% of sCOD. As digestion time progressed with increase in OLR and COD levels, by day 119, the tCOD – sCOD increased to 5.2 g L<sup>-1</sup> which represent about 32.5% of tCOD and 48.1% of sCOD. The ratio of sCOD/tCOD was 78% on day 1 to

about 68% by day 119. High COD solubilisation could be attributed to increases in digestion temperature (Li *et al.*, 2013a), as the main effect of temperature is to increase soluble COD concentration (Montingelli *et al.*, 2015), by promoting cell wall disruption and breakage making the substrates more accessible for digestion (González-Fernández *et al.*, 2012). From Table 6-2, using the elemental analysis results and from the Buswell equation, 1 gVS of the macroalgae feedstock, theoretically give about  $0.26 \text{ g CH}_4 = 0.36 \text{ L} = 1.04 \text{ g COD}$ . Previously, 1 gVS of a biological sludge been reported as equivalent 1.40 g COD (Prabhudessai *et al.*, 2013), as there is a direct relationship between COD and VS of an organic substrate (Kispergher *et al.*, 2017). This implies in TR 1 for instances, at OLR  $5 \text{ gVS.L}^{-1}.\text{d}^{-1}$ , the methane yield equivalent for 1 gVS obtained was  $301.4 \text{ mL CH}_4 / \text{gVS}$  (Table 7-1), which is  $\leq 19.4\%$  less than the theoretical yield for every g of COD or VS converted to biogas. In the mesophilic reactor (MR 1), tCOD concentration increased from  $5.0 \text{ g L}^{-1}$  on day 1 to  $10.0 \text{ g L}^{-1}$  by day 19 and sCOD, increased from  $3.9$  to  $6.4 \text{ g L}^{-1}$  on day 1 and 19, respectively. The sCOD / tCOD ratio within this period was 78% on day 1 and decreased to 64% by day 19. Presumably, some readily digestible sCOD had been converted to VFAs, causing a pH decline and subsequent of methanogens inhibition (Gurung *et al.*, 2012). This led to low gas productions within the period and an increase in the sCOD contents. Thereafter, tCOD reduced slightly to  $7.5 \text{ g L}^{-1}$  by day 49 but then increased at an OLR of  $3 \text{ gVS.L}^{-1}.\text{d}^{-1}$  to  $9.2 \text{ g L}^{-1}$  on day 56 before remaining relatively stable till day 104 at an OLR  $4 \text{ gVS L}^{-1}.\text{d}^{-1}$ , where it increased to  $11.6 \text{ g L}^{-1}$ , and continued in that trend till day 119 to  $18.0 \text{ g L}^{-1}$ . As both the tCOD and sCOD continued to build as a result of the increase in OLR from day 104, the process also was characterised by a declining pH and increasing level of tVFA in all the mesophilic reactors. From the methane yield obtained for MR 1 at OLR  $5 \text{ gVS.L}^{-1}.\text{d}^{-1}$  ( $318 \text{ mL CH}_4 / \text{gVS}$ ), this is  $\leq 13.2\%$  less than the theoretical methane yield for every g of COD or VS converted to biogas.

The concentration of  $\text{SO}_4^{2-}$  and chloride in the reactors are also shown in Figure 7-10. Some of the  $\text{SO}_4^{2-}$  produced was converted to  $\text{H}_2\text{S}$  and  $\text{HCO}_3^-$  by SRB in using organic compounds (Nkemka and Murto, 2010). The  $\text{SO}_4^{2-}$  concentration for the thermophilic reactor TR 1, was almost negligible on day 1 but increased to  $0.9 \text{ g L}^{-1}$  by day 30 and fluctuated throughout the loading regime to about 0.1

g L<sup>-1</sup> on day 98, and remained at 0.1 g L<sup>-1</sup> by day 119 while in the mesophilic reactor MR 1 showed similar pattern from negligible SO<sub>4</sub><sup>2-</sup> content on day 1 to 0.1 g L<sup>-1</sup> on 30, and varied to 0.3 g L<sup>-1</sup> by day 49, and fluctuated between 0.1 g L<sup>-1</sup> and 0.14 g L<sup>-1</sup> with a final value of 0.3 by day 119.

The COD/SO<sub>4</sub><sup>2-</sup> ratio has been used as a factor to control biogenic H<sub>2</sub>S production (Velasco *et al.*, 2008). When sulphate is present during AD degradation, SRB uses part of carbon substrate to produce H<sub>2</sub>S, competing with methanogens in the process (Omil *et al.*, 1995). SRB competing with methanogens for H<sub>2</sub> is dependent on the COD/SO<sub>4</sub><sup>2-</sup> ratio (Nkemka and Murto, 2010). It is generally reported by several authors that a COD/SO<sub>4</sub><sup>2-</sup> ratio of 10 and above is recommended for successful anaerobic digestion process (Omil *et al.*, 1995; de Smul *et al.*, 1999). A ratio lower than 8 - 10 could cause inhibition of methanogenesis from H<sub>2</sub>S production because the SRB outcompetes the methanogens when SO<sub>4</sub><sup>2-</sup> is high (Omil *et al.*, 1995; Aspé *et al.*, 1997). The COD/SO<sub>4</sub><sup>2-</sup> ratio in the current study, greatly exceeds the ratio of 10, as a result of the OLR and elemental composition of the macroalgae substrate, hence methanogens had a growth advantage over the SRB (Nkemka and Murto, 2010). Under those prevailing conditions, inhibition by H<sub>2</sub>S was low and sulphate was not converted fully to H<sub>2</sub>S. Other factors contributing to the low inhibitory effect of H<sub>2</sub>S, was the pH of the reactors which was above 7.0 throughout the experiment, favouring the HS<sup>-</sup> form, but H<sub>2</sub>S can have profound effect at lower pH (Gerardi, 2003). The buffering capacity of HCO<sub>3</sub><sup>-</sup> ions produced during the reduction process of SO<sub>4</sub><sup>2-</sup> to H<sub>2</sub>S is also a contributing factor (Nkemka and Murto, 2010).



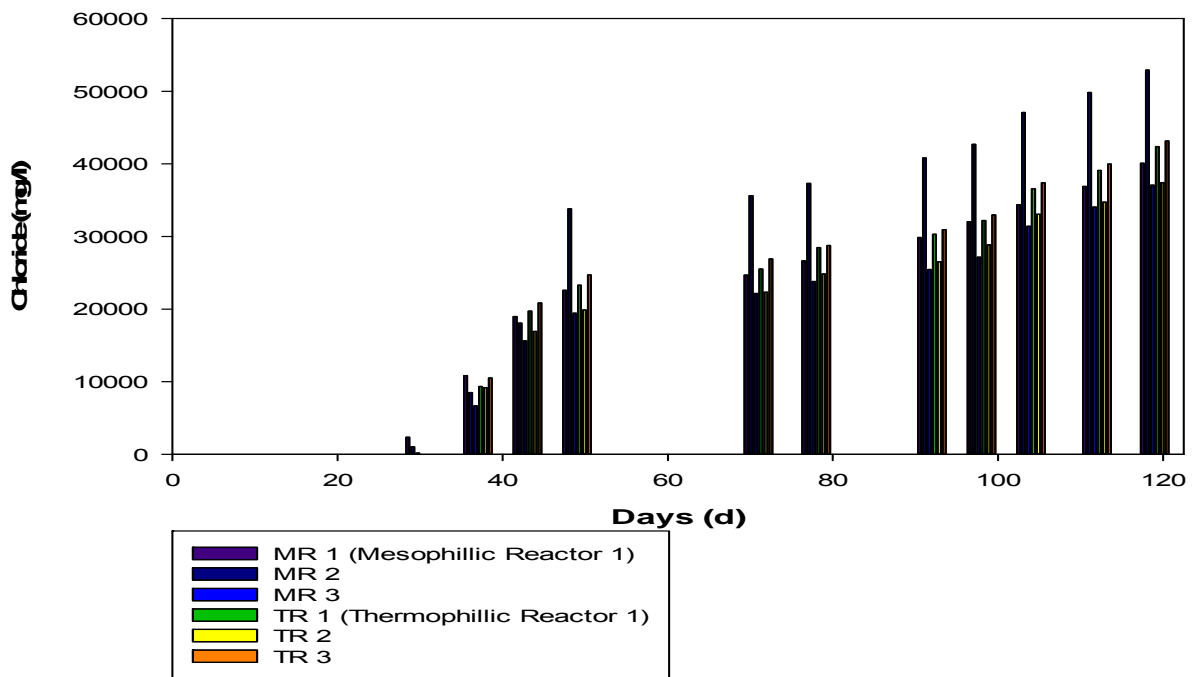
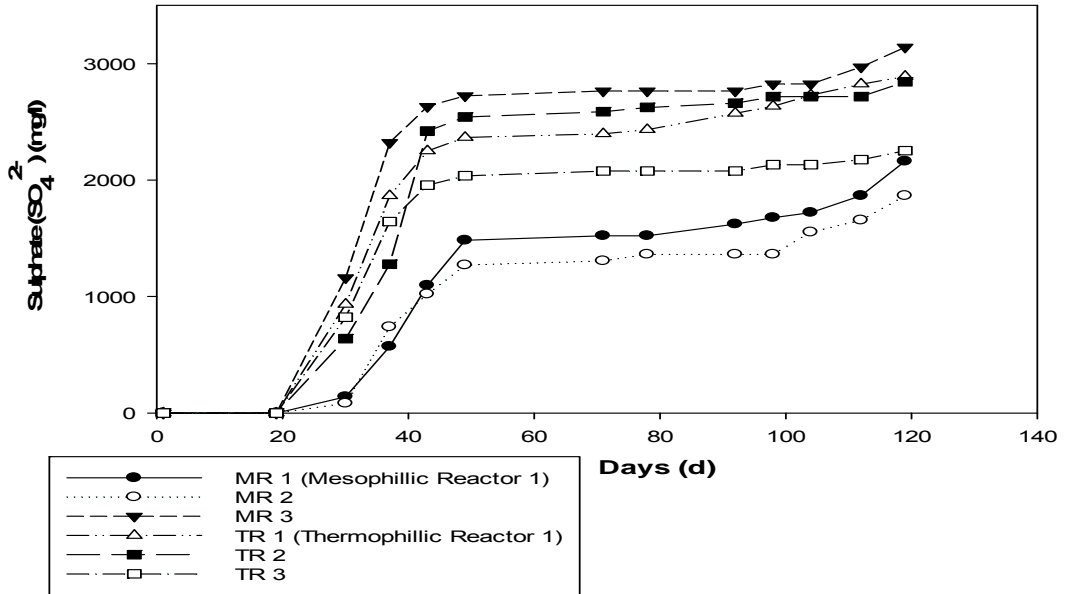


Figure 7-10 A), Concentration profile of sulphate; B), Chloride in mesophilic (MR 1, 2, 3) and thermophilic (TR 1, 2, 3) reactors.

Due to the marine origin of the substrate, high content of both KCl and NaCl were found in the macroalgae feedstock, as shown in X-ray Diffraction (XRD) studies, Appendix B. The concentration of chloride produced during the digestion of the macroalgae feedstock is also shown in Figure 7-10 B. High chloride concentration is a possible concern for the development of mono-

seaweed digesters (Tabassum *et al.*, 2016a). High salinity level, particularly in form of sodium salt, can be inhibitory to bacterial cells, causing them to dehydrate due to increased osmotic pressure (Ward *et al.*, 2014), this results in loss of cell activity and plasmolysis (Uygur, 2006; Wang *et al.*, 2017). At low concentration 350 mg Na<sup>+</sup> /L (~0.8 g/L NaCl) (Wang *et al.*, 2017), chloride is essential for bacterial growth and cellular metabolism (Suwannopadol *et al.*, 2012; Ward *et al.*, 2014).

There was progressive increase in chloride concentration with increases in OLR in all reactors as the experiment progressed. The cumulative chloride content in MR 1 and TR 1 was 40.1 g L<sup>-1</sup> and 42.4 g L<sup>-1</sup>, respectively. The highest concentration of 52.94 g L<sup>-1</sup> was observed for CM 2 with NaHCO<sub>3</sub> addition. Lefebvre *et al.* (2007), has shown that the main adverse effect of increasing Cl concentration in AD systems from 0 - 60 g L<sup>-1</sup> is the reduction in biogas production which depends on the nature of the substrate. In AD systems at various temperatures, inhibitory levels of chloride, range from 5 - 50 g L<sup>-1</sup>, but it has also been shown that acclimatised sludge can operate at a wide range of sodium chloride concentrations (0 - 50 g L<sup>-1</sup>) (Riffat and Krongthamchat, 2006). During, the AD of *L. digitata* and *S. latissima*, it has been shown that acclimatisation of the process allowed stable methane production at efficiencies close to their theoretical maximum even at high OLRs (up to 4 kg VS.m<sup>-3</sup>.d<sup>-1</sup>) when high chloride levels were present up to 14 g L<sup>-1</sup> (Tabassum *et al.*, 2016a). In the current study, the effect of the high levels of chloride on biogas yield was not followed specifically, but the acclimatised inoculum continued to produce biogas at chloride concentrations up to 40 g L<sup>-1</sup>. In their study, Tabassum *et al.* (2016a), could not clearly establish a correlation between the level of chloride and the methane yield for macroalgae.

Figure 7-11, shows the solids concentration profile during the digestion period. In both the thermophilic and mesophilic reactors, the TS ranged between 32 – 54 mg L<sup>-1</sup>, 33 - 58 mg L<sup>-1</sup>, and VS (%TS) between 38.5 - 41.1% and 43.8 - 45.5% respectively as the OLR is increased. At the end of the third feeding cycle, and at the beginning of the higher OLR (4 gVS.L<sup>-1</sup>.d<sup>-1</sup>), the TS continued to increase, reaching up to 53 mg L<sup>-1</sup>- 63 mg L<sup>-1</sup>, during the last OLR period of the experiment in all the reactors. This maximum TS averaged at 40.7% in all the reactors. This observed increase is similar to increases in both the tCOD

and sCOD concentrations, and could be attributed to slower rate of microbial degradation of feedstock and lower yields of methane that can be expected under high substrate loading (Doğan - Subaşı and Demirer, 2016).

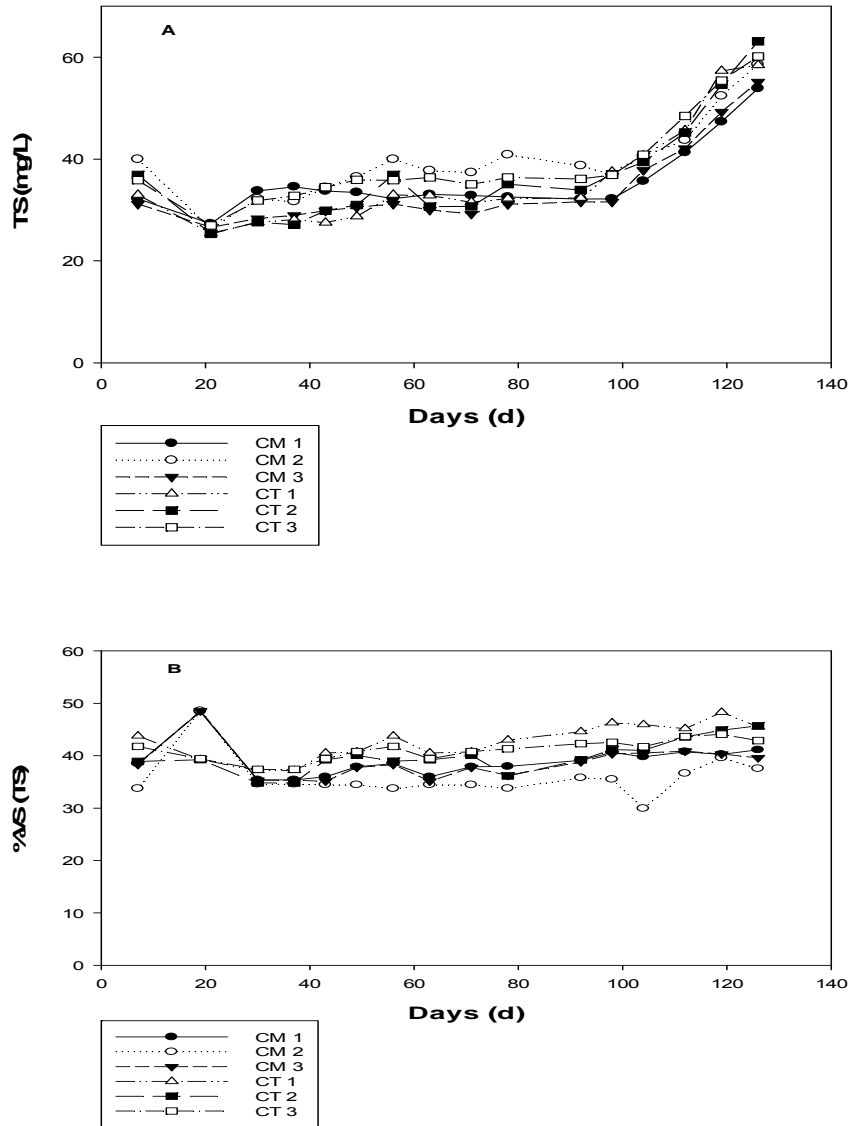


Figure 7-11 A), Concentration profile of total solids; B), Volatile solids in mesophilic (MR 1, 2, 3) and thermophilic (TR 1, 2, 3) reactors.

#### 7.4.4 Statistical Analysis

##### *Two sample t-test*

Statistical analysis was carried out using Minitab 17 or Signal plot 12.5 software to compare the means of cumulative CH<sub>4</sub> produced from the different reactors. Firstly, a two-sample t-test was used to evaluate the difference between the control reactors MR 1 and TR 1. The result of the absolute t value was less than the corresponding critical value ( $1.10 < 1.984$ ), with a p-value of 0.272, hence there is no significant difference between the cumulative CH<sub>4</sub> production of the reactors at the 5% level (95% confidence interval), This implies the two different temperature conditions did not affect the methanogenic processes significantly in reactors MR1 and TR1. From the test of equal variance, using both the Bonett's (F-test) ( $p=0.353$ ), and the Levene's test ( $p=0.496$ ), the p-values are not significant, hence equal variances can be assumed for the two datasets (MR 1 and TR 1) for cumulative CH<sub>4</sub> production.

##### *One way analysis of variance (ANOVA)*

One way analysis of variance (ANOVA) was used to compare the means of cumulative CH<sub>4</sub> production between the different mesophilic reactors (MR 1, 2, 3), and between the different thermophilic reactors (TR 1, 2, 3), separately. Equal variance was assumed for the analysis. For the mesophilic reactors, the  $p = 0.895$  and observed F-ratio is 0.11. Both the 1% and 5% critical value of  $F_{2, 189}$  is 3.09 and 4.89, which is higher than the observed F-ratio. Hence, the significance level is not less than 0.05, implying that there are no real differences between the means of the different mesophilic reactors for the cumulative CH<sub>4</sub> produced. For the thermophilic reactors, the  $p = 0.919$  and observed F-ratio is 0.08. From the critical value of  $F_{2, 189}$  which is also higher than the observed F-ratio, the significance level is also less than 0.05, implying there are no real difference between the means of the different thermophilic reactors. This suggests the amendments of bicarbonate (Reactor 2) and phosphate (Reactor 3), had no actual effect on methane production compared to the unamended reactors (Reactor 1).

### *Two-way analysis of variance*

Figure 7-12 shows the main effect and interaction plot from two-way analysis of variance comparing the means of the cumulative CH<sub>4</sub> production between the mesophilic and thermophilic reactors. The ANOVA Table 7-2 shows that the main effect of the temperature on the reactors is not significant (p-values = 0.673 & 0.074).

Table 7-2 Analysis of variance (ANOVA) for reactors cumulative CH<sub>4</sub> means

Source	DF	Adj SS	Adj MS	F-Value	P-Value
Reactor	2	1266825	633412	0.49	0.673
Temperature	1	15600938	15600938	11.98	0.074
Error	2	2604841	1302420		
Total	5	19472604			

The main effects plot demonstrates response of the cumulative CH<sub>4</sub> means from the reactors with respect to the temperature of the reactors. It is clear that the mesophilic reactors attained a methane yield above the average methane of 2.9 L CH<sub>4</sub>/ reactor (dashed line) among the reactors whereas the thermophilic reactors were less than the average value of 2.9 LCH<sub>4</sub>/ reactor in all the reactors, Figure 7-12 A. From the temperature interaction plot, Figure 7-12 B, it can be deduced that MR 3 with FePO<sub>4</sub> addition performed better after 127 days of digestion at both the mesophilic and thermophilic temperature conditions, while the control reactor MR1 performed almost equally as well as the MR 3 under the mesophilic conditions, but TR 1 under the thermophilic conditions performed the least among the reactors.

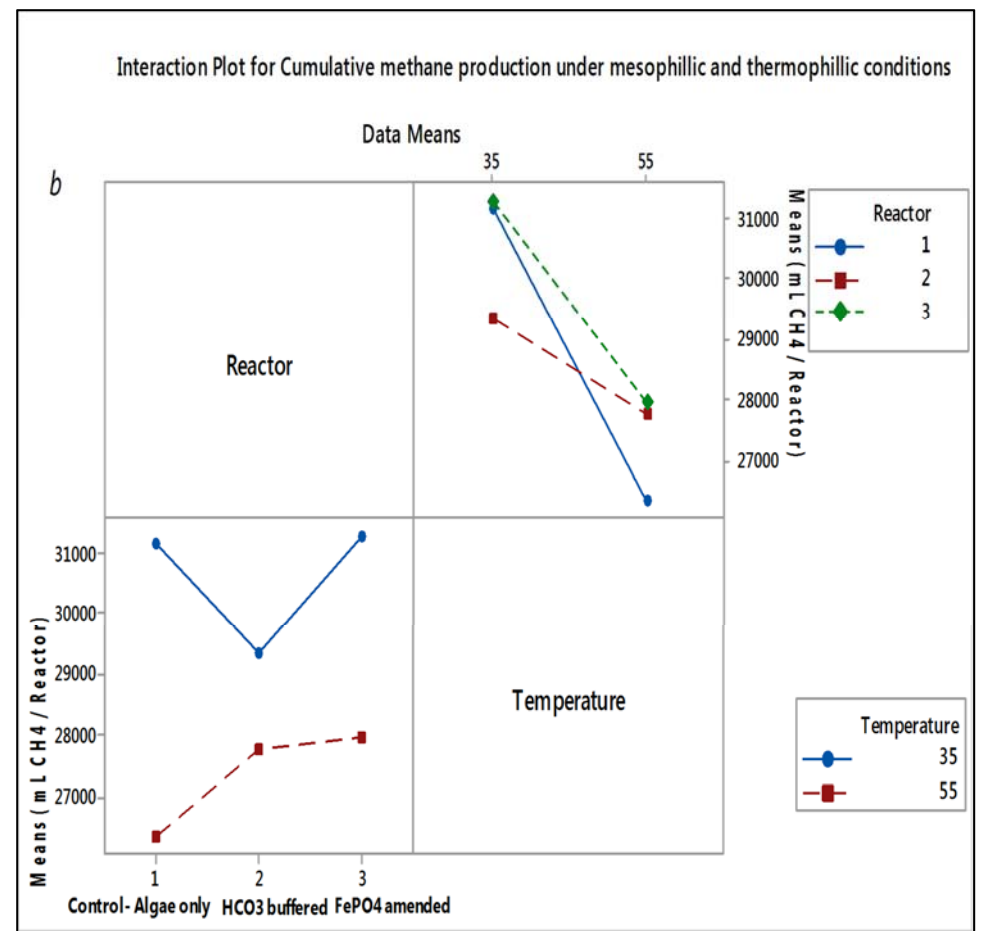
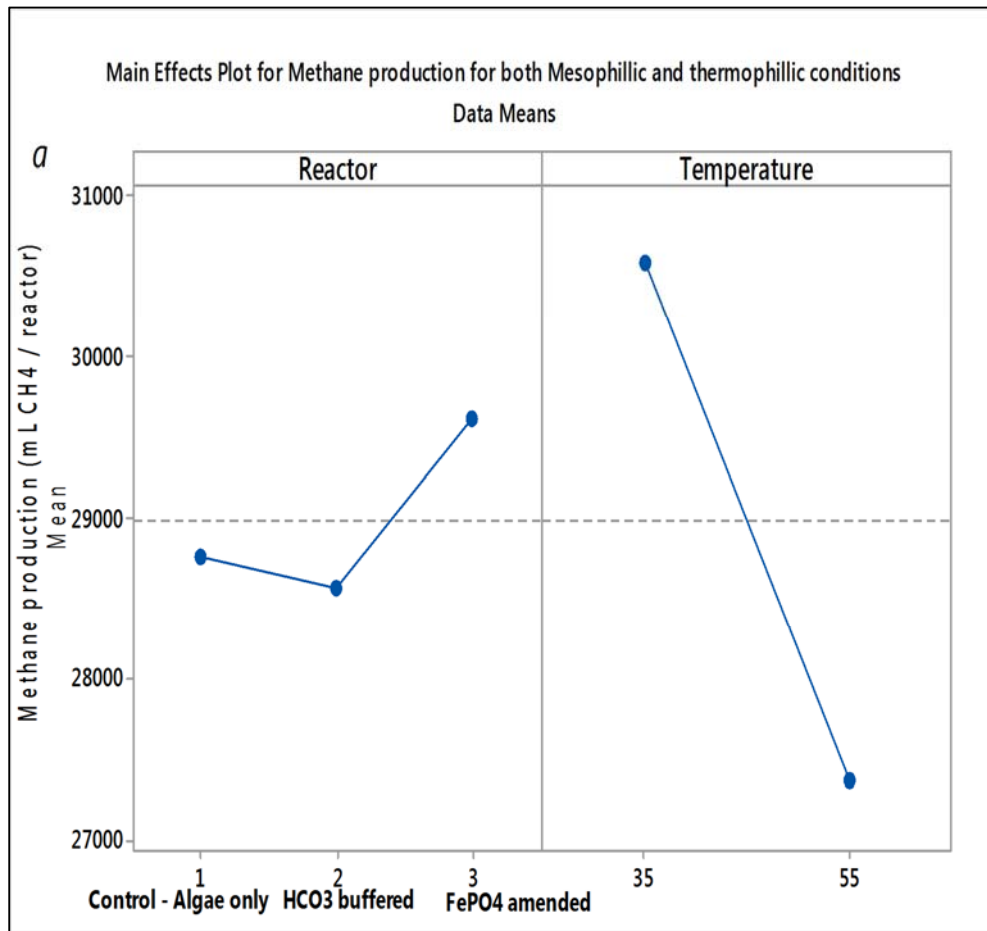


Figure 7-12 Main effects and interaction plot for cumulative CH<sub>4</sub> production for mesophilic (MR 1, 2, 3) and thermophilic (TR 1, 2, 3) reactors.

## 7.5 Conclusion

This laboratory-scale study investigated methane production and composition under mesophilic (35 °C) and thermophilic (55 °C) conditions using *Laminaria digitata* as the sole substrate (mono-digestion). The results show that, marine biomass from brown macroalgae can be used to generate renewable energy-rich biogas, methane (Gurung *et al.*, 2012) because the biomass contains high levels of fermentable sugars and low levels of recalcitrant lignin. However, considering the efficiency of seaweed digestion, certain critical factors, such as high sulphur and chloride content, were shown to affect the methane production rate, and were sometimes problematic for the digestion process. The addition of amendments as NaHCO<sub>3</sub> and FePO<sub>4</sub> was found to show no significant difference to enhance the methane production process, provide improved buffering capacity, and control chloride production in the system. Statistical analysis gave an insight into the variance and effect of temperature on the mean cumulative methane production at mesophilic and thermophilic temperatures, which was not significant. The long-term continuous mono-digestion of *L. digitata* generated similar methane yields of 350 ± 1.23 and 362 ± 0.98 (mL/g VS) but as OLR was increased, the methane yield differed significantly for both the mesophilic and thermophilic reactors. Chloride concentration of 40 g L<sup>-1</sup> did not significantly affect biogas production in all the reactors which can be attributed to acclimatisation of the digestion process to the marine algae.

## Chapter 8. Optimisation of methane production from macroalgae feedstock using regression analysis under mesophilic and thermophilic conditions

### *Abstract*

A multivariate technique was used to optimize methane production from anaerobic digestion of macroalgae under mesophilic and thermophilic conditions. To evaluate the effects and interaction of three reaction variables: COD, VFA, and ammonia on methane production, their data recorded in a time order were subjected to fit and multiple regression analysis, which generated a second order quadratic polynomial equation used to predict the optimised methane production. The ANOVA results showed the developed model for the mesophilic ( $p < 0.003$ ) and thermophilic ( $p < 0.000$ ) reactors are significant. Their  $R^2$  values of 0.97 and 0.99 suggest it was suitable for interpreting the experimental data set and adjusted  $R^2$  of (0.91 and 0.97) indicates good regression models. The interaction terms  $X_2^2$  (*vfAs*) and  $X_1 \times X_2$  (*COD, VFAs*) for mesophilic and thermophilic reactors, has a positive influence on methane production compared to other terms. The model predicted the optimal reactors conditions, derived as  $X_1$ : COD = 6.6 g L<sup>-1</sup>,  $X_2$ : VFAs = 2.8 g L<sup>-1</sup>,  $X_3$ : Ammonia = 1.3 g L<sup>-1</sup> for the mesophilic reactor, and  $X_1$ : COD = 6.7 g L<sup>-1</sup>,  $X_2$ : VFAs = 2.5 g L<sup>-1</sup>,  $X_3$ : Ammonia = 1.1 g L<sup>-1</sup> for the thermophilic reactor.



## 8.2 Materials and methods

### 8.2.1 *Experimental procedure*

In accordance with Section 7.2.1.

### 8.2.2 *Algae collection, pretreatment, and storage*

In accordance with section 7.2.2.

### 8.2.3 *Optimisation methodology used*

The optimisation process employed an approach using fit and multiple regression analysis by exploring the relationships between experimentally determined time series data set, as continuous predictors variables (independent), and an output, as a response variable (dependent), methane produced. The fit regression model was used to fit the data set (response against predictors variables) to generate an ANOVA equations and interactions terms while the multiple regression model was used to optimise methane production by evaluating the influence and interactive effects of the data set (predictor variables). The model employed, use the fit and multiple regression analysis tool in Minitab 17, to obtain the interactions between experimentally determined methane production and observed process parameters. The coefficient of determination ( $R^2$ ) value obtained expresses the adequacy and quality of the model fitness and the interactions terms were evaluated by a p-value of 95% ( $p > 0.05$ ).

The experimental data results (pH, COD, VFA, ammonia, and alkalinity) for both the mesophilic (MR 1) and thermophilic (TR 1) reactors in Section 7.4 were subjected to correction test using matrix plot (Appendix C), to check for correction among the variables known as multiple collinearities, which can cause instability in the model (McGeeney, 2015). The elimination method was then applied to remove correlated parameters using ( $p < 0.05$ ) as shown in Appendix D, for the mesophilic reactor (MR 1) and Appendix E, for thermophilic reactor (TR 1). The parameters COD, VFA and ammonia were then selected as adequate from the outcome of the correction results to fit the model (McGeeney, 2015).

The selected parameters, their data set which were recorded in a time order, data for the continuous digestion process for COD (Figure 7-9 B), VFA (Figure 7-4 A), and ammonia (Figure 7-7 B) shown in Section 7.4 were applied as continuous predictors variables, and fitted against the methane production values of Figure 7-1 A and B shown in Section 7.3 for the reactors MR 1 and TR 1, Table 8-1. These were then used to generate an ANOVA quadratic equation (McGeeney, 2015). The interactions terms in the equation were then used to describe and predict the optimised methane production from optimal predicted conditions of the reactors (MR 1 and TR 1) digestion processes from multiple regression analysis. Multiple regression has been previously used by several authors in various studies for methane optimisation (Sarkar *et al.*, 2014; Tedesco *et al.*, 2014; Kafle and Chen, 2016; Montingelli *et al.*, 2017), and for optimisation of anaerobic digestion of macroalgae (Montingelli *et al.*, 2015).

Table 8-1 Variables used in fit and multiple regression analysis.

Factor	Levels	Response ( Reactors MR 1 and TR 1)
Seaweed specie ( <i>L. digitata</i> )	COD VFA Ammonia	Methane production (mL / gVS <sub>added</sub> .reactor )

## 8.3 Results and Discussion

### 8.3.1 Model equation generation: Mesophilic temperature

For the mesophilic reactor MR 1, the result of the quadratic second –order multiple regression in form of ANOVA is shown in Table 8-2.

Table 8-2 Analysis of Variance (ANOVA) for Mesophilic reactor MR 1

Source	DF	Adj SS	Adj MS	F-Value	P-Value	Rank
Model	9	613793608	68199290	17.77	0.003	Significant
COD	1	27945565	27945565	7.28	0.043	Significant
VFA	1	8020199	8020199	2.09	0.208	5
Ammonia	1	17150329	17150329	4.47	0.088	4
COD*COD	1	19288051	19288051	5.03	0.075	3
VFA*VFA	1	3887407	3887407	1.01	0.360	7
Ammonia*Ammonia	1	2467699	2467699	0.64	0.459	9
COD*VFA	1	2503022	2503022	0.65	0.456	8
COD*Ammonia	1	22705161	22705161	5.92	0.059	2
VFA*Ammonia	1	4071449	4071449	1.06	0.350	6
Error	5	19190894	3838179			
Total	14	632984502				

$$R^2 = 0.9697; \text{Adj.}R^2 = 0.9151$$

The following quadratic equation and 2-way interactions terms was generated, Eqn 8-1:

$$\begin{aligned}
 CH_4 \text{ production (Y)} & & \text{Eqn 8-1} \\
 & = -96148 + 20.71 X_1 + 6.44 X_2 + 49.7 X_3 \\
 & - 0.000835 X_1^2 + 0.000497 X_2^2 - 0.00420 X_3^2 \\
 & - 0.000460 X_1 \times X_2 - 0.00641 X_1 \times X_3 \\
 & - 0.00268 X_2 \times X_3
 \end{aligned}$$

Where  $X_1$ : COD,  $X_2$ : VFA,  $X_3$ : ammonia.

Eqn 8-1, shows the methane production as predicted (Y), as a function of the observed experimental process parameters ( $X_1, X_2, X_3$ ). The relationship between Y and the X variables in the model is statistically significant with a  $p < 0.003$  (Table 8-2). The  $R^2$  value of 0.97 suggests it was appropriate for simulating the experimental data set (Mu *et al.*, 2007a). Since, the goal is to maximise  $CH_4$  production, using the model as a predictive tool, solution to optimal conditions obtained from the model building sequence of the interactive terms using multiple regression is;  $X_1$ : COD = 6.6 mg L<sup>-1</sup>,  $X_2$ : VFAs = 2.8 g L<sup>-1</sup>,  $X_3$ : Ammonia = 1.3 g L<sup>-1</sup>.

Using the coefficients in the Eqn 8-1 (Montingelli *et al.*, 2015), and the ranking in Table 8-2, the predicted impacts of the variables on methane production is:  $X_1 > (X_1 \times X_3) > (X_1 \times X_1) > X_3 > X_2 > (X_2 \times X_3) > (X_2 \times X_2) > (X_1 \times X_2) > (X_2 \times X_2)$ , with  $X_1$  (COD) concentration having the most impacts, followed by the interactions of COD and ammonia concentration ( $X_1 \times X_3$ ), with ammonia interactions ( $X_2 \times X_2$ ), being the least. The impact between COD and VFAs ( $X_1 \times X_2$ ), and ammonia interactions ( $X_2^2$ ) are of the same magnitude.

## Multiple Regression for CH<sub>4</sub> Yield Effects Report

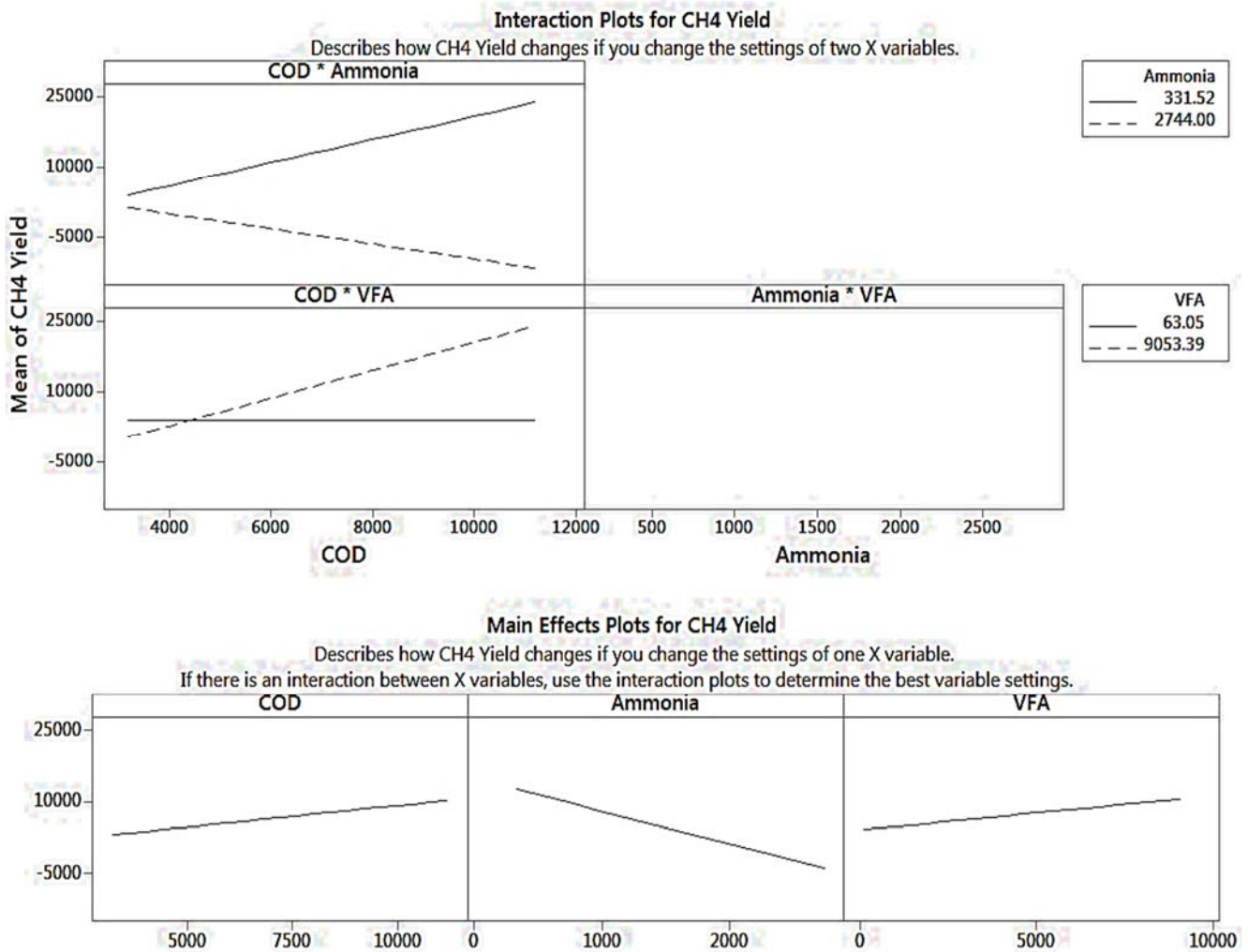


Figure 8-1 Main effects plot for mesophilic reactor (MR 1) on methane production.

The main effects and interactions among the various variables from multiple regression analysis are shown in Figure 8-1. It can be seen that for predictors  $X_1$  and  $X_2$ , they have a positive gradient, and as their value increases, the methane production increases up to a maximum concentration of  $9.1 \text{ g L}^{-1}$  for VFAs, with the COD concentration ( $11.2 \text{ g L}^{-1}$ ) having the most effect. The effect of ammonia shows a negative correlation, with low concentration having a higher impact on methane production. The interaction terms showed quite an interesting phenomenon, for optimal process conditions, ammonia concentration up to  $331 \text{ mg L}^{-1}$  will give an increasing methane production with increasing COD concentration up to  $4.0 - 10.0 \text{ g L}^{-1}$ , whereas with high ammonia concentration approximately  $\sim 2.7 \text{ g L}^{-1}$ , the reverse is the case,

producing low methane as the COD concentration increases. The relationship between COD and VFAs shows that optimal VFAs concentration up to  $9.1 \text{ g L}^{-1}$  will aid methane yield with increasing COD concentration. At a low VFA concentration of  $63.1 \text{ g L}^{-1}$ , the methane yield seems to be almost constant producing virtually very low methane as the COD concentration increases. This is not unexpected as VFAs are intermediates produced in AD process which serves as precursors for methane formation (Trisakti *et al.*, 2017), but higher concentration can cause inhibitory and detrimental effects which could lead to a slow production of biogas (Paritosh *et al.*, 2017).

### 8.3.2 Surface and contour plots analysis for mesophilic reactor

The results of the interaction effects on surface and contour plots for the mesophilic reactor MR 1 are shown in Figure 8-3. From the COD/ammonia interaction surface plot, better methane production will be obtained with a COD  $> 5.0 \text{ g L}^{-1}$ , and an ammonia concentration up to  $1.0 \text{ g L}^{-1}$ . Increase in COD concentration up to  $10.0 \text{ g L}^{-1}$  with a lower concentration of ammonia will eventually produce a low methane yield. Higher concentration of ammonia close to  $2.0 \text{ g L}^{-1}$  with increase in COD concentration will cause a sharp drop in the methane production with a negative response, indicating inhibition of the process.

The interaction between COD and VFAs has a very low impact on the process, and indicates that as VFAs concentration increases up to  $10.0 \text{ g L}^{-1}$ , COD  $< 5.0 \text{ g L}^{-1}$  will tend to give process optimal conditions, yielding high methane production. The impacts of the interactions of ammonia and VFAs has on the predicted outcome of methane production shows that as the ammonia concentration reduces to below  $1.0 \text{ g L}^{-1}$  with a corresponding increasing VFAs up to  $10.0 \text{ g L}^{-1}$  more methane production will be achieved.

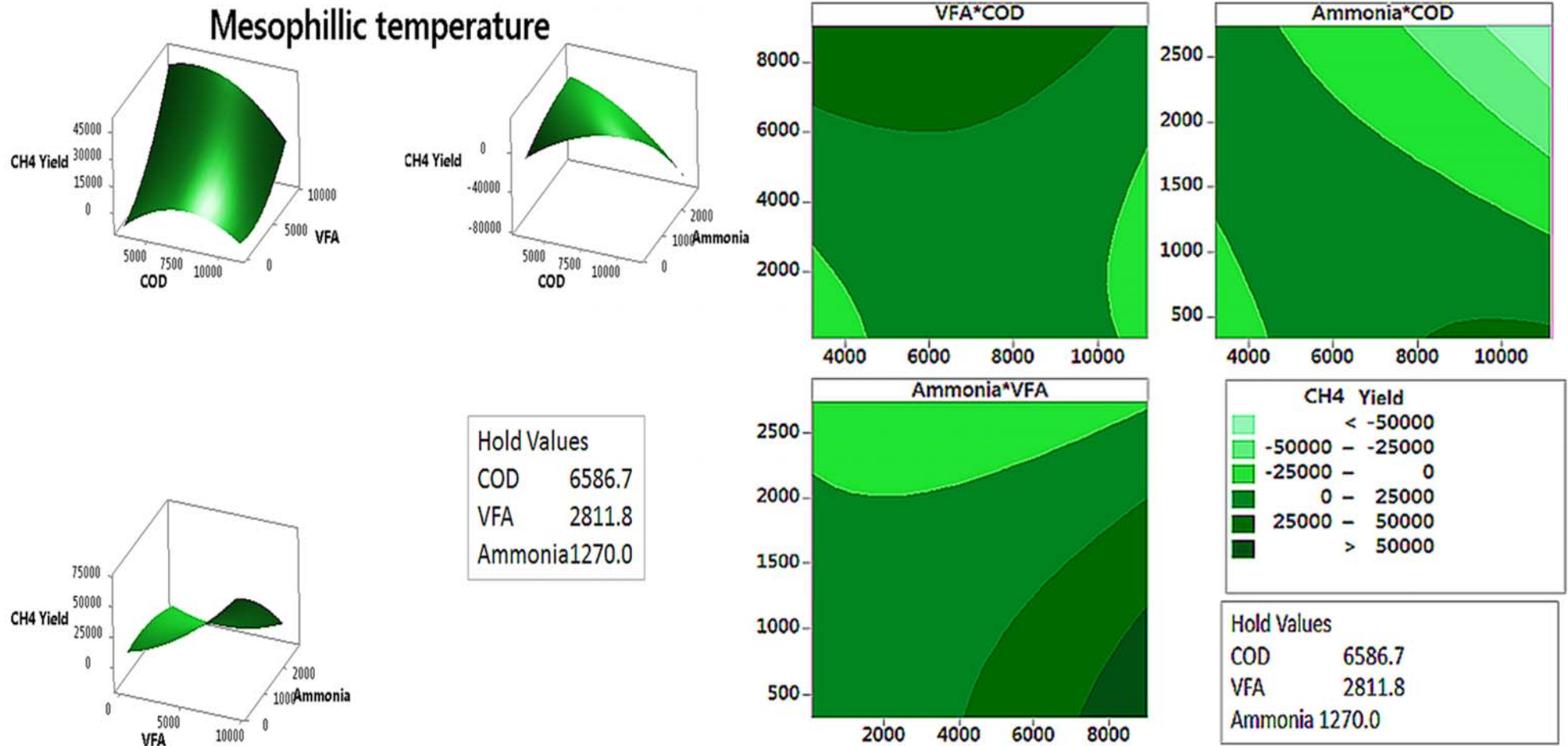


Figure 8-2 Surface and contour plots for mesophilic reactor (MR 1).

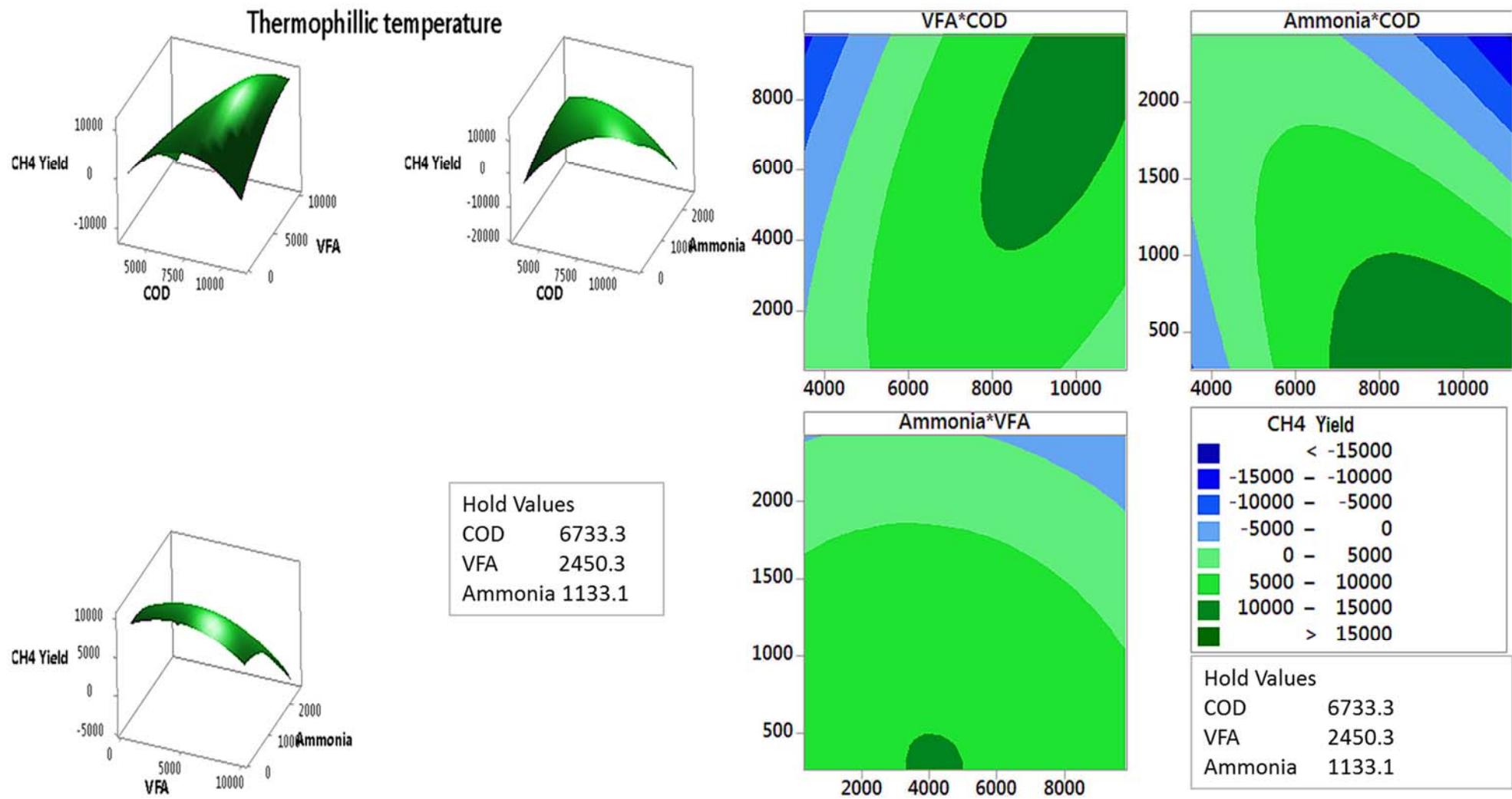


Figure 8-3 Surface and contour plots for thermophilic reactor (TR 1)

The results of the contour plots gave a more refined and clearer picture of the interactions of the process parameters, which is similar to the observations from the surface plot. From the curvature of the interactions between COD and ammonia shows that lower ammonia concentration below 500 mg L<sup>-1</sup> with an increasing COD concentration up to 10.0 g L<sup>-1</sup> will give a high yield up to 25 – 50 L CH<sub>4</sub> / reactor but within a very low margin. COD range 5.0 ≤ 10.0 g L<sup>-1</sup>, and ammonia 1.5 ≤ 2.5 g L<sup>-1</sup> regions will give a good range of optimal methane production. Process inhibition is likely to occur when the COD > 5.0 g L<sup>-1</sup> and ammonia concentration > 2.5 g L<sup>-1</sup> producing a negative response in the process. The curvature for the impact of COD and VFA interactions shows optimal conditions will be achieved at COD values 5.0 ≤ 9.0 g L<sup>-1</sup>, and VFAs of 6.0 ≤ 8.0 g L<sup>-1</sup> without any process instability during the continuous digestion of the macroalgae feedstock. The interaction effect between ammonia, and VFAs from the curvature results shows high methane production at VFAs up to 8.0 g L<sup>-1</sup> when the concentration of ammonia is < 1.0 g L<sup>-1</sup>. At ammonia concentration > 2.0 g L<sup>-1</sup> even with VFAs concentration in the range of 2.0 – 8.0 g L<sup>-1</sup> process inhibition is likely to occur with a negative response in methane production.

### 8.3.3 Model equation generation: Thermophilic temperature

For the thermophilic reactor TR 1, the result of the quadratic second-order multiple regression in form ANOVA is also shown in Table 8-3.

Table 8-3 Analysis of Variance (ANOVA) for Response surface model at thermophilic temperature (TR 1)

Source	DF	Adj SS	Adj MS	F-Value	P-Value	Rank
Model	9	494217822	54913091	60.47	0.000	Significant
COD	1	23442024	23442024	25.81	0.004	Significant 1
VFA	1	57117	57117	0.06	0.812	8
Ammonia	1	9391511	9391511	10.34	0.024	4
COD*COD	1	9925304	9925304	10.93	0.021	3
VFA*VFA	1	420622	420622	0.46	0.526	6
Ammonia*Ammonia	1	2453196	2453196	2.70	0.161	5
COD*VFA	1	334892	334892	0.37	0.570	7
COD*Ammonia	1	16716834	16716834	18.41	0.008	2
VFA*Ammonia	1	3696	3696	0.00	0.952	9
Error	5	4540550	908110			
Total	14	498758372				

R<sup>2</sup> = 0.9909; Adj.R<sup>2</sup> = 0.9745



The following quadratic equation and its 2-way interactions terms were generated, Eqn 8-2:

$$\begin{aligned}
 \text{CH}_4 \text{ production (Y)} & \qquad \qquad \qquad \text{Eqn 8-2} \\
 &= -33561 + 9.33 X_1 - 1.07 X_2 + 16.34 X_3 \\
 &\quad - 0.000471 X_1^2 - 0.000110 X_2^2 - 0.00209 X_3^2 \\
 &\quad + 0.000300 X_1 \times X_2 - 0.002185 X_1 \times X_3 \\
 &\quad - 0.00009 X_2 \times X_3
 \end{aligned}$$

Where  $X_1$ : COD,  $X_2$ : VFA,  $X_3$ : Ammonia.

The relationship between  $Y$  and the  $X$  variables in the model is statistically significant with a  $p < 0.000$ . The regression coefficient  $R^2$ , is 0.99, indicating a perfect fit for the model. Solution to optimal conditions from the model building sequence of the interactive terms using multiple regression gave;  $X_1$ : COD = 6.7 g L<sup>-1</sup>,  $X_2$ : VFAs = 2.5 g L<sup>-1</sup>,  $X_3$ : Ammonia = 1.1 g L<sup>-1</sup>.

From the coefficients in Eqn 8-2, and the ranking in Table 8-3, the predicted impacts of the variables on methane yield is:  $X_1 > (X_1 \times X_3) > X_1^2 > X_3 > X_3^2 > X_2^2 > (X_1 \times X_2) > X_2 > (X_2 \times X_3)$ , with  $X_1$  (COD) concentration having the most impacts. The impact between COD ( $X_1^2$ ) and ammonia ( $X_2$ ) interactions are of the same magnitude.

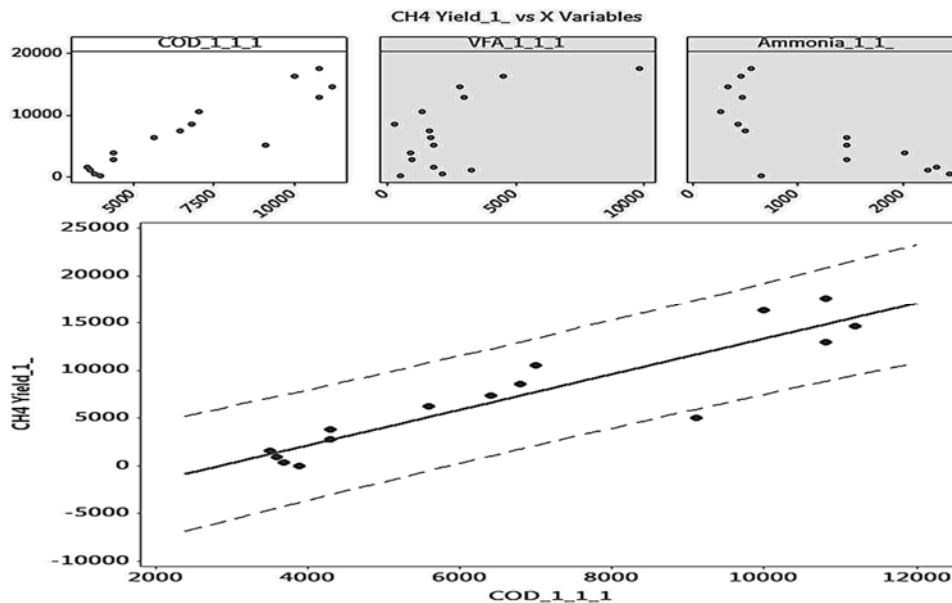


Figure 8-4 Main effects plot for thermophilic reactor (TR I) on methane yield

Using multiple regression analysis, the main effects and interactions among the various variable in the thermophilic reactor (TR 1) are shown in Figure 8-4. The predicted impacts of the variables on methane production are strongly related to the COD concentration but not strongly with the VFAs or ammonia concentrations, as shown, Figure 8-4. As the COD increases, the predicted methane production increases. The regression coefficient (0.834) suggests it was adequate to simulate the experimental data, hence, while the COD concentration play a critical in methane production, the other interactions among these parameters did not significantly affect the methane produced in the thermophilic reactor.

The results of the surface and contour plots for the thermophilic reactor TR 1 is also shown in Figure 8-3. The graphs show from the COD/ammonia interaction, the characteristics of the surface plot is similar to what was obtained in the mesophilic reactor MR 1 (Figure 8-2). Higher methane production can be obtained with a COD  $> 5.0 \text{ g L}^{-1}$  and an ammonia concentration up to  $1.0 \text{ g L}^{-1}$ . However, as the COD concentration continues to increase up to  $10.0 \text{ g L}^{-1}$  with a lower concentration of ammonia, the process will tend to produce less quantity of methane. At high concentration of ammonia close to  $2.0 \text{ g L}^{-1}$  a sharp drop in methane production will be obtained with a negative response, indicating inhibition of the process. This effect is more pronounce with the mesophilic reactor. At COD  $< 5.0 \text{ g L}^{-1}$ , with a reduction in ammonia concentration  $< 1.0 \text{ g L}^{-1}$ , a drop in methane production will also gradually occur.

The interaction between COD and VFAs indicates that as VFAs concentration increases up to  $10.0 \text{ g L}^{-1}$  an increase in COD up to  $7.0 \text{ g L}^{-1}$  will tend to give process optimal conditions, yielding high methane production. Below, this COD concentration  $< 5.0 \text{ g L}^{-1}$  or above  $7.0 \text{ g L}^{-1}$ , reduction in VFAs concentrations will tend to lower the methane production, and eventually lead to reactor failure, due to negative output in the gas yields. The impacts of the interaction of ammonia and VFAs on the predicted outcome of methane production, shows as the ammonia concentration reduces to below  $1.0 \text{ g L}^{-1}$  with a corresponding increase in VFAs up to  $10.0 \text{ g L}^{-1}$ , more methane production will be achieved, but is quickly inhibited, when the ammonia concentration increases up to  $2.0 \text{ g L}^{-1}$ , tending towards very low methane production.

From results of the contour plots, the curvature of the interactions between COD and ammonia shows lower ammonia concentration below 500 mg L<sup>-1</sup>, with an increasing COD  $\geq 8.0$  g L<sup>-1</sup> will give a high yield up to 15 L CH<sub>4</sub> / reactor. When the COD concentration is  $> 7.0$  g L<sup>-1</sup>, and ammonia  $> 1.5$  g L<sup>-1</sup> the process will tend to produce low quantity of methane, leading to an inhibited state where the gas production will be completely seized with a negative output. The curvature for the impact of COD and VFA interactions shows optimal conditions will be achieved at COD values between 5.0 – 9.0 g L<sup>-1</sup>, and VFAs concentrations of 6.0 – 8.0 g L<sup>-1</sup>, without any instability to the continuous digestion process. Below, COD  $< 4.0$  g L<sup>-1</sup> and VFAs  $> 2.0$  g L<sup>-1</sup>, process inhibition might start to set in, leading to low methane production and outright process failure.

The interaction effect between ammonia and VFAs from the curvature results shows optimal gas production at VFAs up to 4.0 g L<sup>-1</sup>, when the concentration of ammonia is  $< 500$  mg L<sup>-1</sup>. At ammonia concentration  $> 2.0$  g L<sup>-1</sup> with VFAs concentration in the range of 6.0 – 8.0 g L<sup>-1</sup>, process inhibition is likely to occur with a negative response in methane output. At ammonia concentration  $< 15.0$  g L<sup>-1</sup>, methane production will occur at VFAs concentration up 1.0 – 8.0 g L<sup>-1</sup>.

## 8.4 Conclusion

Brown seaweed, *L. digitata* spp. is regarded as a desirable feedstock for methane production (Montingelli *et al.*, 2015). Various methods of pre-treatment (Carlsson *et al.*, 2012; Pham *et al.*, 2013a), co-digestion (Vivekanand *et al.*, 2012) and process control monitoring has been used to improve methane production during anaerobic digestion of the feedstock. Optimisation techniques are normally used in anaerobic digestion process to propose areas where improvements could be made when commercialisation is considered (Ward *et al.*, 2008). Optimisation refers to as process performance improvement for maximum benefit, and traditionally applied by monitoring the influence of one factor at a time on an experimental response (Bezerra *et al.*, 2008). Experimental results; pH, COD, VFA, Ammonia, and alkalinity were subjected to correlation analysis using matrix plot, and identified correlated parameters were back eliminated, reducing the parameters to COD, VFA, and ammonia which were adequate to simulate the regression model in both the

mesophilic and thermophilic reactors. Surface and contour plots were to describe the optimisation process and to evaluate the effects and interaction of COD, VFA and ammonia on methane production. The model regression analysis generated a second-order quadratic equation in form of ANOVA in both the mesophilic and thermophilic reactors. Solution to optimal conditions from the equation for optimised methane production were derived as  $X_1$ : COD = 6.6 g L<sup>-1</sup>,  $X_2$ : VFAs = 2.8 g L<sup>-1</sup>,  $X_3$ : Ammonia = 1.3 g L<sup>-1</sup> for the mesophilic reactor and  $X_1$ : COD = 6.7 g L<sup>-1</sup>,  $X_2$ : VFAs = 2.5 g L<sup>-1</sup>,  $X_3$ : Ammonia = 1.1 g L<sup>-1</sup> for the thermophilic reactor.

## Chapter 9. Co-digestion of macroalgae with simulated food waste (SFW)

### *Abstract*

This study examined anaerobic digestion by mono and co-digestion of *Laminaria digitata* (LD) with a simulated food waste (SFW) in batch and continuous experiments. Different mix ratios of LD and SFW, namely,  $LD_{100:0\%}$ ,  $LD_{90:10\%}$ ,  $LD_{75:25\%}$ ,  $LD_{50:50\%}$  were assessed. Results from the batch reactors indicated the mono-digested feedstock  $LD_{100:0\%}$  produced the highest cumulative methane yield at  $207 \pm 0.07$  mL  $\text{CH}_4 \cdot \text{gVS}^{-1}$  after 34 days. The co-digested mix ratios in the batch test exhibited both antagonistic ( $LD_{90:10\%}$ ) and synergetic ( $LD_{75:25\%}$ ) effects. In the continuous reactors,  $LD_{90:10\%}$  was found to be optimal for the highest cumulative methane production ( $175 \pm 0.17$  L/ reactor) after 85 days and achieved a maximum biomethane efficiency factor BEF (0.93) at an OLR  $4 \text{ gVS} \cdot \text{L}^{-1} \cdot \text{d}^{-1}$ . The mono-digestion of  $LD_{100:0\%}$  in continuous reactors was characterized by the accumulation of high total volatile fatty acids (tVFA), reduced pH, and an increased FOS: TAC ratio as the OLR was increased, which led to reactor failure. Acclimatization to high salinity was evident in the co-digested reactor in the presence of low ammonia concentration at high loading rate. Co-digestion of *L. digitata* with SFW seem to cause the dilution of inhibitory components which was not evident in the mono-digested reactor.

## 9.1 Introduction

This chapter investigates the potential of anaerobic co-digestion of macroalgae and simulated food waste at different ratios. An introduction to the background material for this chapter has been given already in Section 2.14 and 2.15.

## 9.2 Materials and Methods

### 9.2.1 *Substrate, inoculum and chemical analysis*

The algae feedstock and chemical analysis used was prepared according to Section 3.1 and 3.2.

### 9.2.2 *Synthetic food waste preparation.*

The synthetic food waste components, Table 9-1 were selected and prepared according to methods reported by (Mata-Alvarez *et al.*, 1992) and (Li *et al.*, 2017). A representative sample, 50g of each food substrate was weighed, then first chopped into small sizes (1 – 5 cm) with a kitchen knife before maceration and blending for approximately 2 minutes in a kitchen blender (James martin ZX 865) to produce a homogenous mixture of approximately 0.5 - 1 mm typical size, Figure 9-1.

Table 9-1 Selected types of food substrates used.

Fruits (g)	Vegetables (g)	Meat and Fish waste (g)
Apples	Tomatoes	Pork/ham/bacon
Oranges	Onions	Beef
Peaches	Pepper	Fish / Shell fish
Melon	Potatoes	Lamb
Pears	Beans	Chicken
Kiwi	Carrots	Seafood
Water Melon	Cabbage	Sardines
Pineapples	Cucumber	Cod
Tangerines	Mushroom	Mussels
Strawberries	Broccoli	Embed
Grapes	Lettuce	others
Lemons		Cakes
		Rice



Figure 9-1 Homogenous prepared food feedstock for the digesters

### 9.2.3 Experimental procedure

The batch studies including gas measurement and kinetics was carried out according to Section 6.3.1 and 6.3.2. The continuous reactor study comprised a series of 4 identical, 1-litre continuous stirred tank reactors (CSTR) (R 1 - R 4) operating simultaneously for 85 days under different mix ratios ( $LD_{100\%}$ ,  $LD_{90:10\%}$ ,  $LD_{75:25\%}$ , and  $LD_{10:90\%}$ .) but with the same daily feeding regime, with a hydraulic residence time of 25 days. Details of reactor systems are given in Section 3.1.1. The different mix ratios used for both the batch and continuous reactors are given in Table 9-2.

Table 9-2 Ratios of LD with SFW used in both batch and continuous reactors study.

Ratios	Algae 100: 0 SFW	Algae 90: 10 SFW	Algae 75: 25 SFW	Algae 50: 50 SFW	Algae 25: 75 SFW	Algae 10: 90 SFW	Algae 0: 100 SFW
Batch test	$LD_{100\%}$	$LD_{90:10\%}$	$LD_{75:25\%}$	$LD_{50:50\%}$	$LD_{25:75\%}$	$LD_{10:90\%}$	$FW_{100\%}$
Continuous reactors	R 1 ( $LD_{100\%}$ )	R 2 ( $LD_{90:10\%}$ )	R 3 ( $LD_{75:25\%}$ )	R 4 ( $LD_{50:50\%}$ )			

The initial inoculum concentration was  $10 \text{ gVS.L}^{-1}$ , and was pre-acclimatised with macroalgae ( $1 \text{ gVS}$ ) feedstock daily for 9 days, then degassed for 3 – 5 days before the start of experiment. The organic loading rate OLR ( $\text{g VS.L}^{-1} \text{ d}^{-1}$ ) was increased stepwise after acclimatization from  $2 \text{ g VS.L}^{-1} \text{ d}^{-1}$  on day 1 of the experiment to  $3 \text{ g VS.L}^{-1} \text{ d}^{-1}$  on day 26, thereafter, to  $4 \text{ g VS.L}^{-1} \text{ d}^{-1}$  on day 39 and, finally to  $5 \text{ g VS.L}^{-1} \text{ d}^{-1}$  on day 55, till the end of the experiment. Biogas production rate was measured daily.

In the batch trials the antagonistic or synergistic effects of co-digestion on methane yields was evaluated based on the following equations (Labatut *et al.*, 2011; Cogan and Antizar-Ladislao, 2016);

$$Effects = CH_{4MY} - \sum CH_{4WMY} \quad \text{Eqn 9-1}$$

$$\sum CH_{4WMY} = LD_{CH_{4MY}} \times P.LD + FW_{CH_{4MY}} + P.FW \quad \text{Eqn 9-2}$$

Where;  $CH_{4MY}$  is experimental determined methane yield of substrates.

$CH_{4WMY}$  is weighted average methane yield.

$LD_{CH_{4MY}}$  is methane yield for *L. digitata*.

$FW_{CH_{4MY}}$  is methane yield for food waste,

$P$  is the percentage of the substrate in the mixture

If  $CH_{4MY} > CH_{4WMY}$  (*synergetic effect*) and  $CH_{4WMY} > CH_{4MY}$  (*antagonist effect*).

The biodegradability index (BI) is defined as ratio of  $BMP_{exp} / BMP_{theo}$  (Allen *et al.*, 2015; Tabassum *et al.*, 2017).

The % VS reduction efficiency is given as; (Wisconsin Department of Natural Resources, 1992)

$$\% efficiency = \% vs in - \% vs out \div [\% vs in - (\% vs in \times \% vs out)] \times 100 \quad \text{Eqn 9-3}$$

Where vs is the volatile solids.

## 9.3 Results and Discussion

### 9.3.1 Characterisation of macroalgae and food substrates

The chemical characteristics and elemental analysis of the macroalgae, food and inoculum samples used in the batch and continuous processes are shown in Table 9-3. Based on the elemental analysis results obtained in Table 9-3, and using methods as reported by (Membere *et al.*, 2015), the stoichiometric equation of the algal samples were evaluated and applied in the Buswell equation to calculate the theoretical methane yield and composition shown in Table 9-4, together with the experimental BMP yield, degradation constant (k) and biodegradability index (BI). Table 9-8 shows the trace element profile before, and at the end of, the experimental



reactor runs. From Table 9-3, the total solids (%TS) of the algae feedstock is 86.8% with the organic fraction (% VS) constituting about 61.2 % of the TS. This indicates the biomass feedstock comprises mainly organic matter, which is the predominant precursor to methane formation during AD (Lin *et al.*, 2009). The methane yield is affected by the type and composition of the marine biomass (Nkemka and Murto, 2010). The %TS of the co-substrate (FW) is 10.1% with a %VS content of 61.2 %. The C: N ratio for both the macroalgae (11.7: 1) and food substrate (11.0: 1) are quite similar as shown in Table 9-3 but are still under the ideal range of 15:1 - 30 :1 suggested as optimum conditions for AD operation (Wang *et al.*, 2012; Allen *et al.*, 2013b; Xu *et al.*, 2013). *L. digitata* has been reported as having a range between 10.9: 1 - 31.9: 1 (Adams *et al.*, 2011a).

Table 9-3 Characteristics of inoculum, macroalgae, and food used for batch and continuous processes.

Characteristics	Inoculum	Macroalgae	Food
% TS	25.6 (0.11)	86.8 (0.03)	10.1 (0.07)
% VS (% TS)	51.8 (0.08)	61.2 (0.07)	94.3 (0.12)
% Moisture	*	13.3 (0.10)	89.9 (0.08)
TKN (g/kg)	*	5.0 (0.18)	2.0 (0.22)
Ammonia (g/L)	1.76 (0.05)	1.68 (1.10)	0.42 (0.59)
Protein %TS (kg)	*	2.7 (0.18)	1.23 (0.45)
Alkalinity (g CaCO <sub>3</sub> /l)	10.5 (0.03)	*	*
TVFAs (g/L)	3.40 (0.16)	*	*
% C (% TS)		24.4 (0.36)	40.2 (0.30)
% H% (% TS)		5.0 (0.02)	7.1 (0.13)
% N% (% TS)		2.1 (0.44)	3.7 (0.85)
% S (%TS)		0.6 (0.15)	0.3 (0.02)
% O (% TS)		38.1 (0.02)	40.7 (0.15)
% Ash content		29.8 (0.01)	8.0 (0.18)
% TOC	7.4 (0.19)	29.5 (0.05)	5.3 (0.17)
C:N		11.7: 1 (0.21)	11.0: 1 (0.07)
C:S		40.7: 1 (0.11)	134: 1 (0.19)

\* Not assessed

In brown algae, the *Laminaria* genus has the capability to take up and store nitrate, with the nitrate content accounting for a major proportion of the TAN (Young *et al.*, 2007). Low C:N ratio < 15 can lead to elevated ammonia levels causing digestion instability (Allen *et al.*, 2015). The low C: N ratio obtained for the substrates indicates they might be problematic during the digestion process leading possibly to accumulation of toxic level of total ammonia nitrogen (TAN) (Miao *et al.*, 2014; Thorin

*et al.*, 2017), which inhibits methanogens (Allen *et al.*, 2014), and in turn decreases methane yields (Allen *et al.*, 2013b). Co-digestion of anaerobic feedstocks with food waste (FW) has been proposed as a way to improve the C: N ratio (Mata-Alvarez *et al.*, 2011), and help enhance stable process stability (Cogan and Antizar-Ladislao, 2016). Another important factor that should be considered during anaerobic digestion of macroalgae is the production of H<sub>2</sub>S. An elevated level of dissolved H<sub>2</sub>S is toxic and inhibits methanogens in AD process (Peu *et al.*, 2012). H<sub>2</sub>S is produced from sulphur reduction which is proportional to the amount of biodegradable carbon in a feedstock (Peu *et al.*, 2012). The C: S ratio in a feedstock has been used to predict the concentration of H<sub>2</sub>S in biogas (Peu *et al.*, 2012). A C: S ratio of 40 is recommended as minimum ratio for substrate below which accumulation of higher level of H<sub>2</sub>S is observed as shown in seaweed fermentation experiments (Allen *et al.*, 2014). From Table 9-3, the C: S of macroalgae is 41: 1 while the foods substrate is 134: 1. A range of 29 - 60.3: 1 has been reported for *L. digitata* (Adams *et al.*, 2011a). Co-digestion of both substrates is expected to improve the C: S and C: N ratios positively enhancing the digestion process synergistically.

Table 9-4 Design mix used in the batch and continuous operations with BMP results of experimental and theoretical methane (CH4) yields.

	<i>LD</i> <sub>100</sub> %	<i>LD</i> <sub>90:10</sub> %	<i>LD</i> <sub>75:25</sub> %	<i>LD</i> <sub>50:50</sub> %	<i>LD</i> <sub>25:75</sub> %	<i>LD</i> <sub>10:90</sub> %	<i>FW</i> <sub>100</sub> %
<i>C</i>	24.4 (0.11)	26.0 (0.10)	28.4 (0.09)	32.3 (0.04)	36.2 (0.15)	38.6 (0.13)	40.2 (0.30)
<i>H</i>	5.0 (0.09)	5.2 (0.13)	5.5 (0.11)	6.1 (0.07)	6.6 (0.04)	6.9 (0.10)	7.1 (0.14)
<i>N</i>	2.1 (0.08)	2.3 (0.11)	2.5 (0.04)	2.9 (0.06)	3.3 (0.07)	3.5 (0.19)	3.7 (0.08)
<i>O</i>	38.1 (0.11)	38.3 (0.22)	38.7 (0.10)	39.4 (0.13)	40.1 (0.09)	40.5 (0.05)	40.7 (0.63)
<i>S</i>	0.64 (0.60)	0.61 (0.09)	0.57 (0.15)	0.49 (0.19)	0.42 (0.17)	0.37 (0.08)	0.34 (0.02)
C:N	11.6 (0.21)	11.3 (0.27)	11.4 (0.31)	11.1 (0.22)	11.0 (0.35)	11.0 (0.51)	10.9 (0.07)
C:S	40.7 (0.11)	43.3 (0.16)	49.8 (0.18)	65.9 (0.10)	86.2 (0.41)	104.3 (0.16)	118.2 (0.19)
Theo (L CH <sub>4</sub> /kg VS)	290.6	305.9	327.1	358.9	338.6	401.4	389.5
Theo (L Biogas /kg VS)	403.3	420.2	443.5	478.5	508.6	525.5	535.7
Theo % CH <sub>4</sub>	44.7	45.6	46.7	48.3	49.4	50.0	50.4
BMP (L CH <sub>4</sub> /kg VS)	207	167	174.3	115.3	83.9	43.0	30.8
BMP (L Biogas /kg VS)	619	477	430	280	206	104	80
Bio-degradability Index (BI)	0.77	0.53	0.52	0.32	0.22	0.11	0.08
K (d <sup>-1</sup> )	0.25	0.33	0.26	0.29	0.21	0.33	0.24
R <sup>2</sup>	0.98	0.99	0.99	0.98	0.98	0.95	0.87
pH	7.6	7.54	7.59	7.59	7.6	7.54	7.5

Table 9-5 Kinetic analysis of the different mix ratio using the modified Gompertz equation

Parameter	Modified Gompertz						
	<i>LD</i> <sub>100 %</sub>	<i>LD</i> <sub>90:10 %</sub>	<i>LD</i> <sub>75:25 %</sub>	<i>LD</i> <sub>50:50 %</sub>	<i>LD</i> <sub>25:75 %</sub>	<i>LD</i> <sub>10:90 %</sub>	<i>FW</i> <sub>100 %</sub>
Biomethane potential from Gompertz Model (ml)- predicted	215.4	179.2	183	129.1	101.9	61.0	51.9
Max biomethane potential from Gompertz Model (ml)- predicted	228.4	187.6	194.4	138.5	110.2	66.6	56.9
R <sub>B</sub> (ml/day)	32.2	37.6	27.1	18.1	9.8	7.4	4.6
Lag phase ( $\lambda$ )	0.5	0.2	0.6	1.1	1.8	1.9	2.5
T <sub>50</sub> (days)	3	2	3	3	3	2	2
R <sup>2</sup>	0.96	0.97	0.96	0.94	0.94	0.9	0.91
RMSE	14.2	10.1	12.4	10.1	7.8	5.8	4.5

## 9.4 Batch studies: CH<sub>4</sub> production

The biomethane potential for each LD to SFW ratio was measured under controlled conditions (35 °C) for 34 days. The daily and cumulative biogas and methane production profiles are shown in Figure 9-2 and Figure 9-3. In assessing the data, biogas contribution from the inoculum was deducted from the cumulative yield. In all the reactors pre-acclimatization of inoculum with macroalgae resulted in negligible lag time in biogas production. The extent of cell wall degradation is known to be critical for the rate of conversion of algae biomass to biogas (Mussnug *et al.*, 2010). Pre-treatment has been shown to aid the decomposition of cells, enhancing methane productivity (Zhang *et al.*, 2016). Pre-treatment of the macroalgae samples by maceration ensured rapid digestibility of some macroalgae components with naturally large particle size by promoting cell-wall disruption (Membere *et al.*, 2015), since the macroalgae has a relatively thick cell walls (Zhang *et al.*, 2016) which are tough and protective making them particularly resistant to microbial attack, producing low methane yields during the AD process (Mussnug *et al.*, 2010).

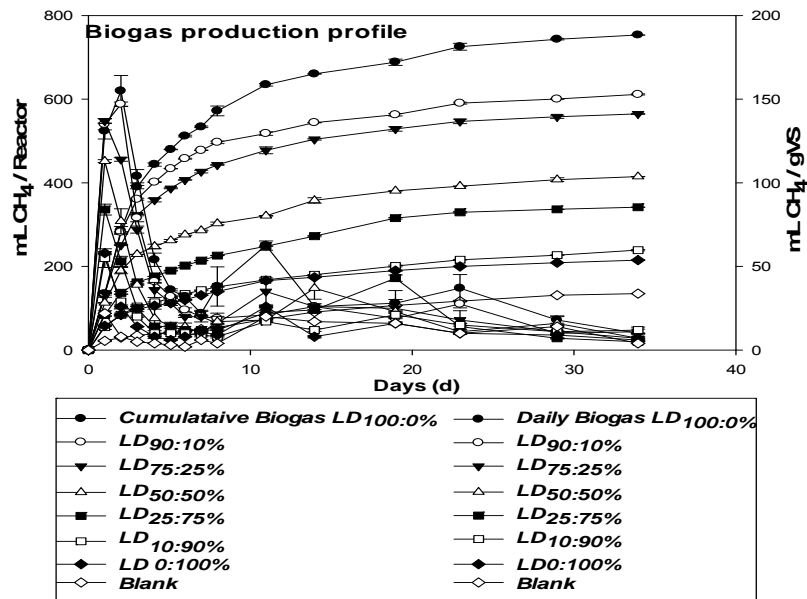


Figure 9-2 Cumulative and daily biogas profile for different design mix of algae to food ratio.

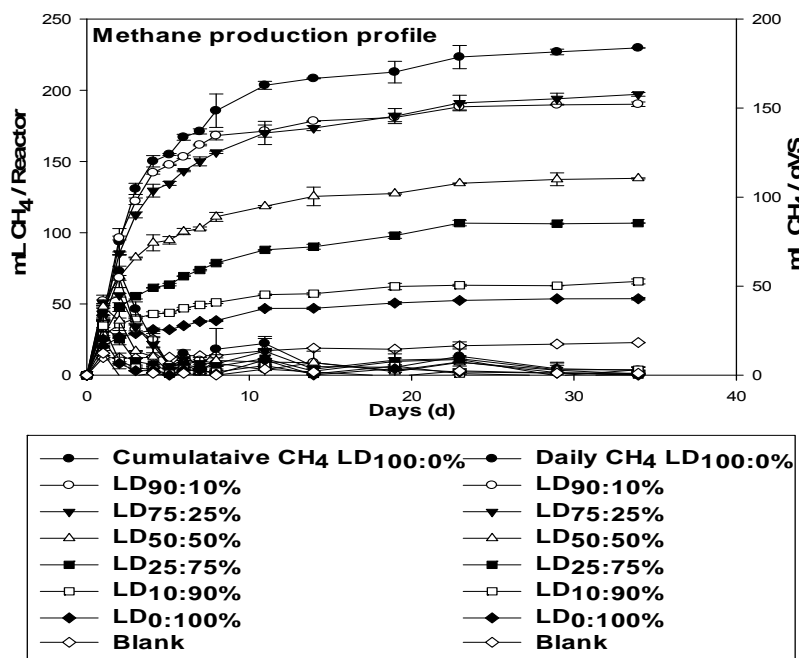


Figure 9-3 Cumulative and daily methane profile for different design mix of algae to food ratio.

Figure 9-3 shows the reactors with  $LD_{100\%}$  ratio produced the highest biogas and evaluated  $CH_4$  yield (MY) at  $619 \pm 0.99$  mL biogas  $g^{-1}$  VS and  $207 \pm 1.10$  mL  $CH_4$   $g$  VS $^{-1}$ , respectively. This was followed by  $LD_{90:10\%}$  ratio at  $477 \pm 0.07$  mL biogas  $g$  VS $^{-1}$  with a slightly lower  $CH_4$  yield of  $167 \pm 1.43$  mL  $CH_4$   $g$  VS $^{-1}$  compared to  $174 \pm 1.89$  mL  $CH_4$   $g$  VS $^{-1}$  obtained for the  $LD_{75:25\%}$  ratio as shown in Table 9-4. The results indicate that as the proportion of SFW ratio added to the mixture increases, the methane yield decreases with 100% SFW ( $LD_{0:100\%}$ ) producing the lowest BMP yield of 30 mL  $CH_4$   $g$  VS $^{-1}$ . This value is low compared to reported BMP values for FW of between 0.44 - 0.48 L  $CH_4$   $g$  VS $^{-1}$  (Zhang *et al.*, 2011), 0.18 L  $CH_4$   $g$  VS $^{-1}$  (Cogan and Antizar-Ladislao, 2016), 0.392 L  $CH_4$   $g$  VS $^{-1}$  (Yong *et al.*, 2015) and 0.18 to 0.73 L  $CH_4$   $g$  VS $^{-1}$  (Gunaseelan, 2004). This dissimilarity in the reported BMP values of FW can be ascribed as a function of the characteristics of the food waste mixture used, with respect to the %TS and %VS content, as the chemical composition of the FW mainly determines its degradability (Paritosh *et al.*, 2017). The approximate 3 fold difference in these BMP yields from FW could be due to the heterogeneous nature of the FW and variability in nutrient content between regions (Yong *et al.*, 2015). The characteristics of the FW used in this study was chosen in order to minimise operational disturbance of the process as single digestion of FW as shown to induce high VFA accumulation with low pH (Yao *et al.*, 2016), and an elevated ammonia /ammonium ion concentrations as a results of high protein content in most FW (Banks *et al.*, 2011). The BMP result for 100% *Laminaria* feedstock,  $LD_{100\%}$ , of 207 mL  $CH_4$   $g$  VS $^{-1}$  is in very close agreement with reported values of  $218 \pm 4.1$  mL  $CH_4$   $g$  VS $^{-1}$  (Allen *et al.*, 2015), 219 mL  $CH_4$   $g$  VS $^{-1}$  (Adams *et al.*, 2011b), and quite close to 184 mL  $CH_4$   $g$  VS $^{-1}$  (Vanegas and Bartlett, 2013a), but lower than 280 mL  $CH_4$   $g$  VS $^{-1}$  (Chynoweth *et al.*, 1993) for *L. digitata*. However, it is higher than 141 mL  $CH_4$   $g$  VS $^{-1}$  reported for *L. digitata* (Membere *et al.*, 2015), and 173 mL  $g$  VS $^{-1}$  for *Laminaria japonica* (Barbot *et al.*, 2015). Factors like seasonal variation, species types and geographical location influence the composition of the algae and its BMP yield (Adams *et al.*, 2011b). All the reactors achieved between 45 - 54%  $CO_2$  compositions in the biogas, except for the no substrate control reactor which had a maximum of 14% (data not shown). This agrees with 51 - 54%  $CO_2$  in biogas reported for co-digestion of macroalgae with FW (Cogan and Antizar-Ladislao, 2016).

#### 9.4.1 Kinetics of CH<sub>4</sub> production

The theoretical methane potential ( $BMP_{theo}$ ) for the different mix ratios calculated using the Buswell equation (Section 2.18.2) is given in Table 9-4. The  $BMP_{theo}$  values are higher than all experimental  $BMP_{exp}$  yields. As the proportion of FW increased the estimated  $BMP_{theo}$  increased due to the higher percentage of carbon and hydrogen in the co-substrate (FW). Although, the Buswell equation neglects cellular synthesis (Labatut *et al.*, 2011), which involves the maintenance and anabolism of the microbial community (Tabassum *et al.*, 2017), and does not account for around 12% of carbon which is consumed by the cell protoplasm (Cogan and Antizar-Ladislao, 2016), the  $BMP_{theo}$  yields will therefore be overestimated (Tabassum *et al.*, 2017). The difference between  $BMP_{theo}$  and  $BMP_{exp}$  ranges from 29% for  $LD_{100}$  %, to 92%  $FW_{100}$  %. The high variation and low yields obtained with higher proportions of FW could be due to the characteristics of the SFW feedstock, and its suitability for digestion, but could also have been due to the lack of pre-acclimatization of the microorganisms to the SFW substrate before the start of the experiment, and the pH of the inoculum used (7.5 - 7.6). Compared to other AD processes, reactors operating on FW commonly operate at high pH > 8 level (Cogan and Antizar-Ladislao, 2016) due to the breakdown of proteins producing elevated ammonia (Serna-Maza *et al.*, 2014). Table 9-4 shows the biodegradability index (BI) as described in Section 9.2.3. Since, the BI is an indication of the biomass degradation efficiency, high BI index corresponds to higher digestion efficiency (Tabassum *et al.*, 2017). The  $LD_{100}$  % had the highest BI of 0.67, followed by 0.53 for  $LD_{90:10}$  %, 0.52 for  $LD_{75:25}$  %, and  $SFW_{100}$  % having the lowest value of 0.08. Reported BI values range from 0.19 to 0.78 for different macroalgal species, 0.46 for *L. digitata* (Allen *et al.*, 2015), and 0.47 – 0.54 for co-digested macroalgae substrates (Allen *et al.*, 2014). Generally, the  $BMP_{exp}$  profiles in Figure 9-3 showed no sign of a prolonged lag phase, which can hamper the accuracy of a kinetic assessment (Allen *et al.*, 2015), except for the mix ratios with higher content of SFW (1.06 d for  $LD_{50:50}$  %, 1.77 d for  $LD_{25:75}$  %, 1.85 d for  $LD_{10:90}$  % and 2.52  $SFW_{100:0}$  %) compared to 6 days reported for digested brown algae (Gurung *et al.*, 2012).

The kinetic constant corresponds to the slope of the curve after the lag phase (López *et al.*, 2015). The almost immediate steep curve (without lag) for all the

mix ratios was an indication of fast degradation rates (k), and a result of using the *Laminaria*-acclimatised inoculum (Membere *et al.*, 2015). The hydrolysis rate constant was obtained by fitting the data set to the first order rate model using Matlab software. All the different mix ratios had a similar kinetic decay constants (k) ranging from 0.25 for  $LD_{100:0}$  %, 0.29 for  $LD_{50:50}$  %, 0.24  $FW_{100:0}$  %, and 0.33 being the highest for  $LD_{90:10}$  % and  $LD_{10:90}$  % shown in Table 9-4. A k value of 0.19 (Allen *et al.*, 2015), 0.33 - 0.36 (Membere *et al.*, 2015) has been reported previously for *L. digitata*, and a range of 0.12 - 0.17 for FW (Browne *et al.*, 2014).  $T_{50}$  is the substrate half-life, regarded as the time taken to produce half of the methane (Allen *et al.*, 2013a). The half-life ( $T_{50}$  days) for all the mix ratios was a maximum of 3 days with a  $T_{90}$  (90 % of methane production) of between 14 - 19 days, suggesting substrates were readily degradable, and a retention time of 20 - 30 days could be adequate and applied in a continuous digestion process. The modified Gompertz model also exhibited a good fit of the data set, with a correlation coefficient ( $R^2$ ) ranging from 0.90 - 0.96, and the RMSE value (which represents a statistical indicator to measure the model error (Deepanraj *et al.*, 2015a; Yang *et al.*, 2016) range from 4.5 - 14.2 mL CH<sub>4</sub> g VS<sup>-1</sup>.

#### 9.4.2 Antagonistic or synergistic effects of co-digestion on methane yields

One method of evaluating the potential performance of co-digesting substrates is to determine any synergistic or antagonistic effects. In the current study, these were evaluated based on a method by Cogan and Antizar-Ladislao (2016) and (Labatut *et al.*, 2011); given as the difference between an experimentally determined methane yield ( $CH_{4MY}$ ) and sum of a weighted average of the individual substrates, ( $CH_{4WMY}$ ), Eqn 9-1 and Eqn 9-2. Labatut *et al.* (2011) stated that a synergistic effect results if the CH<sub>4</sub> yield of the mix co-substrates is higher compared to the sum of their individual weighted average CH<sub>4</sub> yield, while an antagonistic effect results when the individual weighted average CH<sub>4</sub> yield is higher. Various factors have been attributed to causing either synergetic effects, such as trace elements, alkalinity, enzymes or other amendments not present in individual samples which can aid biodegradability of the substrate, or antagonist effects such as elevated VFA or pH inhibition and ammonia toxicity (Labatut *et al.*, 2011; Cogan and Antizar-Ladislao, 2016), and



rapid acidification of some component of the FW leading to methanogen inhibition (Rao and Baral, 2011). Table 9-6 is a summary of the effects obtained for the different mix ratios (*LD: SFW*) used. The results indicate that synergistic effects were observed for *LD*<sub>75:25</sub> % and *LD*<sub>25:75</sub> %. For instance, the weighted average methane yield (*CH*<sub>4</sub> *WMY*) for *LD*<sub>75:25</sub> % is 163 mL CH<sub>4</sub> g VS<sup>-1</sup> whereas the methane yield (*CH*<sub>4</sub> *MY*) of the co-digested substrate of *LD*<sub>75:25</sub> % is 174 mL CH<sub>4</sub> g VS<sup>-1</sup>. Since the positive differential in CH<sub>4</sub> yield is greater than the SD (1.24 mL CH<sub>4</sub> gVS<sup>-1</sup>), then the synergetic effects of co-digestion of *LD*<sub>75:25</sub> % brought about an increase of 6.5% in methane yield. However, the co-digestion of the mix ratios of *LD*<sub>90:10</sub> %, *LD*<sub>50:50</sub> % and *LD*<sub>10:90</sub> % produced antagonistic effects in methane yield. Comparing their *CH*<sub>4</sub> *WMY* and *CH*<sub>4</sub> *MY* values with the SD, shows a decrease of 13.4%, 3.1%, and 12.7% respectively in methane yield of the mixed substrate when juxtaposed with the weighted average of the individual substrate.

Table 9-6 Antagonistic or synergistic effects of co-digestion on methane yields.

LD: FW ratios	CH <sub>4</sub> <i>MY</i>	CH <sub>4</sub> <i>WMY</i>	Differential (CH <sub>4</sub> <i>MY</i> -CH <sub>4</sub> <i>WMY</i> )	% CH <sub>4</sub> increase	Effects
LD <sub>100</sub> %	207 ± 0.07	207	-	-	n/a
LD <sub>90:10</sub> %	167 ± 1.54	189.4	-22.4	-13.4	Antagonist
LD <sub>75:25</sub> %	174.3 ± 1.24	163.0	11.4	6.5	Synergistic
LD <sub>50:50</sub> %	115.3 ± 0.43	118.9	-3.6	-3.1	Antagonist
LD <sub>25:75</sub> %	83.9 ± 0.03	74.8	9.0	10.8	Synergistic
LD <sub>10:90</sub> %	43.0 ± 1.78	48.4	-5.5	-12.7	Antagonist
FW <sub>100</sub> %	30.8 ± 0.81	30.8	-	-	n/a

## 9.5 Continuous co-digestion studies

Figure 9-4 and Figure 9-5 outlines the daily and cumulative biogas production profile, % methane content and cumulative methane production of the different mix ratios in the continuous digestion studies. Figure 9-6 - Figure 9-9 shows the variation in the MY and the FOS: TAC ratio for tested OLRs for mono-digestion and co-digestion of the macroalgae and stimulated food waste. The daily biogas production for the mix ratios is shown in Figure 9-4 A. The biogas production increased as the OLR was increased from 2 gVS.L<sup>-1</sup>.d<sup>-1</sup> - 5 gVS.L<sup>-1</sup>.d<sup>-1</sup>, and achieved stable and steady production, except for the *LD*<sub>100%</sub> reactor which

showed signs of reactor instability from day 60 with reduction in biogas production at OLR 5 gVS L<sup>-1</sup> d<sup>-1</sup>. From Figure 9-4 B, the *LD*<sub>90:10%</sub> mix ratio produced the highest cumulative biogas production (175 ± 0.17 L / reactor) after 85 days of digestion followed by *LD*<sub>100%</sub> (173 ± 0.27 L / reactor) with the lowest value from *LD*<sub>50:50%</sub> (113 ± 0.07 L / reactor). The cumulative methane production, Figure 9-5 B, evaluated from the biogas production also followed similar trend with the highest for *LD*<sub>90:10%</sub> (42.77 ± 0.19 L / reactor, *LD*<sub>100%</sub> (40.068 ± 0.20 L / reactor) while the lowest was for *LD*<sub>50:50%</sub> (28.86 ± 0.09 L / reactor).

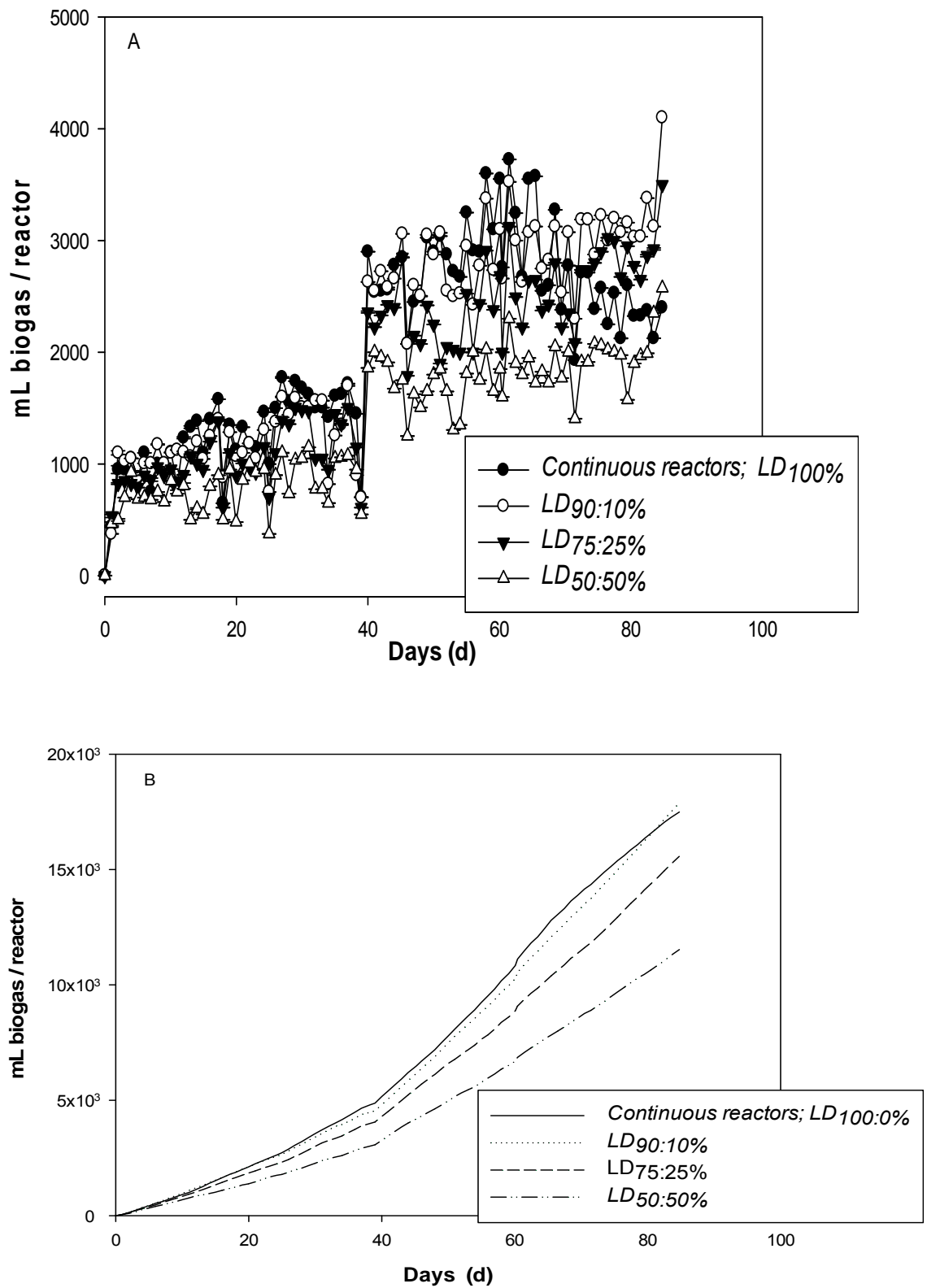


Figure 9-4 Continuous reactors, co-digestion mixtures; A), Daily biogas production; B), Cumulative biogas production.

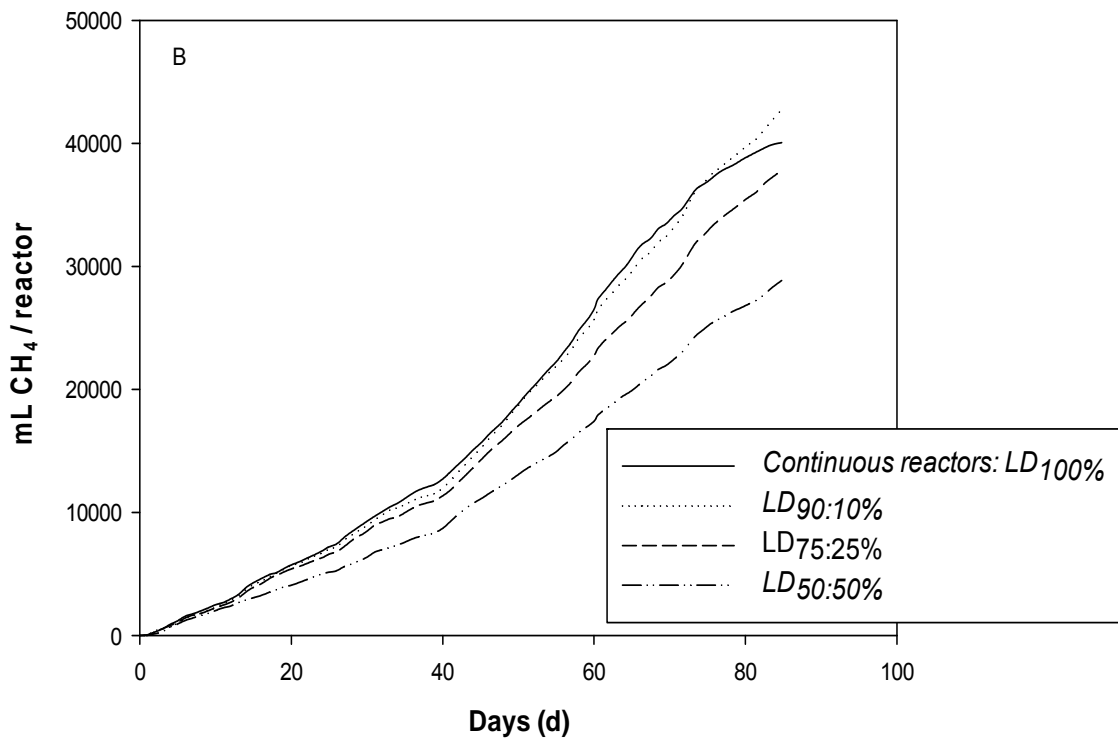
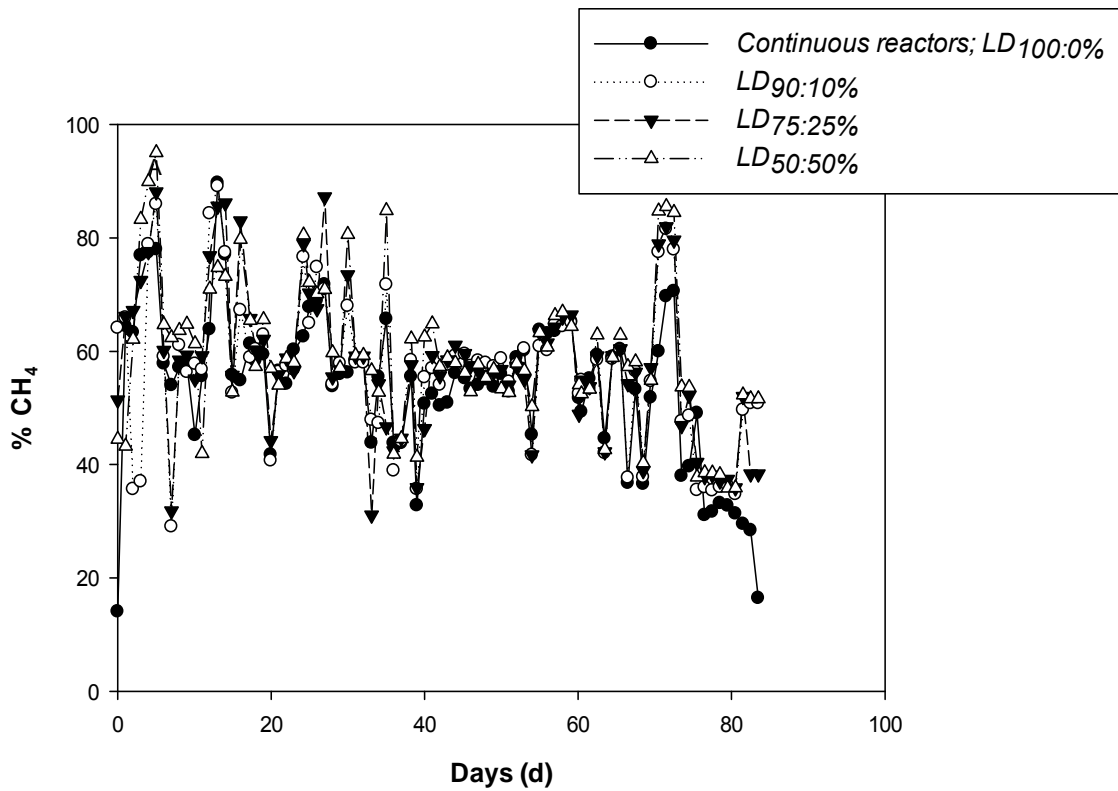


Figure 9-5 Continuous reactors, co-digestion mixtures; A), % Methane; B), Cumulative methane production.

The methane content of the biogas, Figure 9-5 A, increased from 14 % for LD<sub>100%</sub> and between 25% - 44% for the other reactors on commencement of the

digestion process after acclimatization and remained in a steady range of between 45% - 60% as the OLR was increased stepwise except for  $LD_{100\%}$  which showed signs of inhibition (unsteady state) at OLR 5 with a sharp reduction of the methane content from day 75 to around 38% and continued to drop to around 16% by the end of the experimental. Generally, from Figure 9-5 A, there was a reduction in biogas production in all the reactors on day 39 in the OLR 3 regime, as a result of an unplanned drop in temperature to about 22 °C (equipment failure) before recovering, this lead to a drop in pH in all reactors to around 7.0 - 7.1 and increase in tVFAs to between 15 g L<sup>-1</sup>- 20 g L<sup>-1</sup>, Figure 9-10 A and C.

#### 9.5.1 Assessment of mono-digestion of $LD_{100\%}$ (100% *L. digitata*, 0% food waste)

The variation in CH<sub>4</sub> production and methane yield (MY) for R 1 ( $LD_{100\%}$ ) with respect to increasing OLR from 2 - 5 gVS.L<sup>-1</sup>.d<sup>-1</sup> over the length of the experiment is shown in Figure 9-6. An assessment of the reactor process is given in Table 9-7. Generally, it is assumed for the continuous processes, stable digestion is achieved with a FOS: TAC ratio between 0.2 - 0.4 and when the MY value approaches the BMP value (Allen *et al.*, 2014). From Table 9-7, for  $LD_{100\%}$  the biomethane efficiency factor (BEF) was estimated as 0.70, 0.61, 0.72 and 0.57 for OLR 2, 3, 4 and 5, respectively. The drop in BEF to 0.47 at OLR 5 is due to the higher loading rate which resulted in corresponding accumulation of tVFAs, reaching a maximum value of 15.5 g L<sup>-1</sup> (Figure 9-10 C), a drop in pH to around 6.75 (Figure 9-10 A), and an increased FOS: TAC ratio to 2 at the end the run (Figure 9-6). Although the average pH observed at the different OLR is between 7.38 - 7.11, Table 9-7, then dropped to around 6.75 at OLR 5 indicating potential methanogen inhibition, which could lead to reactor failure if the process continued. Herrmann *et al.* (2016) have reported that at low pH, inhibition due to free ammonia decreases with methane production, but does not cease completely. This is reflected in the continued reduction of both CH<sub>4</sub> production and MY from day 75.

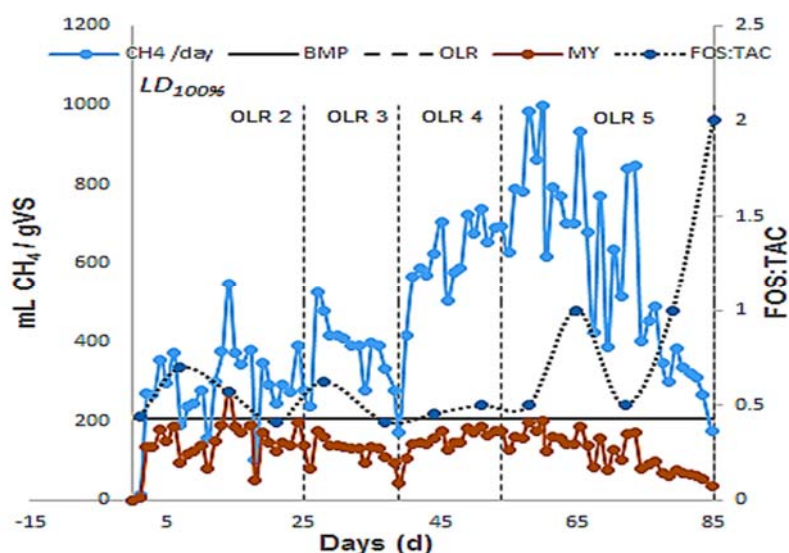


Figure 9-6 Assessment of continuous reactors, mono-digestion of *L. digitata* R1 ( $LD_{100\%}$ ): Variations in  $CH_4$  production, MY, BMP ( $mL CH_4/gVS$ ), and FOS:TAC ratio with increasing OLR ( $gVS.L^{-1}.d^{-1}$ ). Vertical dashed line indicates organic loading rate (OLR).

The average methane content in the biogas also dropped from 59% - 47% and to 16% by day 85 Figure 9-5 A. The C: N ratio was 11.69: 1 a figure that is regarded as non-optimal, as an unbalanced ratio (Section 9.3.1) has been identified as a limiting factor during AD of algal biomass (Fernández-Rodríguez *et al.*, 2014). AD process inhibition has been reported with C: N ratios less than 20: 1 (Sialve *et al.*, 2009b). A feedstock with low C: N ratio could result in elevated TAN and tVFAs accumulated in the digester (Zhong *et al.*, 2012). The TAN values observed showed a decreasing trend as the OLR is increased but are similar and within acceptable levels for 100% *L. digitata* (Tabassum *et al.*, 2016a). From Figure 9-11 A, the alkalinity value was found to increase from  $11.5 g.L^{-1}$  to  $16.0 g.L^{-1}$  by day 44 before dropping to around  $9.0 g.L^{-1}$  on day 85 while the COD and %TS increased from 13 -  $29 g L^{-1}$  and 31% - 66%, respectively. The cumulative sulphate ( $SO_4^{2-}$ ) concentration in the reactor showed slight increase ( $10.3 g.L^{-1}$  -  $11.5 g.L^{-1}$ ) as the OLR was increased between day 20 and 85, whereas the cumulative concentration of chloride showed progressive increases from  $5.0 g.L^{-1}$  on day 1 to around  $90 g.L^{-1}$  by the end of the experiment. In AD processes presence of high sodium ( $Na^+$ ) and  $SO_4^{2-}$  has been shown to inhibit methanogens (Lakaniemi *et al.*, 2011). The inhibitory level of chloride (salinity) is currently not clearly defined (Herrmann *et*

*al.*, 2016; Tabassum *et al.*, 2016a), but concentrations of Na<sup>+</sup> (100 - 200 mg L<sup>-1</sup>) is needed for growth of methanogens (Mottet *et al.*, 2014). Salinity concentration above 10 g kg<sup>-1</sup> are considered as highly saline (Tabassum *et al.*, 2016a) and can cause inhibition by increasing the osmotic pressure and dehydration of bacteria cells wall (Ward *et al.*, 2014), resulting in cell plasmolysis and cell death (Mottet *et al.*, 2014). Mottet *et al.* (2014) showed in their study that salinity levels of 15 g L<sup>-1</sup> can cause decrease in methane production with an acclimatised inoculum, and above 75 g L<sup>-1</sup> methanogenesis is severely hampered. The salinity concentration of up to 17 g L<sup>-1</sup> has been reported as not detrimental for mono-digestion of *L. digitata* (Tabassum *et al.*, 2016a), but has been shown to be inhibitory to methane production (Herrmann *et al.*, 2016) . From the results obtained in the current study, it could be concluded that mono-digestion of *L. digitata* would not be feasible at OLR above 5 gVS.L<sup>-1</sup>.d<sup>-1</sup>.

Table 9-7 Performance characteristics of the continuous reactors R1 - R4

OLR (kg VS / L / d)	BMP (L CH <sub>4</sub> / kg VS)	SMY (L CH <sub>4</sub> / kg VS)	Bio-methane efficiency factor (BEF)	CH <sub>4</sub> (%)	HRT (days)	FOS:TAC	TAN	PH
R 1 LD <sub>100%</sub> (100% L. Digitata, 0% Food waste)								
OLR 2	207 ± 0.07	143.99	0.86	59.86	25	0.42	1.43	7.38
OLR 3		126.55	0.76	57.2	13	0.51	1.12	7.36
OLR 4		148.36	0.89	52.97	16	0.47	1.07	7.34
OLR 5		118.96	0.71	47.87	31	1	0.7	7.11
R2 LD <sub>90:10%</sub> (90% L. Digitata, 10% Food waste)								
OLR 2	167 ± 1.54	139.97	0.84	61.11	25	0.41	1.53	7.41
OLR 3		112.56	0.67	58.18	13	0.40	1.17	7.38
OLR 4		155.86	0.93	56.17	16	0.48	1.24	7.41
OLR 5		138.09	0.83	52.3	31	0.39	0.89	7.46
R3 LD <sub>75:25%</sub> (75% L. Digitata, 25% Food waste)								
	174.31 ±							
OLR 2	1.24	132.05	0.76	65.48	25	0.28	1.42	7.39
OLR 3		108.35	0.62	57.52	13	0.4	1.09	7.37
OLR 4		127.48	0.73	55.18	16	0.43	0.98	7.38
OLR 5		121.49	0.70	52.99	31	0.43	0.74	7.42
R4 LD <sub>50:50%</sub> (50% L. Digitata, 50% Food waste)								
	115.31 ±							
OLR 2	0.43	102.86	0.89	67.43	25	0.28	1.23	7.37
OLR 3		79.02	0.69	62.29	13	0.33	1.11	7.29
OLR 4		98.90	0.85	56.51	16	0.38	0.91	7.31
OLR 5		92.28	0.80	55.21	31	0.66	0.79	7.32

### 9.5.2 Assessment of co-digestion of LD<sub>90:10%</sub> (90% *L. digitata*, 10% food waste)

The reactor R 2, LD<sub>90:10%</sub> contained the lowest feed level of food waste among the mixed ratio reactors (R 2 – R 4). In the batch trials (Section 9.4), certain mix ratios showed antagonistic effects on the digestion process (Table 9-6), which is contrary to what was observed during the continuous digestion process as the Reactor 2, with the LD<sub>90:10%</sub> feed, produced both the highest cumulative biogas and methane, Figure 9-5 B. This enhanced efficiency can be attributed to acclimatisation of the biomass microorganism to the food substrate, a process which was absent in the short duration batch tests. Synergy can be brought about by improved and balanced C: N ratio, which can be achieved by blending feedstock components, preventing ammonia inhibition, and by improving the bioavailability of nutrients (Herrmann *et al.*, 2016). Figure 9-7 shows the variation in CH<sub>4</sub> production together with the MY and FOS: TAC ratio. The co-digestion process operated steadily with increase the in methane yield as the



OLR was increased, with OLR 4 gVS.L<sup>-1</sup>.d<sup>-1</sup> producing the highest MY yield close to the BMP value, Table 9-7. Hence, the process can be said to be efficient in biogas production, and considered to be mainly operationally stable with signs of reactor instability within the first 10 days, since the FOS: TAC ratio fluctuated between 0.1 - 0.6 throughout duration of the experiment. Although stable digestion is characterized by FOS: TAC ratio of ≤ 0.4 (Mauky *et al.*, 2017), or given as ≤ 0.3 (Herrmann *et al.*, 2016), between 0.3 - 0.8 indicates risk of instability and ≥ 0.8 suggests instability (Schnürer *et al.*, 2017). This demonstrates better performance of LD<sub>90:10%</sub> compared to LD<sub>100%</sub> which failed at OLR 5 g VS L<sup>-1</sup> d<sup>-1</sup>.

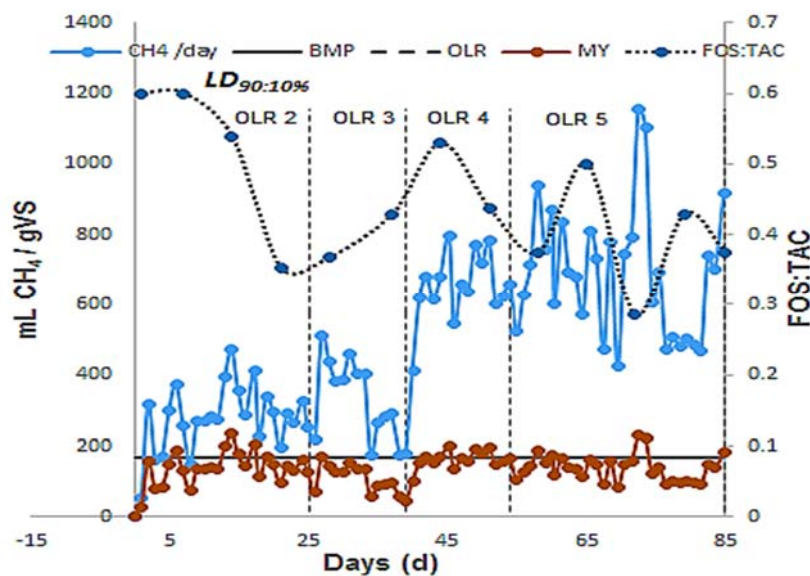


Figure 9-7 Assessment of continuous reactors, co-digestion of *L. digitata* R2 (LD<sub>90:10%</sub>): Variations in CH<sub>4</sub> production, MY, BMP (mL CH<sub>4</sub>/ gVS), and FOS: TAC ratio with increasing OLR (gVS.L<sup>-1</sup>.d<sup>-1</sup>). Vertical dashed line indicates organic loading rate (OLR).

The BEF obtained at OLR 2, OLR 3, OLR 4 and OLR 5 were 0.84, 0.67, 0.93, and 0.83 respectively, Table 9-7. At OLR 4, the average BEF value of 0.93 was close to maximum signifying an acclimatized inoculum and better performance of the reactor. The average pH was between 7.41 - 7.46 over the OLR tested, which probably resulted from ammonia buffering capacity of the reactor (Procházka *et al.*, 2012). High buffering results in less accumulation of tVFA at increased OLR (Alvarez and Lidén, 2008). The % methane content in the biogas reduced from 61% - 52% as the OLR was increased. The TAN values

(1.53 - 0.89 mg L<sup>-1</sup>) are below the threshold value (1.7 - 5 g L<sup>-1</sup>) for inhibition to occur (Zhong *et al.*, 2012). Analysis from Figure 9-13 A, as the OLR increases the %TS content increased from 29 - 56% while the COD concentration also increased from 8.7 g L<sup>-1</sup> - 18.2 g L<sup>-1</sup>. The %VS destruction varied from 51% - 38% representing 43.6% by the end of the run. The alkalinity value was between 12 g L<sup>-1</sup> - 11 g L<sup>-1</sup> while the maximum tvFA concentration obtained, was 6.6 g L<sup>-1</sup> on day 79 at an OLR of 5 gVS.L<sup>-1</sup>.d<sup>-1</sup> (Figure 9-10 C). At this concentration, reduction in methane yield was evident (Figure 9-7), but not sufficient to cause failure as the MY fluctuated from 221 mL CH<sub>4</sub> gVS<sup>-1</sup> on day 74 to 121 mL CH<sub>4</sub> gVS<sup>-1</sup> on day 75 and, continued in this trend before recovering, Figure 9-7. The performance of an AD process has a direct correlation with concentration of the tvFA (Zhong *et al.*, 2012) and above 6 g L<sup>-1</sup>, both biogas and the ratio of methane to CO<sub>2</sub> produced is greatly inhibited (Siegert and Banks, 2005). The cumulative trend of SO<sub>4</sub><sup>2-</sup> and chloride concentration increased from 0.5 - 82 g L<sup>-1</sup> and 5 - 69 g L<sup>-1</sup> respectively.

### 9.5.3 Assessment of co-digestion of LD<sub>75:25</sub> % (75% *L. digitata*, 25% food waste)

The continuous fermentation data of R 3 LD<sub>75:25</sub> % are shown in Figure 9-8 and Table 9-7. The methane production rate fluctuated from an average value of 132 mL CH<sub>4</sub> gVS<sup>-1</sup>.d<sup>-1</sup> to 122 mL CH<sub>4</sub> gVS<sup>-1</sup>.d<sup>-1</sup> which coincided with an increase in OLR from 2 g VS.L<sup>-1</sup>.d<sup>-1</sup> - 5 g VS.L<sup>-1</sup>.d<sup>-1</sup> within 85 days of operation. From the batch trial (Section 9.4) a BMP of 174 ± 1.24 mL CH<sub>4</sub> gVS<sup>-1</sup> was obtained for LD<sub>75:25</sub> % compared to 163 mL CH<sub>4</sub> gVS<sup>-1</sup> for the weighted average methane yield (CH<sub>4</sub> WMY), giving an increase of 6.5% in CH<sub>4</sub> yield which had a synergetic effect from the co-digestion mix. From Figure 9-4 B the cumulative biogas production for LD<sub>75:25</sub> % is 156 ± 9.20 L biogas / reactor while from Figure 9-5 C the cumulative methane production is 38 ± 1.72 L CH<sub>4</sub> / reactor, these are less by 11% and 5.6% to the cumulative biogas and methane produced for LD<sub>100</sub> % with no co-digestion mix. Comparing LD<sub>75:25</sub> % to LD<sub>100</sub> % it is evident that it performed better as the reactor continued to produce biogas after day 75 with no sign of instability and reactor failure as experienced in LD<sub>100</sub> %. From Table 9-8, the BEF are 0.76, 0.62, 0.73 and 0.70 for OLR 2, OLR 3, OLR 4 and OLR 5 respectively. The average pH ranged between 7.39 - 7.42. The FOS: TAC ratio

fluctuated slightly within 0.28 - 0.43 as the OLR was increased, indicating the good stability of the process.

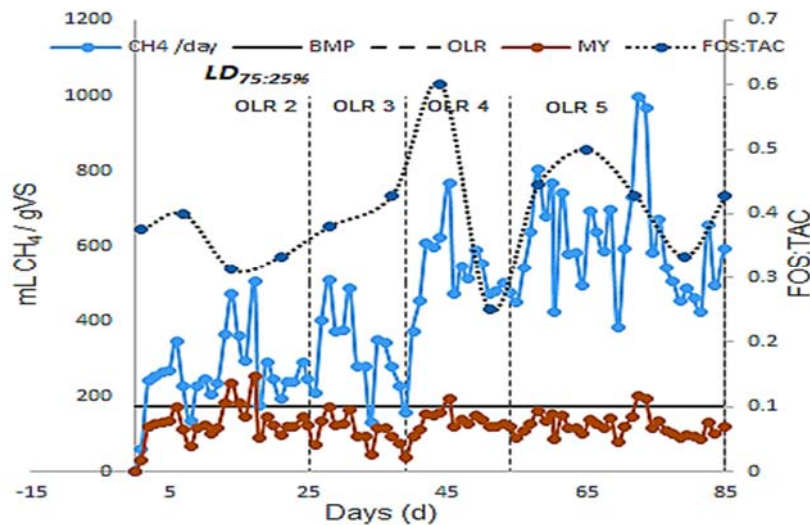


Figure 9-8 Assessment of continuous reactors, co-digestion of *L. digitata* R3 ( $LD_{75:25\%}$ ): Variations in  $CH_4$  production, MY, BMP ( $mL CH_4/gVS$ ), and FOS:TAC ratio with increasing OLR ( $gVS.L^{-1}.d^{-1}$ ). Vertical dashed line indicates organic loading rate (OLR).

The average % methane concentration of the biogas in  $LD_{75:25\%}$  reactor was highest (66%) at OLR 2 and lowest (53%) at OLR 5. This decreasing trend was reflected in average MY value of  $132 mL CH_4 gVS^{-1}$ ,  $128 mL CH_4 gVS^{-1}$  and  $122 mL CH_4 gVS^{-1}$  for OLR 2, OLR 4 and OLR 5, respectively except OLR 3 with  $108 mL CH_4 gVS^{-1}$  which experienced drop in temperature from  $35\text{ }^\circ C$  to around  $22\text{ }^\circ C$  on day 39, hence the average low MY obtained for OLR 3. The TAN value ranged from  $1.42 g.L^{-1}$  –  $0.74 g.L^{-1}$  as the OLR increased from 2 - 5  $gVS L^{-1}.d^{-1}$ . Analysis of Figure 9-13 E, both the %TS (30% - 44%) and COD ( $12.0 g.L^{-1}$  -  $17.2 g.L^{-1}$ ) concentration increased with increases in OLR from 2  $gVS.L^{-1}.d^{-1}$  - 5  $gVS.L^{-1}.d^{-1}$ . The %VS destruction was from 53% at OLR 2 to 35% at OLR 5, representing about 50% VS reduction efficiency which entered the reactor as feed. For all OLR, the alkalinity value was between  $11 g.L^{-1}$  –  $10 g.L^{-1}$ . The cumulative trend of chloride and  $SO_4^{2-}$  concentration increased from  $4.5 g L^{-1}$  –  $75 g L^{-1}$  and  $0.5 g L^{-1}$  –  $4.7 g L^{-1}$  respectively, while the tVFA ranged from  $2.6 g.L^{-1}$  at OLR 2 to  $2.3 g.L^{-1}$  at OLR 5 with a maximum FOS:TAC ratio of 0.43 at OLR 5 indicating a stable digestion process.

### 9.5.4 Assessment of co-digestion of $LD_{50:50\%}$ (50% *L. digitata*, 50% food waste)

This mix  $LD_{50:50\%}$  reactor (R 4) consists of equal amount of *L. digitata* and food waste. In the continues study, the cumulative biogas and methane production were  $113 \pm 2.43$  L biogas/reactor and  $29 \pm 2.01$  LCH<sub>4</sub> / reactor respectively, Figure 9-4 B and Figure 9-5 C. The MY was 103 mL CH<sub>4</sub> gVS<sup>-1</sup>, 79 mL CH<sub>4</sub> gVS<sup>-1</sup>, 99 mL CH<sub>4</sub> gVS<sup>-1</sup>, 93 mL CH<sub>4</sub> gVS<sup>-1</sup> at OLR 2, OLR 3, OLR 4 and OLR 5, respectively (Figure 9-9). The BMP value obtained (Section 9.4) was  $115 \pm 0.43$  mL CH<sub>4</sub> gVS<sup>-1</sup> which was less than  $119$  mL CH<sub>4</sub> gVS<sup>-1</sup> obtained for the weighted average methane yield (CH<sub>4</sub> WMY) (Table 9-6) by -3.11%, indicating an antagonistic effect on the co-digestion mix during the batch trials (Section 9.4). Comparing  $LD_{50:50\%}$  to the mono-digested reactor ( $LD_{100\%}$ ), at the OLR 5 regime it continued to produce gas with no sign of the instability that was experienced in  $LD_{100\%}$ , hence the antagonistic effect experienced in the batch test did not replicate itself during the continuous trials. Nutrients supplemented from the food waste and better acclimatization to the food substrate by the microbial community at the higher OLR could have played a role in the high stability of the reactor R4.

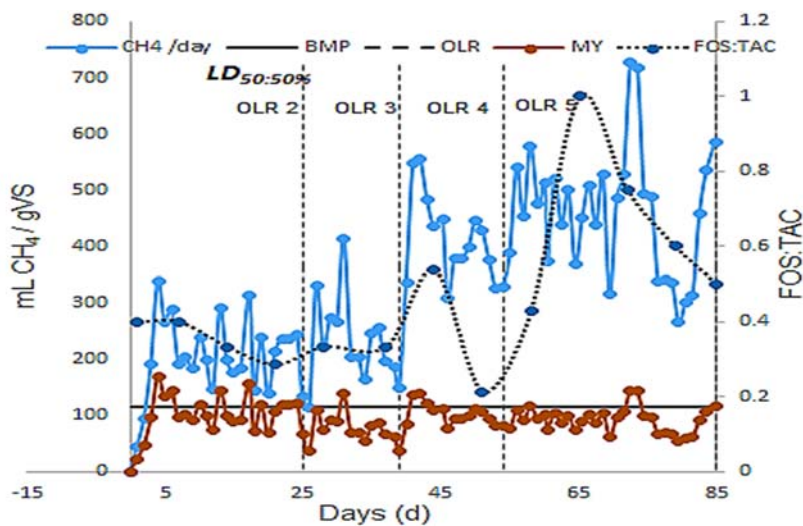


Figure 9-9 Assessment of continuous reactors, co-digestion of *L. digitata* R4 ( $LD_{50:50\%}$ ): Variations in CH<sub>4</sub> production, MY, BMP (mL CH<sub>4</sub>/ gVS), and FOS: TAC ratio with increasing OLR (gVS.L<sup>-1</sup>.d<sup>-1</sup>). Vertical dashed line indicates organic loading rate (OLR).

The % methane composition in the biogas continued to decline slightly as the OLR was increased stepwise, from 67% at OLR 2, 62% at OLR 3, 56% at OLR 4 and to 55% at OLR 5, Table 9-7. The BEF was 0.89 at the initial OLR 2 after 25 days within the first HRT, but dropped to 0.69 at OLR 3 and improved again to 0.85 at OLR 4. Similar stable pH trend (7.37 - 7.32) was observed compared to other co-digested mix ratios (*LD*<sub>90:10%</sub>, and *LD*<sub>75:25%</sub>) with the exception of *LD*<sub>100%</sub> (7.38 - 6.75). The FOS: TAC ratio increased from 0.4 – 1.0 indicating reactor imbalance at OLR 5 feeding regime, but declined to 0.5 before the end of the 3.5 HRT period. This normalised the instability in the reactor which was reflected by the recovery and continuous production of biogas from day 75, Figure 9-9. There was no tVFA accumulation which averaged between 2.6 g.L<sup>-1</sup> - 2.3 g.L<sup>-1</sup>. The TAN also followed similar decreasing trend to other co-digested mix ratios (1.2 g L<sup>-1</sup>- 0.8 g L<sup>-1</sup>) as the OLR was increased. The %TS had a stable operating range from 27% - 31% with a %VS reduction from 52% - 39% representing about 41% of VS reduction efficiency of R 4. The COD concentration increased slightly from 14 g.L<sup>-1</sup> to 16 g.L<sup>-1</sup> while the alkalinity content of the reactor remains stable between 11 g.L<sup>-1</sup> - 9 g.L<sup>-1</sup>. As the OLR is increased from OLR 2 - OLR 5, the cumulative trend of SO<sub>4</sub><sup>2-</sup> concentration showed an increase from 0.4 g.L<sup>-1</sup> to 3.9 g.L<sup>-1</sup> while that of chloride increased from 4.2 g.L<sup>-1</sup> to 54 g.L<sup>-1</sup>, respectively.

#### 9.5.5 Comparison of *LD*<sub>100%</sub> with other *LD*<sub>LD%:FW%</sub> mix reactors

##### *Process operational parameters*

##### *pH, VFA, and FOS: TAC ratio*

The pH of all the co-digested mix reactors (*LD*<sub>90:10%</sub>, *LD*<sub>75:25%</sub>, and *LD*<sub>50:50%</sub>) fluctuated between 7.60 - 7.20 compared to the mono-digested reactor (*LD*<sub>100%</sub>) which started to drop sharply from 7.10 on day 78 to 6.65 by day 85, Figure 9-10 A. pH is regarded as one of the critical indicators for digester performance (Wang *et al.*, 2012), because it promotes favorable condition for growth of microorganisms and overall performance of the digesters (Ravi *et al.*, 2018). Optimum pH range has been suggested as between 6.8 – 7.2 for methanogens (Turovskii, 2006). The VFA produced in the acidogenesis phase can induce a drop in pH (Turovskii, 2006). The *LD*<sub>100%</sub> reactor produced the highest tVFA

which increased from 2.7 g L<sup>-1</sup>- 15.5 g L<sup>-1</sup> as the OLR increased from 2 gVS. L<sup>-1</sup>.d<sup>-1</sup> – 5 gVS. L<sup>-1</sup>.d<sup>-1</sup>, this was followed by *LD*<sub>90:10%</sub> (3.3 g L<sup>-1</sup> – 6.6 g L<sup>-1</sup>), *LD*<sub>75:25%</sub> (2.6 g L<sup>-1</sup> – 2.3 g L<sup>-1</sup>), and the lowest being *LD*<sub>50:50%</sub> (1.7 g L<sup>-1</sup> – 2.21 g L<sup>-1</sup>).

Accumulated levels of undissociated VFA cause detrimental effects on the AD process by penetrating the cell membranes damaging intracellular macromolecules (Cotter and Hill, 2003). The VFA range of 2.0 g L<sup>-1</sup>– 3.0 g L<sup>-1</sup> is regarded as the optimum required for metabolic activity (Paritosh *et al.*, 2017). At OLR 5 gVS. L<sup>-1</sup>.d<sup>-1</sup>, for *LD*<sub>100%</sub> a maximum VFA concentration of 15.5 g L<sup>-1</sup> was seen leading to reactor failure while at the maximum concentration of 6.63 g L<sup>-1</sup> for *LD*<sub>90:10%</sub> the effect was low gas production at the same loading rate. As can be seen from Figure 9-10 C on day 39 there was an increase in VFAs concentration in all the reactors to between (14 g L<sup>-1</sup> - 21 g L<sup>-1</sup>) with a corresponding decrease in pH (to 7.0 - 7.1), this was due to a drop in temperature of the reactors to around 22 °C, caused by equipment failure, before recovering again. The temperature of the reactors plays a critical role for the AD microorganisms as the conversion of acetic acid to methane is highly temperature dependent (Paritosh *et al.*, 2017). The FOS: TAC ratio showed the largest increase for *LD*<sub>100%</sub>, reaching up to 2 at OLR 5. The other co-digested reactors were all within the stable digestion ratio of 0.2 - 0.5, except for *LD*<sub>50:50%</sub> which showed signs of instability at FOS: TAC ratio of 1 at OLR 5, before normalising.

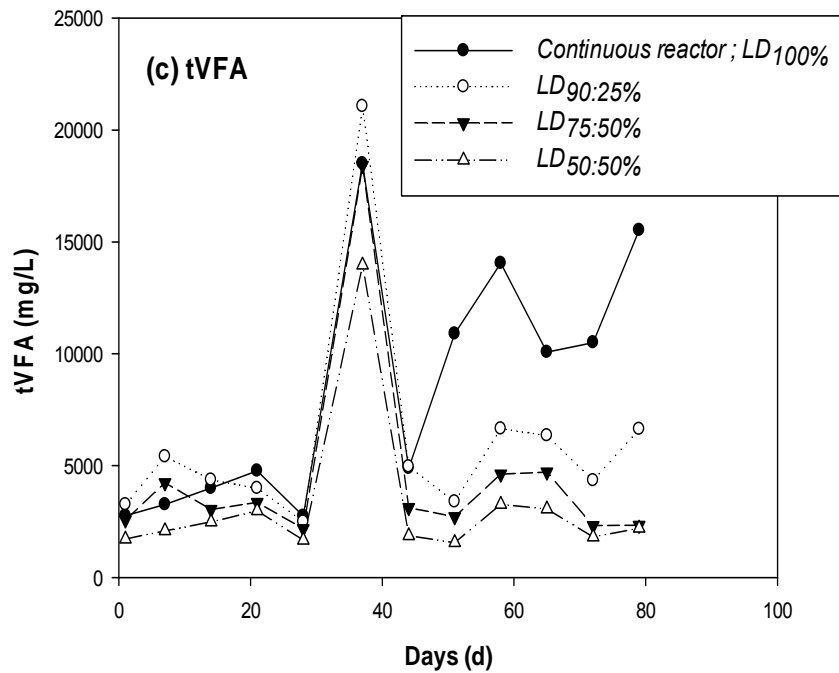
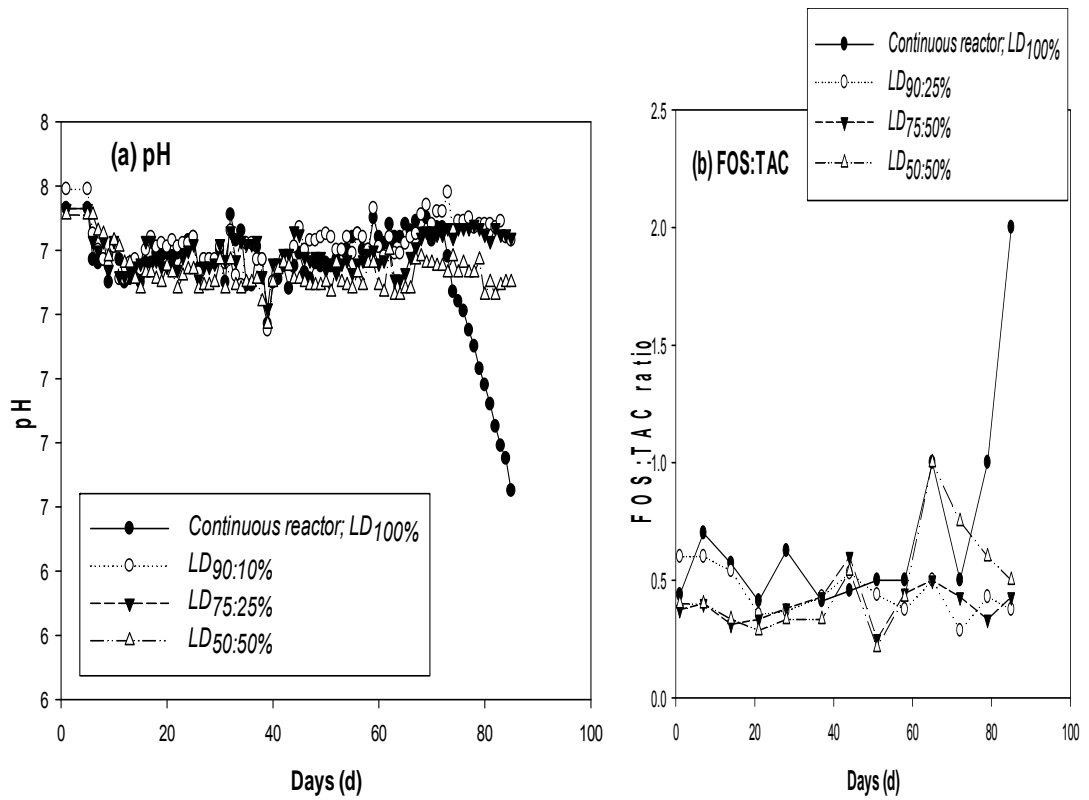


Figure 9-10 Continuous reactors, co-digestion mixtures (A), pH; (B), FOS: TAC ratio; (C), Total volatile fatty acid (tVFAs)

## *Alkalinity and Ammonia*

Methane-forming bacteria produce alkalinity in three forms; CO<sub>2</sub>, bicarbonate, and ammonia (Turovskii, 2006). Ammonia production with its buffering capacity is also controlled by the C: N ratio of the substrates which can affect the performance of the process (Wang *et al.*, 2012). The alkalinity value in all the reactors ranged between approximately 8 g.L<sup>-1</sup>– 12 g.L<sup>-1</sup>, Figure 9-11 A. Alkalinity has been shown to have a synergetic effect on anaerobic digestion of food waste (Shujun *et al.*, 2015), as ammonium bicarbonate alkalinity can maintain a neutral pH in microbial cells known as “metabolism generated alkalinity” (Shujun *et al.*, 2015). High amounts of TAN and FAN concentration present in solution are known causes of digester instability with the FAN being more toxic to anaerobes (Kayhanian, 1999; Poirier *et al.*, 2017). Although the inoculum ammonia concentration was 1.76 g L<sup>-1</sup> at the start of the experiment, both the TAN and FAN concentration shows a similar decreasing trend in all the reactors including the mono-digested reactor (*LD*<sub>100%</sub>) ranging from 1.6 g L<sup>-1</sup> - 0.6 g.L<sup>-1</sup> and 0.06 g.L<sup>-1</sup> – 0.02 g.L<sup>-1</sup>, respectively, Figure 9-11 B and Figure 9-12 A. Reported inhibitory concentration for ammonia is > 3.0 g.L<sup>-1</sup> at any pH and between 1.5 g.L<sup>-1</sup> - 3.0 g.L<sup>-1</sup> at pH ≥ 7.4 (Calli *et al.*, 2005), and for food waste digestion TAN inhibition can occur at > 2 g.L<sup>-1</sup>(Chen *et al.*, 2016). FAN inhibitory concentration has been reported to be between 0.099 g L<sup>-1</sup>- 0.15 g L<sup>-1</sup> (Ahring *et al.*, 1992), and 0.15 g L<sup>-1</sup> - 1.2 g L<sup>-1</sup> (Poirier *et al.*, 2017). The values obtained for both TAN and FAN are mostly below the reported inhibitory levels.



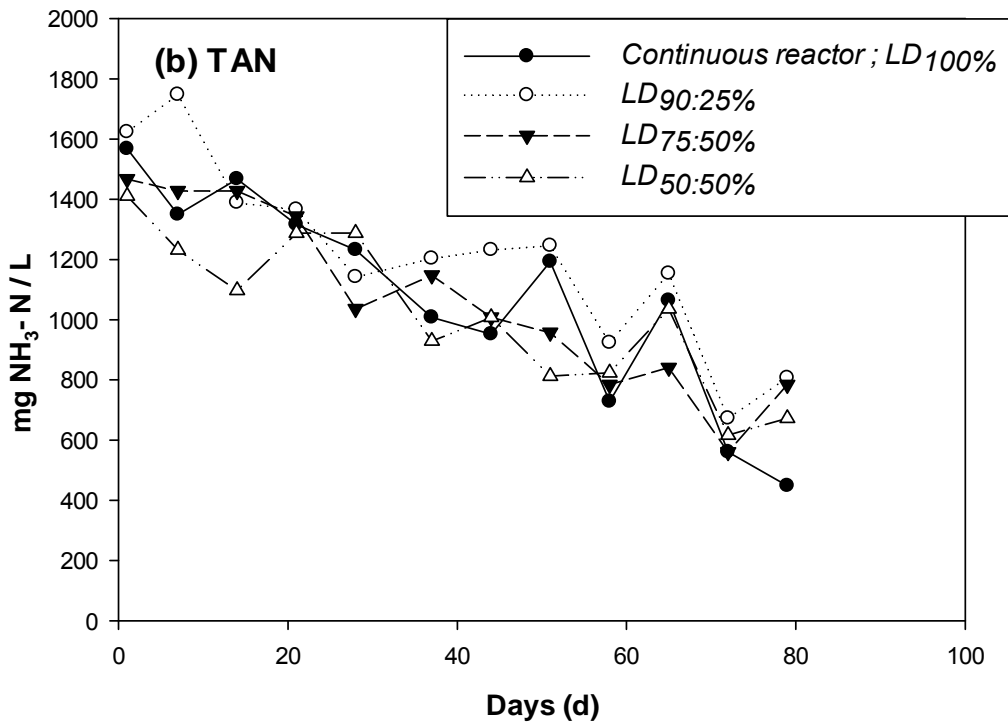
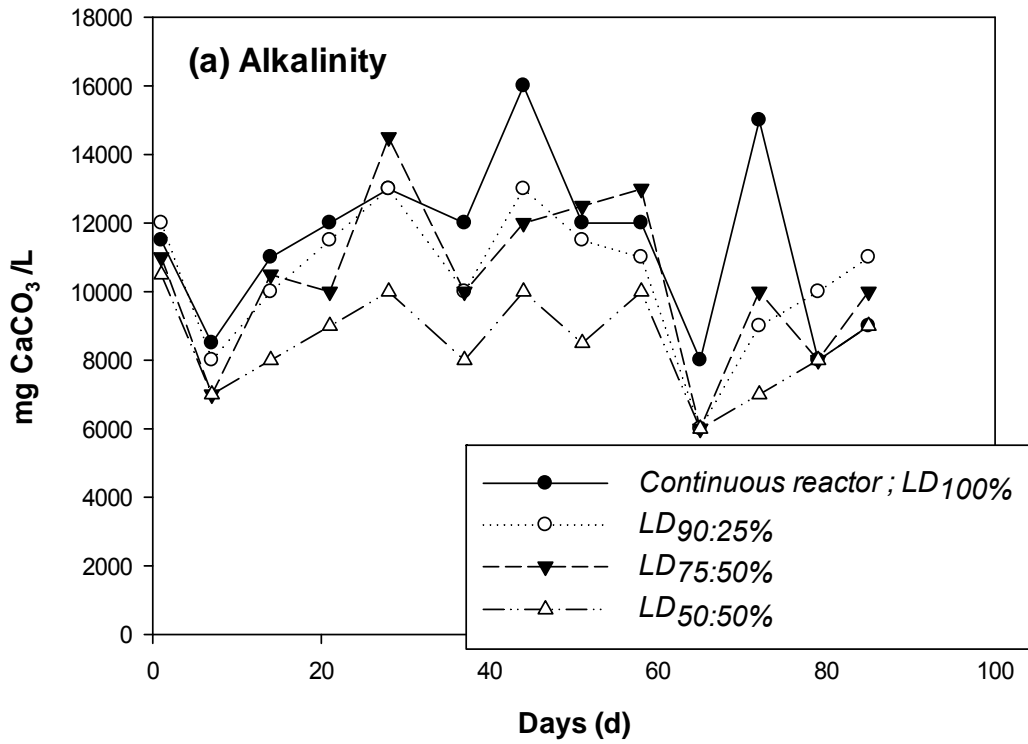


Figure 9-11 Continuous reactors, co-digestion mixtures; (A), Alkalinity; (B), Total ammonia nitrogen (TAN).

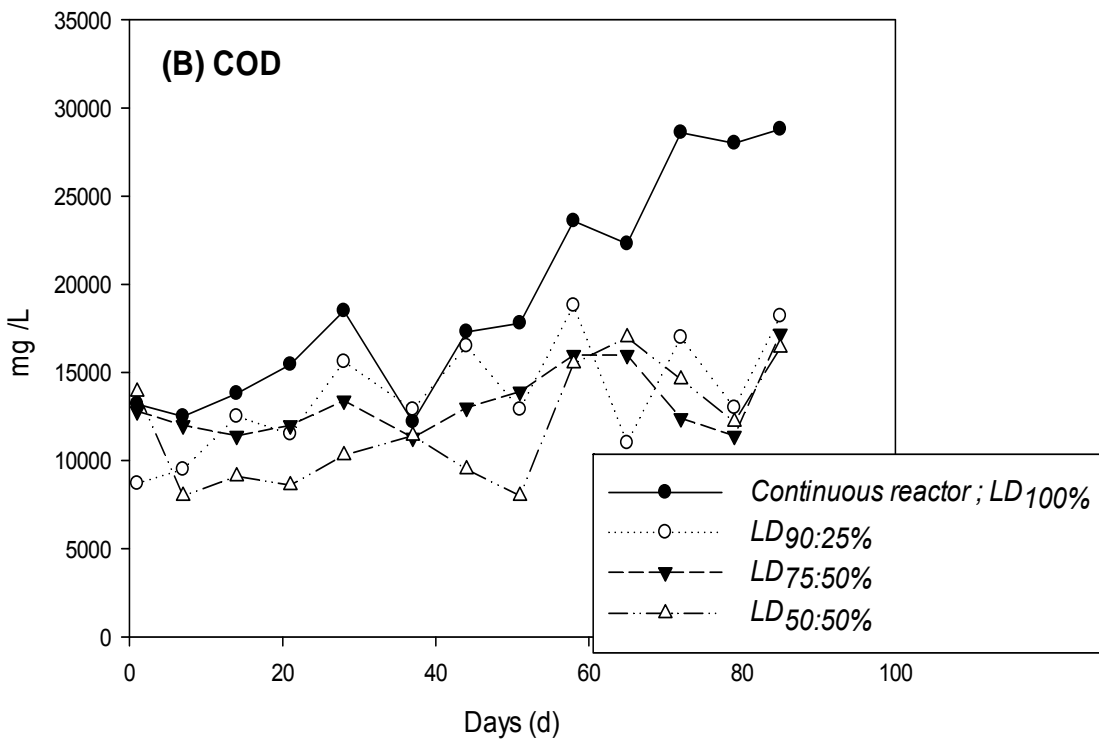
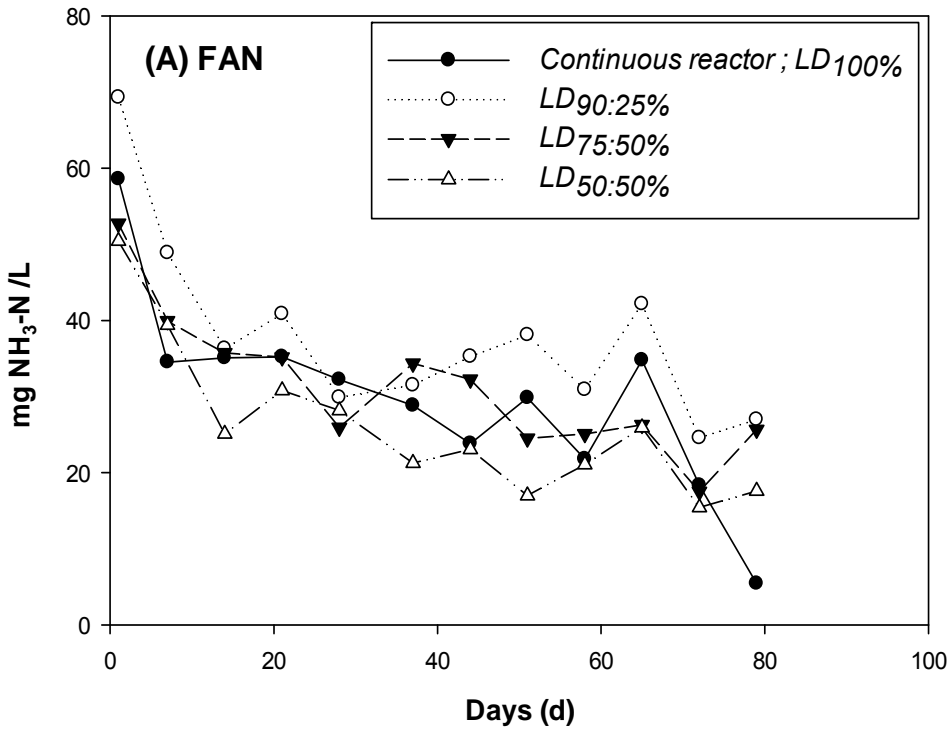


Figure 9-12 Continuous reactors, co-digestion mixtures; (A), Free ammonia nitrogen (FAN); (B), Chemical oxygen demand (COD)

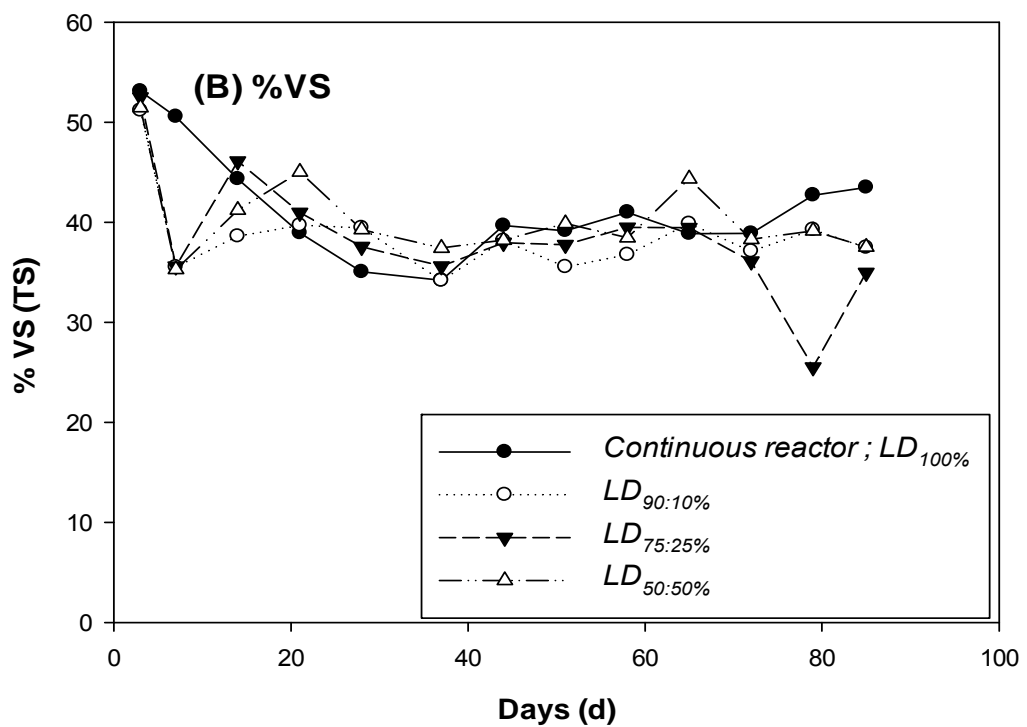
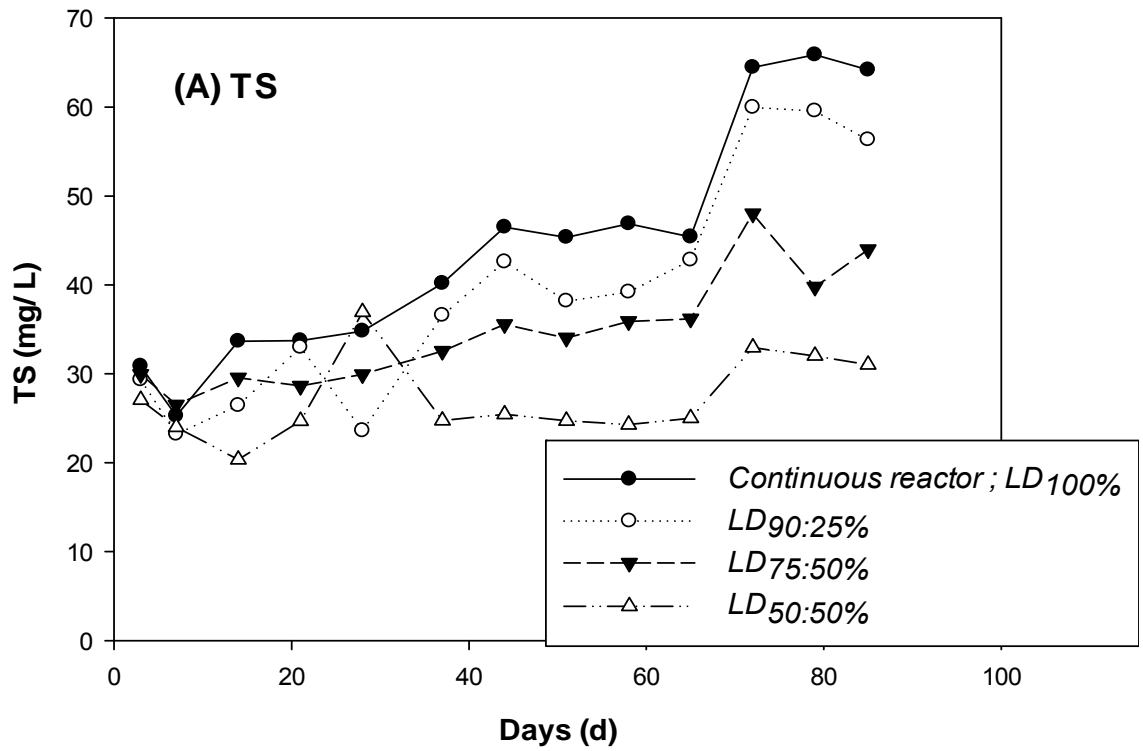


Figure 9-13 Continuous reactors, co-digestion mixtures; (A), Total solid; (%TS)  
(B), Volatile solid (%VS)

### *COD, total and volatile solids*

As the OLR is increased, the COD concentration also increased in the reactors, with the highest observed for R<sub>1</sub> (*LD*<sub>100%</sub>) (13 g.L<sup>-1</sup> to 29 g.L<sup>-1</sup>), and the other co-digestion mix reactors within approximately 9 g.L<sup>-1</sup> to 15 g.L<sup>-1</sup>, Figure 9-12 B.

The difference in COD concentration between *LD*<sub>100%</sub> and the other reactors is close to 48% by the end of the experiment indicating the instability in the mono-digested reactor and the inefficiency of the microbes to degrade the feed due to low pH, high tVFA concentrations, and high FOS: TAC ratio in the reactor.

Since, AD of feedstock causes COD conversion to methane (González-Fernández *et al.*, 2013), COD values can aid the evaluation of the potential of biogas and methane production by dividing the amounts of COD added and reduced in the digesters (Sunada *et al.*, 2012).

The %TS for *LD*<sub>100%</sub> increased from 31 mg L<sup>-1</sup> - 64 mg L<sup>-1</sup>, an increase of 52% as the OLR was increased, compared to *LD*<sub>50:50%</sub> (27 mg L<sup>-1</sup> - 31 mg L<sup>-1</sup>), an increase of 15%, which showed the lowest increase among the co-digested reactors, Figure 9-13 A. Increase in TS affects the performance of AD process by changing the microbial composition of the system, and pyrosequencing results have shown high shifts in bacterial community can occur with increasing total solids contents (Yi *et al.*, 2014). Thus, increase in OLR brings about increase in TS with a corresponding increase in the concentration of potentially inhibitory compounds, such as ammonia and heavy metals, with a decrease in mass transfer effects (An *et al.*, 2017). The degree of VS destruction among all the reactors was similar, averaging from 51% - 37%, which equates to around 44% VS removal efficiency, Figure 9-13 B. Information regarding VS reduction can indicate the nature of actual solids matrix of substrates fed to digesters (P. Chastain and Bryan Smith, 2015)

### *Chloride concentration*

The chloride concentration gradually increased in all the reactors as the OLR was increased and are for *LD*<sub>100%</sub> (2.5 g.L<sup>-1</sup> - 45 g.L<sup>-1</sup>), *LD*<sub>90:10%</sub> (2.6 g.L<sup>-1</sup> - 34.72 g.L<sup>-1</sup>), *LD*<sub>75:25%</sub> (2.25 g.L<sup>-1</sup> - 37.49 g.L<sup>-1</sup>), *LD*<sub>50:50%</sub> (2.12 g.L<sup>-1</sup> - 27.01 g.L<sup>-1</sup>) shown in Figure 9-14.

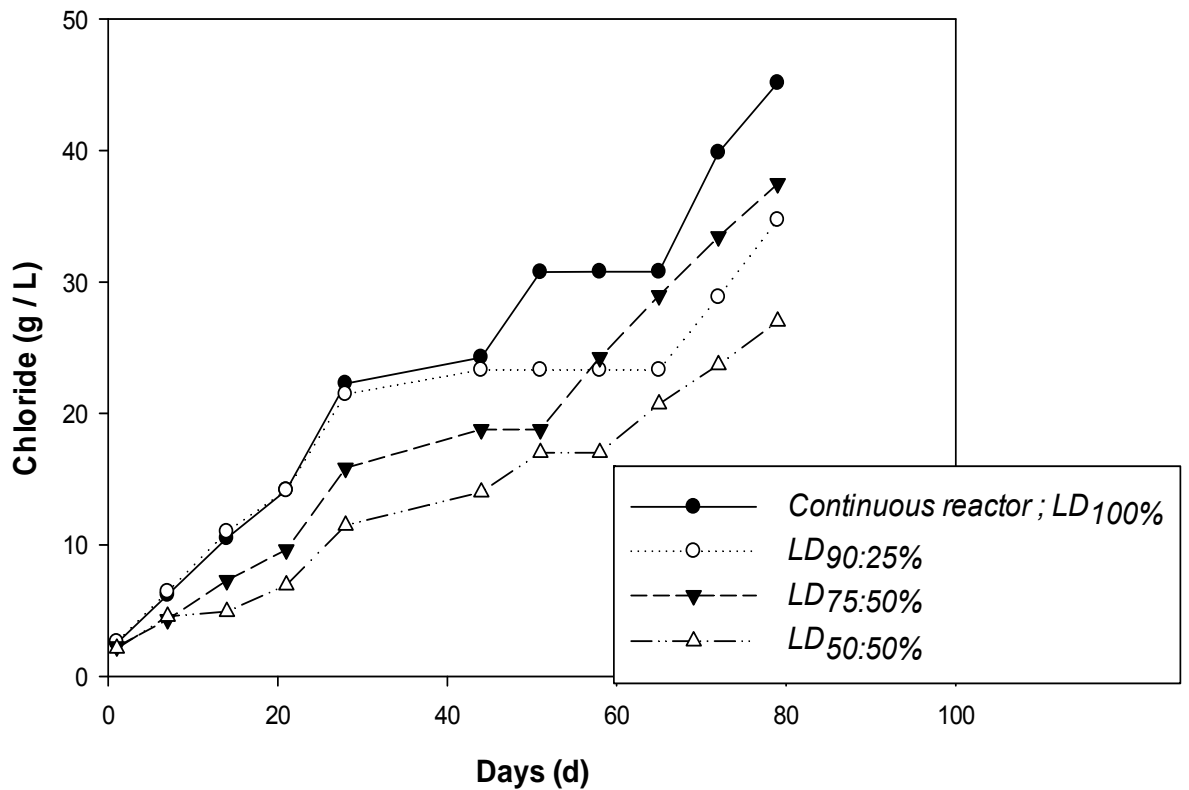


Figure 9-14 Continuous reactors, co-digestion mixtures; Chloride concentration.

Previously, sodium chloride has been identified as an inhibitor of AD process (Allen *et al.*, 2014), although needed in small concentrations by microorganisms (Suwannopadol *et al.*, 2012). A wide range (5 – 20 g.L<sup>-1</sup>) of chloride inhibitory values have been reported (Tabassum *et al.*, 2016a). The high cumulative chloride concentration and BEF obtained in this study might not be unconnected with acclimatization of the process, as reported for studies carried out on seaweed (Tabassum *et al.*, 2016a). Another important observation is the low TAN level obtained in all the reactors at OLR 5. Hierholtzer and Akunna (2012) observed tolerance to high salinity level when ammonia levels were low. In the current study as the content of food waste in the reactors with mix ratio increased, both sulphate and chloride concentrations reduced through simple washout (SFW contained low chloride).

#### 9.5.6 Metal Concentrations

The concentration of the inoculum, *L. digitata* and food waste feedstocks and the final reactor contents at the end of the run were all analyzed for the

essential trace elements required by microorganism for growth and stable digestion process, Table 9-8. Both the macro and micronutrients are required for stable growth of anaerobic microorganisms (Gerardi, 2003). From the results, the algae feedstock showed highest concentrations of Ca, K, Mg, and Na, compared to other elements found. A similar trend has been reported by other studies (Adams *et al.*, 2011a). Davis *et al.* (2003) stated that the cell walls polysaccharides and protein of seaweed contains many binding sites (anionic carboxyl, phosphate and sulphate groups) for metal absorption which may results in high metal content. This is determined largely by environmental factors where the algae grows, such as such nutrient content, turbidity, salinity and heavy metal contamination (Ródenas de la Rocha *et al.*, 2009). The concentration of the inoculum also followed similar higher values in these elements as it had previously been fed with algae feedstock in other studies. Most of these essential trace metals reported in Table 9-8 are required by microorganism for their growth at low concentrations (Thanh *et al.*, 2016) but have the potential to curb production of VFA by inhibiting acidogenic microorganisms (Cogan and Antizar-Ladislao, 2016).

Table 9-8 Essential trace elements concentration of algae and stimulated food waste feedstock, inoculum, and continuous reactors R1, R2, R3 and R4.

Trace elements	Inoculum	algae feedstock	Food substrate	LD100 %	LD90:10 %	LD75:25 %	LD50:50 %
----------------	----------	-----------------	----------------	---------	-----------	-----------	-----------

	start of Run (mg/l)			end of run (mg/l)			
Al	11.61	0.00	2.67	2.52	3.03	4.53	5.00
As	0.00	0.00	0.00	1.02	1.17	0.00	0.53
B	0.74	2.10	0.41	4.39	3.72	5.41	4.37
Ba	0.92	0.18	0.05	0.96	0.52	0.75	0.66
Ca	355	206	30.13	479	514	729	514
Cd	0.00	0.02	0.00	0.04	0.00	0.00	0.00
Co	0.07	0.00	0.01	0.04	0.05	0.00	0.05
Cr	0.14	0.04	0.13	0.08	0.10	0.17	0.34
Cu	0.84	0.03	0.11	0.63	0.13	0.23	0.32
Fe	21.4	3.58	1.45	8.38	10.56	14.4	17.67
K	702	496	139	2229	2119	3162	2652
Mg	135	130	8.14	316	277	397	282
Mn	2.24	0.07	0.24	0.29	0.43	0.55	0.68
Na	78	93	6.19	270	256	353	289
Ni	0.12	0.10	0.12	0.20	0.26	0.32	0.44
Pb	0.28	0.00	0.00	0.17	0.27	0.00	0.00
Si	0.00	0.00	0.13	2.29	1.84	5.25	6.19
V	0.00	0.00	0.00	0.02	0.06	0.03	0.06
Zn	5.19	0.83	28.20	2.44	0.04	2.43	2.65
Ti	0.14	0.01	0.03	0.00	1.82	0.05	0.08
Se	0.77	0.00	0.00	0.00	0.00	0.00	0.74

For the three most inhibitory elements (Cu > Zn > Cr), the concentration reported to cause 50% inhibition of VFA production by acidogenic microorganisms, and 50% inhibition of VFA degradation by methanogenic organisms are 17 mg L<sup>-1</sup>, 3.5 mg L<sup>-1</sup>, 0.9 mg L<sup>-1</sup>, and 14.7 mg L<sup>-1</sup>, 16 mg L<sup>-1</sup>, 12.5 mg L<sup>-1</sup>, respectively (Lin, 1993). The maximum concentration found in Table 9-8 for Cu, Zn and Cr is 0.63 mg L<sup>-1</sup> for *LD*<sub>100%</sub>, 2.65 mg L<sup>-1</sup> and 0.34 mg L<sup>-1</sup> for *LD*<sub>50:50%</sub>, values which are below the inhibitory values. For Na and Ca, the reported critical levels of 6 - 30 g L<sup>-1</sup> (Cogan and Antizar-Ladislao, 2016) and 8 g L<sup>-1</sup> (Chen et al., 2008) were higher than observed in the current study. K concentration for the reactors ranged between 2.2 - 3.16 mg L<sup>-1</sup>, moderate inhibition has been reported at 2.5 - 4.5 g L<sup>-1</sup> and strong inhibition at 12 g L<sup>-1</sup> respectively (Turovskii, 2006). A literature survey about the stimulatory ranges of some trace metals for anaerobic digestion biomass for Co, Fe, Ni, and Se were reported to be 0.05 - 0.19, 0 - 0.39, 0.11 - 0.25 and 0.008 - 0.79 mg L<sup>-1</sup> (Demirel and Scherer, 2011). The reported values in Table 9-8 are mostly within these stimulatory ranges and not high enough to cause process inhibition, except for the mono-digested reactor *LD*<sub>100%</sub> which showed instability at high OLR with a value of 0.63 mg L<sup>-1</sup> for Cu, which was more than the strongly inhibitory concentration limit of 0.5 mg L<sup>-1</sup> reported for soluble Cu (Turovskii, 2006). This implies that co-digesting the macroalgae with food waste brought

about dilution of potential toxicity of inhibitory compounds in the reactors while bringing about optimization and stability of the reactors.

## 9.6 Conclusion

Batch and continuous trials of mono-digestion  $LD_{100:0\%}$  and co-digestion of *L. digitata* with food waste were carried out at different mix ratios. The  $LD_{100:0\%}$  reactor produced the highest BMP yield in the batch test. In the continuous trial,  $LD_{90:10\%}$  was found to be optimal for the highest cumulative methane production after 85 days of fermentation as the OLR was increased step-wise. Although in the batch experiment this mix ratio ( $LD_{90:10\%}$ ) showed an antagonistic effect on the digestion, this result was not obtained in the continuous trial. The mono-digestion of  $LD_{100\%}$  was characterised by the accumulation of high tVFA and an increased FOS: TAC ratio as the OLR was increased, leading to the reactor failure. Co-digestion of *L. digitata* and food waste was beneficial as it brings about acclimatization to high salinity level in presence of low ammonia concentration, and dilution of potential inhibitory compounds which were not evident in the mono-digested reactor.



## Chapter 10. Anaerobic digestion of macroalgae with trace element supplementation: Batch and continuous studies

### Abstract

Trace elements are essential for the enzyme cofactors involved in the metabolism of methane formation and are needed in a balanced anaerobic digestion process. This study investigates the effect of trace element supplementation (TES) on mesophilic anaerobic digestion treating brown algae, *Laminaria digitata* (LD) in both batch and continuous (CSTR) reactors. Two set of Experiment 1 and 2 (batch and continuous) reactors were carried out with and without trace element addition, and their performance compared.

In Experiment 1, five (batch 500 ml and 1L CSTR) reactors were operated with the addition of metals as Reactor 1 - control (TES 0), Reactor 2 (TES 1 - 0.1 mg/l Se, 0.1 mg/l W), Reactor 3 (TES 2 - 0.1 mg/l Se, 0.1 mg/l W, 0.5 mg/l Co, 0.1 mg/l Mo), Reactor 4 (TES 3 - 0.1 mg/l Se, 0.1 mg/l W, 0.5 mg/l Co, 0.1 mg/l Mo, 0.5 mg/l Ni, 0.05 mg/l Cu) and Reactor 5 (TES 4 - 0.1 mg/l Se, 0.1 mg/l W, 0.5 mg/l Co, 0.1 mg/l Mo, 0.5 mg/l Ni, 0.05 mg/l Cu, 0.5 mg/l Fe, 0.1 mg/l Zn). The results obtained from the first batch test (BT 1) show that TES 1 - 4 reactors achieved an increase in methane yield of between 17 - 26% compared to the control reactor without TES after 22 days of incubation. In CSTR reactors, the results show that trace elements addition (daily) with an HRT of 25 days allowed for a stable anaerobic digestion in three different combinations TES 2-4 at an organic loading rate of 2 gVS.L<sup>-1</sup>.d<sup>-1</sup> used throughout the experiment, but did not give any advantage over the reactor without TES 0.

In Experiment 2, two (batch 500 ml and 1L CSTR) reactors were operated with and without TES 4 mix. From the results of the second batch test (BT 2), the TES 4 reactor achieved an increase in methane yield of 50% compared to the control reactor without TES 0 after 40 days of incubation. While in the second CSTR test, where there was a step-wise increase in OLR from 2 - 5 gVS.L<sup>-1</sup>.d<sup>-1</sup>, and weekly addition of the TES 4 mix, the reactor showed better performance compared to the reactor without TES 0 which was characterised by high tVFA,

increased FOS: TAC ratio and a drop in pH of the reactor resulting to instability and process failure.

Therefore, it can be concluded that TES brought about an increase in methane yield, with weekly addition of TES in long term continuous digestion process being the preferred option.

## 10.1 Introduction

This chapter investigates the effect of trace element supplementation (TES) on anaerobic digestion of macroalgae. An introduction to the background material for this chapter has been given already in Section 2.17.

## 10.2 Materials and methods

### 10.2.1 *Substrates and chemical analysis*

The algae feedstock and chemical analyses are described in Section 3.1 and 3.2.

### 10.2.2 *Inoculum*

The inoculum used was collected from a full-scale running anaerobic digester (Cockle Park Farm, Newcastle) operating on grass silage (Section 3.1.2). The initial trace element concentration of the inoculum is shown in Table 10-2.

### 10.2.3 *Design of the Experiment*

#### *Batch*

The batch tests (BT 1 and 2) were carried out according to (Membere *et al.*, 2015). The inoculum to substrate ratio used was 3:1. Trace elements mix of (Selenium se, Molybdenum Mo, Cobalt Co, Tungsten W, Iron Fe, Nickel Ni, Zinc Zn, and Copper Cu) in four different combination TES 1 - 4 were added to the reactor bottles as shown in Table 10-1. The dose added were calculated based on trace metal content of the inoculum, algae substrate and stimulatory ranges reported in literature (Moosbrugger *et al.*, 1990; Demirel and Scherer, 2011), and also to avoid attaining toxic concentrations (Banks *et al.*, 2012). The tests were carried out by supplementing 370 ml of inoculum with the trace element matrix, before making the volume to 500 ml with distilled water. The reactors with TES 1 - 4 were compared to a control reactor without TES. For BT 1, 2 ml of each prepared mix were added in reactors TES 1 – 4, while in BT 2, only 2 ml of TES 4 mix were used. The inoculum used was acclimatised prior to the start of the experiment and allowed to degas for between 3 - 5 days. Biogas produced were collected using gas bags and all measured gas volume were normalized to standard temperature and pressure (Section 4.2.7).

Table 10-1 Experimental design for both batch and CSTRs with trace element concentration.

Substrate and trace element additions	Batch		CSTR reactors
Algae (control)	TES 0		R TES 0
Algae + Se ,Mo	TES 1		R TES 1
Algae + Se , Mo, Co, W	TES 2		R TES 2
Algae + Se, Mo , Co, W , Fe , Ni	TES 3		R TES 3
Algae + Se, Mo, Co, W, Fe , Ni, Zn, Cu	TES 4		R TES 4
Trace element compound used and concentration added (mg/l)			
Na <sub>2</sub> SeO <sub>4</sub> .6H <sub>2</sub> O - Selenium Se	0.1	FeCl <sub>2</sub> . 4H <sub>2</sub> O -Iron Fe	0.5
Na <sub>2</sub> MO <sub>4</sub> .2H <sub>2</sub> O - Molybdenum Mo	0.1	NiCl <sub>2</sub> . 4H <sub>2</sub> O - Nickel Ni	0.5
CoCl <sub>2</sub> . 6H <sub>2</sub> O - Cobalt Co	0.5	ZnCl <sub>2</sub> - Zinc Zn	0.1
Na <sub>2</sub> WO <sub>4</sub> .2H <sub>2</sub> O - Tungsten W	0.1	CuCl <sub>2</sub> . 2H <sub>2</sub> O- Copper Cu	0.05

#### 10.2.4 Continuous reactors

Two set of CSTR (Experiment 1 and 2) were also carried out.

In Experiment 1, five set of 1 L (1.2 L capacity) reactors (RTES 0 - 4) were operated with and without trace elements in four different combination (RTES 1-4) as shown in Table 10-1. The reactors were inoculated with 1L of acclimatised inoculum and operated at a constant OLR (2 gVS.L<sup>-1</sup> d<sup>-1</sup>). Feeding was carried out by daily removal of digestate through an outlet port followed by addition of the substrate and 1ml of the trace element mix in the reactor.

In Experiment 2, only two set of the 1 L reactors (R 1 and R 2) were used. In reactor 2, 5 ml of the TES 4 mix was added once a week. The organic loading rate OLR (g VS.L<sup>-1</sup> d<sup>-1</sup>) was increased stepwise after acclimatization from 2 g VS.L<sup>-1</sup> d<sup>-1</sup> on day 1 of the experiment to 3 g VS.L<sup>-1</sup> d<sup>-1</sup> on day 26, thereafter, to 4 g VS.L<sup>-1</sup> d<sup>-1</sup> on day 39 and, finally to 5 g VS.L<sup>-1</sup> d<sup>-1</sup> on day 55, till the end of the experiment.

## 10.3 Results and discussion

### 10.3.1 Biomethane potential

In Batch 1 and 2, biomethane production potential was measured under controlled conditions (35 °C) for 22 and 40 days, respectively, and was stopped when no further gas production was noticed. The daily, cumulative CH<sub>4</sub> and biogas production obtained for the TES 4 mix reactor for BT 1 and 2 is shown in Figure 10-1 A and B, respectively. Contribution from background CH<sub>4</sub> produced by the inoculum was deducted from the cumulative production in evaluating the data as recommended by (Membere *et al.*, 2015). In BT 1, the control reactor (TES 0) without metals supplementation generated  $237 \pm 0.19$  mL CH<sub>4</sub>/g VS with methane content increasing up to 70%. The highest methane yield achieved was  $299 \pm 1.14$  mL CH<sub>4</sub>/g VS from the TES 4 reactor. This was followed closely by TES 1, 2 and 3 ( $293 \pm 1.66$ ,  $284 \pm 0.09$ ,  $278 \pm 1.84$  ml CH<sub>4</sub>/g VS), respectively (data not shown). The results obtained compared to the control, shows supplementation with the various mix of metals improved methane yield by 17 – 26%. Results obtained from BT 2 carried out using only TES 4 mix which produced the highest methane yield from BT 1 is shown in Figure 10-2 B. The cumulative methane production after 40 days for TES 4 is  $440 \pm 0.49$  ml CH<sub>4</sub>/g VS compared to  $293 \pm 1.02$  ml CH<sub>4</sub>/g VS obtained for the reactor TES 0 without trace element addition. This represents an increase of about 50% in methane yield indicating trace element addition aided in more biogas production. Studies carried out by (Facchin *et al.*, 2013) using Co, Ni, Mo, Se, and W improved methane yield by 45 – 65% while the addition of Co and Ni mix has shown to increase methane yield by 13.5% (Zhang *et al.*, 2017a). Kayhanian and Rich (1995) using Co, Fe, Cu, Ni, Mo, Se, W, and Zn nutrient addition also had elevated gas production by 30%, with increased digester stability. The variability in gas production for TES 4 mix between BT 1 and 2 could be due to the inoculum used, as the methane yield for an organic substrate for a defined inoculum is directly influenced by the degree of solubilisation (Raposo *et al.*, 2011a), while the slowest step of either hydrolysis (solubilisation), acidogenesis or methanogenesis, determines the degradation rate (Jash and Ghosh, 1996).

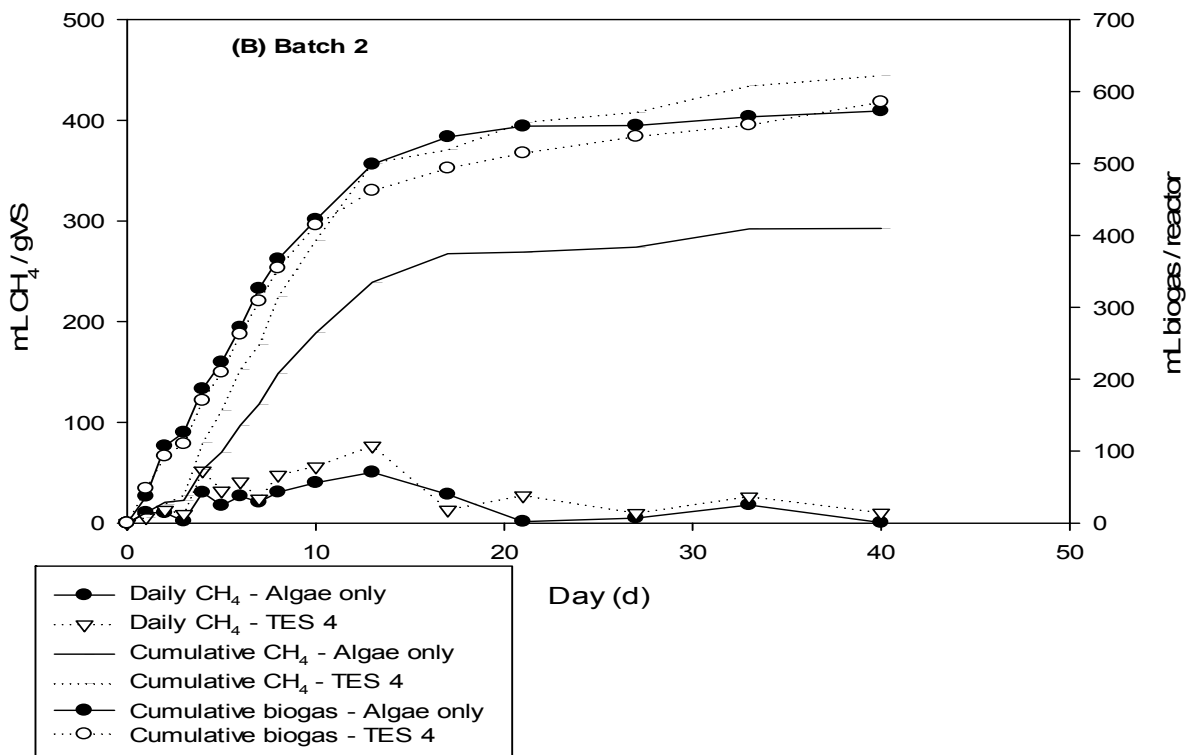
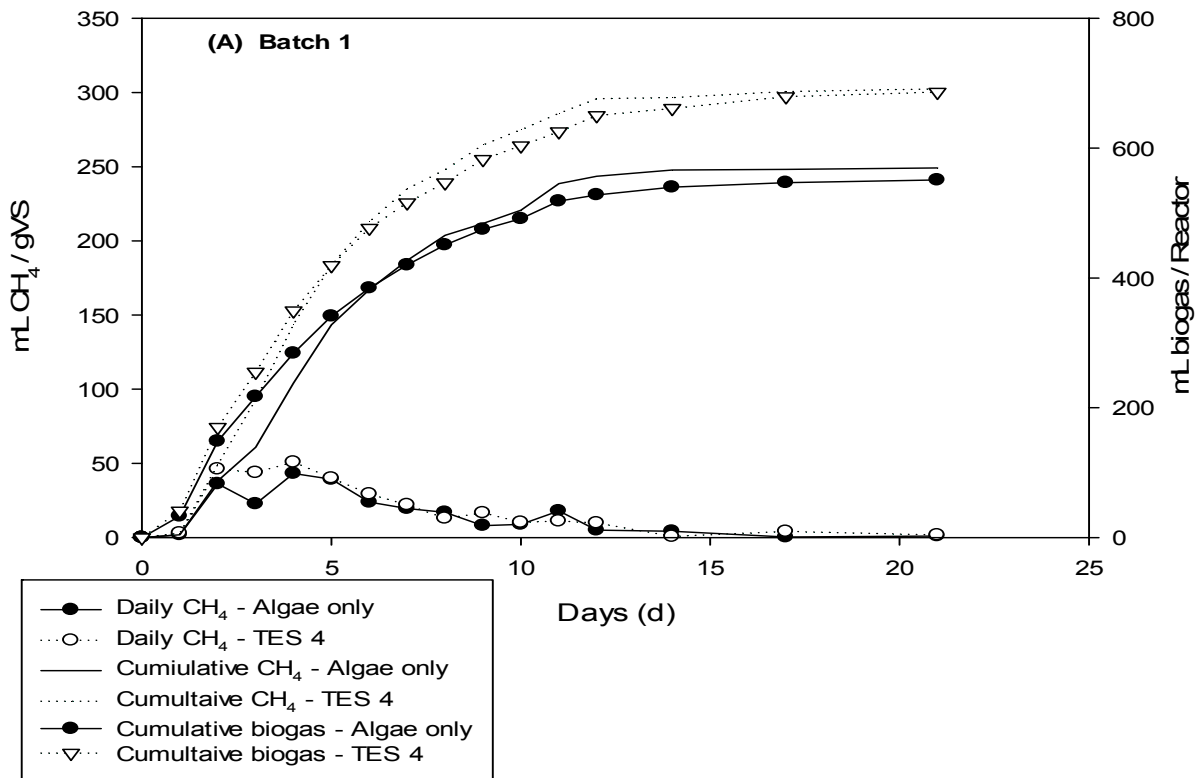


Figure 10-1 Cumulative biogas and methane yield for Batch test 1 and 2

The maximum rate of methane production was obtained in the control reactors compared to TES reactors. For BT 1 and 2, 115 ml CH<sub>4</sub> /gVS.d was obtained on day 2 and 77 ml CH<sub>4</sub> /gVS.d on day 13. The cumulative biogas production in BT 1 for the control and TES 4 are 551 and 686 mL biogas/reactor compared to BT 2, 573 and 586 ml biogas/reactor, respectively.

### 10.3.2 *Continuous reactors (Experiment 1)*

The continuous digesters (RTES 0 – 4) were fed once a day over a period of 90 days on the algae substrate. The volumetric methane production rate of the reactors with and without supplementations is shown in Figure 10-2 and Figure 10-3, respectively. The cumulative methane production, % methane and H<sub>2</sub>S content in the reactors are shown in Figure 10-4 and Figure 10-5.

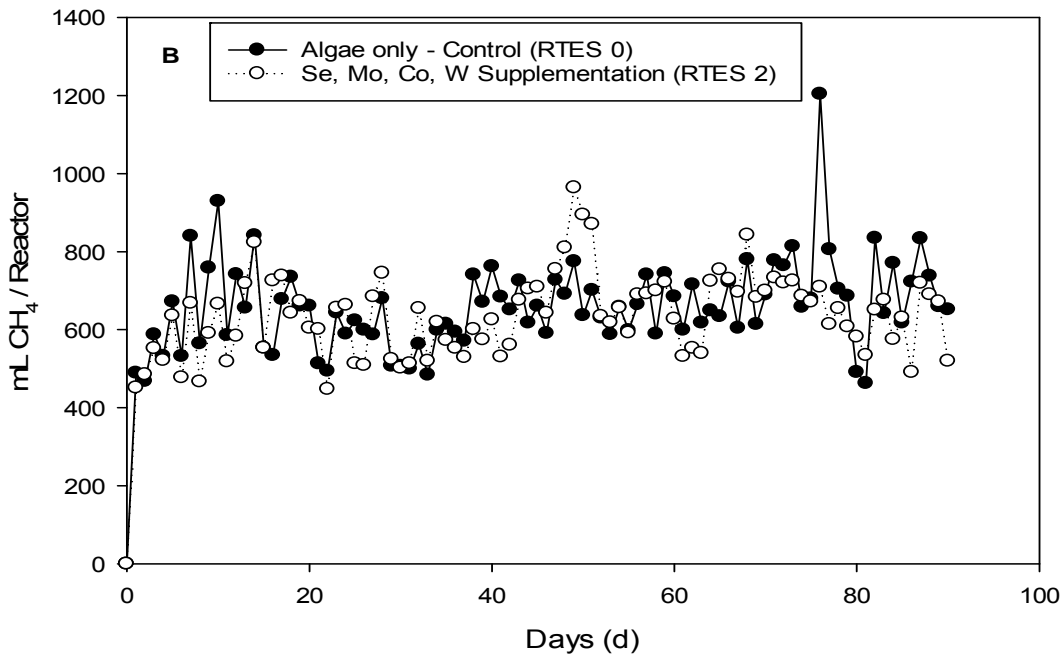
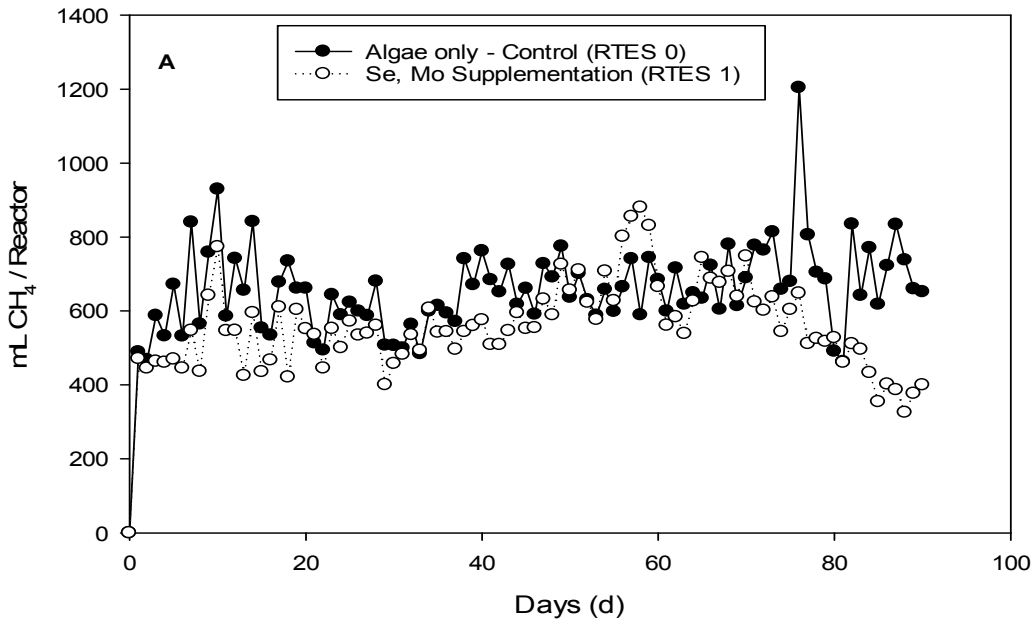


Figure 10-2 A), Daily volumetric methane production in continuous reactors (RTES 0 and RTES 1); B), Daily volumetric methane production in continuous reactors (RTES 0 and RTES 2).



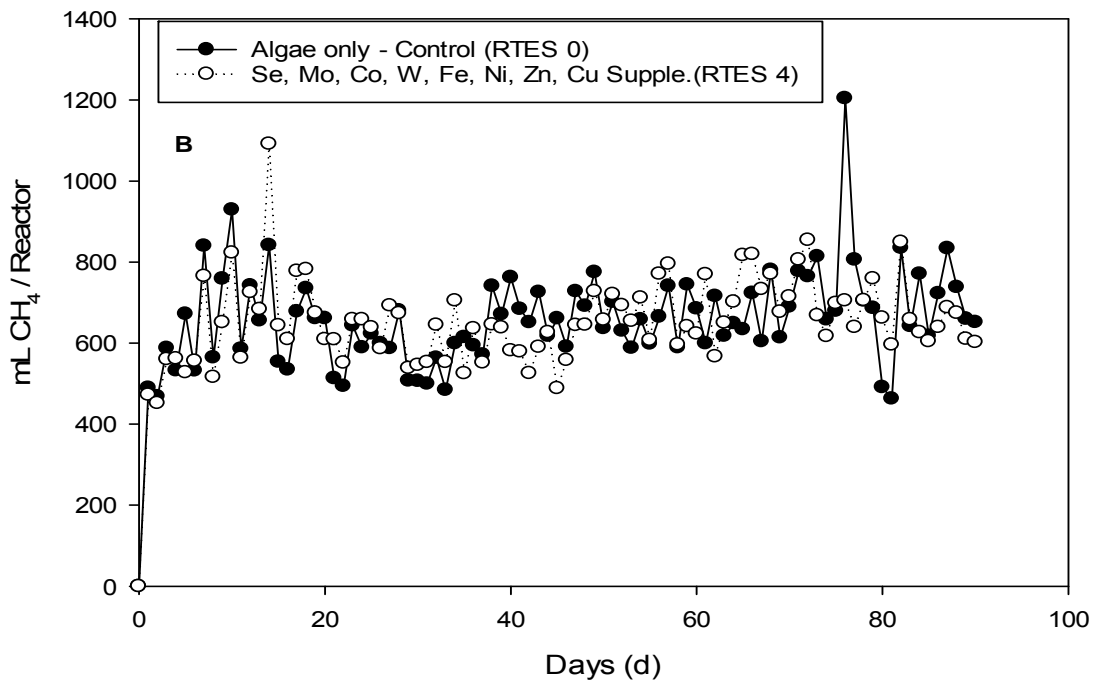
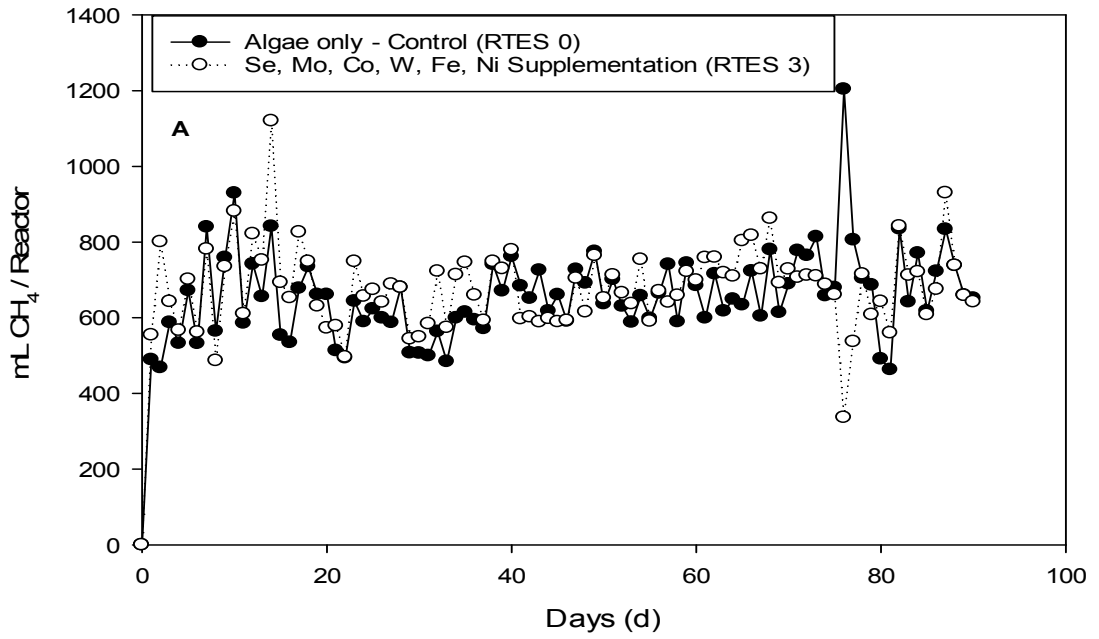


Figure 10-3 A), Daily volumetric methane production in continuous reactors (RTES 0 and RTES 3); B), Daily volumetric methane production in continuous reactors (RTES 0 and RTES 4).

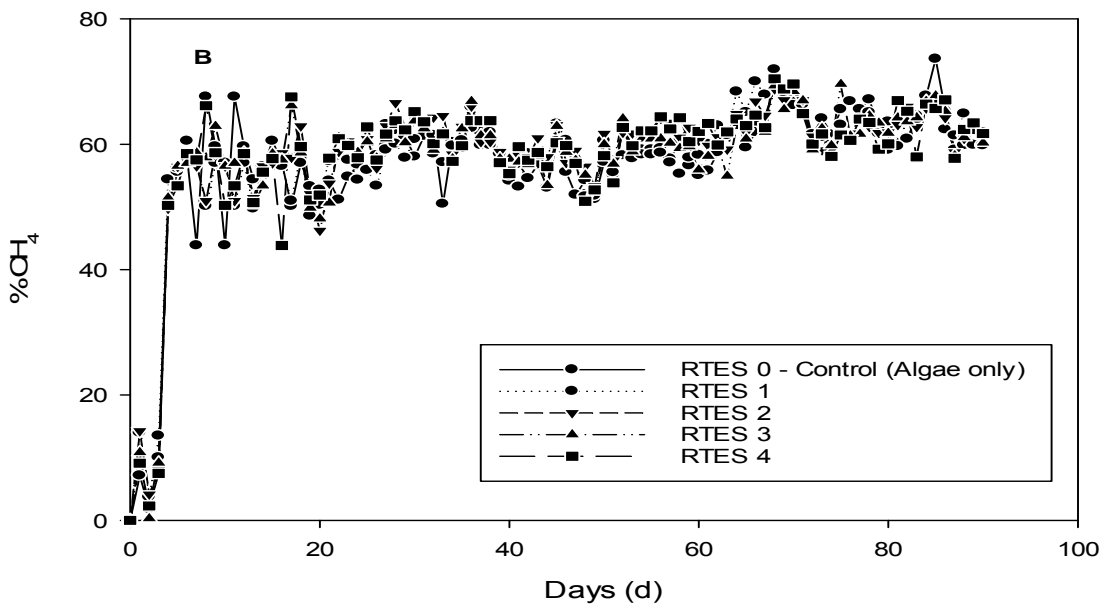
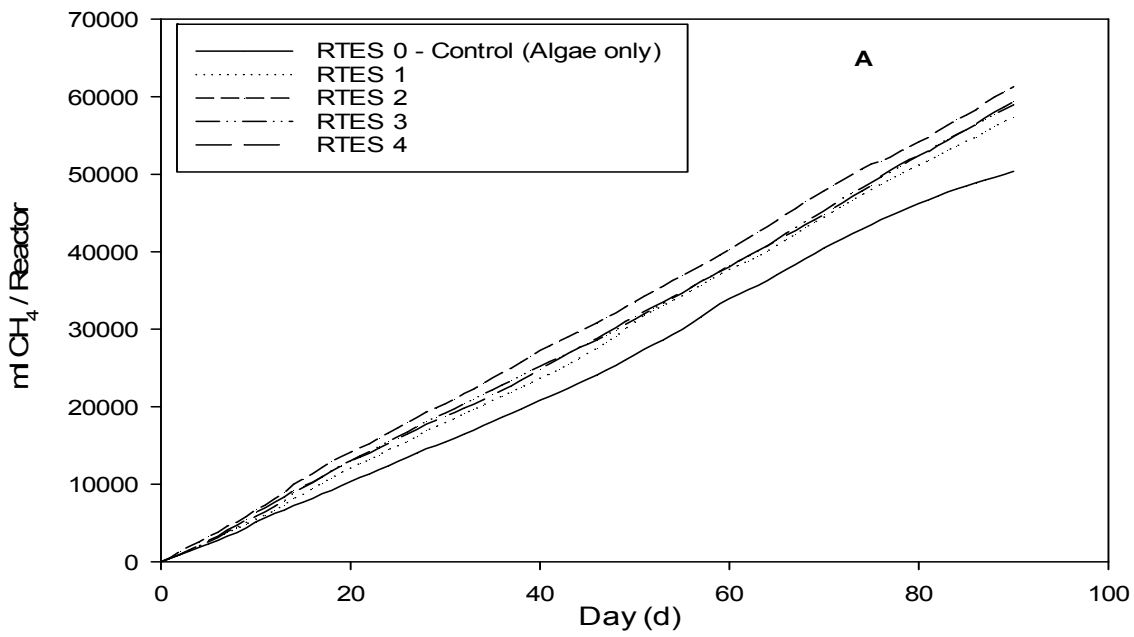


Figure 10-4 A), Cumulative methane production; and B), % Methane content in continuous reactors (RTES 0 – 4).

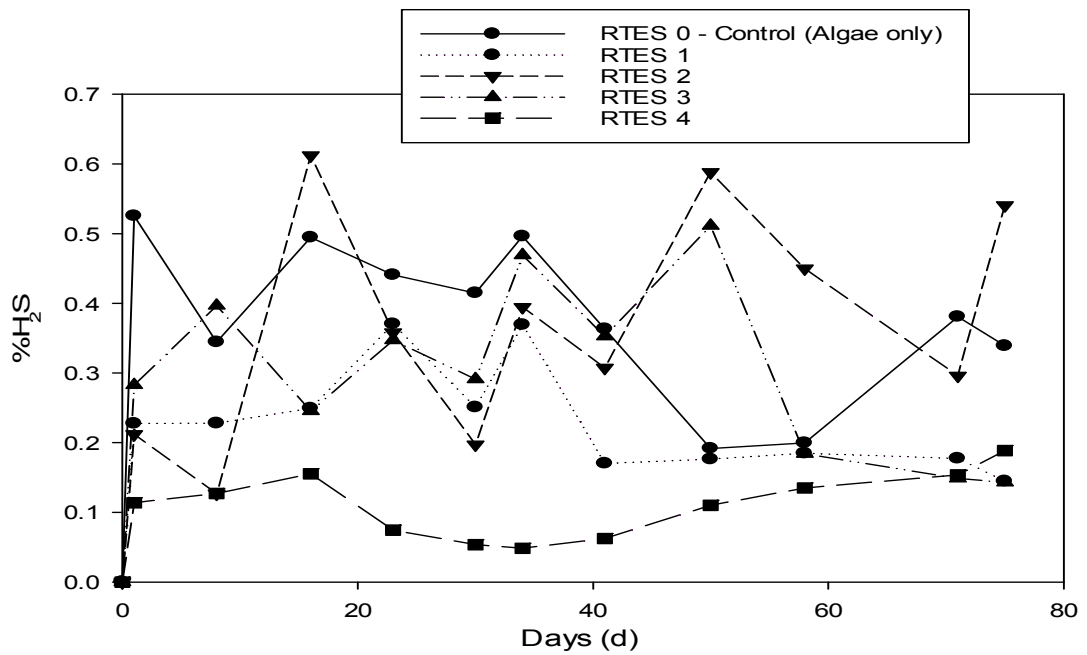


Figure 10-5 % Hydrogen sulphide production in continuous reactors (RTES 0 – 4).

Table 10-2 shows the trace element contribution from the algae and inoculum before the start of digestion and at the end of the test. The supplemented reactors performance were compared to the control. The methane yields for the reactors are obtained from average data of between 5 - 15 days of stable and pseudo-steady gas production, regarded as when the deviation is less than 5-10% for consecutive five days (Li *et al.*, 2013a).

Table 10-2 : Trace element concentration in algae substrate and inoculum at the start of the experiment, and the concentration in the reactors at the end of the experiment.

Start of Experiment			End of experiment				
Trace element	Algae	Innoculum / Control	Control RTES 0	Reactor 2 RTES 1	Reactor 3 RTES 2	Reactor 4 RTES 3	Reactor 5 RTES 4
	mg/l	mg/l	No metal additions	Se ,Mo (mg/l)	Se , Mo, Co, W (mg/l)	Se, Mo , Co, W , Fe , Ni (mg/l)	Se, Mo, Co, W, Fe , Ni, Zn, Cu (mg/l)
K	737	2597	963	1175	984	991	1083
Al	0.74	3.20	1.21	0.64	1.15	1.37	0.46
Ca	191	600	235	228	266	291	241
Cd	0.00	0.01	0.00	0.00	0.00	0.00	0.00
Co	0.00	0.02	0.00	0.01	1.41	1.95	1.72
Cu	0.08	2.55	0.12	0.11	0.12	0.14	1.16
Fe	1.94	9.33	2.85	1.93	2.28	17	1.41
Mg	153	285	210	229	178	192	186
Mo	0.03	0.09	0.04	2.29	2.31	2.48	2.32
Na	143	464	206	252	208	207	225
Ni	0.13	0.31	0.14	0.12	0.11	10.15	8.95
P	32	186	45	35	39	44	30
Pb	0.00	0.06	0.00	0.18	0.01	0.01	0.00
S	48	63	47	51	39	47	42
Se	0.00	0.01	0.01	1.37	1.43	1.89	1.59
W	0.00	0.19	0.01	0.02	0.38	0.50	0.44

### *Performance of the reactors (Experiment 1)*

#### *RTES 1 (Se and Mo mix)*

Both Se and Mo are component of an enzyme formate dehydrogenase (FDH) (Kayhanian and Rich, 1995), which plays an essential role in energy supply to methylotrophic bacteria's (Tishkov and Popov, 2004). They are part of metals needed for a balanced digestion process (Facchin *et al.*, 2013). At the start of the experiment the initial inoculum concentration of Se and Mo are 0.01 and 0.09 mg l<sup>-1</sup>, this was supplemented in the continuous reactor (RTES 1) by Na<sub>2</sub>SeO<sub>4</sub>.6H<sub>2</sub>O – Selenium (Se), and Na<sub>2</sub>MO<sub>4</sub>.2H<sub>2</sub>O - Molybdenum (Mo) at a dose of 0.1 mg L<sup>-1</sup> daily. From Table 10-2, at the end of the experiment, concentration of Se and Mo had increased slightly to 1.4 and 2.3 mg L<sup>-1</sup>, respectively. The stimulatory ranges reported for Se and Mo are 0.062 and 0.11 - 0.25 mg/kg<sup>-1</sup>, respectively, and at Se concentration above 1.5 mg L<sup>-1</sup>, Zhang *et al.* (2010b) has reported evidence of toxicity on digestion process. Figure 10-2 A shows the performance of the Se and Mo supplemented reactor compared to the control. The volumetric methane production evaluated for the supplemented

and control reactors are 595 and 633 mL CH<sub>4</sub> / reactor while the methane yield are 297 and 317 mL CH<sub>4</sub>/g VS. The cumulative methane produced after 90 days of fermentation, shown in Figure 10-4 A was 5.04 and 5.94 L CH<sub>4</sub> /reactor, respectively. The average methane content in the reactors fluctuated between 58 - 65%, and is similar for both reactors (Figure 10-4 B). The H<sub>2</sub>S concentration in the gas phase with the RTES 1 reactor ranged between 0.14 to 0.36% (v/v) compared to the control reactor which peaked at 0.33% (v/v) within the duration of the experiment, Figure 10-5. The results show RTES 1 (Se and Mo) had a negative effect on methane production compared to the control reactor, a phenomenon which could be attributable to the negative or positive impact intracellular trace metal concentration can have on cell metabolism in AD (Bourven *et al.*, 2017). Since, the trace metals Se and Mo are important in formate oxidation which is a breakdown product of propionic acid, the negative effect cannot be attributed to inhibition caused by propionic acid oxidation (Dong *et al.*, 1994), because it is the lack of it that can trigger accumulation of formate (Banks *et al.*, 2012). Both Se and Mo are required in the synthesis of formate dehydrogenase, which is needed for formate oxidation and by extension the enzymes required for hydrogentrophic methane production (Banks *et al.*, 2012).

The volumetric biogas and methane production for the RTES 1 reactor decreased from day 80 till the end of the experiment, Figure 10-2 A. This period was characterized by decline in pH below 6.7, Figure 10-7 A, when feeding was stopped, and an increase in VFAs production from < 0.5 up to 4.3 g L<sup>-1</sup>, Figure 10-6 A. This is reflected in the FOS: TAC value > 0.5, Figure 10-6 B, showing the instability of the reactor supplemented with RTES 1 continued to increase from day 80, accumulating VFAs (Ripley *et al.*, 1986). It has been shown that supplementation of Se and Mo in reactors help to prevent VFA accumulation (Ariunbaatar *et al.*, 2016) but VFA quickly build up when the OLR is high at which point increasing Se and Mo mix makes no difference, and other factors become limiting which are responsible for the VFAs accumulation (Banks *et al.*, 2012). In this study, using an OLR of 2 gVS.L<sup>-1</sup>.d<sup>-1</sup>, RTES 1 after day 50 began to show rapid buildup of VFAs. The performance of the continuous control reactor (RTES 0) could be attributed to the availability of rich nutrient compounds such as K, P, Mg and S needed by microorganism (Kayhanian and

Rich, 1995; Romero-Güiza *et al.*, 2016; Paritosh *et al.*, 2017). These compounds were present in high concentrations in the algae substrate and inoculum before and at the end of the experiment, Table 10-2, and could have played a stimulatory role in the stability of the control reactor. In their work Facchin *et al.* (2013) found out that supplementation of reactors with inoculum having high level of background trace element had a negative effect on biogas production. The pH of the control reactor declined slightly from 7.5 to 7.2, having a low VFAs concentration  $< 0.5 \text{ g L}^{-1}$  and the FOS: TAC ratio remained below 0.5 over the duration of the experiment.

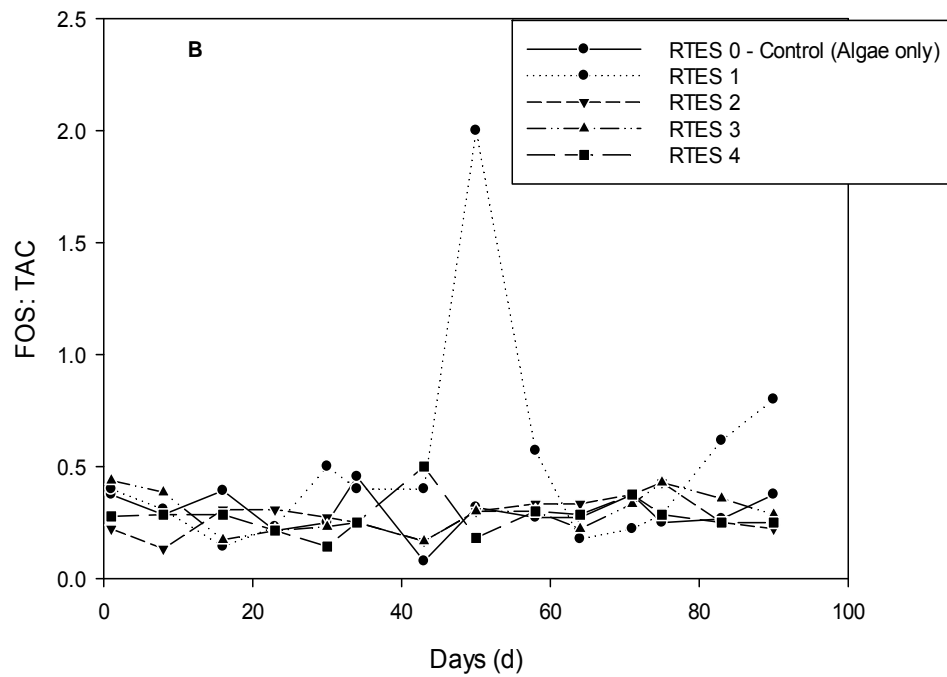
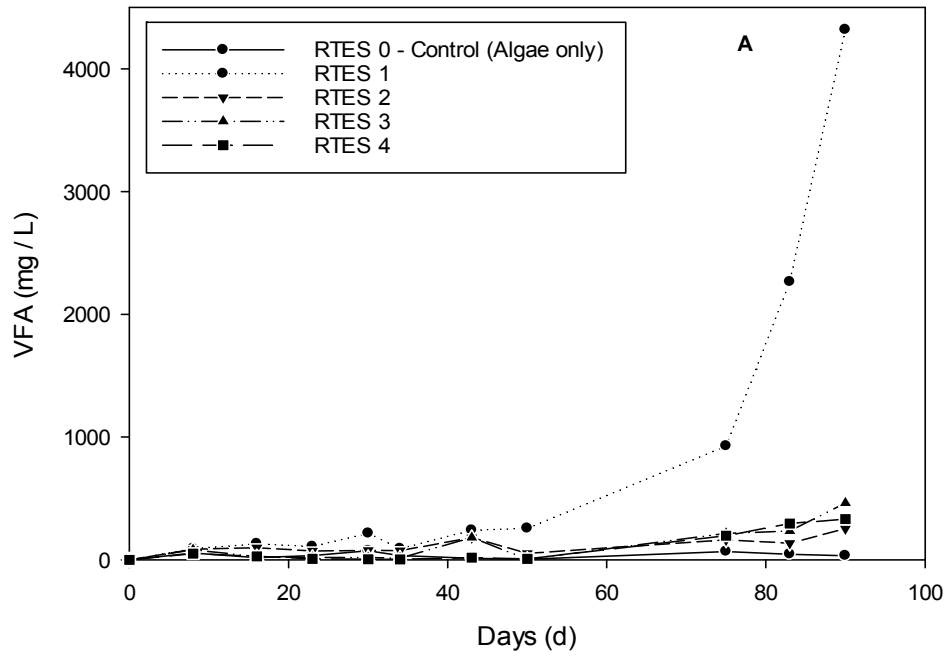


Figure 10-6 A), Volatile fatty acids profile; and B), FOS: TAC ratio in continuous reactors RTES 0 - 4.

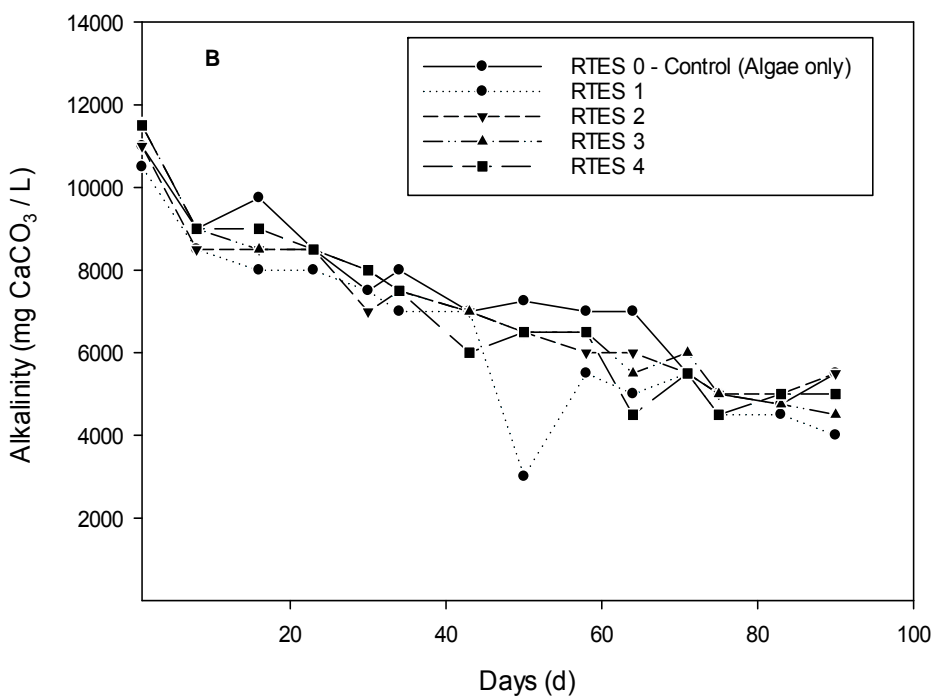
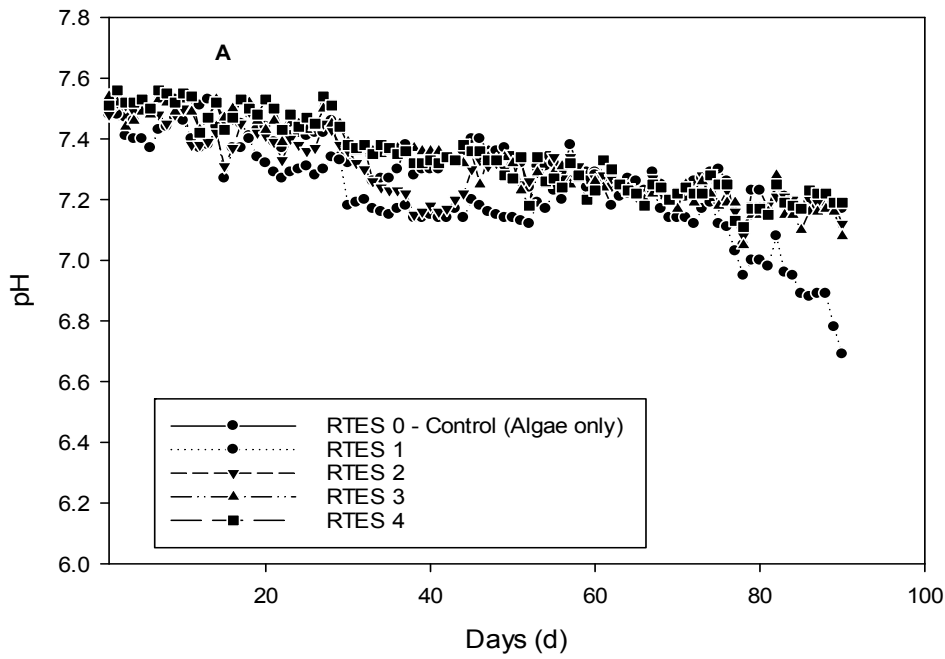


Figure 10-7 A), pH, and B), Alkalinity profile in continuous reactors RTES 0 - 4.



### ***RTES 2 (Se, Mo, Co, W mix)***

In addition to Se and Mo, both Co and W were added to the continuous reactor (RTES 2) in form of  $\text{CoCl}_2 \cdot 6\text{H}_2\text{O}$  – Cobalt (Co) and  $\text{Na}_2\text{WO}_4 \cdot 2\text{H}_2\text{O}$  – Tungsten (W) W at a dose of 0.5 and 0.1 mg L<sup>-1</sup> daily. Cobalt is present in methyl-H<sub>4</sub>SPT, a coenzyme of M methyl-transferase complex of the methanogens (Pobeheim *et al.*, 2010). It is also used by the enzyme, carbon monoxide dehydrogenase (CODH) which participates in acetate-formation, while Tungsten is a part of the FDH enzyme (Kayhanian and Rich, 1995). At the start of the experiment the initial inoculum concentration of Co and W are 0.02 and 0.19 mg L<sup>-1</sup>, after addition of RTES 2 mix and at the end of the feeding period, their concentration increased to 1.41 and 0.38 mg L<sup>-1</sup> compared to 0.01 and 0.02 mg L<sup>-1</sup> for RTES 1, and 0.01 and 0.01 mg L<sup>-1</sup> for the control reactor (RTES 0). Stimulatory concentration ranges reported are 0.05 - 0.19 mg kg<sup>-1</sup> for W, and for Co it is 0.22 mg kg<sup>-1</sup> (Kayhanian and Rich, 1995; Banks *et al.*, 2012). The results of methane production from the continuous reactors, RTES 2 compared to the control RTES 0 is shown in Figure 10-2 B. The volumetric methane production rate are 641 and 633 mL /reactor.d<sup>-1</sup> with a methane yield of 321 and 317 mL CH<sub>4</sub>/g VS, respectively. The cumulative methane produced, also shown in Figure 10-4 A are 5.7 and 5.9 L CH<sub>4</sub> /reactor, respectively. The methane content is similar to that observed in RTES 1, averaging between 55 - 65% for both reactors, Figure 10-4 B. The H<sub>2</sub>S concentration in the gas phase of the reactors fluctuated throughout the experiment between 0.19 - 0.58% (v/v) but peaked on day 34 at 0.61% (v/v) for the RTES 2 while in the control RTES 0 it ranged from 0.14 - 0.37% (v/v), Figure 10-5. The results obtained show the performance of the RTES 2 reactor and the control RTES 0 are similar.

### ***RTES 3 (Se, Mo, Co, W, Fe, Ni mix)***

Additionally, Fe, Ni were added to the combination of elements used in the continuous reactor (RTES 2), and this mixture used to supplement continuous reactor (RTES 3). Fe was added in the form of  $\text{FeCl}_2 \cdot 4\text{H}_2\text{O}$  at a dose of 0.5 mg L<sup>-1</sup>, and Ni as  $\text{NiCl}_2 \cdot 4\text{H}_2\text{O}$  at a dose of 0.5 mg L<sup>-1</sup>. While Fe is found in higher concentrations in methanogenic biomass and plays active roles in reduction processes, Ni is used by cells present in the compound F<sub>430</sub>, a component of methyl-coenzyme M reductase complex used in catalyzing formation of methane (Yao *et al.*, 2016). Nickel is found in every methanogenic bacteria and

in sulphate reducing bacteria through the enzyme carbon monoxide dehydrogenase (CODH) (Kayhanian and Rich, 1995), which contains the factor F420 (Yao *et al.*, 2016). From Table 10-2, the initial concentration of Fe and Ni from the inoculum at the beginning of the fermentation process was 9.33 and 0.31 mg L<sup>-1</sup>, respectively, which increased to about 16.45 and 10.15 mg L<sup>-1</sup> for RTES 3 and 1.93 and 0.12 mg L<sup>-1</sup> for RTES 0, respectively, by the end of the experiment. Kayhanian and Rich (1995) has reported the stimulatory concentration range for Fe as 0 - 0.39 mg L<sup>-1</sup> and Ni 0.11 - 0.25 mg L<sup>-1</sup>. The daily volumetric methane production rate shown in Figure 10-3 A, for the RTES 3 and control RTES 0 are 668 and 633 mL CH<sub>4</sub>/ reactor.d, respectively. Their methane yield is 334 and 317 ml CH<sub>4</sub>/ gVS while the cumulative methane produced after 90 days is 6.1 and 5.9 L CH<sub>4</sub>/ reactor, respectively. The H<sub>2</sub>S concentration in the gas phase for the reactors fluctuated throughout the duration of the experiment between 0.19 - 0.58% (v/v) but peaked on day 34 at 0.61% (v/v) for the RTES 3 while in the RTES 0 it ranged from 0.14 - 0.37% (v/v). The methane content (58 - 68%) and H<sub>2</sub>S (0.14 - 0.51% (v/v)) obtained was similar to what was obtained in RTES 1 and 2. The results show the performance of the RTES 3 was similar to the control RTES 0.

#### *RTES 4 (Se, Mo, Co, W, Fe, Ni, Zn, Cu mix)*

The continuous reactor (RTES 4), was supplemented further with Zn and Cu in addition to the combination mix used in RTES 3. Zn was added in the form of ZnCl<sub>2</sub> and Cu as CuCl<sub>2</sub>. 2H<sub>2</sub>O at a dose of 0.1 and 0.05 mg L<sup>-1</sup>. Both Zn and Cu are found in large concentrations in methanogenic bacteria but reports of their stimulatory effects are scarce (Kayhanian and Rich, 1995). Figure 10-3 B shows the daily volumetric methane production rate which averaged around 668 and 633 mL CH<sub>4</sub>/ reactor.d for the RTES 4 and RTES 0 continuous reactors, respectively. The methane yield obtained was 319 and 317 mL CH<sub>4</sub>/gVS, with a cumulative methane production of 5.90 and 5.94 L CH<sub>4</sub>/ reactor, respectively. The H<sub>2</sub>S concentration in the gas phase was lowest for RTES 4 (0.04 - 0.18% (v/v)) compared to the other reactors. The methane content (53 - 67%) obtained was also similar to what was obtained in RTES 1, 2 and 3. The results shows performance of the RTES 4 compared to the control RTES 0 were also similar.

### *TES reactors process performance (Experiment 1)*

Results of other process performances for the five continuous reactors (RTES 0 – 4) are shown in Figure 10-6 - Figure 10-9. The effect of these process parameters on AD process has been discussed previously in Section 2.11.

The total alkalinity values shown in Figure 10-7 B for the reactors including the control at the start of the experiment was around  $10.0 \text{ g L}^{-1}$ , and gradually reduced to  $5.0 \text{ g L}^{-1}$  except in the RTES 1 digester which dropped to around  $2.8 \text{ g L}^{-1}$  on day 50, reflecting the drop in pH and increase in VFAs, before recovering at day 58.

The TKN and TAN concentration (Figure 10-8 A and B) in all the reactors were also similar, declining from a start value of  $\sim 2.2$  and  $1.7 \text{ g L}^{-1}$  to  $1.3$  and  $< 0.2 \text{ g L}^{-1}$ , respectively. Work by Banks *et al.* (2012) showed continued reduction in TAN concentration in both supplemented and control reactors, with no direct reason being identified for the reduction in the supplemented reactor, while Lindorfer *et al.* (2012) tried to show a correlation between biological nitrogen fixation by TAN and an increase in microbial biomass in the effluent.

The VFAs profile (Figure 10-6 A) shows the starting inoculum in the reactors which had been acclimatized with algae substrate, contained a high concentration of VFAs which declined rapidly at the start of the experiment when OLR was increased in both the RTES 1 - 4 and control RTES 0 reactors. The VFA concentrations in all the RTES reactors, except the reactor with Se and Mo (RTES 1), were all below  $500 \text{ mg L}^{-1}$  at the end of the experiment. This agrees with results reported for digesters dosed with multiple trace elements where stable digestion was achieved, and VFA concentrations did not exceed  $500 \text{ mg L}^{-1}$  (Banks *et al.*, 2012).

The soluble COD (sCOD) concentration profile for the digesters are shown in Figure 10-9. The average sCOD concentration at the start of the experiment was around  $10.0 \text{ g L}^{-1}$  which reduced to  $\sim 4.0 \text{ g L}^{-1}$  except in RTES 2 (Se and Mo) where it was  $\sim 8.0 \text{ g L}^{-1}$ . The RTES 4 digester performed better for sCOD reduction compared to all other reactors, with RTES 2 digester having the lowest performance.

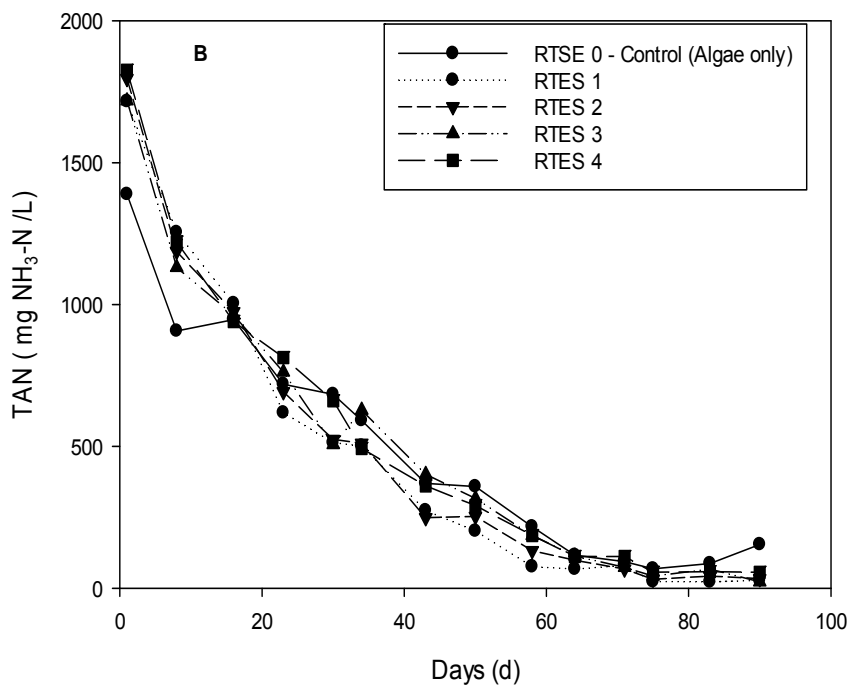
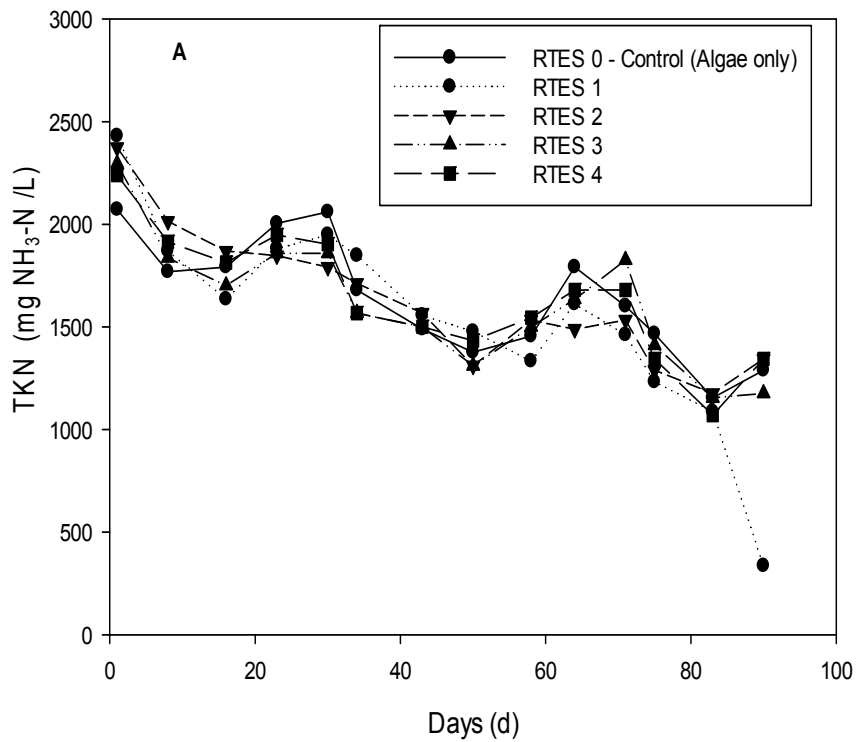


Figure 10-8 A), TKN; and B), TAN concentration profile in continuous reactors RTES 0 - 4.

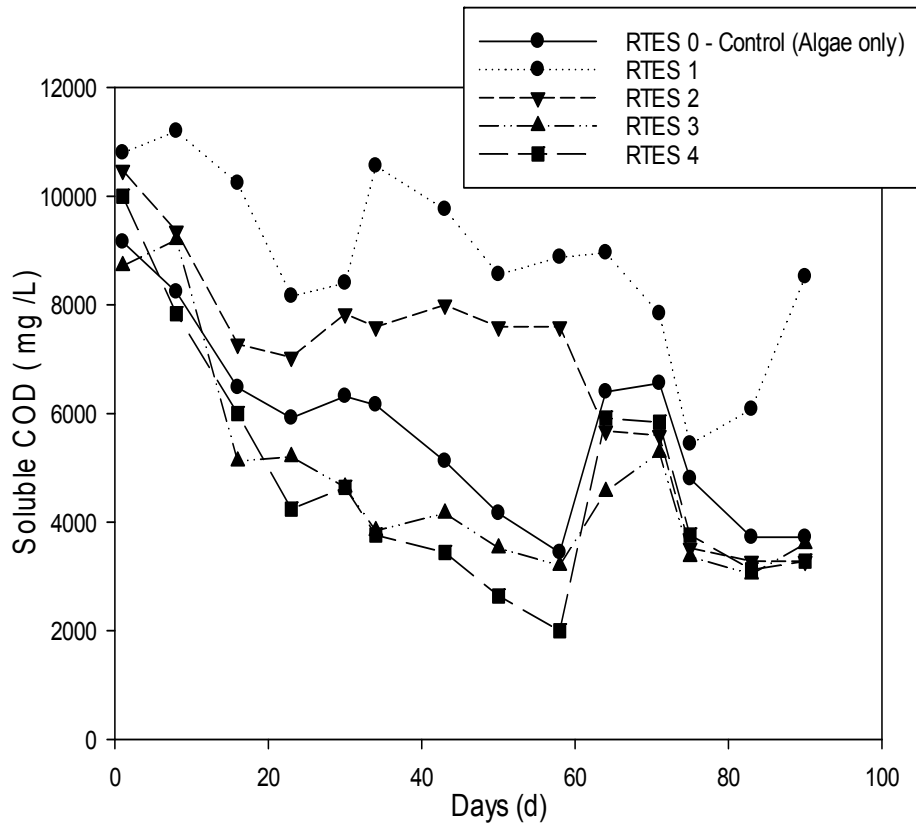


Figure 10-9 Soluble COD concentration profile in continuous reactors RTES 0 - 4.

### 10.3.3 Continuous reactors (Experiment 2)

The continuous digesters (R 1 and R 2) were fed with the algae feedstock once a day over a period of 85 days. In reactor 2, 5 ml of TES – 4 mix was added weekly. Table 10-2 shows the background trace element contribution from the algae and inoculum before the start of digestion and at the end of the experiment.

The variation in CH<sub>4</sub> production and Methane yield (MY) for R 1 and R 2 (TES – 4) with respect to increasing OLR from 2 - 5 gVS.L<sup>-1</sup>.d<sup>-1</sup> over the length of the experiment is shown in Figure 10-10.

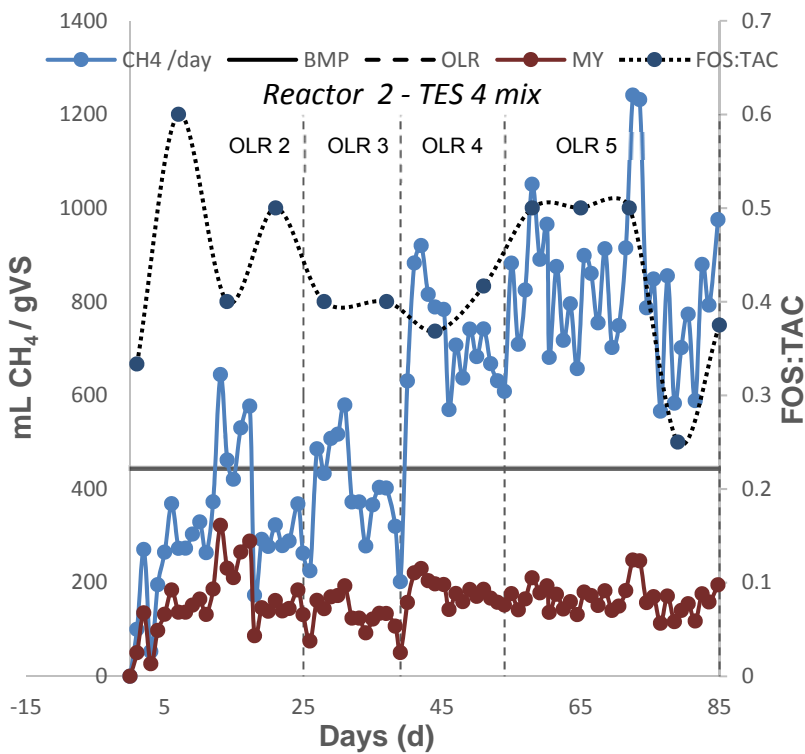
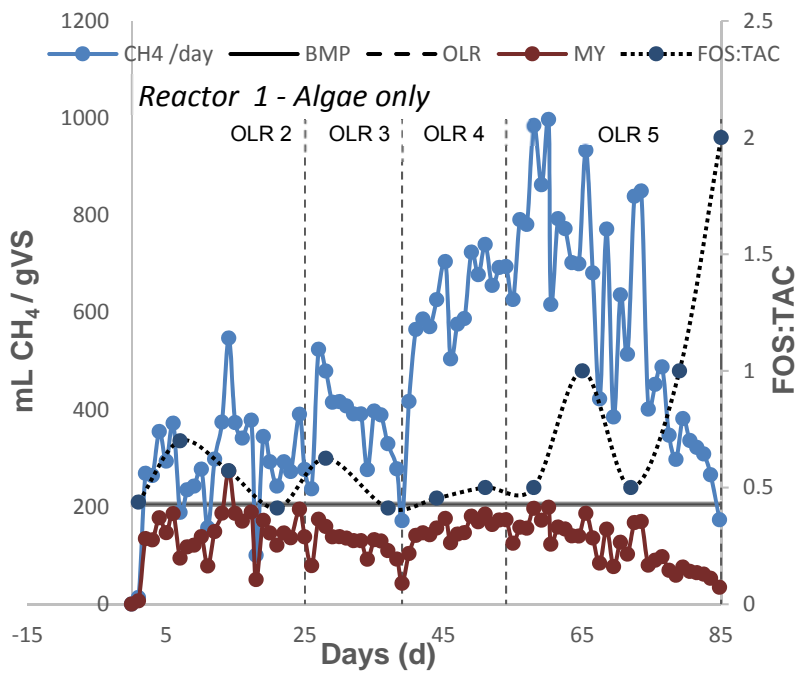


Figure 10-10 Assessment of continuous reactors, reactor 1 and reactor 2 (TES-4) mix: Variations in CH<sub>4</sub> production, MY, BMP ( $\text{mL CH}_4/\text{gVS}$ ), and FOS: TAC ratio with increasing OLR ( $\text{gVS}\cdot\text{L}^{-1}\cdot\text{d}^{-1}$ ). Vertical dashed line indicates organic loading rate (OLR).

A summary of the reactor performance is given in Table 10-4. It has been stated previously that for the continuous process, stable digestion is achieved with a FOS: TAC ratio is between 0.2 - 0.4 and when the MY value approaches the BMP value (Allen *et al.*, 2014).

From Table 10-4, for R 1 and R 2 (TES 4 mix), the biomethane efficiency factor (BEF) averaged between 0.69 - 0.57 and 0.3 – 0.4, respectively, as the OLR was increased from 2 – 5 gVS.L<sup>-1</sup>.d<sup>-1</sup>. The BEF (ratio of the experimental to theoretical methane yield) shows that R 2 with TES 4 addition is not working at optimum yield conditions as higher value of BEF is an indication of better substrate degradation (Allen *et al.*, 2015). The methane yields obtained for TES 4 at OLR 2, 3, 4 and 5 (159, 135, 172 and 166 mL CH<sub>4</sub>/ gVS) were all higher than (144, 127, 148 and 119 mL CH<sub>4</sub>/ gVS) obtained for R 1 (without TES mix) at the same OLR, indicating an increase of 11%, 6%, 16% and 39%, respectively. The % methane decreased slightly in both R 1 and R 2 (TES 4) from 60% to 48%, and from 61% to 56%, respectively.

The tvFA profiles, Figure 10-11 A show that as the OLR was increased, there was a gradual increase in the tvFA in both the TES 4 and control reactors, ranging from ~ 2.7 g L<sup>-1</sup> and 4.7 g L<sup>-1</sup>, respectively, on day 1, to 10.9 g L<sup>-1</sup> and 5.2 g L<sup>-1</sup> on day 51, then to 15.5 g L<sup>-1</sup> and 3.7 g L<sup>-1</sup> by day 85. The continued increase of tvFA from day 51 in the control reactor was characterized by a reduction in methane yield, increase in FOS: TAC ratio from 0.5 - ≥ 2 (Figure 10-10), indicating reactor instability. This caused an increase in COD from 17.8 – 28.8 g L<sup>-1</sup>, Figure 10-12 B, and a drop in pH from 7.40 – 6.45, Figure 10-11 B, leading to reactor failure. However, the TES 4 reactor with FOS: TAC ratio 0.5 - 0.25, COD 10.0 – 14.0 g L<sup>-1</sup>, and pH within 7.52 – 7.58 from day 51, was relatively stable.

The total alkalinity values in the reactor TES 4 and control at the start of the experiment were around 10.0 g L<sup>-1</sup>, which gradually increased to around ~1.7 g L<sup>-1</sup> before reducing to ~ 11.0 g L<sup>-1</sup> in TES 4 and ~ 9.0 g L<sup>-1</sup> in R 1, respectively, Figure 10-12 A. The TAN concentration in both reactors continued to decline as the OLR was increased from a start value of ~ 1.7 and 1.6 g L<sup>-1</sup> to 0.86 and < 0.45 g L<sup>-1</sup> for TES 4 and control reactors, respectively.

Table 10-3 Summary of the results for the continuous reactors with and without trace element supplementation (Experiment 2).

Start of experiment			End of experiment	
Trace elements	Inoculum/control	algae feedstock	Control Reactor 1	Reactor 2 (TES 4 Mix)
	mg/l	mg/l	No metal addition (mg/l)	Se, Mo, Co, W, Fe, Ni, Zn, Cu (mg/l)
Al	11.61	0.00	2.52	2.86
As	0.00	0.00	1.02	0.0
B	0.74	2.10	4.39	4.69
Ba	0.92	0.18	0.96	0.49
Ca	355	206	479	371
Cd	0.00	0.02	0.04	0.0
Co	0.07	0.00	0.04	2.93
Cr	0.14	0.04	0.08	0.08
Cu	0.84	0.03	0.63	0.34
Fe	21.41	3.58	8.38	13.92
K	702	496	2229	3054
Mg	135	130	316	351
Mn	2.24	0.07	0.29	0.34
Na	78	93	270	338
Ni	0.12	0.10	0.20	3.33
Pb	0.28	0.00	0.17	0.0
Si	0.00	0.00	2.29	4.0
V	0.00	0.00	0.02	0.0
Zn	5.19	0.83	2.44	2.5
Ti	0.14	0.01	0.00	0.02
Se	0.77	0.00	0.00	0.63

Table 10-4 Summary of the results for the continuous reactors with and without trace element supplementation (Experiment 2).

OLR (kg VS / L / d)	BMP (L CH <sub>4</sub> / kg VS)	MY(L CH <sub>4</sub> / kg VS)	CH <sub>4</sub> efficiency factor	CH <sub>4</sub> (%)	FOS:TAC	pH
<i>R 1 Control- (Algae only)</i>						
	207 ± 0.07					
OLR 2		144	0.70	60	0.40	7.38
OLR 3		127	0.61	57	0.50	7.36
OLR 4		148	0.72	53	0.47	7.34
OLR 5		119	0.57	48	1	7.11
<i>Reactor 2 - TES 4 mix (Se, Mo, Co, W, Fe, Ni, Zn, Cu)</i>						
OLR 2	440 ± 0.11	159	0.36	61	0.37	7.38
OLR 3		135	0.30	60	0.40	7.36
OLR 4		172	0.39	56	0.39	7.35
OLR 5		166	0.37	56	0.43	7.29



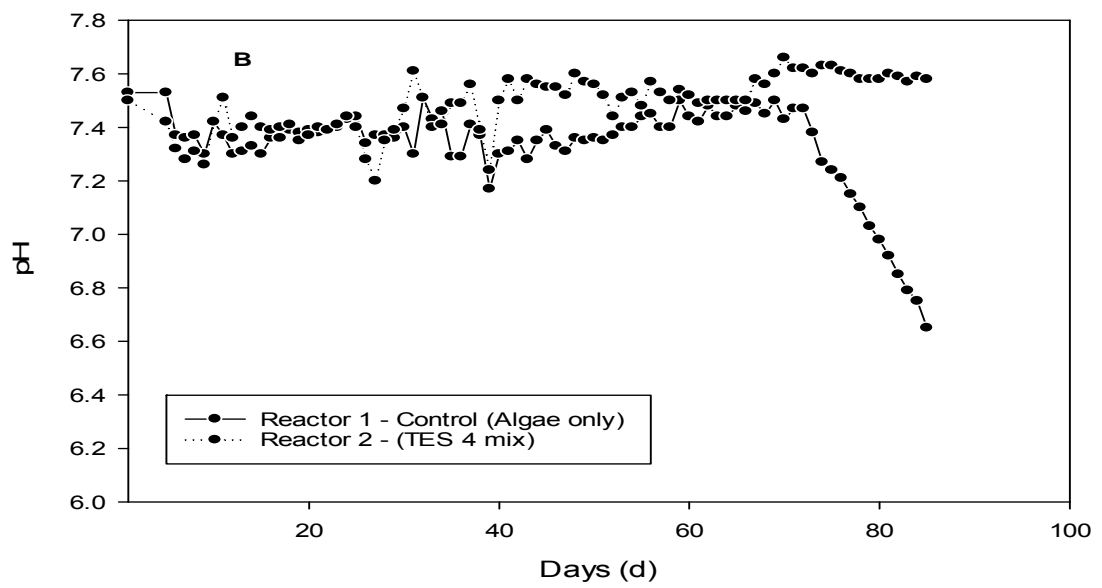
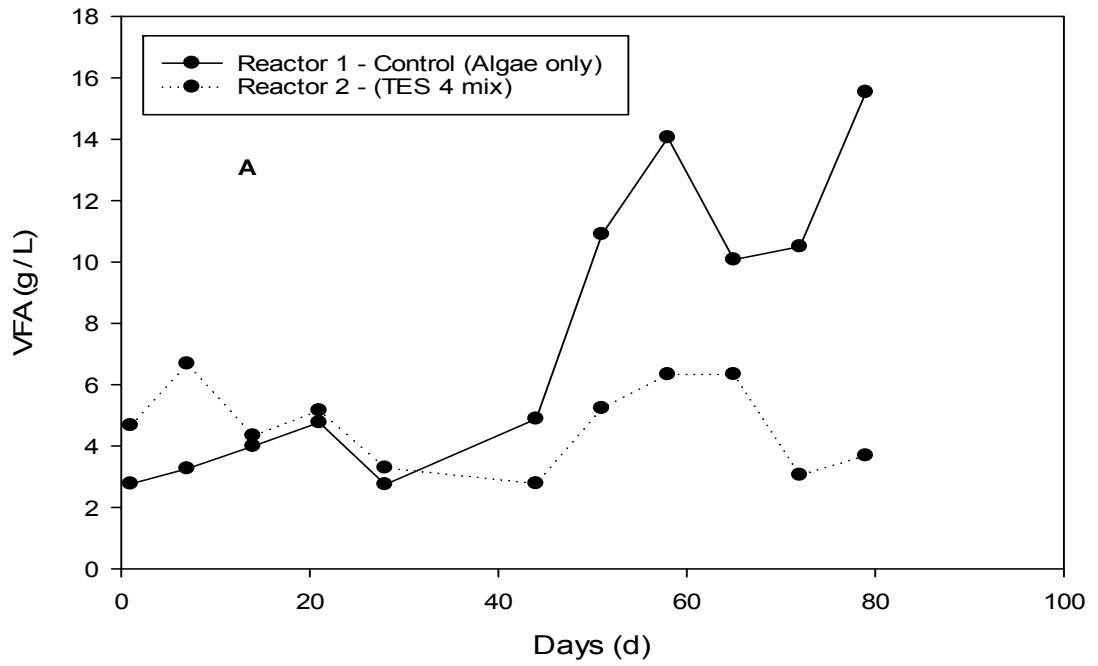


Figure 10-11 A), Volatile fatty acid; and B), pH concentration profile in continuous reactors R 1 and R 2 (TES 4 mix).

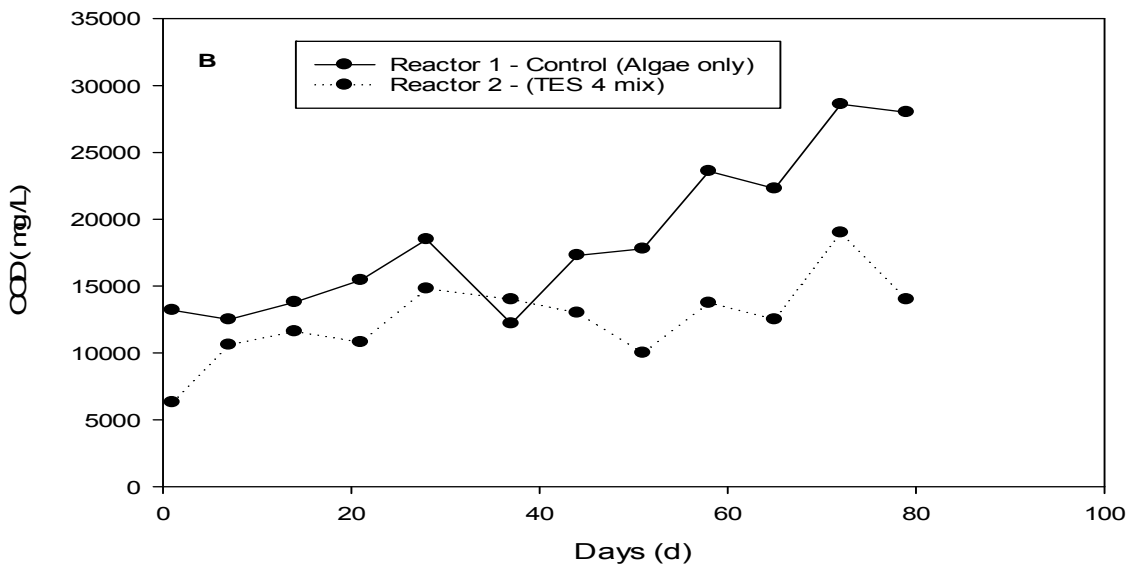
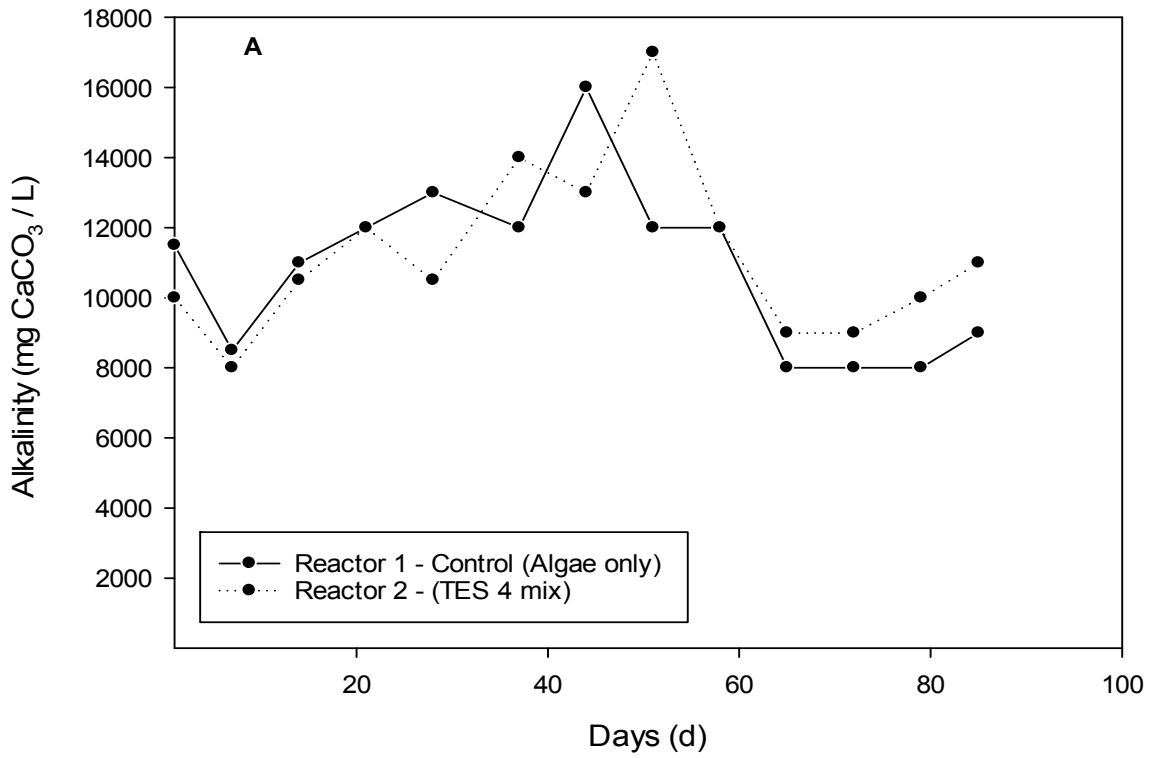


Figure 10-12 A), Alkalinity; and B), COD concentration profile in continuous reactors R 1 and R 2 (TES 4 mix).

## 10.4 Conclusion

Trace elements are needed by microorganism for growth but if added in excess amounts to anaerobic digesters they can lead to inhibition (Thanh *et al.*, 2016). The addition of both micro and macro nutrients for AD processes have been reported previously (Romero-Güiza *et al.*, 2016). The results obtained from the current batch experiments show that the methane yield of the TES 1 - 4 reactors was between 17 - 50% higher than the control reactor (without TES). In the continuous reactors, Experiment 1, where the OLR of  $2 \text{ gVS.L}^{-1}.\text{d}^{-1}$  was maintained throughout the duration of the experiment, and where the TES 1 - 4 mix was added daily in reactors (RTES 1 – 4), results showed no significant difference in performance of these reactors compared to the control reactor (RTES 0) without metal addition. In the second continuous reactor (Experiment 2), where there was a step-wise increase in OLR from  $2 - 5 \text{ gVS.L}^{-1}.\text{d}^{-1}$ , and a weekly addition of TES 4 mix, the TES 4 reactor (R 2) showed better performance compared to the control reactor without TES (R 1), which was characterised by high tVFA, increased FOS: TAC ratio and a drop in pH,, leading to reactor failure.

## Chapter 11. General discussion and conclusion

Renewable energy sources can provide an alternative to current fossil fuel supplies worldwide only if methods are available to extract, use and store the energy conveniently at a cheaper cost. The development of renewable energy has seen a recent increase in the amount of research on anaerobic digestion technologies because it is an environmentally friendly option. Although relatively small amounts of municipal solid waste (MSW) are currently converted to methane in dedicated digester systems, that situation is set to change substantially in the near future as food waste, biodegradable municipal waste fractions, energy crops, and potentially seaweed, are used either as mono or co-digested feedstocks for these systems. Currently, attention has turned to the use of marine biomass to either replace or supplement terrestrial biomass as a source of feedstock for biofuel production. In 2015 a communication by the EU Environment Committee stated that at least 1.25% of energy consumption in transport by 2020 should come from advanced biofuels from seaweed or certain types of waste (European Parliament, 2015). Seaweed also known as macroalgae is considered as a major alternative feedstock, and *L. digitata*, in particular, has been reported as a viable feedstock due to its high content of fermentable carbohydrates (Tabassum *et al.*, 2017). Seaweeds are evolutionarily diverse and abundant in the world's oceans and coastal waters, and as biomass can be biologically degraded, and sometimes are detrimental to the amenity of coastal bays by causing eutrophication in water bodies. Therefore, they offer a vast renewable energy resource for countries throughout the world that have available coastline, yet energy production from them is still limited due to economic viability. Sustainable bio-energy production using macroalgae as feedstock offers one way to overcome this inherent economic barrier. Potentially, this limitation will be overcome with increases in research on anaerobic digestion technologies based on mixed co-digestion of renewable feedstocks (energy crops, municipal solid waste, and lignocellulose biomass) and energy policy targets like Kyoto protocol, Directive 2009/28/EC, and US Renewable Fuels Standard. One encouraging area for the potential of large-scale biofuel production from macroalgae is the growing innovative technologies used in its cultivation and storage (Integrated farming (polyculture), natural

seaweed seabeds, Tank/ lagoons, and ponds). Because macroalgae have high levels of carbohydrates, low lipid and negligible lignin content they can be converted efficiently into biogas and liquid fuels, and more recently bio-oils from thermal processes such as pyrolysis. Biomaterials produced from macroalgae include alginates for gel production, carrageenan, agars and phycocolloids and  $^1\text{H}$  NMR had historically been used for structural analysis of extracted alginates.

Algae biomass has demonstrated an ability to remain intact and undigested during anaerobic digestion, because the cell wall is resistant to bacteria attack. Pre-treatment is one way of overcoming this challenge. Samples of *Laminaria digitata* used in this study were all pre-treated and dried, with results from the BMP evidently showing the potential of this biomass for large-scale fuel production. In *Chapter 4* a modified BMP test method developed in the current study using Supel™ inert gas sampling bags as biogas collection and storage system, was well suited for use with macroalgae. The BMP results on pre-treated and dried *Laminaria* samples gave yields of between  $141 \pm 5.77$  mL  $\text{CH}_4$  gVS $^{-1}$  and  $207 \pm 0.07$  mL  $\text{CH}_4$  gVS $^{-1}$ .

In *Chapter 5* it was shown that *Laminaria digitata* exhibited a stepwise degradation pathway similar to thermal decomposition of the different biopolymers observed using TGA and from the pyrograms obtained from Py-GC/MS, sixty-four compounds were identified present in all samples, twenty which have been previously reported as major pyrolysis products.  $^1\text{H}$  NMR analysis identified the monad, diad, and triad frequencies (homopolymeric mannuronic and guluronic) blocks with their alternating block fractions and the average block lengths. The M/G ratio value of the alginates extracted from *L. digitata* collected from *UK* shores shows it can be used to produce soft and elastic gels. Alginates have a major consequence for efficient AD because alginates degrades to glyceraldehyde-3-phosphate and pyruvate during anaerobic digestion but it has been shown that about 13 – 15% of the alginate remained insoluble during alginate degradation (Moen *et al.*, 1997), as accumulated alginate in the periplasm of a cell is reported to have a lethal effect on cells (Rehm and Moradali, 2017). This presumably can amount to within 1.3 – 6% of the macroalgae feedstock that remain as particulate matter in solution during digestion because alginate constitute about 10 - 40% of the macroalgae

components. Methods that enhance their solubilisation during anaerobic digestion can aid in higher biogas production.

In the continuous fermentation study, *Chapter 7* the effect of temperature showed the mesophilic temperature range was better than the thermophilic condition, and can be more cost-effective. Optimisation techniques described in *Chapter 8* can be used for process improvements by using modelling approach to predict optimal reactors conditions for optimised methane production which can be beneficial when commercialisation is considered. Results from the study of mono and co-digestion of the *L digitata* feedstock with food waste in *Chapter 9* shows that co-digestion has inherent advantages and would be the preferred option for long-term continuous digestion as the mono-feedstock was characterised by reactor instability and eventual failure, while all the co-digested mixed feedstock reactors were stable. Synergy and beneficial effects were observed with mixed feedstocks which enhanced continuous gas production at high loading rates as a result of the microbial community acclimatization to high salinity (chloride) level in the presence of low ammonia concentration and dilution of inhibitory components which were not evident in the mono-digested reactor.

In *Chapter 10* the addition of trace elements with particular reference to TES 4 mixture (Se, Mo, Co, W, Fe, Ni, Zn, Cu), and at the concentrations used in this study was found to be beneficial and improved methane yield with process stability in the continuous reactor when added weekly. This demonstrates that at the right combination and dosing levels, trace element supplementation in anaerobic reactors treating macroalgae will have a positive impact.

In conclusion, the current study shows that the use of brown macroalgae, *L digitata* as a biomass resource for biofuel production has an enormous potential and is feasible. By encouraging research into new technologies and techniques for integrated cultivation, and a biofinery centred on anaerobic digestion of the algal biomass, the use of its residual after extraction processes, and co-digestion, this macroalgae on a large-scale can actualize its potential to be used as an alternative renewable feedstock.

## 11.1 Recommendation

Biofuel production sustainability is presently a major limitation to the achievement of EU 2020 vision of reaching 1.25% of transport fuel from seaweed. The current study shows the feasibility of using macroalgae for biogas production via anaerobic digestion (AD), in which the produced biogas could then be treated and converted to electrical power for heating and transport purposes. AD has the advantage of being a low cost, and low maintenance technology which is capable of working on feedstocks from a wide range of seaweed species. In order to achieve a net energy gain in the production of biofuel from seaweed, the location, cultivation, harvesting and storage of seaweed are key factors to consider. The UK for instance can be considered to be strategically placed to leverage from its long coastline (populated with many different types of seaweed), strong research base in anaerobic digestion on seaweed across several universities, and the vast experience in AD from current pilot and commercial anaerobic digesters, in order to bring about the much needed step from laboratory based studies to full-scale processes and commercialisation. This will not only contribute towards meeting the EU-set target, but will also create employment opportunities, and clean up the ocean water bodies affected by seaweed eutrophication.

In order for the UK to be a lead player in sustainable energy development from this point of view, an integrated systems approach (ISP) should be encouraged. This will involve seaweed cultivation with existing aquaculture resources and co-digestion with other waste streams together conversion processes for heat and steam for upcoming facilities.

With respect to the outcome of this study, the following points are highlighted and could be beneficial if taken into consideration during the set-up of large-scale facilities;

- ✓ While mono-digestion of seaweed is feasible, co-digestion with other waste materials will be a better option for overall energy balance in large scale operations and should be investigated in long-term processes.
- ✓ A balance between appropriate HRT and OLR should be applied during its anaerobic digestion of this macroalgae feedstock.

- ✓ The mesophilic temperature range was shown to be advantageous and should be recommended for large scale production in preference to thermophilic digestion.
- ✓ Integrated approach in seaweed cultivation, bio-products extraction and energy generation with currently existing units should be encouraged to reduce cultivation costs.
- ✓ The use of trace element in seaweed digestion will increase an overall gas yield

#### 11.1.1 *Areas recommended for further studies using brown seaweed.*

- ✓ Cost benefit analysis of the use of LD in large scale operation (from cultivation to biofuels production).
- ✓ The cost of seaweed harvesting is a major limitation in the aquaculture production process, studies with respect to cost effective innovative technology in seaweed cultivation are needed.
- ✓ Pre-treatment targeted at salt removal as a solution to problems related to salt accumulation / inhibition.
- ✓ Studies on optimum nitrogen concentrations together with sulphide inhibition should be investigated.
- ✓ Biofuels other than methane such as bio-butanol should be investigated from brown algae feedstock.



## Chapter 12. References

- Adams, J.M., Gallagher, J.A. and Donnison, I.S. (2008) 'Fermentation study on *Saccharina latissima* for bioethanol production considering variable pre-treatments', *Journal of Applied Phycology*, 21(5), p. 569.
- Adams, J.M.M., Ross, A.B., Anastasakis, K., Hodgson, E.M., Gallagher, J.A., Jones, J.M. and Donnison, I.S. (2011a) 'Seasonal variation in the chemical composition of the bioenergy feedstock *Laminaria digitata* for thermochemical conversion', *Bioresource Technology*, 102(1), pp. 226-234.
- Adams, J.M.M., Toop, T.A., Donnison, I.S. and Gallagher, J.A. (2011b) 'Seasonal variation in *Laminaria digitata* and its impact on biochemical conversion routes to biofuels', *Bioresource Technology*, 102(21), pp. 9976-9984.
- Ağdağ, O.N. and Sponza, D.T. (2007) 'Co-digestion of mixed industrial sludge with municipal solid wastes in anaerobic simulated landfilling bioreactors', *Journal of Hazardous Materials*, 140(1–2), pp. 75-85.
- Ahring, B.K., Angelidaki, I. and Johansen, K. (1992) 'Anaerobic treatment of manure together with industrial waste', *Water science and technology*, 25(7), pp. 311-318.
- Ahring, B.K., Sandberg, M. and Angelidaki, I. (1995) 'Volatile fatty acids as indicators of process imbalance in anaerobic digestors', *Applied Microbiology and Biotechnology*, 43(3), pp. 559-565.
- Aitken, D. and Antizar-Ladislao, B. (2012) 'Achieving a green solution: limitations and focus points for sustainable algal fuels', *Energies*, 5(5), pp. 1613-1647.
- Aitken, D., Bulboa, C., Godoy-Faundez, A., Turrion-Gomez, J.L. and Antizar-Ladislao, B. (2014) 'Life cycle assessment of macroalgae cultivation and processing for biofuel production', *Journal of Cleaner Production*, 75, pp. 45-56.
- Allen, E., Browne, J., Hynes, S. and Murphy, J.D. (2013a) 'The potential of algae blooms to produce renewable gaseous fuel', *Waste Management*, 33(11), pp. 2425-2433.
- Allen, E., Browne, J.D. and Murphy, J.D. (2013b) 'Evaluation of the biomethane yield from anaerobic co-digestion of nitrogenous substrates', *Environmental technology*, 34(13-14), pp. 2059-2068.
- Allen, E., Wall, D.M., Herrmann, C. and Murphy, J.D. (2014) 'Investigation of the optimal percentage of green seaweed that may be co-digested with dairy slurry to produce gaseous biofuel', *Bioresource Technology*, 170, pp. 436-444.

- Allen, E., Wall, D.M., Herrmann, C., Xia, A. and Murphy, J.D. (2015) 'What is the gross energy yield of third generation gaseous biofuel sourced from seaweed?', *Energy*, 81, pp. 352-360.
- Allen, S.G. (1974) *Chemical analysis of ecological materials*. Oxford: Blackwell.
- Altaş, L. (2009) 'Inhibitory effect of heavy metals on methane-producing anaerobic granular sludge', *Journal of Hazardous Materials*, 162(2–3), pp. 1551-1556.
- Alvarez, R. and Lidén, G. (2008) 'Semi-continuous co-digestion of solid slaughterhouse waste, manure, and fruit and vegetable waste', *Renewable Energy*, 33(4), pp. 726-734.
- Alves, A., Sousa, R.A. and Reis, R.L. (2013) 'A practical perspective on ulvan extracted from green algae', *Journal of Applied Phycology*, 25(2), pp. 407-424.
- Alves, M.M., Mota Vieira, J.A., Álvares Pereira, R.M., Pereira, M.A. and Mota, M. (2001) 'Effects of lipids and oleic acid on biomass development in anaerobic fixed-bed reactors. Part II: Oleic acid toxicity and biodegradability', *Water Research*, 35(1), pp. 264-270.
- Amsler, C.D. and Fairhead, V.A. (2006) 'Defensive and sensory chemical ecology of brown algae', in Callow, J.A. (ed.) *Advances in Botanical Research, Vol 43: Incorporating Advances in Plant Pathology*. pp. 1-91.
- An, D., Wang, T., Zhou, Q., Wang, C., Yang, Q., Xu, B. and Zhang, Q. (2017) 'Effects of total solids content on performance of sludge mesophilic anaerobic digestion and dewaterability of digested sludge', *Waste Management*, 62(Supplement C), pp. 188-193.
- Anastasakis, K., Ross, A.B. and Jones, J.M. (2011) 'Pyrolysis behaviour of the main carbohydrates of brown macro-algae', *Fuel*, 90(2), pp. 598-607.
- Angelidaki, I. and Ahring, B.K. (1993) 'Thermophilic anaerobic digestion of livestock waste: the effect of ammonia', *Applied Microbiology and Biotechnology*, 38(4), pp. 560-564.
- Angelidaki, I., Alves, M., Bolzonella, D., Borzacconi, L., Campos, J.L., Guwy, A.J., Kalyuzhnyi, S., Jenicek, P. and Van Lier, J.B. (2009) 'Defining the biomethane potential (BMP) of solid organic wastes and energy crops: a proposed protocol for batch assays', *Water science and technology ; journal of the International Association on Water Pollution Research*, Vol.59(5), pp. 927-34
- Angelidaki, I., Ellegaard, L. and Ahring, B.K. (1993) 'A mathematical model for dynamic simulation of anaerobic digestion of complex substrates: focusing on ammonia inhibition', *Biotechnology and bioengineering*, 42(2), pp. 159-166.

Angelidaki, I., Ellegaard, L. and Ahring, B.K. (1999) 'A comprehensive model of anaerobic bioconversion of complex substrates to biogas', *Biotechnology and bioengineering*, 63(3), pp. 363-372.

Angelidaki, I. and Sanders, W. (2004) 'Assessment of the anaerobic biodegradability of macropollutants', *Re/Views in Environmental Science & Bio/Technology*, 3(2), pp. 117-129.

Antonopoulou, G., Stamatelatou, K. and Lyberatos, G. (2010) 'Exploitation of rapeseed and sunflower residues for methane generation through anaerobic digestion: the effect of pretreatment', *CHEMICAL ENGINEERING*, 20.

APHA (2005) *Standard Methods for the Examination of Water and Wastewater*. American Public Health Association.

Apostolidis, E., Karayannakidis, P.D., Kwon, Y.-I., Lee, C.M. and Seeram, N.P. (2011) 'Seasonal Variation of Phenolic Antioxidant-mediated  $\alpha$ -glucosidase Inhibition of *Ascophyllum nodosum*', *Plant Foods for Human Nutrition*, 66(4), pp. 313-319.

Appels, L., Baeyens, J., Degrève, J. and Dewil, R. (2008) 'Principles and potential of the anaerobic digestion of waste-activated sludge', *Progress in energy and combustion science*, 34(6), pp. 755-781.

Ariunbaatar, J., Esposito, G., Yeh, D.H. and Lens, P.N.L. (2016) 'Enhanced anaerobic digestion of food waste by supplementing trace elements: role of Selenium (VI) and Iron (II)', *Frontiers in Environmental Science*, 4, p. 8.

Arnold, T.M. and Targett, N.M. (2000) 'Evidence for metabolic turnover of polyphenolics in tropical brown algae', *Journal of chemical ecology*, 26(6), pp. 1393-1410.

Aspé, E., Marti, M.C. and Roeckel, M. (1997) 'Anaerobic treatment of fishery wastewater using a marine sediment inoculum', *Water Research*, 31(9), pp. 2147-2160.

Astals, S., Nolla-Ardèvol, V. and Mata-Alvarez, J. (2013) 'Thermophilic co-digestion of pig manure and crude glycerol: Process performance and digestate stability', *Journal of Biotechnology*, 166(3), pp. 97-104.

ASTM F2259. (2012) 'Standard Test Method for Determining the Chemical Composition and Sequence in Alginate by Proton Nuclear Magnetic Resonance (1H NMR) Spectroscopy', ASTM International, West Conshohocken, PA, 2012, <https://doi.org/10.1520/F2259-10R12E01>", *ASTM International, West Conshohocken, PA, 2012*.

Ayala-Parra, P., Liu, Y., Field, J.A. and Sierra-Alvarez, R. (2017) 'Nutrient recovery and biogas generation from the anaerobic digestion of waste biomass

from algal biofuel production', *Renewable Energy*, 108(Supplement C), pp. 410-416.

Banks, C.J., Chesshire, M., Heaven, S. and Arnold, R. (2011) 'Anaerobic digestion of source-segregated domestic food waste: Performance assessment by mass and energy balance', *Bioresource Technology*, 102(2), pp. 612-620.

Banks, C.J., Zhang, Y., Jiang, Y. and Heaven, S. (2012) 'Trace element requirements for stable food waste digestion at elevated ammonia concentrations', *Bioresource Technology*, 104, pp. 127-135.

Barbot, Y., Thomsen, C., Thomsen, L. and Benz, R. (2015) 'Anaerobic Digestion of Laminaria japonica Waste from Industrial Production Residues in Laboratory- and Pilot-Scale', *Marine Drugs*, 13(9), p. 5947.

Barsanti, L. (2006) *Algae : anatomy, biochemistry, and biotechnology*. Boca Raton, Fla. London.

Barsanti, L. and Gualtieri, P. (2014) *Algae: anatomy, biochemistry, and biotechnology*. CRC press.

Batstone, D.J., Keller, J., Angelidaki, I., Kalyuzhnyi, S.V., Pavlostathis, S.G., Rozzi, A., Sanders, W.T.M., Siegrist, H. and Vavilin, V.A. (2002) 'The IWA Anaerobic Digestion Model No 1(ADM 1)', *Water Science & Technology*, 45(10), pp. 65-73.

Begum, L. (2014) *Advanced processes and technologies for enhanced anaerobic digestion*. Ontario: Ontario : Green Nook Press.

Bezerra, M.A., Santelli, R.E., Oliveira, E.P., Villar, L.S. and Escaleira, L.A. (2008) 'Response surface methodology (RSM) as a tool for optimization in analytical chemistry', *Talanta*, 76(5), pp. 965-977.

Bird, K., Chynoweth, D. and Jerger, D. (1990) 'Effects of marine algal proximate composition on methane yields', *Journal of Applied Phycology*, 2(3), pp. 207-213.

Bixler, H.J. and Porse, H. (2011) 'A decade of change in the seaweed hydrocolloids industry', *Journal of Applied Phycology*, 23(3), pp. 321-335.

Bjornsson, L., Murto, M. and Mattiasson, B. (2000) 'Evaluation of parameters for monitoring an anaerobic co-digestion process', *Applied Microbiology And Biotechnology*, 54(6), pp. 844-849.

Blanco, L. and Isenhouer, M. (2010) 'Powering America: The impact of ethanol production in the Corn Belt states', *Energy Economics*, 32(6), pp. 1228-1234.

Bleakley, S. and Hayes, M. (2017) 'Algal Proteins: Extraction, Application, and Challenges Concerning Production', *Foods*, 6(5), p. 33.

Boe, K. (2006) *Online monitoring and control of the biogas process*. Technical University of Denmark Danmarks Tekniske Universitet, Department of Systems Biology Institut for Systembiologi, PhD Thesis.

Bohutskyi, P. and Bouwer, E. (2013) 'Biogas Production from Algae and Cyanobacteria Through Anaerobic Digestion: A Review, Analysis, and Research Needs', in Lee, J.W. (ed.) *Advanced Biofuels and Bioproducts*. New York, NY: Springer New York, pp. 873-975.

Bojko, M., Madsen, F., Olsen, C.E. and Engelsen, S.B. (2002) 'Physico-chemical characterization of floridean starch of red algae', *Starch/Stärke*, 54, pp. 66-74.

Bold, H.C. and Wynne, M.J. (1985) *Introduction to the algae : structure and reproduction*. 2nd ed.. edn. Englewood Cliffs, N.J.: Englewood Cliffs, N.J. : Prentice-Hall.

Bolzonella, D., Fatone, F., Pavan, P. and Cecchi, F. (2005) 'Anaerobic fermentation of organic municipal solid wastes for the production of soluble organic compounds', *Industrial & engineering chemistry research*, 44(10), pp. 3412-3418.

Bourven, I., Casellas, M., Buzier, R., Lesieur, J., Lenain, J.F., Faix, A., Bressolier, P., Maftah, C. and Guibaud, G. (2017) 'Potential of DGT in a new fractionation approach for studying trace metal element impact on anaerobic digestion: the example of cadmium', *International Biodeterioration & Biodegradation*, 119, pp. 188-195.

BP Global (2015) *Sustainability Report 2015*. Available at: <http://www.bp.com/content/dam/bp/pdf/sustainability/group-reports/bp-sustainability-report-2015.pdf> (Accessed: 13.01.17).

BP Global (2016) *BP Statistical Review of World Energy June 2016*. Available at: <http://www.bp.com/content/dam/bp/pdf/energy-economics/statistical-review-2016/bp-statistical-review-of-world-energy-2016-full-report.pdf> (Accessed: 13.01.17).

Brennan, L. and Owende, P. (2010) 'Biofuels from microalgae—A review of technologies for production, processing, and extractions of biofuels and co-products', *Renewable and Sustainable Energy Reviews*, 14(2), pp. 557-577.

Briand, X. and Morand, P. (1997) 'Anaerobic digestion of *Ulva* sp. 1. Relationship between *Ulva* composition and methanisation', *Journal of Applied Phycology*, 9(6), pp. 511-524.

Brodie, J., Wilbraham, J., Pottas, J. and Guiry, M.D. (2016) 'A revised check-list of the seaweeds of Britain', *Journal of the Marine Biological Association of the United Kingdom*, pp. 1-25.

Browne, J.D., Allen, E. and Murphy, J.D. (2014) 'Assessing the variability in biomethane production from the organic fraction of municipal solid waste in batch and continuous operation', *Applied Energy*, 128, pp. 307-314.

Bruhn, A., Dahl, J., Nielsen, H.B., Nikolaisen, L., Rasmussen, M.B., Markager, S., Olesen, B., Arias, C. and Jensen, P.D. (2011a) 'Bioenergy potential of *Ulva lactuca*: Biomass yield, methane production and combustion', *Bioresource Technology*, 102(3), pp. 2595-2604.

Bruhn, A., Dahl, J., Nielsen, H.B., Nikolaisen, L., Rasmussen, M.B., Markager, S., Olesen, B., Arias, C. and Jensen, P.D. (2011b) 'Bioenergy potential of *Ulva lactuca*: Biomass yield, methane production and combustion', *Bioresource technology*, 102(3), pp. 2595-2604.

Brus, J., Urbanova, M., Czernek, J., Pavelkova, M., Kubova, K., Vyslouzil, J., Abbrent, S., Konefal, R., Horský, J., Vetchy, D., Vysloužil, J. and Kulich, P. (2017) 'Structure and Dynamics of Alginate Gels Cross-Linked by Polyvalent Ions Probed via Solid State NMR Spectroscopy', *Biomacromolecules*.

Bryers, J.D. (1985) 'Structured modeling of the anaerobic digestion of biomass particulates', *Biotechnology and bioengineering*, 27(5), pp. 638-649.

Buck, B.H. and Buchholz, C.M. (2004) 'The offshore-ring: A new system design for the open ocean aquaculture of macroalgae', *Journal of Applied Phycology*, 16(5), pp. 355-368.

Bunker, F. (2012) *Seaweeds of Britain and Ireland*. Plymouth : Wild Nature Press.

Burke, D.A. (2001) 'Dairy waste anaerobic digestion handbook', *Environmental Energy Company*, 6007, pp. 17-27.

Burton, C.H. and Turner, C. (2003) *Manure management: Treatment strategies for sustainable agriculture*. Editions Quae.

Burton, T., Lyons, H., Lerat, Y., Stanley, M. and Rasmussen, M.B. (2009) 'A review of the potential of marine algae as a source of biofuel in Ireland'.

Buschmann, A.H., Camus, C., Infante, J., Neori, A., Israel, Á., Hernández-González, M.C., Pereda, S.V., Gomez-Pinchetti, J.L., Golberg, A., Tadmor-Shalev, N. and Critchley, A.T. (2017) 'Seaweed production: overview of the global state of exploitation, farming and emerging research activity', *European Journal of Phycology*, 52(4), pp. 391-406.

- Buswell, A.M. and Mueller, H.F. (1952) 'Mechanism of methane fermentation', *Industrial & Engineering Chemistry*, 44(3), pp. 550-552.
- Bux, F. and Chisti, Y. (2016) *Algae Biotechnology: Products and Processes*. Springer International Publishing.
- Buyukkamaci, N. and Filibeli, A. (2004) 'Volatile fatty acid formation in an anaerobic hybrid reactor', *Process Biochemistry*, 39(11), pp. 1491-1494.
- Calli, B., Mertoglu, B., Inanc, B. and Yenigun, O. (2005) 'Effects of high free ammonia concentrations on the performances of anaerobic bioreactors', *Process Biochemistry*, 40(3), pp. 1285-1292.
- Calumpong, H.P., Maypa, A.P. and Magbanua, M. (1999) 'Population and alginate yield and quality assessment of four *Sargassum* species in Negros Island, central Philippines', *Hydrobiologia*, 398(0), pp. 211-215.
- Carere, C.R., Sparling, R., Cicek, N. and Levin, D.B. (2008) 'Third Generation Biofuels via Direct Cellulose Fermentation', *International Journal of Molecular Sciences*, 9(7), pp. 1342-1360.
- Carlsson, M., Lagerkvist, A. and Morgan-Sagastume, F. (2012) 'The effects of substrate pre-treatment on anaerobic digestion systems: A review', *Waste Management*, 32(9), pp. 1634-1650.
- Chae, K.J., Yim, S.K., Choi, K.H., Park, W.K. and Lim, D.K. (2002) *Latin American Workshop and Symposium on Anaerobic Digestion*, 7. UNAM. Available at: <http://www.bvsde.paho.org/bvsacd/unam7/swine.pdf>.
- Chai, T. and Draxler, R.R. (2014) 'Root mean square error (RMSE) or mean absolute error (MAE)?', *Geoscientific Model Development Discussions*, 7, pp. 1525-1534.
- Champagne, P. (2008) 'Chapter 9 - Biomass A2 - Letcher, Trevor M', in *Future Energy*. Oxford: Elsevier, pp. 151-170.
- Chan, C.-X., Ho, C.-L. and Phang, S.-M. (2006) 'Trends in seaweed research', *Trends in Plant Science*, 11(4), pp. 165-166.
- Chang, H.N., Kim, N.-J., Kang, J. and Jeong, C.M. (2010) 'Biomass-derived volatile fatty acid platform for fuels and chemicals', *Biotechnology and Bioprocess Engineering*, 15(1), pp. 1-10.
- Charles, W., Walker, L. and Cord-Ruwisch, R. (2009) 'Effect of pre-aeration and inoculum on the start-up of batch thermophilic anaerobic digestion of municipal solid waste', *Bioresource Technology*, 100(8), pp. 2329-2335.

Chen, H., Wang, W., Xue, L., Chen, C., Liu, G. and Zhang, R. (2016) 'Effects of Ammonia on Anaerobic Digestion of Food Waste: Process Performance and Microbial Community', *Energy & Fuels*, 30(7), pp. 5749-5757.

Chen, H., Zhou, D., Luo, G., Zhang, S. and Chen, J. (2015) 'Macroalgae for biofuels production: Progress and perspectives', *Renewable and Sustainable Energy Reviews*, 47(Supplement C), pp. 427-437.

Chen, P.H. and Oswald, W.J. (1998) 'Thermochemical treatment for algal fermentation', *Environment International*, 24(8), pp. 889-897.

Chen, Y., Cheng, J.J. and Creamer, K.S. (2008) 'Inhibition of anaerobic digestion process: A review', *Bioresource Technology*, 99(10), pp. 4044-4064.

Chen, Y., Luo, J., Yan, Y. and Feng, L. (2013) 'Enhanced production of short-chain fatty acid by co-fermentation of waste activated sludge and kitchen waste under alkaline conditions and its application to microbial fuel cells', *Applied Energy*, 102(Supplement C), pp. 1197-1204.

Chen, Z.L., Liu, Z.Z., Sun, X.R., Huang, X.H. and Zhan, J. (2012) *Applied Mechanics and Materials*. Trans Tech Publ.

Cherubini, F. (2010) 'The biorefinery concept: Using biomass instead of oil for producing energy and chemicals', *Energy Conversion and Management*, 51(7), pp. 1412-1421.

Chisti, Y. (2007) 'Biodiesel from microalgae', *Biotechnology Advances*, 25(3), pp. 294-306.

Cho, A. (2010) 'Energy's tricky tradeoffs', *Science (New York, N.Y.)*, 329(5993), p. 786.

Choi, J.-W., Choi, J.H., Suh, D.J. and Kim, H. (2015) 'Feasibility of *Laminaria japonica* as a feedstock for fast pyrolysis in a bubbling fluidized-bed reactor', *Journal of Analytical and Applied Pyrolysis*, 112, pp. 141-149.

Choong, Y.Y., Norli, I., Abdullah, A.Z. and Yhaya, M.F. (2016) 'Impacts of trace element supplementation on the performance of anaerobic digestion process: A critical review', *Bioresource Technology*, 209(Supplement C), pp. 369-379.

Chung, I.K., Beardall, J., Mehta, S., Sahoo, D. and Stojkovic, S. (2011) 'Using marine macroalgae for carbon sequestration: a critical appraisal', *Journal of Applied Phycology*, 23(5), pp. 877-886.

Chynoweth, D.P., Owens, J.M. and Legrand, R. (2001) 'Renewable methane from anaerobic digestion of biomass', *Renewable Energy*, 22(1-3), pp. 1-8.



- Chynoweth, D.P., Turick, C.E., Owens, J.M., Jerger, D.E. and Peck, M.W. (1993) 'Biochemical methane potential of biomass and waste feedstocks', *Biomass and Bioenergy*, 5(1), pp. 95-111.
- Cogan, M. and Antizar-Ladislao, B. (2016) 'The ability of macroalgae to stabilise and optimise the anaerobic digestion of household food waste', *Biomass and Bioenergy*, 86, pp. 146-155.
- Collado-Vides, L. (2001) 'Clonal architecture in marine macroalgae: ecological and evolutionary perspectives', *Evolutionary Ecology*, 15(4-6), pp. 531-545.
- Colleran, E., Pender, S., Philpott, U., O'Flaherty, V. and Leahy, B. (1998) 'Full-scale and laboratory-scale anaerobic treatment of citric acid production wastewater', *Biodegradation*, 9(3-4), pp. 233-245.
- Connan, S., Delisle, F., Deslandes, E. and Gall, E.A. (2006) 'Intra-thallus phlorotannin content and antioxidant activity in Phaeophyceae of temperate waters', *Botanica Marina*, 49(1), pp. 39-46.
- Costa, J.C., Gonçalves, P.R., Nobre, A. and Alves, M.M. (2012) 'Biomethanation potential of macroalgae *Ulva* spp. and *Gracilaria* spp. and in co-digestion with waste activated sludge', *Bioresource Technology*, 114, pp. 320-326.
- Cotter, P.D. and Hill, C. (2003) 'Surviving the acid test: responses of gram-positive bacteria to low pH', *Microbiology and Molecular Biology Reviews*, 67(3), pp. 429-453.
- D'Este, M., Alvarado-Morales, M., Ciofalo, A. and Angelidaki, I. (2017) 'Macroalgae *Laminaria digitata* and *Saccharina latissima* as Potential Biomasses for Biogas and Total Phenolics Production: Focusing on Seasonal and Spatial Variations of the Algae', *Energy & Fuels*, 31(7), pp. 7166-7175.
- Daglia, M. (2012) 'Polyphenols as antimicrobial agents', *Current Opinion in Biotechnology*, 23(2), pp. 174-181.
- Daroch, M., Geng, S. and Wang, G. (2013) 'Recent advances in liquid biofuel production from algal feedstocks', *Applied Energy*, 102(Supplement C), pp. 1371-1381.
- Das, D. and Veziroglu, T.N. (2008) 'Advances in biological hydrogen production processes', *International Journal of Hydrogen Energy*, 33(21), pp. 6046-6057.
- Dāsa, D. (2015) *Algal Biorefinery: An Integrated Approach*. Place of publication not identified : Springer Science and Business Media.
- Davis, T.A., Volesky, B. and Mucci, A. (2003) 'A review of the biochemistry of heavy metal biosorption by brown algae', *Water Research*, 37(18), pp. 4311-4330.

- de Baere, L.A., Devocht, M., Van Assche, P. and Verstraete, W. (1984) 'Influence of high NaCl and NH<sub>4</sub>Cl salt levels on methanogenic associations', *Water Research*, 18(5), pp. 543-548.
- de Smul, A., Goethals, L. and Verstraete, W. (1999) 'Effect of COD to sulphate ratio and temperature in expanded-granular-sludge-blanket reactors for sulphate reduction', *Process Biochemistry*, 34(4), pp. 407-416.
- de Wild, P.J. (2015) 'Biomass Pyrolysis for Hybrid Biorefineries', *Industrial Biorefineries and White Biotechnology*, p. 341.
- Dębowski, M., Zieliński, M., Grala, A. and Dudek, M. (2013) 'Algae biomass as an alternative substrate in biogas production technologies—Review', *Renewable and Sustainable Energy Reviews*, 27(0), pp. 596-604.
- Deepanraj, B., Sivasubramanian, V. and Jayaraj, S. (2015a) 'Experimental and kinetic study on anaerobic digestion of food waste: The effect of total solids and pH', *Journal of Renewable and Sustainable Energy*, 7(6), p. 063104.
- Deepanraj, B., Sivasubramanian, V. and Jayaraj, S. (2015b) 'Kinetic study on the effect of temperature on biogas production using a lab scale batch reactor', *Ecotoxicology and Environmental Safety*, 121, pp. 100-104.
- Demirbas, A. (2007) 'Progress and recent trends in biofuels', *Progress in Energy and Combustion Science*, 33(1), pp. 1-18.
- Demirbas, A. (2009a) 'Biofuels Securing the Planet's Future Energy Needs' SpringerLink. London  
New York: London : Springer London.
- Demirbas, A. (2009b) 'Biofuels securing the planet's future energy needs', *Energy Conversion and Management*, 50(9), pp. 2239-2249.
- Demirbas, A. (2010) 'Use of algae as biofuel sources', *Energy Conversion and Management*, 51(12), pp. 2738-2749.
- Demirbaş, A. (2001) 'Biomass resource facilities and biomass conversion processing for fuels and chemicals', *Energy Conversion and Management*, 42(11), pp. 1357-1378.
- Demirbas, A. and Arin, G. (2002) 'An Overview of Biomass Pyrolysis', *Energy Sources*, 24(5), pp. 471-482.
- Demirbas, A. and Demirbas, M.F. (2010) *Algae Energy: Algae as a New Source of Biodiesel*. Springer London.

- Demirbas, A. and Fatih Demirbas, M. (2011) 'Importance of algae oil as a source of biodiesel', *Energy Conversion and Management*, 52(1), pp. 163-170.
- Demirel, B. and Scherer, P. (2011) 'Trace element requirements of agricultural biogas digesters during biological conversion of renewable biomass to methane', *Biomass and Bioenergy*, 35(3), pp. 992-998.
- Denton, A., Chapman, A.R.O. and Markham, J. (1990) 'Size-specific concentration of phlorotannins (anti-herbivore compounds) in three species of Fucus', *MARINE ECOLOGY PROGRESS SERIES* 65, pp. 103-104.
- Derenne, S., Largeau, C., Berkaloff, C., Rousseau, B., Wilhelm, C. and Hatcher, P.G. (1992) 'Non-hydrolysable macromolecular constituents from outer walls of *Chlorella fusca* and *Nanochlorum eucaryotum*', *Phytochemistry*, 31(6), pp. 1923-1929.
- Deublein, D. and Steinhauser, A. (2011) *Biogas from waste and renewable resources : an introduction*. 2nd, rev. and expanded ed.. edn. Weinheim: Weinheim : Wiley-VCH.
- Dimroth, P. and Thomer, A. (1989) 'A primary respiratory Na<sup>+</sup> pump of an anaerobic bacterium: the Na<sup>+</sup>-dependent NADH:quinone oxidoreductase of *Klebsiella pneumoniae*', *Archives of Microbiology*, 151(5), pp. 439-444.
- Doğan-Subaşı, E. and Demirel, G.N. (2016) 'Anaerobic digestion of microalgal (*Chlorella vulgaris*) biomass as a source of biogas and biofertilizer', *Environmental Progress & Sustainable Energy*.
- Dolfing, J. and Bloeman, W.G.B.M. (1985) 'Activity measurements as a tool to characterize the microbial composition of methanogenic environments', *Journal of Microbiological Methods*, 4(1), pp. 1-12.
- Dominguez-Faus, R., Powers, S.E., Burken, J.G. and Alvarez, P.J. (2009) 'The water footprint of biofuels: A drink or drive issue?', *Environmental Science & Technology*, 43(9), pp. 3005-3010.
- Dong, X., Plugge, C.M. and Stams, A.J.M. (1994) 'Anaerobic degradation of propionate by a mesophilic acetogenic bacterium in coculture and triculture with different methanogens', *Applied and environmental microbiology*, 60(8), pp. 2834-2838.
- Donoso-Bravo, A., Mailier, J., Martin, C., Rodríguez, J., Aceves-Lara, C.A. and Wouwer, A.V. (2011) 'Model selection, identification and validation in anaerobic digestion: A review', *Water Research*, 45(17), pp. 5347-5364.
- Doublet, J., Boulanger, A., Ponthieux, A., Laroche, C., Poitrenaud, M. and Cacho Rivero, J.A. (2013) 'Predicting the biochemical methane potential of wide range of organic substrates by near infrared spectroscopy', *Bioresource Technology*, 128(0), pp. 252-258.

- Draget, K.I., Moe, S.T., Skjak-Bræk, G. and Smidsrød, O. (2016) '9 Alginates', *Food polysaccharides and their applications*, 160, p. 289.
- Draget, K.I., Smidsrød, O. and Skjåk-Bræk, G. (2005) 'Alginates from algae', *Biopolymers Online*.
- Ehimen, E.A., Sun, Z.F., Carrington, C.G., Birch, E.J. and Eaton-Rye, J.J. (2011) 'Anaerobic digestion of microalgae residues resulting from the biodiesel production process', *Applied Energy*, 88(10), pp. 3454-3463.
- Eisenberg DM, Benemann JR, Weissman JC and WJ, O. (1981) 'Large-scale freshwater microalgae biomass production for fuel and fertilizer, final report', *Golden, Colorado: Solar Energy Research Institute*.
- Engineering ToolBox. (2008) 'Solubility of Gases in Water', [https://www.engineeringtoolbox.com/gases-solubility-water-d\\_1148.htm](https://www.engineeringtoolbox.com/gases-solubility-water-d_1148.htm), accessed 04/04/2018.
- Eom, S.H., Kim, Y.M. and Kim, S.K. (2012) 'Antimicrobial effect of phlorotannins from marine brown algae', *Food and Chemical Toxicology*, 50(9), pp. 3251-3255.
- European Environment Agency. (2003) ' Europe's Environment: The Third Assessment, Environmental Assessment Report No 10. EEA, Copenhagen.'
- European Parliament (2015) 'Environment Committee backs switchover to advanced biofuels'.
- Experts, D. (2017) *The General Science Compendium for IAS Prelims General Studies CSAT Paper 1, UPSC & State PSC*.
- Facchin, V., Cavinato, C., Fatone, F., Pavan, P., Cecchi, F. and Bolzonella, D. (2013) 'Effect of trace element supplementation on the mesophilic anaerobic digestion of foodwaste in batch trials: The influence of inoculum origin', *Biochemical Engineering Journal*, 70, pp. 71-77.
- Fang, H.H.P. (2010) *Environmental anaerobic technology : applications and new developments*. London: London : Imperial College Press.
- FAO (1997) *Renewable Biological Systems for Alternative Sustainable Energy Production (FAO Agricultural Services Bulletin-128)*. [Online]. Available at: <http://www.fao.org/docrep/w7241e/w7241e00.htm#Contents>.
- FAO (2001) 'The state of world fisheries and aquaculture 2000, Electronic edition'.

FAO (2010) 'Food and Agriculture Organization of the United Nations. Fishery and Aquaculture Statistic'.

FAO (2014) 'Fishery and Aquaculture Statistics. Aquaculture production 1950-2012 (FishstatJ). In: FAO Fisheries and Aquaculture Department [online or CD-ROM]. Rome. Updated 2014.'. <http://www.fao.org/fishery/statistics/software/fishstatj/en>.

Fargione, J., Hill, J., Tilman, D., Polasky, S. and Hawthorne, P. (2008) 'Land Clearing and the Biofuel Carbon Debt', *Science*, 319(5867), pp. 1235-1238.

Feijoo, G., Soto, M., Méndez, R. and Lema, J.M. (1995) 'Sodium inhibition in the anaerobic digestion process: Antagonism and adaptation phenomena', *Enzyme and Microbial Technology*, 17(2), pp. 180-188.

Fernández-Rodríguez, M.J., Rincón, B., Feroso, F.G., Jiménez, A.M. and Borja, R. (2014) 'Assessment of two-phase olive mill solid waste and microalgae co-digestion to improve methane production and process kinetics', *Bioresource Technology*, 157(Supplement C), pp. 263-269.

Fertah, M., Belfkira, A., Dahmane, E.m., Taourirte, M. and Brouillette, F. (2014) 'Extraction and characterization of sodium alginate from Moroccan *Laminaria digitata* brown seaweed', *Arabian Journal of Chemistry*.

Florin, N. and Harris, A. (2007) 'Hydrogen production from biomass', *The Environmentalist*, 27(1), pp. 207-215.

Funami, T., Fang, Y., Noda, S., Ishihara, S., Nakauma, M., Draget, K.I., Nishinari, K. and Phillips, G.O. (2009) 'Rheological properties of sodium alginate in an aqueous system during gelation in relation to supermolecular structures and Ca<sup>2+</sup> binding', *Food Hydrocolloids*, 23(7), pp. 1746-1755.

Galí, A., Benabdallah, T., Astals, S. and Mata-Alvarez, J. (2009) 'Modified version of ADM1 model for agro-waste application', *Bioresource Technology*, 100(11), pp. 2783-2790.

Gallert, C., Bauer, S. and Winter, J. (1998) 'Effect of ammonia on the anaerobic degradation of protein by a mesophilic and thermophilic biowaste population', *Applied Microbiology And Biotechnology*, 50(4), pp. 495-501.

Gao, K. and McKinley, K.R. (1994) 'Use of macroalgae for marine biomass production and CO<sub>2</sub> remediation: a review', *Journal of Applied Phycology*, 6(1), pp. 45-60.

Garcia, J.-L., Patel, B.K.C. and Ollivier, B. (2000) 'Taxonomic, phylogenetic, and ecological diversity of methanogenic Archaea', *Anaerobe*, 6(4), pp. 205-226.

Gayh, U. (2012) *Process intensification of biological desulphurisation of biogas*. PhD thesis. Technischen Universität Hamburg-Harburg [Online]. Available at:

[http://doku.b.tu-harburg.de/volltexte/2012/1154/pdf/Dissertation\\_Ulrike\\_Gayh\\_5.pdf](http://doku.b.tu-harburg.de/volltexte/2012/1154/pdf/Dissertation_Ulrike_Gayh_5.pdf) (Accessed: 30-11.2013).

Gerardi, M.H. (2003) *The Microbiology of Anaerobic Digesters*. Wiley. Available at: <http://NCL.ebib.com/patron/FullRecord.aspx?p=162768>.

Ghadiryfar, M., Rosentrater, K.A., Keyhani, A. and Omid, M. (2016) 'A review of macroalgae production, with potential applications in biofuels and bioenergy', *Renewable and Sustainable Energy Reviews*, 54(Supplement C), pp. 473-481.

Gikas, P. and Romanos, P. (2006) 'Effects of tri-valent (Cr(III)) and hexa-valent (Cr(VI)) chromium on the growth of activated sludge', *Journal of Hazardous Materials*, 133(1-3), pp. 212-217.

Ginkel, S.V., Sung, S. and Lay, J.-J. (2001) 'Biohydrogen production as a function of pH and substrate concentration', *Environmental science & technology*, 35(24), pp. 4726-4730.

Goh, C.S. and Lee, K.T. (2010) 'A visionary and conceptual macroalgae-based third-generation bioethanol (TGB) biorefinery in Sabah, Malaysia as an underlay for renewable and sustainable development', *Renewable and Sustainable Energy Reviews*, 14(2), pp. 842-848.

Goldemberg, J. (2006) 'The ethanol program in Brazil', *Environmental Research Letters*, 1(1).

González-Delgado, Á.-D. and Kafarov, V. (2011) 'Microalgae based biorefinery: Issues to consider', *CT&F-Ciencia, Tecnología y Futuro*, 4(4), pp. 5-22.

González-Fernández, C., Sialve, B., Bernet, N. and Steyer, J.P. (2012) 'Thermal pretreatment to improve methane production of *Scenedesmus* biomass', *Biomass and Bioenergy*, 40, pp. 105-111.

González-Fernández, C., Sialve, B., Bernet, N. and Steyer, J.P. (2013) 'Effect of organic loading rate on anaerobic digestion of thermally pretreated *Scenedesmus* sp. biomass', *Bioresour. Technology*, 129, pp. 219-223.

Grady, C.P.L. (1999) *Biological wastewater treatment*. 2nd ed. rev. and expanded.. edn. New York: New York : Marcel Dekker.

Grady Jr, C.P.L., Daigger, G.T., Love, N.G. and Filipe, C.D.M. (2011) *Biological wastewater treatment*. CRC press.

Grasdalen, H. (1983) 'High-field, 1H-n.m.r. spectroscopy of alginate: sequential structure and linkage conformations', *Carbohydrate Research*, 118, pp. 255-260.

Grasdalen, H., Larsen, B. and Smisrod, O. (1981) '<sup>13</sup>C-n.m.r. studies of monomeric composition and sequence in alginate', *Carbohydrate Research*, 89(2), pp. 179-191.

Greben, H., Maree, J.P. and Mnqanqeni, S. (2000) 'Comparison between sucrose, ethanol and methanol as carbon and energy sources for biological sulphate reduction', *Water Science And Technology*, 41(12), pp. 247-253.

Grosser, A., Neczaj, E., Singh, B.R., Almås, Å.R., Brattebø, H. and Kacprzak, M. (2017) 'Anaerobic digestion of sewage sludge with grease trap sludge and municipal solid waste as co-substrates', *Environmental Research*, 155(Supplement C), pp. 249-260.

Guiry, M.D. (2017) 'The Seaweed Site: information on marine algae'. Available at: <http://www.seaweed.ie/index.php>.

Guiry, M.D. and Blunden, G. (1991) *Seaweed resources in Europe : uses and potential*. Chichester, West Sussex, England

New York.

Gunaseelan, V.N. (2004) 'Biochemical methane potential of fruits and vegetable solid waste feedstocks', *Biomass and Bioenergy*, 26(4), pp. 389-399.

Gunnerson, C.G. and Stuckey, D.C. (1986) 'Anaerobic digestion', *Tech. Pap*, 49, pp. 2181-2187.

Gurung, A., Van Ginkel, S.W., Kang, W.-C., Qambrani, N.A. and Oh, S.-E. (2012) 'Evaluation of marine biomass as a source of methane in batch tests: A lab-scale study', *Energy*, 43(1), pp. 396-401.

Guwy, A.J. (2004) 'Equipment used for testing anaerobic biodegradability and activity', *Reviews in Environmental Science and Biotechnology*, 3(2), pp. 131-139.

Guwy, A.J., Dinsdale, R.M., Kim, J.R., Massanet-Nicolau, J. and Premier, G. (2011) 'Fermentative biohydrogen production systems integration', *Bioresource Technology*, 102(18), pp. 8534-8542.

Hansen, K.H., Angelidaki, I. and Ahring, B.K. (1999) 'Improving thermophilic anaerobic digestion of swine manure', *Water Research*, 33(8), pp. 1805-1810.

Hansen, T.L., Schmidt, J.E., Angelidaki, I., Marca, E., Jansen, J.L.C., Mosbæk, H. and Christensen, T.H. (2004) 'Method for determination of methane potentials of solid organic waste', *Waste Management*, 24(4), pp. 393-400.

Hanssen, J.F., Indergaard, M., Østgaard, K., Bævre, O.A., Pedersen, T.A. and Jensen, A. (1987) 'Anaerobic digestion of *Laminaria* spp. and *Ascophyllum nodosum* and application of end products', *Biomass*, 14(1), pp. 1-13.

- Hansson, G. (1983) 'Methane production from marine, green macro-algae', *Resources and Conservation*, 8(3), pp. 185-194.
- Harada, H., Uemura, S. and Momonoi, K. (1994) 'Interaction between sulfate-reducing bacteria and methane-producing bacteria in UASB reactors fed with low strength wastes containing different levels of sulfate', *Water Research*, 28(2), pp. 355-367.
- Hardy, F.G., Guiry, M.D. and Arnold, H.R. (2006) *A Check List and Atlas of the Seaweeds of Britain and Ireland*. British Phycological Society.
- Hartmann, H. and Ahring, B.K. (2005) 'Anaerobic digestion of the organic fraction of municipal solid waste: Influence of co-digestion with manure', *Water Research*, 39(8), pp. 1543-1552.
- Hashimoto, A.G. (1986) 'Ammonia inhibition of methanogenesis from cattle wastes', *Agricultural Wastes*, 17(4), pp. 241-261.
- Hashimoto, A.G., Varel, V.H. and Chen, Y.R. (1981) 'Ultimate methane yield from beef cattle manure: effect of temperature, ration constituents, antibiotics and manure age', *Agricultural Wastes*, 3(4), pp. 241-256.
- Haug, A., Larsen, B. and Smidsrod, O. (1963) 'The Degradation of Alginates at Different pH Values', *Acta Chem. Scand*, 17(5), p. 538.
- Haug, A., Myklestad, S., Larsen, B. and Smidsrød, O. (1967) 'Correlation between chemical structure and physical properties of alginates', *Acta Chem Scand*, 21(3), pp. 768-78.
- Henze, M. and Harremoes, P. (1983) 'Anaerobic treatment of wastewater in fixed film reactors—a literature review', *Water science and technology*, 15(8-9), pp. 1-101.
- Herrmann, C., Kalita, N., Wall, D., Xia, A. and Murphy, J.D. (2016) 'Optimised biogas production from microalgae through co-digestion with carbon-rich co-substrates', *Bioresource Technology*, 214(Supplement C), pp. 328-337.
- Hierholtzer, A. (2013) *Investigating factors affecting the anaerobic digestion of seaweed: modelling and experimental approaches*. University of Abertay Dundee.
- Hierholtzer, A. and Akunna, J. (2012) 'Modelling sodium inhibition on the anaerobic digestion process ', *Water Science And Technology*, 66(7), pp. 1565-1573.
- Hierholtzer, A., Chatellard, L., Kierans, M., Akunna, J.C. and Collier, P.J. (2013) 'The impact and mode of action of phenolic compounds extracted from brown seaweed on mixed anaerobic microbial cultures', *Journal of Applied Microbiology*, 114(4), pp. 964-973.



- Hill, D.T., Cobb, S.A. and Bolte, J.P. (1987) 'Using Volatile Fatty Acid Relationships to Predict Anaerobic Digester Failure', 30(2), p. 496.
- Hills, D.J. and Roberts, D.W. (1981) 'Anaerobic digestion of dairy manure and field crop residues', *Agricultural Wastes*, 3(3), pp. 179-189.
- Hilton, B. and Oleszkiewicz, J. (1988) 'Sulfide-Induced Inhibition of Anaerobic Digestion', *Journal of Environmental Engineering*, 114(6), pp. 1377-1391.
- Hinks, J., Edwards, S., Sallis, P.J. and Caldwell, G.S. (2013) 'The steady state anaerobic digestion of *Laminaria hyperborea* – Effect of hydraulic residence on biogas production and bacterial community composition', *Bioresource Technology*, 143(0), pp. 221-230.
- Hobson, P.N. (1993) *Anaerobic digestion : modern theory and practice*. London  
New York: London  
New York : Elsevier Applied Science.
- Hoek, C., Mann, D. and Jahns, H.M. (1995) *Algae: An Introduction to Phycology*. Cambridge University Press.
- Holm-Nielsen, J.B., Al Seadi, T. and Oleskovicz-Popiel, P. (2009) 'The future of anaerobic digestion and biogas utilization', *Bioresource Technology*, 100(22), pp. 5478-5484.
- Holmes, B. and Jones, N. (2003) 'Brace yourself for the end of cheap oil', *New Scientist*, 179(2406), pp. 9-10.
- Hong, Y., Chen, W., Luo, X., Pang, C., Lester, E. and Wu, T. (2017) 'Microwave-enhanced pyrolysis of macroalgae and microalgae for syngas production', *Bioresource Technology*, 237, pp. 47-56.
- Horn, S.J., Aasen, I. and Ostgaard, K. (2000a) 'Ethanol production from seaweed extract', *Journal Of Industrial Microbiology & Biotechnology*, 25(5), pp. 249-254.
- Horn, S.J., Aasen, I.M. and Østgaard, K. (2000b) 'Production of ethanol from mannitol by *Zymobacter palmae*', *Journal of Industrial Microbiology and Biotechnology*, 24(1), pp. 51-57.
- Horn, S.J., Moen, E. and Østgaard, K. (1999) *Sixteenth International Seaweed Symposium*. Springer.
- Horton, R. and Hawkes, D. (1981) 'The Design of Anaerobic Digesters', *Studies in Environmental Science* 9, pp. 143-150.

Huang, H.-J., Ramaswamy, S., Al-Dajani, W., Tschirner, U. and Cairncross, R.A. (2009) 'Effect of biomass species and plant size on cellulosic ethanol: A comparative process and economic analysis', *Biomass and Bioenergy*, 33(2), pp. 234-246.

Hughes, A., Kelly, M., Black, K. and Stanley, M. (2012) 'Biogas from Macroalgae: is it time to revisit the idea?', *Biotechnology for Biofuels*, 5(1), p. 86.

Hughes, A.D., Black, K.D., Campbell, I., Heymans, J.J., Orr, K.K., Stanley, M.S. and Kelly, M.S. (2013) 'Comments on 'Prospects for the use of macroalgae for fuel in Ireland and UK: An overview of marine management issues'', *Marine Policy*, 38, pp. 554-556.

IEA (2009) *IEA Bioenergy Task 42 Biorefinery*. Available at: <http://www.iea-bioenergy.task42-biorefineries.com/>.

Ince, O., Ince, B.K. and Yenigun, O. (2001) 'Determination of potential methane production capacity of a granular sludge from a pilot-scale upflow anaerobic sludge blanket reactor using a specific methanogenic activity test', *Journal of Chemical Technology and Biotechnology*, 76(6), pp. 573-578.

Isaacson, R. (1991) *Methane from Community Wastes*. Taylor & Francis.

ISO, D. (2009) 'Water Quality-Determination of Selected Elements by Inductively Coupled Plasma Optical Emission Spectrometry (ICP-oes)'.

Jabłoński, S.J., Biernacki, P., Steinigeweg, S. and Łukaszewicz, M. (2015a) 'Continuous mesophilic anaerobic digestion of manure and rape oilcake – Experimental and modelling study', *Waste Management*, 35(0), pp. 105-110.

Jabłoński, S.J., Biernacki, P., Steinigeweg, S. and Łukaszewicz, M. (2015b) 'Continuous mesophilic anaerobic digestion of manure and rape oilcake – Experimental and modelling study', *Waste Management*, 35, pp. 105-110.

Jahedsaravani, A., Marhaban, M.H. and Massinaei, M. (2014) 'Prediction of the metallurgical performances of a batch flotation system by image analysis and neural networks', *Minerals Engineering*, 69(Supplement C), pp. 137-145.

Janda, K., Kristoufek, L. and Zilberman, D. (2012) 'Biofuels: Policies and impacts', *Agricultural Economics*, 58(8), pp. 372-386.

Janke, L., Leite, A., Nikolausz, M., Schmidt, T., Liebetrau, J., Nelles, M. and Stinner, W. (2015) 'Biogas production from sugarcane waste: assessment on kinetic challenges for process designing', *International journal of molecular sciences*, 16(9), pp. 20685-20703.

Jard, G., Marfaing, H., Carrère, H., Delgenes, J.P., Steyer, J.P. and Dumas, C. (2013) 'French Brittany macroalgae screening: Composition and methane

potential for potential alternative sources of energy and products', *Bioresource Technology*, 144, pp. 492-498.

Jash, T. and Ghosh, D.N. (1996) 'Studies on the solubilization kinetics of solid organic residues during anaerobic biomethanation', *Energy*, 21(7-8), pp. 725-730.

Jensen, A. (1993) 'Present and future needs for algae and algal products', *Hydrobiologia*, 260(1), pp. 15-23.

John, R.P., Anisha, G.S., Nampoothiri, K.M. and Pandey, A. (2011a) 'Micro and macroalgal biomass: A renewable source for bioethanol', *Bioresource Technology*, 102(1), pp. 186-193.

John, R.P., Anisha, K.M., Nampoothiri, A. and Pandey, A. (2011b) 'Micro and macroalgal biomass: A renewable source for bioethanol', *Bioresource Technology*, 102(1), pp. 186-193.

Jones, C.S. and Mayfield, S.P. (2012) 'Algae biofuels: versatility for the future of bioenergy', *Current Opinion in Biotechnology*, 23(3), pp. 346-351.

Jormalainen, V. and Honkanen, T. (2008) 'Macroalgal chemical defenses and their roles in structuring temperate marine communities', in *Algal chemical ecology*. Springer, pp. 57-89.

Jung, K.-W., Kim, D.-H. and Shin, H.-S. (2011) 'Fermentative hydrogen production from *Laminaria japonica* and optimization of thermal pretreatment conditions', *Bioresource Technology*, 102(3), pp. 2745-2750.

Jung, K.A., Lim, S.R., Kim, Y. and Park, J.M. (2013) 'Potentials of macroalgae as feedstocks for biorefinery', *Bioresource Technology*, 135, pp. 182-190.

Kafle, G.K. and Chen, L. (2016) 'Comparison on batch anaerobic digestion of five different livestock manures and prediction of biochemical methane potential (BMP) using different statistical models', *Waste Management*, 48(Supplement C), pp. 492-502.

Kafle, G.K. and Kim, S.H. (2011) 'Sludge exchange process on two serial CSTRs anaerobic digestions: Process failure and recovery', *Bioresource Technology*, 102(13), pp. 6815-6822.

Kafle, G.K. and Kim, S.H. (2013) 'Anaerobic treatment of apple waste with swine manure for biogas production: Batch and continuous operation', *Applied Energy*, 103(0), pp. 61-72.

Kaparaju, P., Serrano, M. and Angelidaki, I. (2010) 'Optimization of biogas production from wheat straw stillage in UASB reactor', *Applied Energy*, 87(12), pp. 3779-3783.

- Kaspar, H.F. and Wuhrmann, K. (1978) 'Kinetic parameters and relative turnovers of some important catabolic reactions in digesting sludge', *Applied and Environmental Microbiology*, 36(1), pp. 1-7.
- Kayhanian, M. (1999) 'Ammonia inhibition in high-solids biogasification: an overview and practical solutions', *Environmental Technology*, 20(4), pp. 355-365.
- Kayhanian, M. and Rich, D. (1995) 'Pilot-scale high solids thermophilic anaerobic digestion of municipal solid waste with an emphasis on nutrient requirements', *Biomass and bioenergy*, 8(6), pp. 433-444.
- Khairuddin, N., Manaf, L.A., Hassan, M.A., Halimoon, N. and Ghani, W.A.W.A.K. (2016) 'High Solid Anaerobic Co-Digestion of Household Organic Waste with Cow Manure for Mass and Energy Recovery', *Polish Journal of Environmental Studies*, 25(4), pp. 1549-1554.
- Khalid, A., Arshad, M., Anjum, M., Mahmood, T. and Dawson, L. (2011) 'The anaerobic digestion of solid organic waste', *Waste Management*, 31(8), pp. 1737-1744.
- Khanal, S. (2009) *Anaerobic Biotechnology for Bioenergy Production : Principles and Applications*. Wiley. Available at: <http://ncl.ebib.com/patron/FullRecord.aspx?p=427765>.
- Khanal, S.K. (2011) *Anaerobic Biotechnology for Bioenergy Production: Principles and Applications*. Wiley.
- Khanal, S.K., Surampalli, R.Y., Zhang, T.C., Lamsal, B.P., Tyagi, R.D. and Kao, C.M. (2010). American Society of Civil Engineers.
- Kida, K., Shigematsu, T., Kijima, J., Numaguchi, M., Mochinaga, Y., Abe, N. and Morimura, S. (2001) 'Influence of Ni<sup>2+</sup> and Co<sup>2+</sup> on methanogenic activity and the amounts of coenzymes involved in methanogenesis', *Journal of Bioscience and Bioengineering*, 91(6), pp. 590-595.
- Kim, J., Kim, H. and Lee, C. (2017) 'Ulva biomass as a co-substrate for stable anaerobic digestion of spent coffee grounds in continuous mode', *Bioresource Technology*, 241(Supplement C), pp. 1182-1190.
- Kim, S.-K. (2011) *Handbook of marine macroalgae: Biotechnology and applied phycology*. John Wiley & Sons.
- Kim, S.-K. (2015) *Springer Handbook of Marine Biotechnology*. Berlin, Heidelberg: Springer Berlin Heidelberg: Berlin, Heidelberg.
- Kim, S.K. and Chojnacka, K. (2015) *Marine Algae Extracts: Processes, Products, and Applications, 2 Volume Set*. Wiley.

- Kim, S.K. and Lee, C.G. (2014) *Marine Bioenergy: Trends and Developments*. Taylor & Francis Group.
- Kingsbury, J.M. (1984) 'Seaweeds', *BioScience*, 34(5), pp. 334-334.
- Kinley, R. (2017) 'Climate change after Paris: from turning point to transformation', *Climate Policy*, 17(1), pp. 9-15.
- Kirk, R.E. and Othmer, D.F. (1997) *Encyclopedia of chemical technology*. Wiley-Interscience.
- Kispergher, E.M., D'Aquino, C.A., Costa Junior, L.C.d., Mello, T.C.d., Weinschutz, R. and Mathias, A.L. (2017) 'EFFECT OF ORGANIC LOAD AND ALKALINITY ON DAIRY WASTEWATER BIOMETHANATION', *Engenharia Agrícola*, 37, pp. 820-827.
- Klass, D.L. (1998) 'Biomass for Renewable Energy, Fuels, and Chemicals'. Elsevier. Available at:  
<http://app.knovel.com/hotlink/toc/id:kpBREFC00E/biomass-renewable-energy/biomass-renewable-energy>.
- Kloareg, B., Demarty, M. and Mabeau, S. (1986) 'Polyanionic characteristics of purified sulphated homofucans from brown algae', *International Journal of Biological Macromolecules*, 8(6), pp. 380-386.
- Kloareg, B. and Quatrano, R.S. (1988) 'Structure of the cell walls of marine algae and ecophysiological functions of the matrix polysaccharides', *OCEANOGRAPHY AND MARINE BIOLOGY: AN ANNUAL REVIEW.*, 26, pp. 259-315.
- Koivikko, R., Loponen, J., Honkanen, T. and Jormalainen, V. (2005) 'CONTENTS OF SOLUBLE, CELL-WALL-BOUND AND EXUDED PHLOROTANNINS IN THE BROWN ALGA *Fucus vesiculosus*, WITH IMPLICATIONS ON THEIR ECOLOGICAL FUNCTIONS', *Journal of Chemical Ecology*, 31(1), pp. 195-212.
- Korres, N., O'Kiely, P., Benzie, J.A.H. and West, J.S. (2013) *Bioenergy production by anaerobic digestion: using agricultural biomass and organic wastes*. Routledge.
- Kositkanawuth, K., Bhatt, A., Sattler, M. and Dennis, B. (2017) 'Renewable Energy from Waste: Investigation of Co-pyrolysis between Sargassum Macroalgae and Polystyrene', *Energy & Fuels*, 31(5), pp. 5088-5096.
- Koster, I.W. and Lettinga, G. (1984) 'The influence of ammonium-nitrogen on the specific activity of pelletized methanogenic sludge', *Agricultural Wastes*, 9(3), pp. 205-216.

Kotsyurbenko, O.R., Glagolev, M.V., Nozhevnikova, A.N. and Conrad, R. (2001) 'Competition between homoacetogenic bacteria and methanogenic archaea for hydrogen at low temperature', *FEMS microbiology ecology*, 38(2-3), pp. 153-159.

Kraan, S. (2013) 'Mass-cultivation of carbohydrate rich macroalgae, a possible solution for sustainable biofuel production', *Mitigation and Adaptation Strategies for Global Change*, 18(1), pp. 27-46.

Kroeker, E.J., Schulte, D.D., Sparling, A.B. and Lapp, H.M. (1979) 'Anaerobic treatment process stability', *Journal of the Water Pollution Control Federation*, 51(4), pp. 718-727.

Kythreotou, N., Florides, G. and Tassou, S.A. (2014) 'A review of simple to scientific models for anaerobic digestion', *Renewable Energy*, 71, pp. 701-714.

Laanbroek, H.J., Geerligs, H.J., Sijtsma, L. and Veldkamp, H. (1984) 'Competition for sulfate and ethanol among *Desulfobacter*, *Desulfobulbus*, and *Desulfovibrio* species isolated from intertidal sediments', *Applied and Environmental Microbiology*, 47(2), pp. 329-334.

Labatut, R.A., Angenent, L.T. and Scott, N.R. (2011) 'Biochemical methane potential and biodegradability of complex organic substrates', *Bioresource Technology*, 102(3), pp. 2255-2264.

Lakaniemi, A.-M., Hulatt, C.J., Thomas, D.N., Tuovinen, O.H. and Puhakka, J.A. (2011) 'Biogenic hydrogen and methane production from *Chlorella vulgaris* and *Dunaliella tertiolecta* biomass', *Biotechnology for biofuels*, 4(1), p. 34.

Larsen, B., Salem, D.M.S.A., Sallam, M.A.E., Mishrikey, M.M. and Beltagy, A.I. (2003) 'Characterization of the alginates from algae harvested at the Egyptian Red Sea coast', *Carbohydrate Research*, 338(22), pp. 2325-2336.

Laurinovic, L., Jasko, J., Skripsts, E. and Dubrovskis, V. (2013). Available at: <http://www.scopus.com/inward/record.url?eid=2-s2.0-84887110215&partnerID=40&md5=3778f0025ec4b849c35abff4ae0c9c7>.

Lauwers, J., Appels, L., Thompson, I.P., Degève, J., Van Impe, J.F. and Dewil, R. (2013) 'Mathematical modelling of anaerobic digestion of biomass and waste: Power and limitations', *Progress in Energy and Combustion Science*, 39(4), pp. 383-402.

Lay, J.J. (2001) 'Biohydrogen generation by mesophilic anaerobic fermentation of microcrystalline cellulose', *Biotechnology and bioengineering*, 74(4), pp. 280-287.

Leduc, L., Ferroni, G. and Trevors, J. (1997) 'Resistance to heavy metals in different strains of *Thiobacillus ferrooxidans*', *World Journal Of Microbiology & Biotechnology*, 13(4), pp. 453-455.

Lee, J.W. (2013) 'Advanced biofuels and bioproducts' Lee, J.W. New York, NY: New York, NY : Springer.

Lefebvre, O., Quentin, S., Torrijos, M., Godon, J.J., Delgenès, J.P. and Moletta, R. (2007) 'Impact of increasing NaCl concentrations on the performance and community composition of two anaerobic reactors', *Applied Microbiology and Biotechnology*, 75(1), pp. 61-69.

Lettinga, G., Rebac, S. and Zeeman, G. (2001) 'Challenge of psychrophilic anaerobic wastewater treatment', *Trends in Biotechnology*, 19(9), pp. 363-370.

Li, C., Champagne, P. and Anderson, B.C. (2011) 'Evaluating and modeling biogas production from municipal fat, oil, and grease and synthetic kitchen waste in anaerobic co-digestions', *Bioresource Technology*, 102(20), pp. 9471-9480.

Li, C., Champagne, P. and Anderson, B.C. (2013a) 'Biogas production performance of mesophilic and thermophilic anaerobic co-digestion with fat, oil, and grease in semi-continuous flow digesters: effects of temperature, hydraulic retention time, and organic loading rate', *Environmental technology*, 34(13-14), pp. 2125-2133.

Li, C. and Fang, H. (2007) 'Inhibition of Heavy Metals on Fermentative Hydrogen Production by Granular Sludge', *Chemosphere*, 63(4), pp. 668-668.

Li, L., Rowbotham, J.S., Greenwell, C.H. and Dyer, P.W. (2013b) 'An introduction to pyrolysis and catalytic pyrolysis: versatile techniques for biomass conversion', in Elsevier.

Li, Y., Jin, Y., Borrion, A., Li, H. and Li, J. (2017) 'Effects of organic composition on the anaerobic biodegradability of food waste', *Bioresource Technology*, 243(Supplement C), pp. 836-845.

Liew, W.H., Hassim, M.H. and Ng, D.K.S. (2014) 'Review of evolution, technology and sustainability assessments of biofuel production', *Journal of Cleaner Production*, 71, pp. 11-29.

Lin, C.-Y. (1993) 'Effect of heavy metals on acidogenesis in anaerobic digestion', *Water Research*, 27(1), pp. 147-152.

Lin, C.-Y. and Chen, C.-C. (1999) 'Effect of heavy metals on the methanogenic UASB granule', *Water Research*, 33(2), pp. 409-416.

Lin, Y., Wang, D., Wu, S. and Wang, C. (2009) 'Alkali pretreatment enhances biogas production in the anaerobic digestion of pulp and paper sludge', *Journal of Hazardous Materials*, 170(1), pp. 366-373.

- Lindorfer, H., Ramhold, D. and Frauz, B. (2012) 'Nutrient and trace element supply in anaerobic digestion plants and effect of trace element application', *Water Science and Technology*, 66(9), pp. 1923-1929.
- Liu, D., Liu, D., Zeng, R.J. and Angelidaki, I. (2006) 'Hydrogen and methane production from household solid waste in the two-stage fermentation process', *Water Research*, 40(11), pp. 2230-2236.
- Liu, G., Zhang, R., El-Mashad, H.M. and Dong, R. (2009) 'Effect of feed to inoculum ratios on biogas yields of food and green wastes', *Bioresource Technology*, 100(21), pp. 5103-5108.
- Liu, T. and Sung, S. (2002) 'Ammonia inhibition on thermophilic aceticlastic methanogens', *Water Science and Technology*, 45(10), pp. 113-120.
- Llaneza Coalla, H., Blanco Fernández, J.M., Morís Morán, M.A. and López Bobo, M.R. (2009) 'Biogas generation apple pulp', *Bioresource Technology*, 100(17), pp. 3843-3847.
- Lo, H.M., Kurniawan, T.A., Sillanpää, M.E.T., Pai, T.Y., Chiang, C.F., Chao, K.P., Liu, M.H., Chuang, S.H., Banks, C.J., Wang, S.C., Lin, K.C., Lin, C.Y., Liu, W.F., Cheng, P.H., Chen, C.K., Chiu, H.Y. and Wu, H.Y. (2010) 'Modeling biogas production from organic fraction of MSW co-digested with MSWI ashes in anaerobic bioreactors', *Bioresource Technology*, 101(16), pp. 6329-6335.
- Lo, K.V., Liao, P.H. and March, A.C. (1985) 'Thermophilic anaerobic digestion of screened dairy manure', *Biomass*, 6(4), pp. 301-315.
- Lobban, C.S., Harrison, P.J. and Duncan, M.J. (1985) *Physiological ecology of seaweeds*. Cambridge University Press.
- Lobban, C.S. and Wynne, M.J. (1981) *The Biology of seaweeds*. Oxford Boston : Blackwell Scientific Publications.
- López, I., Passeggi, M. and Borzacconi, L. (2015) 'Validation of a simple kinetic modelling approach for agro-industrial waste anaerobic digesters', *Chemical Engineering Journal*, 262(0), pp. 509-516.
- Lü, J., Sheahan, C. and Fu, P. (2011) 'Metabolic engineering of algae for fourth generation biofuels production', *Energy & Environmental Science*, 4(7), pp. 2451-2466.
- Lüning, K. and Pang, S. (2003) 'Mass cultivation of seaweeds: current aspects and approaches', *Journal of Applied Phycology*, 15(2), pp. 115-119.
- Luning, L., Van Zundert, E.H.M. and Brinkmann, A.J.F. (2003) 'Comparison of dry and wet digestion for solid waste', *Water science and technology*, 48(4), pp. 15-20.



Luque, R., Campelo, J. and Clark, J. (2011) 'Handbook of Biofuels Production - Processes and Technologies'. Woodhead Publishing. Available at: <http://app.knovel.com/hotlink/toc/id:kpHBPPT002/handbook-biofuels-production/handbook-biofuels-production>.

Lyberatos, G. and Skiadas, V.I. (1999) 'Modelling of Anaerobic Digestion-A Review', *Global Nest: the int.J*, 1(2), pp. 63-76.

Mackie, R.I. and Bryant, M.P. (1981) 'Metabolic activity of fatty acid-oxidizing bacteria and the contribution of acetate, propionate, butyrate, and CO<sub>2</sub> to methanogenesis in cattle waste at 40 and 60 C', *Applied and Environmental Microbiology*, 41(6), pp. 1363-1373.

Madden, P., Al-Raei, A.M., Enright, A.M., Chinalia, F.A., de Beer, D., O'Flaherty, V. and Collins, G. (2014) 'Effect of sulfate on low-temperature anaerobic digestion', *Frontiers in Microbiology*, 5, p. 376.

Madigan, M.T., Martinko, J.M., Bender, K.S., Buckley, D.H., Stahl, D.A. and Brock, T. (2014) *Brock Biology of Microorganisms*. Pearson Education.

Madsen, M., Holm-Nielsen, J.B. and Esbensen, K.H. (2011) 'Monitoring of anaerobic digestion processes: A review perspective', *Renewable and Sustainable Energy Reviews*, 15(6), pp. 3141-3155.

Mähnert, P. and Linke, B. (2009) 'Kinetic study of biogas production from energy crops and animal waste slurry: Effect of organic loading rate and reactor size', *Environmental Technology*, 30(1), pp. 93-99.

Manjusha, C. and Beevi, B.S. (2016) 'Mathematical Modeling and Simulation of Anaerobic Digestion of Solid Waste', *Procedia Technology*, 24(Supplement C), pp. 654-660.

Mao, C., Zhang, T., Wang, X., Feng, Y., Ren, G. and Yang, G. (2017) 'Process performance and methane production optimizing of anaerobic co-digestion of swine manure and corn straw', *Scientific Reports*, 7(1), p. 9379.

Marinho-Soriano, E., Fonseca, P.C., Carneiro, M.A.A. and Moreira, W.S.C. (2006) 'Seasonal variation in the chemical composition of two tropical seaweeds', *Bioresource Technology*, 97(18), pp. 2402-2406.

Martone, P.T., Estevez, J.M., Lu, F., Ruel, K., Denny, M.W., Somerville, C. and Ralph, J. (2009) 'Discovery of Lignin in Seaweed Reveals Convergent Evolution of Cell-Wall Architecture', *Current Biology*, 19(2), pp. 169-175.

Mata-Alvarez, J., Dosta, J., Macé, S. and Astals, S. (2011) 'Codigestion of solid wastes: a review of its uses and perspectives including modeling', *Critical Reviews in Biotechnology*, 31(2), pp. 99-111.

- Mata-Alvarez, J., Llabrés, P., Cecchi, F. and Pavan, P. (1992) 'Anaerobic digestion of the Barcelona central food market organic wastes: Experimental study', *Bioresource Technology*, 39(1), pp. 39-48.
- Mata-Alvarez, J., Macé, S. and Llabrés, P. (2000) 'Anaerobic digestion of organic solid wastes. An overview of research achievements and perspectives', *Bioresource Technology*, 74(1), pp. 3-16.
- Matsui, T. and Koike, Y. (2010) 'Methane fermentation of a mixture of seaweed and milk at a pilot-scale plant', *Journal of Bioscience and Bioengineering*, 110(5), pp. 558-563.
- Mauky, E., Weinrich, S., Jacobi, H.-F., Nägele, H.-J., Liebetrau, J. and Nelles, M. (2017) 'Demand-driven biogas production by flexible feeding in full-scale – Process stability and flexibility potentials', *Anaerobe*, 46(Supplement C), pp. 86-95.
- McCartney, D.M. and Oleszkiewicz, J.A. (1991) 'Sulfide inhibition of anaerobic degradation of lactate and acetate', *Water Research*, 25(2), pp. 203-209.
- McCarty, P.L. (1964) 'Anaerobic waste treatment fundamentals', *Public works*, 95(9), pp. 107-112.
- McFarland, M.J. and Jewell, W.J. (1989) 'In situ control of sulfide emissions during the thermophilic (55°C) anaerobic digestion process', *Water Research*, 23(12), pp. 1571-1577.
- McGeeney, D. (2015) *Practical Statistics workshop III*.
- McHugh, D.J., Food and Agriculture Organization of the United, N. (2003) *A Guide to the Seaweed Industry*. Food and Agriculture Organization of the United Nations.
- McKennedy, J. and Sherlock, O. (2015) 'Anaerobic digestion of marine macroalgae: A review', *Renewable and Sustainable Energy Reviews*, 52(Supplement C), pp. 1781-1790.
- Mechichi, T. and Sayadi, S. (2005) 'Evaluating process imbalance of anaerobic digestion of olive mill wastewaters', *Process Biochemistry*, 40(1), pp. 139-145.
- Melis, A. and Happe, T. (2001) 'Hydrogen production. Green algae as a source of energy', *Plant Physiology*, 127(3), pp. 740-748.
- Membere, E., Edwards, S., Egwu, U. and Sallis, P. (2015) 'Bio-methane potential test (BMP) using inert gas sampling bags with macroalgae feedstock', *Biomass and Bioenergy*, 83, pp. 516-524.

- Mendez, R., Lema, J.M. and Soto, M. (1995) 'Treatment of seafood-processing wastewaters in mesophilic and thermophilic anaerobic filters', *Water Environment Research*, 67(1), pp. 33-45.
- Metcalf, E.E. and Eddy, H. (2003) 'Wastewater engineer treatment disposal, reuse', *New York: McGraw*.
- Meynell, P.-J. (1982) *Methane: planning a digester*. Prism Press.
- Miao, C., Chakraborty, M. and Chen, S. (2012) 'Impact of reaction conditions on the simultaneous production of polysaccharides and bio-oil from heterotrophically grown *Chlorella sorokiniana* by a unique sequential hydrothermal liquefaction process', *Bioresource Technology*, 110, pp. 617-627.
- Miao, H., Wang, S., Zhao, M., Huang, Z., Ren, H., Yan, Q. and Ruan, W. (2014) 'Codigestion of Taihu blue algae with swine manure for biogas production', *Energy Conversion and Management*, 77, pp. 643-649.
- Michel, G., Tonon, T., Scornet, D., Cock, J.M. and Kloareg, B. (2010) 'The cell wall polysaccharide metabolism of the brown alga *Ectocarpus siliculosus*. Insights into the evolution of extracellular matrix polysaccharides in Eukaryotes', *The New Phytologist*, 188(1), pp. 82-97.
- Michele, P., Giuliana, D.I., Carlo, M., Sergio, S. and Fabrizio, A. (2015) 'Optimization of solid state anaerobic digestion of the OFMSW by digestate recirculation: A new approach', *Waste Management*, 35, pp. 111-118.
- Migliore, G., Alisi, C., Sprocati, A.R., Massi, E., Ciccoli, R., Lenzi, M., Wang, A. and Cremisini, C. (2012) 'Anaerobic digestion of macroalgal biomass and sediments sourced from the Orbetello lagoon, Italy', *Biomass and Bioenergy*, 42, pp. 69-77.
- Milledge, J.J., Smith, B., Dyer, P.W. and Harvey, P. (2014) 'Macroalgae-derived biofuel: a review of methods of energy extraction from seaweed biomass', *Energies*, 7(11), pp. 7194-7222.
- Miyashita, K., Mikami, N. and Hosokawa, M. (2013) 'Chemical and nutritional characteristics of brown seaweed lipids: A review', *Journal of Functional Foods*, 5(4), pp. 1507-1517.
- Moen, E., Horn, S. and Østgaard, K. (1997) 'Alginate degradation during anaerobic digestion of *Laminaria hyperborea stipes*', *Journal of Applied Phycology*, 9(2), pp. 157-166.
- Møller, H.B., Sommer, S.G. and Ahring, B.K. (2004) 'Methane productivity of manure, straw and solid fractions of manure', *Biomass and Bioenergy*, 26(5), pp. 485-495.

- Monnet, F. (2003) 'An introduction to anaerobic digestion of organic wastes', *Remade Scotland*, pp. 1-48.
- Monod, J. (1949) 'The growth of bacterial cultures', *Annual Reviews in Microbiology*, 3(1), pp. 371-394.
- Montingelli, M.E., Benyounis, K.Y., Quilty, B., Stokes, J. and Olabi, A.G. (2017) 'Influence of mechanical pretreatment and organic concentration of Irish brown seaweed for methane production', *Energy*, 118(Supplement C), pp. 1079-1089.
- Montingelli, M.E., Tedesco, S. and Olabi, A.G. (2015) 'Biogas production from algal biomass: A review', *Renewable and Sustainable Energy Reviews*, 43(0), pp. 961-972.
- Moosbrugger, R.E., Loewenthal, R.E. and Marais, G.R. (1990) 'Pelletisation in a UASB system with protein (casein) as substrate', *Water SA*, 16(3), pp. 171-178.
- Mottet, A., Habouzit, F. and Steyer, J.P. (2014) 'Anaerobic digestion of marine microalgae in different salinity levels', *Bioresource Technology*, 158(Supplement C), pp. 300-306.
- Mu, Y., Yu, H.-Q. and Wang, G. (2007a) 'A kinetic approach to anaerobic hydrogen-producing process', *Water research*, 41(5), pp. 1152-1160.
- Mu, Y., Yu, H.Q. and Wang, G. (2007b) 'A kinetic approach to anaerobic hydrogen-producing process', *Water Research*, 41(5), pp. 1152-1160.
- Müller, J., Lehne, G., Schwedes, J., Battenberg, S., Näveke, R., Kopp, J., Dichtl, N., Scheminski, A., Krull, R. and Hempel, D.C. (1998) 'Disintegration of sewage sludges and influence on anaerobic digestion', *Water Science and Technology*, 38(8–9), pp. 425-433.
- Müller, T., Walter, B., Wirtz, A. and Burkovski, A. (2006) 'Ammonium Toxicity in Bacteria', *Current Microbiology*, 52(5), pp. 400-406.
- Muraoka, D. (2004) 'Seaweed resources as a source of carbon fixation', *Bulletin-Fisheries Research Agency Japan*, pp. 59-64.
- Muruganandam, B., Saravanane, R., Lavanya, M. and Sivacouniarw, R. (2008) 'Effect of Inoculum-Substrate Ratio on Acclimatization of Pharmaceutical Effluent in an Anaerobic Batch Reactor', *Journal of Environmental, Science & Engineering*, 50(3), pp. 191-196.
- Mussnug, J.H., Klassen, V., Schlüter, A. and Kruse, O. (2010) 'Microalgae as substrates for fermentative biogas production in a combined biorefinery concept', *Journal of Biotechnology*, 150(1), pp. 51-56.

Naik, S.N., Goud, V.V., Rout, P.K. and Dalai, A.K. (2010) 'Production of first and second generation biofuels: A comprehensive review', *Renewable and Sustainable Energy Reviews*, 14(2), pp. 578-597.

Nallathambi Gunaseelan, V. (1997) 'Anaerobic digestion of biomass for methane production: A review', *Biomass and Bioenergy*, 13(1), pp. 83-114.

Nandi, R., Saha, C.K., Huda, M.S. and Alam, M.M. (2017) 'Effect of mixing on biogas production from cow dung'.

Nayono, S., Gallert, C. and Winter, J. (2009) 'Foodwaste as a co-substrate in a fed-batch anaerobic biowaste digester for constant biogas supply', *Water Science And Technology*, 59(6), pp. 1169-1178.

Nedwell, D.B., Raffaelli, D.G. and Fitter, A.H. (1999) *Estuaries*. Elsevier Science.

Newman, D. and Kolter, R. (2000) 'A role for excreted quinones in extracellular electron transfer', *Nature*, 405(6782), pp. 94-97.

Nielsen, H.B. and Angelidaki, I. (2008) 'Strategies for optimizing recovery of the biogas process following ammonia inhibition', *Bioresource Technology*, 99(17), pp. 7995-8001.

Nielsen, H.B. and Heiske, S. (2011) 'Anaerobic digestion of macroalgae: Methane potentials, pre-treatment, inhibition and co-digestion', *Water Science and Technology*, 64(8), pp. 1723-1729.

Nigam, P.S. and Singh, A. (2011) 'Production of liquid biofuels from renewable resources', *Progress in Energy and Combustion Science*, 37(1), pp. 52-68.

Nizami, A.-S., Korres, N.E. and Murphy, J.D. (2009) 'Review of the Integrated Process for the Production of Grass Biomethane', *Environmental Science & Technology*, 43(22), pp. 8496-8508.

Nkemka, V.N. and Murto, M. (2010) 'Evaluation of biogas production from seaweed in batch tests and in UASB reactors combined with the removal of heavy metals', *Journal of Environmental Management*, 91(7), pp. 1573-1579.

Nopharatana, A., Pullammanappallil, P.C. and Clarke, W.P. (2007) 'Kinetics and dynamic modelling of batch anaerobic digestion of municipal solid waste in a stirred reactor', *Waste Management*, 27(5), pp. 595-603.

Nordberg, A. and Edstroem, M. 52 (2005) 'Co-digestion of energy crops and the source-sorted organic fraction of municipal solid waste' Nordberg, A., Guiot, S., Pavlostathis, J.B. and van Lier, J.B., pp. 217-222.

- Nowakowski, D.J. and Jones, J.M. (2008) 'Uncatalysed and potassium-catalysed pyrolysis of the cell-wall constituents of biomass and their model compounds', *Journal of Analytical and Applied Pyrolysis*, 83(1), pp. 12-25.
- O'Flaherty, V. and Colleran, E. (1999) 'Effect of sulphate addition on volatile fatty acid and ethanol degradation in an anaerobic hybrid reactor. I: process disturbance and remediation', *Bioresource Technology*, 68(2), pp. 101-107.
- O'Flaherty, V., Colohan, S., Mulkerrins, D. and Colleran, E. (1999) 'Effect of sulphate addition on volatile fatty acid and ethanol degradation in an anaerobic hybrid reactor, II :Microbial interactions and toxic effects', *Bioresour. Technol.*, 68, pp. 109-120.
- O'Flaherty, V., Mahony, T., O'Kennedy, R. and Colleran, E. (1998) 'Effect of pH on growth kinetics and sulphide toxicity thresholds of a range of methanogenic, syntrophic and sulphate-reducing bacteria', *Process Biochemistry*, 33(5), pp. 555-569.
- oilgae (2014), [Online]. Available at: [www.oilgae.com](http://www.oilgae.com) (Accessed: 04.11.2017).
- Okabe, S., Nielsen, P.H., Jones, W.L. and Characklis, W.G. (1995) 'Sulfide product inhibition of *Desulfovibrio desulfuricans* in batch and continuous cultures', *Water Research*, 29(2), pp. 571-578.
- Omil, F., Méndez, R. and Lema, J.M. (1995) 'Anaerobic treatment of saline wastewaters under high sulphide and ammonia content', *Bioresource Technology*, 54(3), pp. 269-278.
- Oremland, R.S. and Taylor, B.F. (1978) 'Sulfate reduction and methanogenesis in marine sediments', *Geochimica et Cosmochimica Acta*, 42(2), pp. 209-214.
- Oude Elferink, S.J.W.H., Visser, A., Hulshoff Pol, L.W. and Stams, A.J.M. (1994) 'Sulfate reduction in methanogenic bioreactors', *FEMS Microbiology Reviews*, 15(2-3), pp. 119-136.
- P. Chastain, J. and Bryan Smith, W. (2015) 'Determination of the Anaerobic Volatile Solids Reduction Ratio of Animal Manure Using a Bench Scale Batch Reactor', *2015 ASABE Annual International Meeting*. St. Joseph, MI. ASABE, p. 1. Available at: <http://elibrary.asabe.org/abstract.asp?aid=46350&t=5>.
- Page, D.I., Hickey, K., Narula, R., Main, A.L. and Grimberg, S.J. (2008) 'Modeling anaerobic digestion of dairy manure using the IWA Anaerobic Digestion Model no. 1 (ADM1)', *Water Science And Technology*, 58(3), pp. 689-695.
- Palmeri, L., Barausse, A. and Jorgensen, S.E. (2013) *Ecological Processes Handbook*. CRC Press.

- Pandey, A., Höfer, R., Taherzadeh, M., Nampoothiri, M. and Larroche, C. (2015) *Industrial Biorefineries & White Biotechnology*. Elsevier.
- Parawira, W. (2004) 'Anaerobic treatment of agricultural residues and wastewater', *University of Lund Department of Biotechnology*.
- Parawira, W., Murto, M., Zvauya, R. and Mattiasson, B. (2004) 'Anaerobic batch digestion of solid potato waste alone and in combination with sugar beet leaves', *Renewable Energy*, 29(11), pp. 1811-1823.
- Paritosh, K., Kushwaha, S.K., Yadav, M., Pareek, N., Chawade, A. and Vivekanand, V. (2017) 'Food Waste to Energy: An Overview of Sustainable Approaches for Food Waste Management and Nutrient Recycling', *BioMed Research International*, 2017, p. 19.
- Park, J.-I., Lee, J., Sim, S.J. and Lee, J.-H. (2009) 'Production of hydrogen from marine macro-algae biomass using anaerobic sewage sludge microflora', *Biotechnology and Bioprocess Engineering*, 14(3), pp. 307-315.
- Parkin, G.F. and Speece, R.E. (1982) 'Modeling toxicity in methane fermentation systems', *J. Environ. Eng. Div., ASCE;(United States)*, 108.
- Parys, S., Kehraus, S., Pete, R., Küpper, F.C., Glombitza, K.-W. and König, G.M. (2009) 'Seasonal variation of polyphenolics in *Ascophyllum nodosum* (Phaeophyceae)', *European Journal of Phycology*, 44(3), pp. 331-338.
- Patel, J.N., Rathod, D.M., Patel, N.A. and Modasiya, M.K. (2012) 'Techniques to improve the solubility of poorly soluble drugs', *International Journal of Pharmacy & Life Sciences*, 3(2).
- Pathak, T.S., Yun, J.-H., Lee, J. and Paeng, K.-J. (2010) 'Effect of calcium ion (cross-linker) concentration on porosity, surface morphology and thermal behavior of calcium alginates prepared from algae (*Undaria pinnatifida*)', *Carbohydrate Polymers*, 81(3), pp. 633-639.
- Pavlostathis, S.G. and Gossett, J.M. (1986) 'A kinetic model for anaerobic digestion of biological sludge', *Biotechnology and Bioengineering*, 28(10), pp. 1519-1530.
- Pedersen, A. (1984) 'Studies on phenol content and heavy metal uptake in fucoids', in Bird, C. and Ragan, M. (eds.) *Eleventh International Seaweed Symposium*. Springer Netherlands, pp. 498-504.
- Peng, S., Scalbert, A. and Monties, B. (1991) 'Insoluble ellagitannins in *Castanea sativa* and *Quercus petraea* woods', *Phytochemistry*, 30(3), pp. 775-778.
- Penman, A. and Sanderson, G.R. (1972) 'A method for the determination of uronic acid sequence in alginates', *Carbohydrate Research*, 25(2), pp. 273-282.

Pesta, G. (2007) 'Anaerobic digestion of organic residues and wastes', in *Utilization of by-products and treatment of waste in the food industry*. Springer, pp. 53-72.

Peu, P., Picard, S., Diara, A., Girault, R., Béline, F., Bridoux, G. and Dabert, P. (2012) 'Prediction of hydrogen sulphide production during anaerobic digestion of organic substrates', *Bioresource Technology*, 121, pp. 419-424.

Peu, P., Sassi, J.F., Girault, R., Picard, S., Saint-Cast, P., Béline, F. and Dabert, P. (2011) 'Sulphur fate and anaerobic biodegradation potential during co-digestion of seaweed biomass (*Ulva* sp.) with pig slurry', *Bioresource Technology*, 102(23), pp. 10794-10802.

Pham, T.N., Um, Y. and Yoon, H.H. (2013a) 'Pretreatment of macroalgae for volatile fatty acid production', *Bioresource Technology*, 146(0), pp. 754-757.

Pham, T.N., Um, Y. and Yoon, H.H. (2013b) 'Pretreatment of macroalgae for volatile fatty acid production', *Bioresource Technology*, 146, pp. 754-757.

Pobeheim, H., Munk, B., Müller, H., Berg, G. and Guebitz, G.M. (2010) 'Characterization of an anaerobic population digesting a model substrate for maize in the presence of trace metals', *Chemosphere*, 80(8), pp. 829-836.

Poirier, S., Madigou, C., Bouchez, T. and Chapleur, O. (2017) 'Improving anaerobic digestion with support media: Mitigation of ammonia inhibition and effect on microbial communities', *Bioresource Technology*, 235(Supplement C), pp. 229-239.

Prabhudessai, V., Ganguly, A. and Mutnuri, S. (2013) 'Biochemical methane potential of agro wastes', *Journal of Energy*, 2013.

Pretorius, W.A. (1969) 'Anaerobic digestion III. kinetics of anaerobic fermentation', *Water Research*, 3(8), pp. 545-558.

Price, J.H. (1979) 'Seaweeds. A color-coded, illustrated guide to common marine plants of the east coast of the United States', *Aquatic Botany*, 7, pp. 399-400.

Procházka, J., Dolejš, P., Máca, J. and Dohányos, M. (2012) 'Stability and inhibition of anaerobic processes caused by insufficiency or excess of ammonia nitrogen', *Applied Microbiology and Biotechnology*, 93(1), pp. 439-447.

Radha, M. and Murugesan, A.G. (2017) 'Enhanced dark fermentative biohydrogen production from marine macroalgae *Padina tetrastratica* by different pretreatment processes', *Biofuel Research Journal*, 4(1), pp. 551-558.

Ragan, M.A. and Glombitza, K.-W. (1986) 'Phlorotannins, brown algal polyphenols', *Progress in phycolgical research*, 4, pp. 129-241.



Ragauskas, A.J., Williams, C.K., Davison, B.H., Britovsek, G., Cairney, J., Eckert, C.A., Frederick, W.J., Hallett, J.P., Leak, D.J., Liotta, C.L., Mielenz, J.R., Murphy, R., Templer, R. and Tschaplinski, T. (2006) 'The Path Forward for Biofuels and Biomaterials', *Science*, 311(5760), pp. 484-489.

Rajagopal, R., Massé, D.I. and Singh, G. (2013) 'A critical review on inhibition of anaerobic digestion process by excess ammonia', *Bioresource Technology*, 143(0), pp. 632-641.

Rao, M.S. and Singh, S.P. (2004) 'Bioenergy conversion studies of organic fraction of MSW: kinetic studies and gas yield–organic loading relationships for process optimisation', *Bioresource Technology*, 95(2), pp. 173-185.

Rao, P.V. and Baral, S.S. (2011) 'Experimental design of mixture for the anaerobic co-digestion of sewage sludge', *Chemical Engineering Journal*, 172(2), pp. 977-986.

Raposo, F., Banks, C.J., Siegert, I., Heaven, S. and Borja, R. (2006) 'Influence of inoculum to substrate ratio on the biochemical methane potential of maize in batch tests', *Process Biochemistry*, 41(6), pp. 1444-1450.

Raposo, F., Borja, R., Martín, M.A., Martín, A., de la Rubia, M.A. and Rincón, B. (2009) 'Influence of inoculum–substrate ratio on the anaerobic digestion of sunflower oil cake in batch mode: Process stability and kinetic evaluation', *Chemical Engineering Journal*, 149(1–3), pp. 70-77.

Raposo, F., Borja, R., Rincon, B. and Jimenez, A.M. (2008) 'Assessment of process control parameters in the biochemical methane potential of sunflower oil cake', *Biomass and Bioenergy*, 32(12), pp. 1235-1244.

Raposo, F., De La Rubia, M.A., Fernández-Cegrí, V. and Borja, R. (2011a) 'Anaerobic digestion of solid organic substrates in batch mode: An overview relating to methane yields and experimental procedures', *Renewable and Sustainable Energy Reviews*, 16(1), pp. 861-877.

Raposo, F., Fernández-Cegrí, V., De la Rubia, M.A., Borja, R., Béline, F., Cavinato, C., Demirer, G., Fernández, B., Fernández-Polanco, M., Frigon, J.C., Ganesh, R., Kaparaju, P., Koubova, J., Méndez, R., Menin, G., Peene, A., Scherer, P., Torrijos, M., Uellendahl, H., Wierinck, I. and de Wilde, V. (2011b) 'Biochemical methane potential (BMP) of solid organic substrates: evaluation of anaerobic biodegradability using data from an international interlaboratory study', *Journal of Chemical Technology & Biotechnology*, 86(8), pp. 1088-1098.

Ras, M., Lardon, L., Bruno, S., Bernet, N. and Steyer, J.P. (2011) 'Experimental study on a coupled process of production and anaerobic digestion of *Chlorella vulgaris*', *Bioresource Technology*, 102(1), pp. 200-206.

Ravi, P.P., Lindner, J., Oechsner, H. and Lemmer, A. (2018) 'Effects of target pH-value on organic acids and methane production in two-stage anaerobic

- digestion of vegetable waste', *Bioresource Technology*, 247(Supplement C), pp. 96-102.
- Redwood, M.D., Paterson-Beedle, M. and MacAskie, L.E. (2009) 'Integrating dark and light bio-hydrogen production strategies: Towards the hydrogen economy', *Reviews in Environmental Science and Biotechnology*, 8(2), pp. 149-185.
- Rehm, B.H.A. and Moradali, M.F. (2017) *Alginates and Their Biomedical Applications*. Springer Singapore.
- Reis, M.A.M., Lemos, P.C., Almeida, J.S. and Carrondo, M.J.T. (1991) 'Evidence for the intrinsic toxicity of H<sub>2</sub>S to sulphate-reducing bacteria', *Applied Microbiology and Biotechnology*, 36(1), pp. 145-147.
- Riffat, R. and Krongthamchat, K. (2006) 'Specific methanogenic activity of halophilic and mixed cultures in saline wastewater', *International Journal of Environmental Science & Technology*, 2(4), pp. 291-299.
- Ripley, L.E., Boyle, W.C. and Converse, J.C. (1986) 'Improved Alkalimetric Monitoring for Anaerobic Digestion of High-Strength Wastes', *Journal (Water Pollution Control Federation)*, 58(5), pp. 406-411.
- Ritschard, R.L. (1992) 'Marine algae as a CO<sub>2</sub> sink', *Water, Air, and Soil Pollution*, 64(1), pp. 289-303.
- Rocca, S., Agostini, A., Giuntoli, J. and Marelli, L. (2015) 'Biofuels from algae: technology options, energy balance and GHG emissions'.
- Ródenas de la Rocha, S., Sánchez-Muniz, F.J., Gómez-Juaristi, M. and Marín, M.T.L. (2009) 'Trace elements determination in edible seaweeds by an optimized and validated ICP-MS method', *Journal of Food Composition and Analysis*, 22(4), pp. 330-336.
- Roesijadi, G., Jones, S.B., Snowden-Swan, L.J. and Zhu, Y. (2010) *Macroalgae as a Biomass Feedstock: A Preliminary Analysis* (PNNL-19944; Other: BM0204010; TRN: US201106%%96 United States 10.2172/1006310 ). ; Pacific Northwest National Laboratory (PNNL), Richland, WA (US). [Online]. Available at: <http://www.osti.gov/scitech/servlets/purl/1006310>.
- Romero-Güiza, M.S., Vila, J., Mata-Alvarez, J., Chimenos, J.M. and Astals, S. (2016) 'The role of additives on anaerobic digestion: A review', *Renewable and Sustainable Energy Reviews*, 58, pp. 1486-1499.
- Ross, A.B., Anastasakis, K., Kubacki, M. and Jones, J.M. (2009) 'Investigation of the pyrolysis behaviour of brown algae before and after pre-treatment using PY-GC/MS and TGA', *Journal of Analytical and Applied Pyrolysis*, 85(1–2), pp. 3-10.

- Ross, A.B., Hall, C., Anastasakis, K., Westwood, A., Jones, J.M. and Crewe, R.J. (2011) 'Influence of cation on the pyrolysis and oxidation of alginates', *Journal of Analytical and Applied Pyrolysis*, 91(2), pp. 344-351.
- Ross, A.B., Jones, J.M., Kubacki, M.L. and Bridgeman, T. (2008) 'Classification of macroalgae as fuel and its thermochemical behaviour', *Bioresource Technology*, 99(14), pp. 6494-6504.
- Rowbotham, J.S., Dyer, P.W., Greenwell, H.C., Selby, D. and Theodorou, M.K. (2013) 'Copper(II)-mediated thermolysis of alginates: a model kinetic study on the influence of metal ions in the thermochemical processing of macroalgae', *Interface Focus*, 3(1), p. 20120046.
- Rozzi, A. and Remigi, E. (2004) 'Methods of assessing microbial activity and inhibition under anaerobic conditions: a literature review', *Re/Views in Environmental Science & Bio/Technology*, 3(2), pp. 93-115.
- Sambusiti, C., Bellucci, M., Zabaniotou, A., Beneduce, L. and Monlau, F. (2015) 'Algae as promising feedstocks for fermentative biohydrogen production according to a biorefinery approach: A comprehensive review', *Renewable and Sustainable Energy Reviews*, 44, pp. 20-36.
- Samson, R. and Leduyt, A. (1986) 'Detailed study of anaerobic digestion of *Spirulina maxima* algal biomass', *Biotechnology and Bioengineering*, 28(7), pp. 1014-1023.
- Sans, C., Mata-Alvarez, J., Cecchi, F. and Pavan, P. (1993) 'Volatile Fatty Acids Production by Anaerobic Fermentation of Urban Organic Wastes', *PREPRINTS OF PAPERS-AMERICAN CHEMICAL SOCIETY DIVISION FUEL CHEMISTRY*, 38, pp. 886-886.
- Sarkar, A., Ranjan Mukhopadhyay, A. and Kumar Ghosh, S. (2014) 'Developing a model for process improvement using multiple regression technique: A case example', *The TQM Journal*, 26(6), pp. 625-638.
- Sawyer, C.N. and Carty, M. (1994) 'PL,'PARKIN, GF" Chemistry for environmental Engineering". Mc Graw-Hill International Editions, Civil Engineering Series.
- Scalbert, A. (1991) 'Antimicrobial properties of tannins', *Phytochemistry*, 30(12), pp. 3875-3883.
- Scherer, P. and Sahm, H. (1981a) 'influence of sulfur-containing compounds on the growth of *Methanosarcina barkeri* in a defined medium ', *Eur.J.Appl.Microbiol.Biotechnol.*, 12, pp. 28-35.
- Scherer, P. and Sahm, H. (1981b) 'Influence of sulphur-containing compounds on the growth of *Methanosarcina barkeri* in a defined medium', *European journal of applied microbiology and biotechnology*, 12(1), pp. 28-35.

Schieder, D., Schneider, R. and Bischof, F. (2000) 'Thermal hydrolysis (TDH) as a pretreatment method for the digestion of organic waste', *Water Science and Technology*, 41(3), pp. 181-187.

Schillo, R.S., Isabelle, D.A. and Shakiba, A. (2017) 'Linking advanced biofuels policies with stakeholder interests: A method building on Quality Function Deployment', *Energy Policy*, 100, pp. 126-137.

Schink, B. (1997) 'Energetics of syntrophic cooperation in methanogenic degradation', *Microbiology and molecular biology reviews*, 61(2), pp. 262-280.

Schneider, O., Sereti, V., Eding, E.H. and Verreth, J.A.J. (2005) 'Analysis of nutrient flows in integrated intensive aquaculture systems', *Aquacultural engineering*, 32(3), pp. 379-401.

Schnürer, A., Bohn, I. and Moestedt, J. (2017) 'Protocol for Start-Up and Operation of CSTR Biogas Processes', *Hydrocarbon and Lipid Microbiology Protocols: Bioproducts, Biofuels, Biocatalysts and Facilitating Tools*, pp. 171-200.

Schnurer, A. and Jarvis, A. (2010) 'Microbiological handbook for biogas plants', *Swedish Waste Management U*, 2009, pp. 1-74.

Schoenwaelder, M.E.A. (2002) 'The occurrence and cellular significance of phycodes in brown algae', *Phycologia*, 41(2), pp. 125-139.

Schuck, S. (2006) 'Biomass as an Energy Source', *International Journal of Environmental Studies*, 63(6), pp. 823-823.

Schwede, S., Kowalczyk, A., Gerber, M. and Span, R. (2011) *World Renewable Energy Congress, Linköping, Sweden*.

Scott, S.A., Davey, M.P., Dennis, J.S., Horst, I., Howe, C.J., Lea-Smith, D.J. and Smith, A.G. (2010) 'Biodiesel from algae: Challenges and prospects', *Current Opinion in Biotechnology*, 21(3), pp. 277-286.

Seadi Al Teodorita, D.R., Heinz Prassl, Michael Köttner, Tobias Finsterwalder, Silke Volk, Rainer Janssen (2008) *Biogas handbook: Lemvig Biogas*. University of Southern Denmark Esbjerg, Niels Bohrs Vej 9-10, DK-6700 Esbjerg, Denmark.

Seagren, E.A., Levine, A.D. and Dague, R.R. (1991) 'High pH effects in anaerobic treatment of liquid industrial by-products', *Purdue Industrial Waste Conference* pp 377-386

Serna-Maza, A., Heaven, S. and Banks, C.J. (2014) 'Ammonia removal in food waste anaerobic digestion using a side-stream stripping process', *Bioresource Technology*, 152(Supplement C), pp. 307-315.

Shobana, S., Kumar, G., Bakonyi, P., Saratale, G.D., Al-Muhtaseb, A.a.H., Nemestóthy, N., Bélafi-Bakó, K., Xia, A. and Chang, J.-S. (2017) 'A review on the biomass pretreatment and inhibitor removal methods as key-steps towards efficient macroalgae-based biohydrogen production', *Bioresource Technology*, 244(Part 2), pp. 1341-1348.

Shujun, C., Jishi, Z. and Xikui, W. (2015) 'Effects of alkalinity sources on the stability of anaerobic digestion from food waste', *Waste Management & Research*, 33(11), pp. 1033-1040.

Sialve, B., Bernet, N. and Bernard, O. (2009a) 'Anaerobic digestion of microalgae as a necessary step to make microalgal biodiesel sustainable', *Biotechnology Advances*, 27(4), pp. 409-416.

Sialve, B., Bernet, N. and Bernard, O. (2009b) 'Anaerobic digestion of microalgae as a necessary step to make microalgal biodiesel sustainable', *Biotechnol Adv*, 27.

Siegert, I. and Banks, C. (2005) 'The effect of volatile fatty acid additions on the anaerobic digestion of cellulose and glucose in batch reactors', *Process Biochemistry*, 40(11), pp. 3412-3418.

Sillanpää, M. and Ncibi, C. (2017) *A Sustainable Bioeconomy: The Green Industrial Revolution*. Springer International Publishing.

Sims, R.E.H., Mabee, W., Saddler, J.N. and Taylor, M. (2010) 'An overview of second generation biofuel technologies', *Bioresource Technology*, 101(6), pp. 1570-1580.

Singh, A., Nigam, P.S. and Murphy, J.D. (2011a) 'Mechanism and challenges in commercialisation of algal biofuels', *Bioresource Technology*, 102(1), pp. 26-34.

Singh, A., Nigam, P.S. and Murphy, J.D. (2011b) 'Renewable fuels from algae: An answer to debatable land based fuels', *Bioresource Technology*, 102(1), pp. 10-16.

Singh, A., Smyth, B.M. and Murphy, J.D. (2010) 'A biofuel strategy for Ireland with an emphasis on production of biomethane and minimization of land-take', *Renewable and Sustainable Energy Reviews*, 14(1), pp. 277-288.

Smyth, B.M., Ó Gallachóir, B.P., Korres, N.E. and Murphy, J.D. (2010) 'Can we meet targets for biofuels and renewable energy in transport given the constraints imposed by policy in agriculture and energy?', *Journal of Cleaner Production*, 18(16–17), pp. 1671-1685.

- Soares, J.P., Santos, J.E., Chierice, G.O. and Cavalheiro, E.T.G. (2004) 'Thermal behavior of alginic acid and its sodium salt', *Eclética Química*, 29(2), pp. 57-64.
- Somma, D., Lobkowicz, H. and Deason, J.P. (2010) 'Growing America's fuel: an analysis of corn and cellulosic ethanol feasibility in the United States', *Clean Technologies and Environmental Policy*, 12(4), pp. 373-380.
- Song, M., Pham, H.D., Seon, J. and Woo, H.C. (2015) 'Overview of anaerobic digestion process for biofuels production from marine macroalgae: A developmental perspective on brown algae', *Korean Journal of Chemical Engineering*, 32(4), pp. 567-575.
- Souto, T.F., Aquino, S.F., Silva, S.Q. and Chernicharo, C.A.L. (2010) 'Influence of incubation conditions on the specific methanogenic activity test', *Biodegradation*, 21(3), pp. 411-424.
- Speece, R.E. (1996a) *Anaerobic biotechnology : for industrial wastewaters*. Nashville: Nashville : Archae Press.
- Speece, R.E. (1996b) *Anaerobic Biotechnology for Industrial Wastewaters* Arche Press , Nashville, TN.
- Spencer, C.M., Cai, Y., Martin, R., Gaffney, S.H., Goulding, P.N., Magnolato, D., Lilley, T.H. and Haslam, E. (1988) 'Polyphenol complexation—some thoughts and observations', *Phytochemistry*, 27(8), pp. 2397-2409.
- Sprott, G.D. and Patel, G.B. (1986) 'Ammonia toxicity in pure cultures of methanogenic bacteria', *Systematic and applied microbiology*, 7(2-3), pp. 358-363.
- Steinberg, P.D. (1995) 'Seasonal variation in the relationship between growth rate and phlorotannin production in the kelp *Ecklonia radiata*', *Oecologia*, 102(2), pp. 169-173.
- Stephen, A.M. and Phillips, G.O. (2016) *Food Polysaccharides and Their Applications*. CRC Press.
- Stern, J.L., Hagerman, A., Steinberg, P., Winter, F. and Estes, J. (1996a) 'A new assay for quantifying brown algal phlorotannins and comparisons to previous methods', *Journal of Chemical Ecology*, 22(7), pp. 1273-1293.
- Stern, J.L., Hagerman, A.E., Steinberg, P.D., Winter, F.C. and Estes, J.A. (1996b) 'A new assay for quantifying brown algal phlorotannins and comparisons to previous methods', *Journal of Chemical Ecology*, 22(7), pp. 1273-1293.

Stern, N. (2006) *Stern Review executive summary, 2006*. [Online]. Available at: [http://www.wwf.se/source.php/1169157/Stern%20Report\\_Exec%20Summary.pdf](http://www.wwf.se/source.php/1169157/Stern%20Report_Exec%20Summary.pdf).

Stevens, C.V. and Verhé, R. (2004) *Renewable bioresources : scope and modification for non-food applications*. Hoboken, N.J.: Hoboken, N.J. : J. Wiley.

Stiller, J.W. and Hall, B.D. (1997) 'The origin of red algae: implications for plastid evolution', *Proceedings of the National Academy of Sciences*, 94(9), pp. 4520-4525.

Strack, D., Heilemann, J., Mömken, M. and Wray, V. (1988) 'Cell wall-conjugated phenolics from coniferae leaves', *Phytochemistry*, 27(11), pp. 3517-3521.

Subramanian, V. and Dakshinamoorthy, B. (2015) 'FT-IR, 1H-NMR and 13C-NMR Spectroscopy of alginate extracted from turbinaria decurrens (Phaeophyta)'

Sunada, N.d.S., Orrico, A.C.A., Orrico Júnior, M.A.P., Vargas Junior, F.M.d., Garcia, R.G. and Fernandes, A.R.M. (2012) 'Potential of biogas and methane production from anaerobic digestion of poultry slaughterhouse effluent', *Revista Brasileira de Zootecnia*, 41, pp. 2379-2383.

Suwannopadol, S., Ho, G. and Cord-Ruwisch, R. (2012) 'Overcoming sodium toxicity by utilizing grass leaves as co-substrate during the start-up of batch thermophilic anaerobic digestion', *Bioresource Technology*, 125, pp. 188-192.

Switzenbaum, M.S., Giraldo-Gomez, E. and Hickey, R.F. (1990) 'Monitoring of the anaerobic methane fermentation process', *Enzyme and Microbial Technology*, 12(10), pp. 722-730.

Sze, P. (1998) *A biology of the algae*. 3rd ed.. edn. Boston, Mass.: Boston, Mass. : WCB/McGraw-Hill.

Tabassum, M.R., Wall, D.M. and Murphy, J.D. (2016a) 'Biogas production generated through continuous digestion of natural and cultivated seaweeds with dairy slurry', *Bioresource Technology*, 219, pp. 228-238.

Tabassum, M.R., Xia, A. and Murphy, J.D. (2016b) 'The effect of seasonal variation on biomethane production from seaweed and on application as a gaseous transport biofuel', *Bioresource Technology*, 209, pp. 213-219.

Tabassum, M.R., Xia, A. and Murphy, J.D. (2016c) 'Seasonal variation of chemical composition and biomethane production from the brown seaweed *Ascophyllum nodosum*', *Bioresource Technology*, 216, pp. 219-226.

- Tabassum, M.R., Xia, A. and Murphy, J.D. (2017) 'Potential of seaweed as a feedstock for renewable gaseous fuel production in Ireland', *Renewable and Sustainable Energy Reviews*, 68(Part 1), pp. 136-146.
- Takagi, M., Abe, S., Suzuki, S., Emert, G.H. and Yata, N. (1977) *Bioconversion Symposium; New Dehli, India*.
- Takashima, M. and Speece, R.E. (1989) 'Mineral nutrient requirements for high-rate methane fermentation of acetate at low SRT', *Research Journal of the Water Pollution Control Federation*, 61(11/12), pp. 1645-1650.
- Targett, N., Coen, L., Boettcher, A. and Tanner, C. (1992) 'Biogeographic comparisons of marine algal polyphenolics: evidence against a latitudinal trend', *Oecologia*, 89(4), pp. 464-470.
- Tchobanoglous, G., Theisen, H. and Vigil, S. (1993) *Integrated solid waste management: engineering principles and management issues*. McGraw-Hill Science/Engineering/Math.
- Tedesco, S., Marrero Barroso, T. and Olabi, A.G. (2014) 'Optimization of mechanical pre-treatment of Laminariaceae spp. biomass-derived biogas', *Renewable Energy*, 62, pp. 527-534.
- Teh, Y.Y., Lee, K.T., Chen, W.-H., Lin, S.-C., Sheen, H.-K. and Tan, I.S. (2017) 'Dilute sulfuric acid hydrolysis of red macroalgae *Euclima denticulatum* with microwave-assisted heating for biochar production and sugar recovery', *Bioresource Technology*.
- Thanh, P.M., Ketheesan, B., Yan, Z. and Stuckey, D. (2016) 'Trace metal speciation and bioavailability in anaerobic digestion: A review', *Biotechnology Advances*, 34(2), pp. 122-136.
- Thorin, E., Olsson, J., Schwede, S. and Nehrenheim, E. (2017) 'Biogas from Co-digestion of Sewage Sludge and Microalgae', *Energy Procedia*, 105(Supplement C), pp. 1037-1042.
- Tiehm, A., Nickel, K., Zellhorn, M. and Neis, U. (2001) 'Ultrasonic waste activated sludge disintegration for improving anaerobic stabilization', *Water Research*, 35(8), pp. 2003-2009.
- Tishkov, V.I. and Popov, V.O. (2004) 'Catalytic mechanism and application of formate dehydrogenase', *Biochemistry (Moscow)*, 69(11), p. 1252.
- Titlyanov, E.A. and Titlyanova, T.V. (2010) 'Seaweed cultivation: Methods and problems', *Russian Journal of Marine Biology*, 36(4), pp. 227-242.
- Tiwari, G.N. (2005) *Renewable energy resources : basic principles and applications*. Harrow, England: Harrow, England : Alpha Science International.



- Torres, M.R., Sousa, A.P.A., Silva Filho, E.A.T., Melo, D.F., Feitosa, J.P.A., de Paula, R.C.M. and Lima, M.G.S. (2007) 'Extraction and physicochemical characterization of Sargassum vulgare alginate from Brazil', *Carbohydrate research*, 342(14), pp. 2067-2074.
- Trisakti, B., Adipasah, H. and Turmuzi, M. (2017) *IOP Conference Series: Materials Science and Engineering*. IOP Publishing.
- Turovskii, I.S. (2006) *Wastewater sludge processing*. Hoboken, N. J.: Hoboken, N. J. : John Wiley & Sons.
- Tursman, J.F. and Cork, D.J. (1988) *Influence of sulfate and sulfate-reducing bacteria on anaerobic digestion technology*. In: Mizradi, A van Wezel , A . (Eds): Alan R.Liss, Inc.
- Twidell, J. and Weir, T. (2015) *Renewable energy resources*. Routledge.
- Ulgati, S. (2001) 'A Comprehensive Energy and Economic Assessment of Biofuels: When "Green" Is Not Enough', *Critical Reviews in Plant Sciences*, 20(1), pp. 71-106.
- Ullah, K., Ahmad, M., Sofia, Sharma, V.K., Lu, P., Harvey, A., Zafar, M., Sultana, S. and Anyanwu, C.N. (2014) 'Algal biomass as a global source of transport fuels: Overview and development perspectives', *Progress in Natural Science: Materials International*, 24(4), pp. 329-339.
- UN (2016) *COP21 | United nations conference on climate change*. [Online]. Available at: <http://www.cop21.gouv.fr/en/> (Accessed: 14.01.17).
- UN (2017) 'Sustainable Development Goals : 17 Goals to transform our world'. 04.01.2017. Available at: <http://www.un.org/sustainabledevelopment/blog/2015/07/un-projects-world-population-to-reach-8-5-billion-by-2030-driven-by-growth-in-developing-countries/>.
- Usov, A.I. (1998) 'Structural analysis of red seaweed galactans of agar and carrageenan groups', *Food Hydrocolloids*, 12(3), pp. 301-308.
- Uygur, A. (2006) 'Specific nutrient removal rates in saline wastewater treatment using sequencing batch reactor', *Process Biochemistry*, 41(1), pp. 61-66.
- Valcke, D. and Verstraete, W. (1983) 'A practical method to estimate the acetoclastic methanogenic biomass in anaerobic sludges', *Journal of the Water Pollution Control Federation*, 55(9), pp. 1191-1195.
- Vallejo, T., Alexandra, M. and Vásquez Suárez, A.L. (2017) 'Anaerobic co-digestion of organic residues from different productive sectors in Colombia: biomethanation potential assessment'.

- Van Alstyne, K.L., McCarthy, J.J., Hustead, C.L. and Kearns, L.J. (1999) 'PHLOROTANNIN ALLOCATION AMONG TISSUES OF NORTHEASTERN PACIFIC KELPS AND ROCKWEEDS', *Journal of Phycology*, 35(3), pp. 483-492.
- Van Haandel, A.C. and Lettinga, G. (1994) *Anaerobic sewage treatment: a practical guide for regions with a hot climate*. John Wiley & Sons.
- Vanegas, C. and Bartlett, J. (2013a) 'Anaerobic Digestion of *Laminaria digitata*: The Effect of Temperature on Biogas Production and Composition', *Waste and Biomass Valorization*, 4(3), pp. 509-515.
- Vanegas, C.H. and Bartlett, J. (2013b) 'Green energy from marine algae: biogas production and composition from the anaerobic digestion of Irish seaweed species', *Environmental Technology*, 34(15), pp. 2277-2283.
- Varel, V.H., Chen, T.H. and Hashimoto, A.G. (1988) 'Thermophilic and mesophilic methane production from anaerobic degradation of the cyanobacterium *Spirulina maxima*', *Resources, Conservation and Recycling*, 1(1), pp. 19-26.
- Várhegyi, G., Bobály, B., Jakab, E. and Chen, H. (2011) 'Thermogravimetric Study of Biomass Pyrolysis Kinetics. A Distributed Activation Energy Model with Prediction Tests', *Energy & Fuels*, 25(1), pp. 24-32.
- VDI (2006) 'VDI 4630 : Fermentation of organic materials -Characterisation of the substrate, sampling, collection of material data, fermentation tests. In: Verein Deutscher Ingenieure (VDI) (Ed.), VDI Handbuch Energietechnik. Berlin: Beuth Verlag GmbH:44-59'.
- Velasco, A., Ramírez, M., Volke-Sepúlveda, T., González-Sánchez, A. and Revah, S. (2008) 'Evaluation of feed COD/sulfate ratio as a control criterion for the biological hydrogen sulfide production and lead precipitation', *Journal of Hazardous Materials*, 151(2-3), pp. 407-413.
- Venkatesan, J., Anil, S. and Kim, S.K. (2017) *Seaweed Polysaccharides: Isolation, Biological and Biomedical Applications*. Elsevier Science.
- Vergara-Fernández, A., Vargas, G., Alarcón, N. and Velasco, A. (2008) 'Evaluation of marine algae as a source of biogas in a two-stage anaerobic reactor system', *Biomass and Bioenergy*, 32(4), pp. 338-344.
- Verma, S. (2002) *Anaerobic digestion of biodegradable organics in municipal solid wastes*. Columbia University.
- Vindis, P., Mursec, B., Janzekovic, M. and Cus, F. (2009) 'The impact of mesophilic and thermophilic anaerobic digestion on biogas production', *Journal of achievements in materials and manufacturing Engineering*, 36(2), pp. 192-198.

- Vivekanand, V., Eijssink, V.G.H. and Horn, S.J. (2012) 'Biogas production from the brown seaweed *Saccharina latissima*: Thermal pretreatment and codigestion with wheat straw', *Journal of Applied Phycology*, 24(5), pp. 1295-1301.
- Wang, J., Wang, G., Zhang, M., Chen, M., Li, D., Min, F., Chen, M., Zhang, S., Ren, Z. and Yan, Y. (2006) 'A comparative study of thermolysis characteristics and kinetics of seaweeds and fir wood', *Process Biochemistry*, 41(8), pp. 1883-1886.
- Wang, K., Yin, J., Shen, D. and Li, N. (2014) 'Anaerobic digestion of food waste for volatile fatty acids (VFAs) production with different types of inoculum: Effect of pH', *Bioresource Technology*, 161(Supplement C), pp. 395-401.
- Wang, S., Hou, X. and Su, H. (2017) 'Exploration of the relationship between biogas production and microbial community under high salinity conditions', *Scientific Reports*, 7, p. 1149.
- Wang, X., Yang, G., Feng, Y., Ren, G. and Han, X. (2012) 'Optimizing feeding composition and carbon–nitrogen ratios for improved methane yield during anaerobic co-digestion of dairy, chicken manure and wheat straw', *Bioresource Technology*, 120, pp. 78-83.
- Ward, A.J., Hobbs, P.J., Holliman, P.J. and Jones, D.L. (2008) 'Optimisation of the anaerobic digestion of agricultural resources', *Bioresource Technology*, 99(17), pp. 7928-7940.
- Ward, A.J., Lewis, D.M. and Green, F.B. (2014) 'Anaerobic digestion of algae biomass: A review', *Algal Research*, 5(0), pp. 204-214.
- Wei, N., Quarterman, J. and Jin, Y.-S. (2013) 'Marine macroalgae: an untapped resource for producing fuels and chemicals', *Trends in Biotechnology*, 31(2), pp. 70-77.
- Wellinger, A., Murphy, J.D. and Baxter, D. (2013) *The Biogas Handbook: Science, Production and Applications*. Elsevier Science.
- West, J., Calumpong, H.P. and Martin, G. (2016) '. Seaweeds'.
- Wiencke, C. and Bischof, K. (2012) 'Seaweed biology: Novel insights into ecophysiology, ecology and utilization', *Ecological Studies*.
- Wiesmann, U., Choi, I.S. and Dombrowski, E.-M. (2007) *Fundamentals of biological wastewater treatment*. John Wiley & Sons.
- Wilkie, A., Goto, M., Bordeaux, F.M. and Smith, P.H. (1986) 'Enhancement of anaerobic methanogenesis from napiergrass by addition of micronutrients', *Biomass*, 11(2), pp. 135-146.

- Wilkie, A.C. (2005) 'Anaerobic digestion: biology and benefits', *Dairy Manure Management: Treatment, Handling, and Community Relations*, pp. 63-72.
- Williamson, P. (1992) 'A Curb on Carbon?', *Ambio*, 21(5), pp. 387-387.
- Wisconsin Department of Natural Resources (1992) *Advanced Anaerobic Digestion Study Guide*. Wisconsin Department of Natural Resources Bureau of Science Services. [Online]. Available at: <http://dnr.wi.gov>.
- Wittmann, C., Zeng, A.P. and Deckwer, W.D. (1995) 'Growth inhibition by ammonia and use of a pH-controlled feeding strategy for the effective cultivation of *Mycobacterium chlorophenolicum*', *Applied Microbiology and Biotechnology*, 44(3), pp. 519-525.
- Wong, T.W., Chan, L.W., Kho, S.B. and Sia Heng, P.W. (2002) 'Design of controlled-release solid dosage forms of alginate and chitosan using microwave', *Journal of Controlled Release*, 84(3), pp. 99-114.
- Wu, X., Yao, W., Zhu, J. and Miller, C. (2010) 'Biogas and CH<sub>4</sub> productivity by co-digesting swine manure with three crop residues as an external carbon source', *Bioresource Technology*, 101(11), pp. 4042-4047.
- Wujcik, W.J. and Jewell, W.J. (1980) *Biotechnol. Bioeng. Symp.:(United States)*. Cornell Univ., NY.
- Xie, S., Wickham, R. and Nghiem, L.D. (2017a) 'Synergistic effect from anaerobic co-digestion of sewage sludge and organic wastes', *International Biodeterioration & Biodegradation*, 116(Supplement C), pp. 191-197.
- Xie, T., Xie, S., Sivakumar, M. and Nghiem, L.D. (2017b) 'Relationship between the synergistic/antagonistic effect of anaerobic co-digestion and organic loading', *International Biodeterioration & Biodegradation*, 124(Supplement C), pp. 155-161.
- Xie, Y. (2016) *Disinfection Byproducts in Drinking Water: Formation, Analysis, and Control*. CRC Press.
- Xu, F., Shi, J., Lv, W., Yu, Z. and Li, Y. (2013) 'Comparison of different liquid anaerobic digestion effluents as inocula and nitrogen sources for solid-state batch anaerobic digestion of corn stover', *Waste Management*, 33(1), pp. 26-32.
- Yang, H., Deng, L., Liu, G., Yang, D., Liu, Y. and Chen, Z. (2016) 'A model for methane production in anaerobic digestion of swine wastewater', *Water Research*, 102(Supplement C), pp. 464-474.
- Yano, T., Nakahara, T., Kamiyama, S. and Yamada, K. (1966) 'Kinetic Studies on Microbial Activities in Concentrated Solutions. Part. I

Effect of Excess Sugars on Oxygen Uptake Rate of a Cell Free Respiratory System', *Agricultural and Biological Chemistry*, 30(1), pp. 42-48.

Yao, W., Yongming, S., Zhenhong, Y., Lianhua, L. and Xinshu, Z. (2016) 'Effect of Trace Elements Supplement on Anaerobic Fermentation of Food Waste', *Nature Environment and Pollution Technology*, 15(2), p. 747.

Yates, J.L. and Peckol, P. (1993) 'Effects of nutrient availability and herbivory on polyphenolics in the seaweed *Fucus vesiculosus*', *Ecology*, pp. 1757-1766.

Yen, H.-W. and Brune, D.E. (2007a) 'Anaerobic co-digestion of algal sludge and waste paper to produce methane', *Bioresource Technology*, 98(1), pp. 130-134.

Yen, H.W. and Brune, D.E. (2007b) 'Anaerobic co-digestion of algal sludge and waste paper to produce methane', *Bioresource Technology*, 98(1), pp. 130-134.

Yi, J., Dong, B., Jin, J. and Dai, X. (2014) 'Effect of Increasing Total Solids Contents on Anaerobic Digestion of Food Waste under Mesophilic Conditions: Performance and Microbial Characteristics Analysis', *PLoS ONE*, 9(7), p. e102548.

Yong, Z., Dong, Y., Zhang, X. and Tan, T. (2015) 'Anaerobic co-digestion of food waste and straw for biogas production', *Renewable Energy*, 78(Supplement C), pp. 527-530.

Young, E.B., Dring, M.J., Savidge, G., Birkett, D.A. and Berges, J.A. (2007) 'Seasonal variations in nitrate reductase activity and internal N pools in intertidal brown algae are correlated with ambient nitrate concentrations', *Plant, cell & environment*, 30(6), pp. 764-774.

Young, L.Y. and Rivera, M.D. (1985) 'Methanogenic degradation of four phenolic compounds', *Water Research*, 19(10), pp. 1325-1332.

Zandvoort, M., van Hullebusch, E., Feroso, F. and Lens, P. (2006) 'Trace metals in anaerobic granular sludge reactors: Bioavailability and dosing strategies', *Engineering In Life Sciences*, 6(3), pp. 293-301.

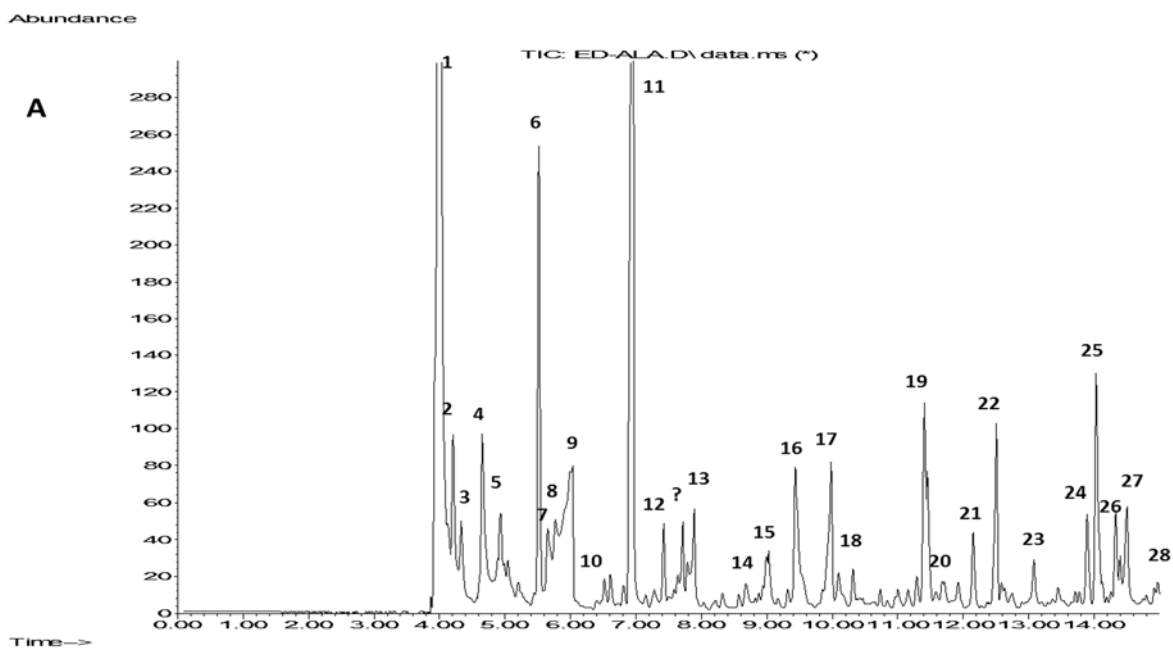
Zayed, G. and Winter, J. (2000) 'Inhibition of methane production from whey by heavy metals – protective effect of sulfide', *Applied Microbiology and Biotechnology*, 53(6), pp. 726-731.

Zhang, C., Su, H., Baeyens, J. and Tan, T. (2014) 'Reviewing the anaerobic digestion of food waste for biogas production', *Renewable and Sustainable Energy Reviews*, 38, pp. 383-392.

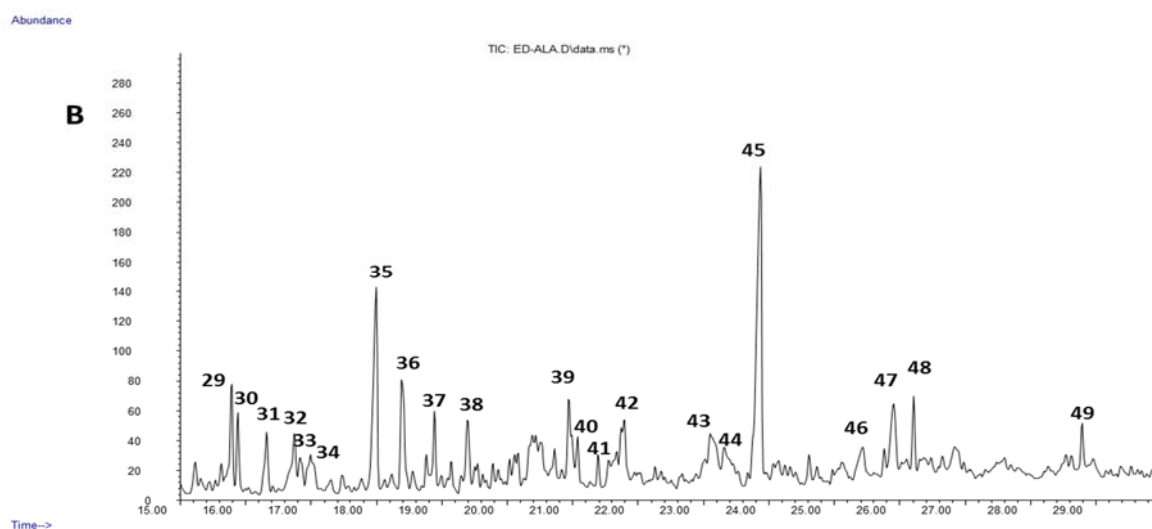
Zhang, C., Su, H. and Tan, T. (2013) 'Batch and semi-continuous anaerobic digestion of food waste in a dual solid-liquid system', *Bioresource Technology*, 145, pp. 10-16.

- Zhang, H., Luo, L., Li, W., Wang, X., Sun, Y., Sun, Y. and Gong, W. (2017a) 'Optimization of mixing ratio of ammoniated rice straw and food waste co-digestion and impact of trace element supplementation on biogas production', *Journal of Material Cycles and Waste Management*, pp. 1-9.
- Zhang, J., Zhang, Y. and Quan, X. (2012a) 'Electricity assisted anaerobic treatment of salinity wastewater and its effects on microbial communities', *Water Research*, 46(11), pp. 3535-3543.
- Zhang, L., Lee, Y.-W. and Jahng, D. (2011) 'Anaerobic co-digestion of food waste and piggery wastewater: Focusing on the role of trace elements', *Bioresource Technology*, 102(8), pp. 5048-5059.
- Zhang, L., Ouyang, W. and Lia, A. (2012b) 'Essential role of trace elements in continuous anaerobic digestion of food waste', *Procedia Environmental Sciences*, 16, pp. 102-111.
- Zhang, L., Xu, C. and Champagne, P. (2010a) 'Overview of recent advances in thermo-chemical conversion of biomass', *Energy Conversion and Management*, 51(5), pp. 969-982.
- Zhang, Q., Hu, J. and Lee, D.-J. (2016) 'Biogas from anaerobic digestion processes: Research updates', *Renewable Energy*, 98(Supplement C), pp. 108-119.
- Zhang, R., El-Mashad, H.M., Hartman, K., Wang, F., Liu, G., Choate, C. and Gamble, P. (2007) 'Characterization of food waste as feedstock for anaerobic digestion', *Bioresource technology*, 98(4), pp. 929-935.
- Zhang, Y., Banks, C. and Walker, M. (2010b) 'Optimising processes for the stable operation of food waste digestion (Defra Project code WR1208)'.
- Zhang, Y., Li, L., Kong, X., Zhen, F., Wang, Z., Sun, Y., Dong, P. and Lv, P. (2017b) 'Inhibition Effect of Sodium Concentrations on the Anaerobic Digestion Performance of Sargassum Species', *Energy & Fuels*, 31(7), pp. 7101-7109.
- Zhong, W., Zhang, Z., Luo, Y., Qiao, W., Xiao, M. and Zhang, M. (2012) 'Biogas productivity by co-digesting Taihu blue algae with corn straw as an external carbon source', *Bioresource Technology*, 114(Supplement C), pp. 281-286.
- Zwietering, M.H., Jongenburger, I., Rombouts, F.M. and Van't Riet, K. (1990) 'Modeling of the bacterial growth curve', *Applied and Environmental Microbiology*, 56(6), pp. 1875-1881.

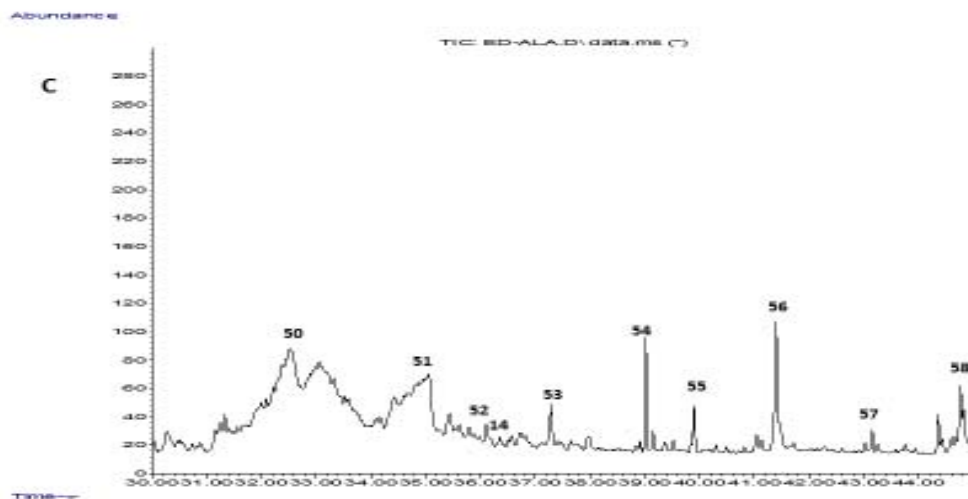
Appendix A. Expanded Py-GC/MS profile at 610°C for *Laminaria digitata* collected in January (Figure A-D)



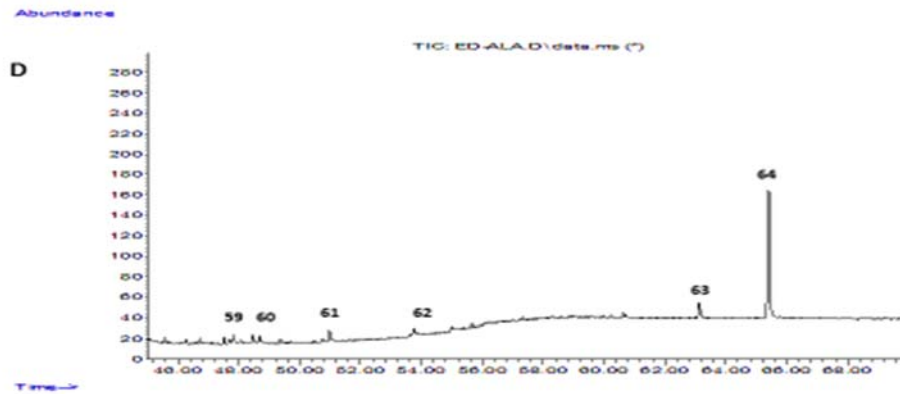
Expanded Py-GC/MS profile at 610°C for *Laminaria digitata* collected in January (identified compounds are listed in Table 3).



Expanded Py-GC/MS profile at 610°C for *Laminaria digitata* collected in January (identified compounds are listed in Table 3).



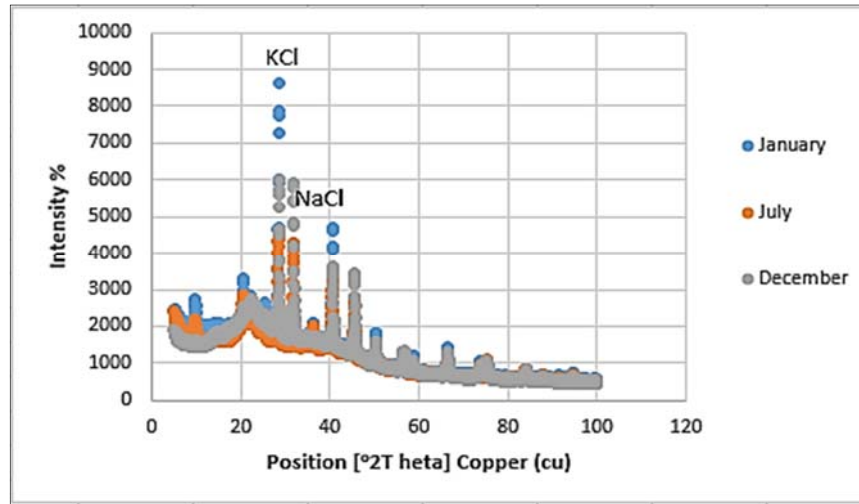
Expanded Py-GC/MS profile at 610°C for *Laminaria digitata* collected in January (identified compounds are listed in Table 3).



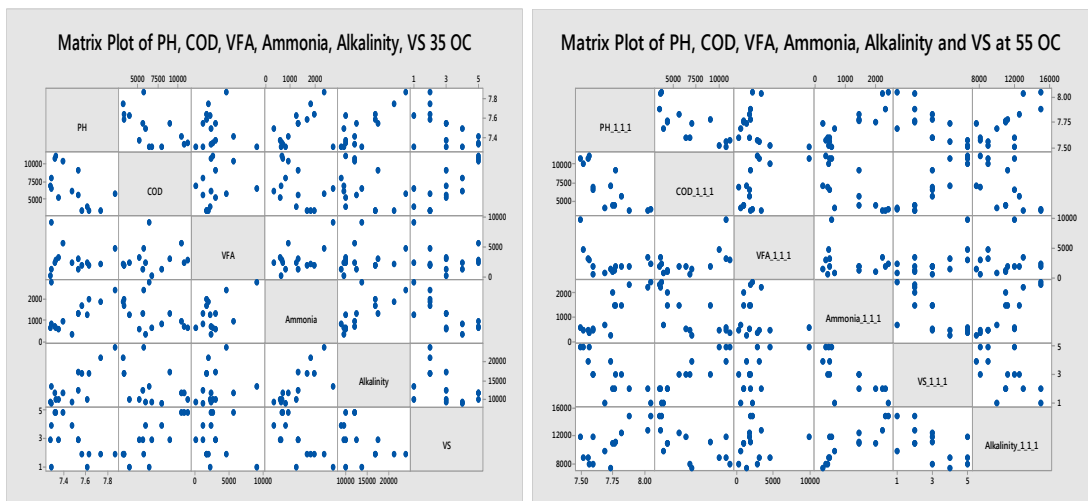
Expanded Py-GC/MS profile at 610°C for *Laminaria digitata* collected in January (identified compounds are listed in Table 3).



Appendix B. X-ray Diffraction intensity graphs for Algae samples collected in January, July, and December 2015.



Appendix C. Matrix plot of COD, VFA and alkalinity for mesophilic and thermophilic reactor



## Appendix D. Correlation: reactor, pH, temperature, COD, VFA, ammonia, VS, and alkalinity (35°C)

	Reactor	PH	TEMP	COD	VFA	
Ammonia						
PH	*					
	*					
TEMP	*	*				
	*	*				
COD	*	-0.591	*			
	*	0.020	*			
VFA	*	-0.077	*	0.183		
	*	0.785	*	0.513		
Ammonia	*	0.530	*	-0.455	0.534	
	*	0.042	*	0.088	0.040	
VS	*	-0.515	*	0.814	-0.193	-
0.741						
	*	0.050	*	0.000	0.492	
0.002						
Alkalinity	*	0.808	*	-0.373	0.193	
0.743						
	*	0.000	*	0.171	0.490	
0.001						
		VS				
Alkalinity	-0.452					
	0.091					

Cell Contents: Pearson correlation  
P-Value

\* NOTE \* All values in column are identical.

## Appendix E. Correlation: reactor, pH, temperature, COD, VFA, ammonia, alkalinity (55 °C)

	Reactor	PH	TEMP
COD			
PH	*		
	*		
TEMP	*	*	
	*	*	
COD	*	-0.767	*
	*	0.001	*
VFA	*	-0.347	*
0.554			
	*	0.205	*
0.032			
Ammonia	*	0.878	*
-0.701			
	*	0.000	*
0.004			
VS	*	-0.740	*
0.911			
	*	0.002	*
0.000			
Alkalinity	*	0.688	*
-0.566			
	*	0.005	*
0.028			
	VFA	Ammonia	VS
Ammonia	-0.187		
	0.504		
VS_1_1_1	0.593	-0.697	
	0.020	0.004	

Alkalinity	0.116	0.823	-0.561
	0.680	0.000	0.030

Cell Contents: Pearson correlation  
P-Value

\* NOTE \* All values in column are identical.